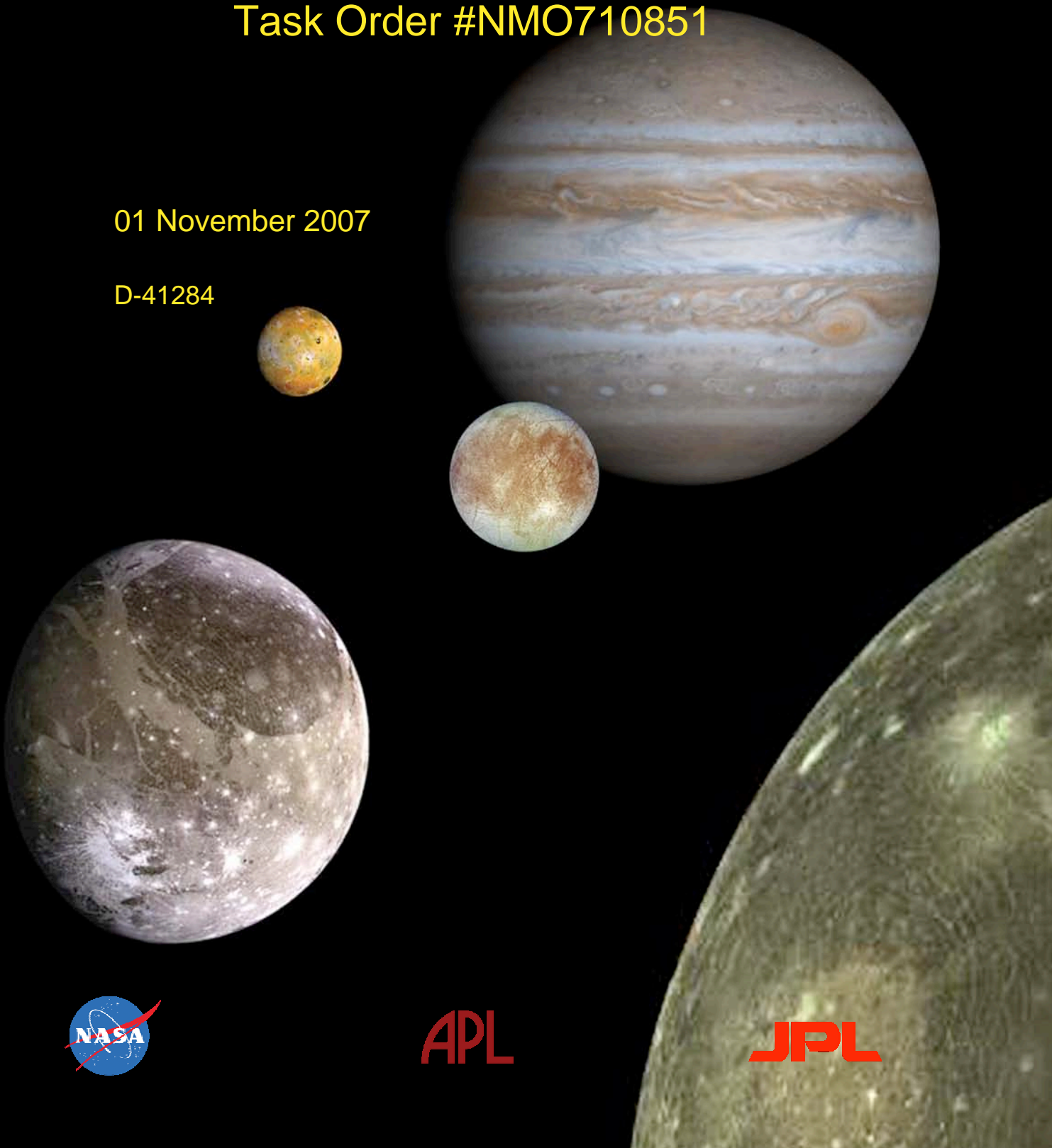


Jupiter System Observer Mission Study: FINAL REPORT

Task Order #NMO710851

01 November 2007

D-41284



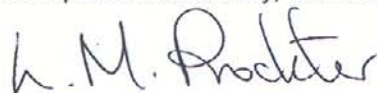
2007 Jupiter System Observer Mission Study: Final Report

Task Order #NMO710851

01 November 2007
D-41284



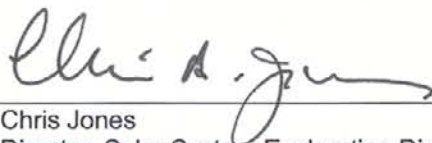
Johnny Kwok
Study Lead
Jet Propulsion Laboratory, California Institute of Technology



Louise Prockter *(signature received by FAX)*
Co-Chair, Science Definition Team
Johns Hopkins University, Applied Physics Laboratory



David Senske
Co-Chair, Science Definition Team
Jet Propulsion Laboratory, California Institute of Technology



Chris Jones
Director, Solar System Exploration Directorate
Jet Propulsion Laboratory, California Institute of Technology



APL

JPL

The research described in this paper was carried out at the Jet Propulsion Laboratory, Caltech Institute of Technology, under a contract with the National Aeronautics and Space Administration.

Table of Contents

FACT SHEET.....	v
1.0 EXECUTIVE SUMMARY	1-1
1.1 Introduction	1-1
1.2 Study Approach	1-1
1.3 Science Definition.....	1-1
1.4 Architecture Development	1-2
1.5 Mission Concept	1-3
1.6 Planning Payload	1-3
1.7 Spacecraft.....	1-3
1.8 Project Implementation	1-4
1.9 Conclusion.....	1-4
2.0 JUPITER SYSTEM SCIENCE GOALS AND OBJECTIVES	2-1
2.1 Introduction: The Jovian System.....	2-1
2.1.1 Science Traceability	2-3
2.1.2 JSO SDT Science Strategy and Structure	2-3
2.2 Science Background, Goals, and Objectives.....	2-5
2.2.1 The Jovian Atmosphere	2-5
2.2.2 The Jovian Magnetosphere	2-10
2.2.3 Io Torus.....	2-13
2.2.4 Galilean Satellites—Surfaces and Interiors	2-14
2.3 Scientific Advancement Achieved by JSO	2-27
3.0 MISSION ARCHITECTURE ASSESSMENT	3-1
3.1 Discriminating Architectural Elements.....	3-1
3.2 Preliminary Mission Architectures Selection.....	3-1
3.3 Intermediate Mission Architectures Selection	3-2
3.3.1 Jovian Tour	3-2
3.3.2 Sub-Satellite.....	3-2
3.3.3 Low Inclination (< 40°) Orbit	3-3
3.3.4 Intermediate Four Architectures.....	3-3
3.4 Final Mission Architectures Selection	3-3
3.4.1 Cost Comparison	3-4
3.4.2 Optical System Aperture.....	3-4
3.4.3 Jupiter Deep Entry Probe.....	3-6
3.4.4 Selection Criteria.....	3-7
3.4.5 Final Two Architectures	3-8
4.0 MISSION CONCEPT IMPLEMENTATION	4-1
4.1 Mission Architecture Overview.....	4-1
4.2 Science Investigation	4-2
4.2.1 Planning Payload.....	4-4
4.2.2 Payload Accommodation.....	4-4

4.2.3	Instrument Descriptions.....	4-6
4.3	Mission Design Overview	4-14
4.3.1	Interplanetary Trajectory	4-15
4.4	Bus Design and Development	4-20
4.4.1	Spacecraft Overview	4-20
4.4.2	Systems Design Approach	4-22
4.4.3	Subsystem Descriptions.....	4-28
4.4.4	Verification and Validation.....	4-41
4.5	Operational Scenarios	4-43
4.5.1	Overcoming the Challenges of Operating in the Jovian System	4-43
4.5.2	Mission Overview	4-44
4.5.3	Science Data Acquisition Scenarios.....	4-49
4.6	JSO Planetary Protection.....	4-57
4.6.1	Requirements	4-57
4.6.2	Implementation	4-58
4.6.3	Probability of Transport to the Ganymedan Sub-Surface.....	4-58
4.7	Trades and Open Issues.....	4-59
4.7.1	Descope Options and Floor Mission	4-59
4.7.2	Lagrange Point Dynamics.....	4-59
4.7.3	Radiation System Design.....	4-60
4.7.4	Radiation Environment Estimation	4-60
4.7.5	Ganymede Approach Trajectory	4-60
4.7.6	Radio Science Capability.....	4-60
4.7.7	Radiation Monitoring System	4-60
4.7.8	Monopulse Pointing	4-60
4.7.9	X-Band Downlink.....	4-60
4.8	Technology Needs	4-60
4.8.1	Radiation Tolerant Sensor Design.....	4-60
4.8.2	Radiation Tolerant Electronic Design	4-61
4.8.3	Qualification of Propulsion System	4-61
4.9	Technical Risk Assessment.....	4-62
4.10	Programmatics	4-64
4.10.1	Schedule.....	4-64
4.10.2	Cost.....	4-66
4.10.3	NEPA Compliance and Launch Approval.....	4-66
5.	DESCOPED MISSION IMPLEMENTATION.....	5-1
5.1	Mission Architecture Overview.....	5-1
5.2	Science Investigation	5-1
5.2.1	Planning Payload.....	5-1
5.2.2	Payload Accommodation.....	5-1
5.2.3	Instrument Description	5-1
5.3	Mission Design	5-1
5.4	Spacecraft Design and Development.....	5-1

5.4.1	Spacecraft Overview	5-1
5.4.2	System Design Approach.....	5-2
5.4.3	Subsystem Descriptions.....	5-3
5.4.4	Verification and Validation.....	5-4
5.5	Operational Scenarios	5-4
5.6	JSO Planetary Protection.....	5-4
5.7	Trades and Open Issues.....	5-4
5.8	Technology Needs	5-4
5.9	Technical Risk Assessment.....	5-4
5.10	Programmatics	5-4
5.10.1	Schedule	5-4
5.10.2	Cost	5-4
5.10.3	NEPA Compliance & Launch Approval.....	5-4
6.0	BACK-UP LAUNCH OPPORTUNITIES	6-1
7.0	SUMMARY	7-1
8.0	TEAM MEMBERS AND ROLES.....	8-1
8.1	Team Overview	8-1
8.2	APL-JPL Outer Planets Steering Group	8-1
8.3	Study Results Review	8-1

APPENDICES

A.	ACRONYMS AND ABBREVIATIONS.....	A-1
B.	REFERENCES.....	B-1
C.	SCIENCE VALUE SUPPORTING DETAIL	C-1
D.	TELECOMMUNICATIONS LINK ANALYSIS.....	D-1
E.	MEL AND PEL.....	E-1

Jupiter System Observer

"Probing the Foundations of Planetary Systems"

Science Goals

Jupiter Atmosphere:

- Understand the processes that maintain the composition, structure, and dynamics of the Jovian atmosphere as a typical example of a gas giant planet

Magnetosphere:

- Understand the magnetospheric environments of Jupiter, its moons, and their interactions

Satellites:

- Understand the mechanisms responsible for formation of surface features and implications for geological history, evolution, and levels of current activity
- Determine the surface compositions and implications for the origin, evolution, and transport of surface materials
- Determine the compositions, origins, and evolution of the atmosphere, including transport of material throughout the Jovian system

Interiors:

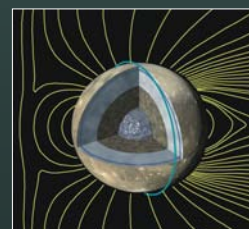
- Determine the interior structures and processes operating in the Galilean satellites in relation to the formation and history of the Jupiter system and potential habitability of the moons

Baseline Planning Payload

Investigations/ Instruments	Characteristics
High-res Camera (HRC)	IFOV = 2.0 μ rad, 50-cm aperture, 10-color filter wheel, shared foreoptics with VHS
VIS-NIR Hyperspectral Imager System (VHS)	0.4 – 5 μ m, IFOV of 10 μ rad, SNR >300, shared 50-cm foreoptics with HRC
Medium res Stereo Camera (MRC)	IFOV of 20 μ rad, 6-cm aperture, monochromatic, near-simultaneous stereo capability
UV Spectrometer (UVS)	EUV 55 – 110 nm, Far UV 110 – 190 nm, and NUV 190 – 350 nm, <0.3-nm spectral resolution, IFOV <1 mrad
Thermal Spectrometer (TS)	7 – 500 μ m, imaging by 2 Fourier Transform Spectrometers, IFOV <250 μ rad, 50 cm aperture
Ground-Penetrating Radar (GPR)	5 MHz dipole & 50 MHz Yagi antennas with 1 to 10 MHz bandwidths
Laser Altimeter (LA)	Multi-beam, 5-spot cross pattern, 1.064 μ m
Magnetometer (MAG)	Dual sensor, 10 m boom, vector magnetic field to accuracy ≤ 0.1 nT, 0.05 s time resolution
Plasma Spectrometer/Energetic Particle Detector (PS/EPD)	Electron, ion beam, and ion mass, energy, and angle distributions at eV to MeV energies, 1 – 30 s resolution
Radio Science Gravity	2 way Doppler, X- & Ka band via telecom subsystem
Radio Science Atmospheres	USO and a one way, dual-frequency downlink from telecom subsystem

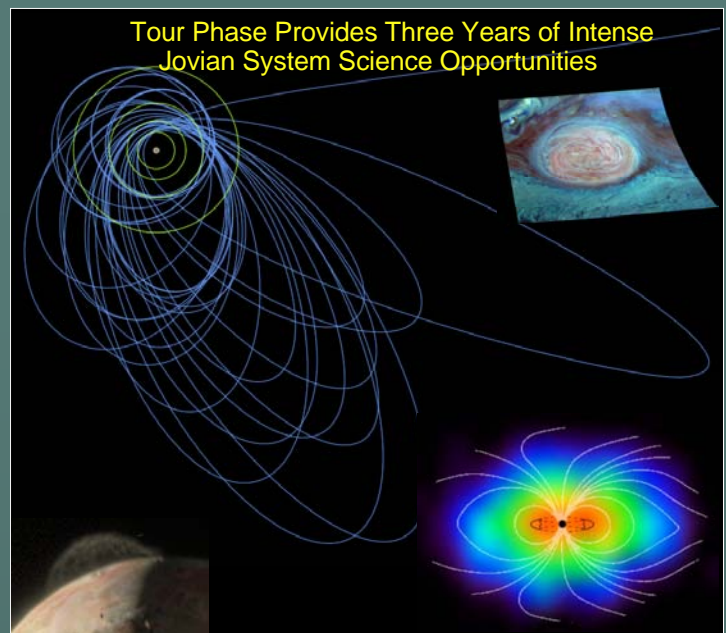
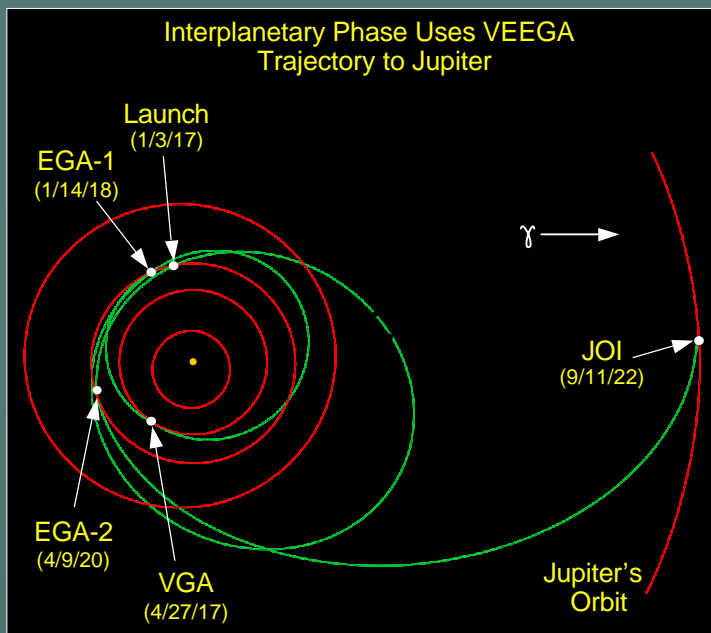
Why JSO?

- JSO will follow-up on discoveries over the last dozen years by Galileo and ground-based observers to study:
 - Jupiter as an analog for understanding known extra-solar planets
 - Jupiter as a natural laboratory for studying magnetospheric phenomenon
 - Ganymede as the only satellite known to have a magnetic field
 - Europa, Ganymede, and Callisto as worlds apparently possessing subterranean oceans
 - Temporal variations in Io's extreme volcanism and Jupiter's turbulent atmosphere



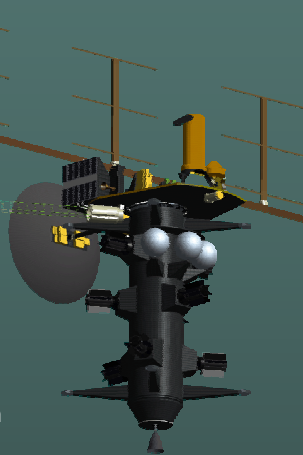
Schedule





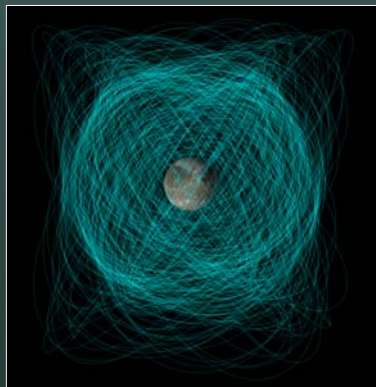
Mission Overview

- Launch on Delta IV-H in January 2017
- Venus-Earth-Earth Gravity Assist (VEEGA) trajectory
- Jupiter Orbit Insertion in September 2022
- 3-year tour of Jovian system, with many close flybys each of Io, Europa, Ganymede, and Callisto, continuous magnetospheric monitoring, regular monitoring of Io and Jupiter's atmosphere
- Ganymede orbit insertion in September 2025
- Initial, elliptical, 200 x 19,000 km orbit
- Transfer to 200 km circular orbit at $\geq 85^\circ$ inclination one year after GOI
- 70m-equivalent DSN coverage during encounters and Ganymede Science phase
- Flight system impacts Ganymede at end-of-mission



Spacecraft

- 7262 kg wet mass
- 228 kg planning payload
- Eight MMRTGs and two 38 A-hr batteries
- Two-axis gimbaled, 2.75 m HGA
- Two-way doppler at both X-/Ka-band for radio science-gravity investigation
- USO for radio science-atmosphere investigation
- 600 kb/s to 70m from 6.5 AU at Ka-band
- 9.6 Gb solid state recorder
- Dual-mode propulsion system; 2705 m/s
- Reaction wheels for long arcs without non-gravity disturbances
- Single-fault tolerant; redundant assemblies
- Radiation-hardened electronics
- 1.8 Mrad radiation design point
- 12-year mission life



Cost

Total Mission Cost \$BFY07	Baseline	Descoped
	Best Estimate: \$3.1 Range: \$2.8 to 3.7	Best Estimate: \$2.7 Range: \$2.4 to 3.2

Science Definition Team

Louise Prockter, Co-Chair (APL)
 Dave Senske, Co-Chair (JPL)
 Elizabeth Turtle (APL)
 Karl Hibbitts (APL)
 Amanda Hendrix (JPL)
 Dave Williams (Arizona State University)
 Geoff Collins (Wheaton College)
 Adam Showman (University of Arizona)
 Jerry Schubert (UCLA)
 Glenn Orton (JPL)
 John Cooper (GSFC)
 Margy Kivelson (UCLA)

1.0 EXECUTIVE SUMMARY

1.1 Introduction

The Jupiter system is a natural laboratory to study diverse and dynamic planetary processes. Its set of planet-sized moons serves as a solar system in miniature. In addition, Jupiter itself is an analog for the majority of extra-solar planets discovered to date. The Galilean moons, from volcanic Io to ancient icy Callisto, embody a variety of geological and geophysical processes, providing a window into solar system history by preserving in their cratering records a chronology dating from the present time back nearly 4.5 billion years. The presence of potential icy satellite subsurface oceans in the icy satellites has profound implications for habitability. The magnetosphere of Jupiter intimately interacts with its system of moons, transferring material throughout the system. Study of the internally generated magnetic field of Ganymede with comparison to the Earth and Mercury provides a basis to better understand planetary dynamos. Gaining insight into the composition and volatile inventory of Jupiter will shed light on how planets accrete from solar nebulae. Hence, a system-level investigation of the Jovian system will illuminate the question of how planetary systems form and evolve.

The NRC Solar System Exploration “Decadal” survey, the 2006 SSE Roadmap, and the 2007 NASA Science Plan all point to the importance of understanding solar system formation and evolution. After the Galileo mission, and with Juno in development, a logical step is for NASA to plan a Jovian system mission that would:

Probe the Foundations of Planetary Systems.

1.2 Study Approach

In January 2007, NASA commissioned JPL to conduct a Jupiter System Observer (JSO) study as an alternative to the Europa Explorer (EE) mission concept, with a set of specific guidelines. (1) The mission should last about 5 years after arriving at Jupiter; (2) It must address five primary science targets: Jupiter, Io, Europa, Ganymede, and Callisto; and (3) The final destination should be in orbit around Ganymede, or in its immediate vicinity. Ganymede is a logical target for a long-lived

observer of the Jovian system because of its diverse geological features, its potential possession of a liquid ocean, because it is one of only three terrestrial bodies in our solar system known to possess an intrinsic magnetic field, and because its radiation environment is less harsh than that of Europa.

NASA appointed a 12-member Science Definition Team (SDT) with diverse planetary science backgrounds to work closely with the engineering team.

The study was divided into two phases. Phase I was to develop target science objectives, and identify possible mission architectures with potential instrumentation and associated science operations scenarios. At the end of phase I, the study team was to select no more than 2 mission architectures. Phase II was to develop the mission concept(s) implementation and to perform a first order cost, schedule and risk assessment.

1.3 Science Definition

The SDT was divided into 4 thematic groups focusing on Jovian atmosphere, magnetosphere, satellite science, and interiors. Other subject matter experts were invited to lead discussions on Jupiter rings, the Io torus, and Jupiter system science from New Horizons. The 4 groups developed the following science goals:

- 1) *Jovian Atmosphere*: Understand the processes that maintain the composition, structure and dynamics of the Jovian atmosphere as a typical example of a Gas Giant Planet
- 2) *Magnetosphere*: Understand the magnetospheric environments of Jupiter, its moons and their interactions
- 3) *Satellite Science*:
 - a) Understand the mechanisms responsible for formation of surface features and implications for geological history, evolution, and levels of current activity
 - b) Determine the surface compositions and implications for the origin, evolution and transport of surface materials
 - c) Determine the compositions, origins, and evolution of the atmosphere, including transport of

material throughout the Jovian system

- d) Determine how the components of the Jovian system operate and interact
- 4) *Interiors*: Determine the interior structures and processes operating in the Galilean Satellites in relation to the formation and history of the Jupiter system and potential habitability of the moons.

From these goals, the SDT developed a hierarchical flow-down of science objectives, investigations, and a comprehensive set of measurements. In all, there are 46 objectives that lead to 140 investigations involving 334 measurements.

1.4 Architecture Development

Establishment of the science objectives, investigations and measurements enabled the identification of key architectural elements such as orbiter, probe, lander, sub-satellite, and the size of optical aperture. Together with options in launch vehicles, interplanetary trajectories, propulsion systems, power sources, and the final orbital state at Ganymede, they become the fundamental set of discriminating architectural elements. Selecting combinations of these elements would constitute the mission architecture. There were over one thousand practical architectures that could be considered.

The study team, using rough order scaling relationships on mass, power, propulsion, LV performance, and qualitative judgment, quickly narrowed the scope of the mission to eleven architectures. The science merit of these architectures was judged against the established objectives, and four were down-selected for further study (see [Table 1.4-1](#)). All four architectures use a Venus-Earth-Earth Gravity-Assist (VEEGA) interplanetary trajectory and the Multi-Mission Radioisotope Thermoelectric Generator (MMRTG).

Architecture 1 uses the Atlas V 551 launch vehicle, which is less expensive but delivers less mass. Architectures 2–4 use the Delta IV-H launch vehicle to provide significant mission flexibility and high science coverage. Architecture 2 plans a low altitude Ganymede orbit as the final destination. Architecture 3 provides the most remote sensing capability with a 1-meter size optical telescope. Architecture 4 supplements an orbiter with a deep probe to extend Galileo’s atmospheric in-situ science. In addition, a set of notional instruments was developed for each architecture that were consistent with meeting the measurement requirements and the mass and power available.

Using JPL’s concurrent engineering team (Team X), preliminary spacecraft designs were conducted and initial cost estimates were generated. Based on the science merit, cost, risk, and technology readiness, architecture 2 was selected as the baseline mission, and architecture 1, which is quite similar to architecture 2 except for the launch vehicle used and the final orbit, was selected to be the descoped mission.

These missions took advantage of several distinguishing physical characteristics of operating in orbit around Ganymede. Relative to a mission that orbits Europa, the radiation flux is about 30 times less severe at Ganymede. This means that for a comparable radiation-tolerant design, a spacecraft at Ganymede would have a much longer life expectancy. This leads to an expandable trade space within the mission architecture where radiation dose is a commodity. For example, part of the allowable dosage is expanded to include 4 Io and 6 Europa flybys. Another distinguishing factor for a Ganymede orbiter is the lower Jovian 3rd-body perturbations at Ganymede. This led to the discovery of a family of long-term stable, large, elliptical, inclined orbits that provide an observational vista point for Jupiter system science.

Table 1.4-1. Four Intermediate Architectures

	1 (Descoped)	2 (Baseline)	3	4
Launch Vehicle	Atlas V 551	Delta IV-H		
Interplanetary Trajectory	VEEGA			
Power Source	MMRTG			
# of S/C	Orbiter			Orbiter + Probe
Optical Aperture	50 cm	50 cm	1 meter	50 cm
Orbit at Ganymede	Elliptical	Low Circular	Elliptical	Elliptical

1.5 Mission Concept

The baseline mission that emerged is a single spacecraft comprised of a bus and a nine-instrument (plus two radio science investigations) payload that launches in January 2017 on a Delta IV-H launch vehicle. A VEEGA interplanetary trajectory with a flight time to Jupiter of 5½ years is used, along with a conventional chemical propulsion system for trajectory adjustments. Upon arrival at Jupiter in September 2022, a close flyby of Io and a large propulsion system burn will establish JSO as only the third artificial satellite of Jupiter (after Galileo and Juno). The mission will conduct a 3-year tour of the Jovian system, using Io, Europa, Ganymede, and Callisto for gravity-assists to reduce JSO's orbital energy, leading to Ganymede Orbit Insertion (GOI) in September 2025. This initial orbit around Ganymede will have a period of 24 hours, an inclination of about 60°, and an eccentricity that brings its periapsis to as low as 200-km altitude. This novel orbit is stable for at least tens of years. Due to Jupiter's gravity effects, the orbit will oscillate between the initial eccentric orbit and a near-circular orbit every 42 days while the periapsis location will vary in latitude and longitude. This novel orbit is ideally suited for long-term characterization of Ganymede's magnetic field while the many low-altitude passages afford important remote sensing, radar, altimetry, and gravity field observations. After approximately one year, a set of orbit transfer maneuvers will place the spacecraft in a 200-km altitude, circular, near-polar orbit. This orbit is ideal for geological, geophysical, and gravity science investigations, while continuing to afford

campaigns of remote sensing of Jupiter and its other moons as well as field and particles measurements.

For the descoped mission the spacecraft will remain in the elliptical orbit for two years (or more) until the end of mission rather than transfer to a low-altitude, circular orbit. The savings in propellant enables the use of the Atlas V 551 rocket.

At the end of the primary mission, the JSO mission will be extended, or the spacecraft will be disposed of onto the surface of Ganymede.

1.6 Planning Payload

The set of measurement requirements recommended by the JSO SDT provided the basis for developing a set of notional science instruments and radio science investigations known as the planning payload, summarized in [Table 1.6-1](#). An Announcement of Opportunity (AO) process is expected in the future to solicit proposals for what will be the actual JSO payload. Using the requirements and the planning payload, a design concept for the spacecraft and its associated operational scenarios was created and measured for its science value.

The high-resolution camera and the hyper-spectral imager share the same 50-cm front optics to save mass and volume. All these instruments have analogous flight proven design as listed. Most of the instrument sensors and electronics require radiation-hard upgrades; an additional 25% was added to the estimated cost of the instrument developments to account for these necessary upgrades.

1.7 Spacecraft

The JSO spacecraft is a redundant, 3-axis

Table 1.6-1. JSO Planning Payload

Instrument/Investigation	Mass (kg)	Power (W)	Similar Instruments
High Resolution Camera + Visible-Near IR Hyperspectral Imager (shared 50 cm optics)	70	95	MRO HiRISE, DI HRI, Cassini NAC
Visible-Near IR Hyperspectral Imager (shared 50 cm optics)			Chandrayaan M ³
Medium Resolution Stereo Camera (No stereo for descoped)	20/15	20/15	Stardust NAVCAM, DAWN Framing Camera, Mars Express HRSC, Chandrayaan Terrain Mapping Camera
UV Spectrometer	15	10	Cassini UVIS
Thermal Spectrometer	43	26	Cassini CIRS
Ground Penetrating Radar	36	45	Mars Express MARSIS, MRO SHARAD
Laser Altimeter	15	21	MGS MOLA, NEAR NLR, LRO LOLA
Magnetometer	4	2	GLL MAG, Polar MAG, Feedsat MAG, ST5 MAG
Plasma Spectrometer/Energetic Particle Detector (No TOF spectrometer for descoped)	25/10	15/10	Cassini CAPS
Radio Science - Gravity and Atmospheres	-	-	Notes: Values are current best estimate for baseline/descoped. Power values are steady-state
Baseline/Descoped Total	228/208	234/224	

stabilized spacecraft. The attitude is controlled by reaction wheels during fine pointing for science. The 2.75-m HGA is 2-axis articulated to allow for Earth communications while pointing the instruments during science observations. The dual Ka and X-band telecommunication system is also used for radio science. The 8 MMRTGs provide 778 W of electrical power at the end of mission. Redundant Li-ion batteries provide for spacecraft modes that require higher power loads, such as main-engine maneuvers and satellite encounters. The descoped mission uses 7 MMRTGs.

The command and data handling architecture includes a fully redundant system based on the RAD 750 computer that performs engineering and selected science functions, including hot-swapping during critical events such as JOI. Redundant 150 Mbyte mass memory is available for engineering data storage and a separate 9.6-Gb solid-state recorder (SSR) is available for science data storage. Both types of data storage use non-volatile, rad-hard chalcogenide memory.

The dual-mode propulsion system uses hydrazine and nitrogen tetroxide. The 890N gimbaled main engine is used for large maneuvers, while the 90N monopropellant engines are used for smaller maneuvers and thrust vector control. The 0.7N thrusters are used for reaction wheel desaturation and backup attitude control. The total propellant load is 4775 kg for the baseline mission, and 2627 kg for the descoped mission.

The launched mass for the baseline mission is 7810 kg, and 5300 kg for the descoped mission. The baseline mission has 1050 kg of mass contingency/reserve; the descoped mission has 1080 kg.

1.8 Project Implementation

The project implementation assumes a development lifecycle duration of 15/15/30/30 months for Phase A/B/C/D respectively. For the January 2017 launch, it means a phase A start in July 2009. The schedule includes a pre-phase A period during 2008 and 2009. This period will be used to reduce risk in several areas and thus reduce cost uncertainty. The JSO planetary protection (PP) implementation assumes the probability of contaminating the Ganymede ocean is vanishingly small and

therefore the bus and instrument components do not require sterilization by dry heat. Pre-phase A includes analysis on this approach leading to a PP implementation decision prior to System Requirements Review. Pre-phase A also includes the formation of the project science team that will continue to refine the mission architecture, establish level 1 science requirements, define descoped options and science floor. The engineering team will conduct sufficient design of the spacecraft to define instrument performance and interfaces (mass, power, volume, data, electrical, mechanical, thermal, radiation tolerance, reliability, pointing, alignment, shared optics, operations, data products, and team responsibilities) in support of the instrument AO.

The total estimated life cycle cost (phase A/B/C/D/E) including the launch vehicle and Radioisotope Power System is \$3.1 BFY07 for the baseline mission, and \$2.7 BFY07 for the descoped mission. Both estimates include 35% reserve (not including LV and RPS) for phase B/C/D based on evaluation of cost/risk factors. The basis of estimate is a combination of semi-grass roots and parametric relationship developed by the JPL Technical Sections and incorporated into the Team X methodology. These cost estimates compared favorably with Cassini.

Previous studies of similar maturity would include -10% to +20% uncertainty in the estimate. So the baseline mission would have a range of \$2.8B to \$3.7B, and the descoped mission would be \$2.4B to \$3.2B

1.9 Conclusion

The JSO mission is a long-term science platform for studying the Jovian system that addresses nearly fifty unique science objectives. It will advance the understanding of fundamental processes of planetary systems, their formation, and evolution. Specifically, it will provide new insight into planetary dynamo processes and lead to a fuller understanding of subsurface oceans. Its scientific results will uniquely advance the NASA mission,

"To advance and communicate scientific knowledge and understanding of the Earth, the solar system, and the universe."

2.0 JUPITER SYSTEM SCIENCE GOALS AND OBJECTIVES

2.1 Introduction: The Jovian System

Building on the science results from previous missions, the Jupiter System Observer (JSO) will provide fundamental new insight into processes of planetary system origin and evolution at spatial and temporal scales up to several orders of magnitude greater than previously attained.

Galileo's observations of moons orbiting the giant planet Jupiter in 1610 were central to developing our understanding of the celestial motion of the solar system. As the most massive body orbiting the Sun, Jupiter governs 63 moons and several rings, creating a solar system in miniature. JSO is a long-duration mission that will study the entire Jupiter system, focusing both on its individual components, including Jupiter's atmosphere, rocky and icy moons, rings, and magnetospheric phenomena, and on the system science that unites them. Moreover, JSO will return a wealth of data that will enable a fuller understanding of a variety of magnetospheric, atmospheric, and geological processes beyond the Jovian system, and will illuminate the question of how planetary systems form and evolve.

JSO is uniquely positioned to address significant unanswered questions about the Jovian system. One of the key outstanding issues is how planetary dynamos operate. Among solid bodies, only Earth, Mercury and Ganymede are known to have dynamo-generated magnetic fields (although Mars may have experienced dynamo activity in the past). Understanding Ganymede's intrinsic magnetic field is therefore a top priority. Furthermore, the one known habitat of life in the Universe, the Earth, has evolved within the protective shield of such a field, so Ganymede offers the opportunity for direct study of a similar magnetic environment. JSO will determine the spatial and temporal characteristics of Ganymede's magnetic field, determining whether it has high-order spatial structure and/or varies in time. JSO will conduct the low-altitude global magnetometer sounding with frequent repeated coverage that is needed to answer these questions by distinguishing the spatial and temporal variability in the intrinsic field from magnetic induction effects.

The four Galilean satellites have undergone markedly different evolution, as is evident from their surfaces. At the system level, JSO will provide critical insight into the tidal interactions responsible for the observed geological activity and differences among the moons. JSO will also investigate specific processes such as how volcanoes operate on Io, how bright terrain formed on Ganymede, and how chaos, ridges and bands formed on Europa. The relative roles of tectonism and volcanism will be examined on all the satellites and the processes that produce their enigmatic landforms will be investigated using a powerful combination of high-resolution global imaging, hyperspectral mapping, topographic measurements and gravity sounding. Subsurface radar sounding will enable compositional or structural horizons to be identified and will be particularly useful for understanding the processes that formed Ganymede's bright terrain. Gravity-topography correlations will be used to determine whether there are mass anomalies associated with resurfaced regions and the nature of the underlying lithosphere.

Establishing whether oceans exist on the icy satellites is key to understanding their evolution and potential habitability. Major questions include whether Europa, Ganymede and Callisto contain oceans, what the three-dimensional distribution of liquid water is in their interiors, and how thick their ice shells are at the present time ([Figure 2.1-1](#)). JSO will address these questions using a combination of approaches. First, the induced dipoles at Europa, Ganymede, and Callisto will be well characterized. Galileo obtained only the minimum number of flybys of Callisto needed to infer an inductive response, and additional flybys will greatly improve our understanding of the strength, orientation, and time variability of the inferred dipole. Once in orbit around Ganymede, JSO will distinguish between an induced dipole and an intrinsic quadrupole. High-resolution spatial and temporal magnetic sounding will allow inferences on the thickness and depth of an ocean and whether it is global. As a second line of investigation, JSO will measure the gravitational and topographic response to the time-variable tidal potential (i.e., measure the second degree Love numbers k_2 and h_2). With

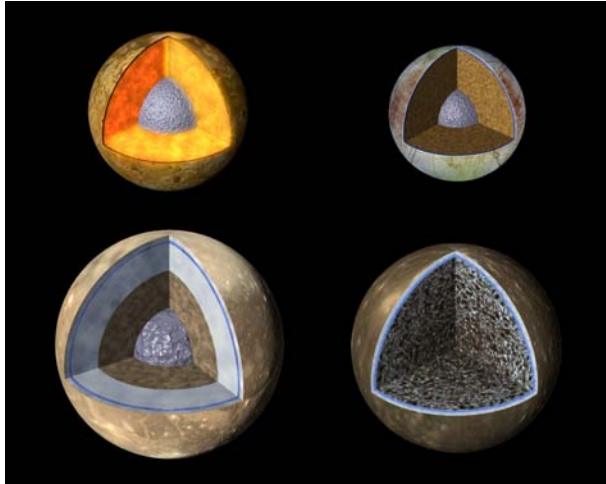


Figure 2.1-1. Interior structure of Galilean satellites (from Schubert et al., 2006).

oceans, the amplitude of the time-variable tides on Europa, Ganymede, and Callisto are ~30, 7, and 5 m; without oceans, these amplitudes decrease by a factor of 10–30. A grounded ice layer (i.e., non-global ocean) will have a complex tidal response that may be measurable for each icy satellite. Gravity data returned from JSO will also help to elucidate questions about the internal mass distribution of the three icy satellites, their degree of differentiation, and whether they are in hydrostatic equilibrium. During orbit around Ganymede, JSO will obtain high-order gravitational harmonics that will enable better mapping of the magnitude and distribution of small-scale gravity anomalies. Finally, JSO will conduct subsurface active (radar) sounding through flybys of Europa and Callisto, and from orbit around Ganymede; current estimates suggest that radar can penetrate ~10 km into a relatively clean, unfractured ice shell.

High-resolution imaging will locate surface features on the satellites with the accuracy needed to address outstanding issues regarding their rotational and orbital states, such as whether they are rotating nonsynchronously, their obliquities and inclinations and whether these change over year-long timescales, and for Ganymede, the libration amplitude. These data will help answer questions such as whether libration and/or nonzero obliquity contributes to tidal heating, and whether the satellites are moving toward or away from

Jupiter. In addition, JSO will make measurements of the heat flow from the satellites at many geometries relative to the Sun, using thermal-IR (10–30 micron) measurements, determine whether “hot spots” exist on Europa and Ganymede, and monitor Io’s volcanism.

After several visits by spacecraft and decades of Earth-based observing, motivation for continued intensive study of Jupiter’s atmosphere by remote sensing lies in the interconnected nature of all of its physical and chemical processes and the lessons they hold for the behavior of planetary atmospheres generally. Jupiter is a vast laboratory of inter-related electromagnetic phenomena, geophysical fluid flow and chemistry. The difficulties faced by previous spacecraft investigations has been in their brevity (flybys by Pioneers 10 and 11, Voyagers 1 and 2, Ulysses, Cassini, and New Horizons), bandwidth-imposed limits on spatial coverage (Galileo), and limitations on spatial resolution and continuity (Earth-based observations). Because of these restrictions, no mission yet flown has obtained the long-term, high-resolution climate database necessary for truly understanding Jupiter’s atmosphere. The Juno mission, scheduled to fly before JSO, will provide crucial information on the spatial variation of the deep water and ammonia abundances, structure of the magnetic field, and the depth of the jet streams, but it will be unable to monitor the upper troposphere and stratosphere in sufficient detail to determine the crucial transport mechanisms for heat, momentum, and condensable vapors that (for example) determine the structure of the jet streams in the atmosphere. In effect, JSO will constitute the first long-term climate sounder for Jupiter’s upper troposphere and stratosphere. A primary goal of the JSO mission will be to provide a broad-based set of synoptic observations of these various atmospheric phenomena over substantial portions of Jupiter’s seasonal and non-seasonal cycles, with extensive spatial coverage, thereby providing a dataset similar to those used to establish a fundamental climatology for the Earth, Mars and Venus. These data will provide powerful constraints on the organization of weather on Jupiter, the structure of the atmosphere near and above the

clouds, the processes that pump Jupiter's jet streams, and the flow of energy and trace constituents among vortices, jets, and waves, thus revolutionizing our understanding of Jupiter's stratosphere.

Likewise, the JSO mission will enable long-term monitoring of Io's hyperactive volcanism. High-resolution observations over various timescales will reveal the physical constraints that contribute to the different eruption styles of plumes, the compositions of lava flows and plains materials, and elucidate the ambiguous relationships between paterae and mountains. The combination of close flybys and distant monitoring over several years will provide invaluable insight into Io's volcanic and tectonic processes.

The JSO mission presents an opportunity to study the Jupiter system and make unprecedented long-term, high-resolution observations of the Io torus, including its sources and wide-ranging effects on the system. Monitoring the torus is essential for investigating correlations between Io's volcanic activity, loss of material from Io, Jupiter's magnetospheric activity, and transport of material into the system as a whole.

JSO will enable long-term, dedicated observations of Jupiter's rings and their intriguing relationships to nearby small satellites. Imaging at many different phase angles and over a range of timescales will enable the rings to be fully characterized and their composition and dynamics to be understood.

Under the imperative of achieving the best overall Jupiter system science, we have identified a number of important and discriminating science focus areas that provide the foundation for specific scientific goals. First, given that Ganymede is one of only three solid-surface bodies in the solar system to possess an internally generated magnetic field, it is necessary to:

- Understand the processes that give rise to the Ganymede internal magnetic field
- Understand Ganymede's internal structure and mass distribution with emphasis on implications for an internal dynamo.

Second, and within the context of these first two objectives and the overall system science, there is a priority to:

- Understand the surface composition of the Galilean satellites, confirm the presence of potential subsurface oceans and provide a framework for relating the surface geology to interior processes.

Finally, as the Jupiter system may be an important analog for extra solar planetary systems, the JSO mission must lead to:

- Understanding the dynamics and structure of the Jupiter atmosphere along with characterization of relations to the magnetosphere and how the components (large and small satellites, rings etc.) of this "miniature solar system" interact

2.1.1 Science Traceability

Results from the Galileo mission in the 1990s generated the highly compelling hypothesis that a subsurface ocean is present at Europa and that liquid layers are most likely present within Ganymede and Callisto. Because of the implications for Jupiter system evolution and potential habitability, there has been consistent science community support for a return to the Jupiter system. Beginning with Europa Orbiter (EO), science drivers were codified to form a traceable basis for such a mission. Subsequently, the NASA commissioned "Solar System Decadal Survey" carried out under the auspices of the National Research Council (New Frontiers in the Solar System: An Integrated Exploration Strategy, 2003) identified Europa as the top science priority for a large-scale mission. This report also stressed the importance of Jupiter, its rings and the magnetosphere environment, along with all of the Galilean satellites to understanding the system as a whole. The overall system science objectives for the Jupiter system led NASA to initiate the Jupiter Icy Moons Orbiter (JIMO) mission. The JIMO Science Definition Team (SDT) generated a comprehensive set of science goals, objectives, investigations and measurements (Greeley et al., 2004a). Although the JIMO mission was indefinitely deferred, the work of the SDT for that mission provides the foundation to the JSO concept discussed here. Much of the cumulative science knowledge of the Jupiter system extending beyond the Decadal and JIMO studies with later Galileo Orbiter and Cassini flyby observations is discussed in chapters of the book *Jupiter - The Planet*,

Satellites and Magnetosphere (Bagenal et al., 2004).

2.1.2 JSO SDT Science Strategy and Structure

The Jovian system provides a unique laboratory to study, in a single place, diverse and dynamic planetary processes. The discovery of extra-solar planetary systems with Jupiter-sized bodies has led to a revolution in thought regarding how these systems form and evolve. The scientific exploration of Jupiter and its diverse set of satellites provide a basis for improving our understanding of dynamical behavior, satellite interactions and geologic events throughout Solar System history. For example, the icy Galilean satellites afford a window into Solar System history by preserving in their cratering records a chronology dating back nearly 4.5 billion years and extending to the present. The continuously erupting volcanoes of Io may derive from an interior magma ocean and, thus, studying Io can provide insight into magma oceans that may have been present within the early Earth and Moon. Ganymede's rare internally-generated magnetic field is an important example of how dynamos work. The confirmation and characterization of icy satellite subsurface oceans will impact considerations of habitability. Characterizing

the dynamics and temperature structure of Jupiter's atmosphere will illuminate the mechanisms by which tides on Jupiter transfer Jupiter's rotational energy to the Galilean satellites and thereby, via the Laplace resonance, drive the satellites' extensive tectonism and volcanism. Understanding the composition and volatile inventory of Jupiter will shed light into how planets accrete from solar nebulae. Finally, like our Sun, Jupiter influences its system through its extensive magnetic field. Taking advantage of this natural laboratory with JSO will advance scientific understanding with the unifying theme: ***Probing the Foundations of Planetary Systems.***

To address the broad range of Jovian system science questions, the JSO SDT divided itself into four focused theme groups, (1) Jovian Atmosphere, (2) Magnetospheres (3) Satellites and (4) Interiors. Guiding the overall process were the "Solar System Decadal Survey," the subsequent NASA Roadmaps, and the Outer Planets Assessment Group (OPAG) "Scientific Goals and Pathways for Exploration of the Outer Solar System" document. The detailed traceability to the Decadal Survey is provided in Appendix C. Specific key elements are summarized in **Table 2.1-1**. These are grouped, and

Table 2.1-1. Traceability of JSO Science to Major Themes and Governing Documents

High level Science Focus	Solar System Exploration (Decadal) Survey	2006 SSE Roadmap and 2007 NASA Science Plan	JSO Science Theme
Physical Processes	Learn how the Sun's retinue of planets originated and evolved	How did the Sun's Family of planets and minor bodies originate?	Satellites Interiors Atmosphere Magnetospheres
	Discover how the basic laws of physics and chemistry, acting over aeons, can lead to the diverse phenomena observed in complex systems, such as planets	How did the solar system evolve to its current diverse state?	
	Understand how physical and chemical processes determine the main characteristics of the planets and their environments, thereby illuminating the workings of the Earth.		
Potential for Habitability	Determine how life developed in the solar system, where it may coexist, whether extant life forms exist beyond Earth and in what ways life modifies planetary environments	What are the characteristics of the solar system that lead to the origin of life?	Satellites Interiors
		How did life begin and evolve on Earth and has it evolved elsewhere in the solar system	
Environment	Explore the terrestrial space environment to discover what potential hazards to Earth's biosphere may exist	What are the hazards and resources in the solar system environment that will affect the extension of human presence in space	Magnetospheres Satellites

paraphrased, from the Decadal Survey into three high-level traceable focus areas, Physical Processes, Potential for Habitability, and Environment.

2.2 Science Background, Goals, and Objectives

Each JSO SDT science theme group compiled a comprehensive set of Goals, Objectives, Investigations and Measurements for studying the Jupiter system. The detailed science flow, including an assessment of science value, for each theme group is provided in Appendix C. Each group prioritized their Objectives and Investigations. Within the Satellites group, each target was prioritized separately. Because there are over 300 measurements, a summary version that focuses on key elements is provided in **Foldout 1** (FO-1: Note that the colors used in this foldout provide a one-to-one mapping with the detailed Goals, Objectives, Investigations and Measurements in Appendix C). Many instruments were considered for the notional payload, but the ones that were selected were chosen based on their ability to meet multiple science goals, and therefore achieve maximum synergy among different science investigations.

The remainder of this section provides a detailed discussion, by theme, of the science to be accomplished by JSO. This discussion deviates somewhat from the overall SDT analysis structure. Specifically, the Satellites and Interiors groups have been combined. Because of the different methods by which satellite surface science and interior geophysics are studied, it was decided to initially keep them separate in defining measurements, investigations, etc. Of course, interior processes are intimately linked to surface composition, geology, tectonics and morphology and, thus, we have combined them in the discussion that follows.

2.2.1 The Jovian Atmosphere

2.2.1.1 Background

Much is known about Jupiter's atmosphere from remote-sensing observations acquired by the Pioneer, Voyager, Hubble, Galileo, Cassini and New Horizons missions. Their remote-sensing observations of the atmosphere have been complemented recently by Earth-based measurements taking advantage of major

advances in the capabilities of modern telescopes and associated instrumentation. In addition, the experiments associated with the Galileo mission's direct probe into Jupiter's atmosphere provided a major advance in our understanding of the structure, composition and dynamics of the atmosphere. Unfortunately, it entered a region that is considered to be anomalously dry with a minimum of cloud opacity (Orton et al., 1996), and several of its results—particularly for volatiles such as NH_3 , H_2O and associated cloud layers—are not considered representative of the planet as a whole. Most of these results have been summarized by Young (2003), Taylor et al. (2004), West et al. (2004), Ingersoll et al. (2004), Moses et al. (2004), Harrington et al. (2004), Yelle and Miller (2004), and Vasavada and Showman (2005).

In 2016, the Juno mission is scheduled to begin microwave remote-sensing and gravitational mapping of Jupiter's deep atmosphere, results that can be linked to Earth-based observations using the JSO instruments. Nonetheless, many questions will remain after Juno about the overlying atmosphere. Juno will greatly boost our understanding of the depth of the jet streams, the small-scale structure of Jupiter's magnetic field, and the deep abundance of water vapor. However, in mapping the upper troposphere and stratosphere, Juno will have neither sufficient spatial resolution, wavelength coverage, nor temporal coverage to constrain the small-scale turbulent processes that transport momentum, heat, and tracers and that are therefore crucial in setting the basic structure of the jets, clouds, belts, zones, and vortices. JSO will provide the first high-resolution, broad-wavelength climate database that will have global coverage over a long-temporal baseline. For example, it remains unclear whether Jupiter's meteorology is primarily powered by deep convection or cloud-layer processes (e.g., thunderstorms, baroclinic instabilities, and other cloud-layer circulations), whether latent heat of water or hydrogen ortho-para conversion play a role in driving the circulation, or whether vertical waves are the principal source of energy driving the unexpectedly warm thermosphere temperature. We know little about the details

SCIENCE THEME	GOALS	OBJECTIVES	INVESTIGATIONS	INSTRUMENT TYPE																																
				Magnetometer	Plasma EPD	PWS	HIC	UV Imager	UV Imaging Spectrometer	UV Hyperspectral Imager	Spectrometer	UV Imaging Spectrometer	Med-Res Imager	Hi-Res Visible Imager (color)	Super Hi-Res Imager	Stereo Imager	VIS-NIR Hyperspectral Imager	VIS-NIR Imaging Spectrometer	Visible Spectrometer	Visible Polarimeter	IR Imager	IR Imaging Spectrometer	Mid-IR Spectrometer	Far-IR Imaging Radiometer	Thermal Imaging Spectrometer	Thermal Imager	Thermal Hyperspectral Imager	Radio	X-ray Imager	Sub-millimeter Sounder	Microwave Radiometer	LIDAR	Laser Altimeter	Ice Penetrating Radar	SAR	
Jupiter Atmosphere	Understand the processes that maintain the composition, structure and dynamics of the Jovian atmosphere as a Type Example of a Gas Giant Planet	Study the composition, structure, chemistry, and dynamics of Jupiter's atmosphere	Study atmospheric dynamics at scales ranging from less than one scale height to the planetary scale; Study the temperature and energy balance of the planet to improve our understanding of the relative roles of radiative solar radiative heating, winds and eddies in driving atmospheric circulation and convection; Study Jupiter's clouds and hazes; Study the composition and chemistry of Jupiter's atmosphere to understand sources and sinks, and dynamics from disequilibrium species; Study the auroral emissions and dynamic effects of the magnetosphere on the upper atmosphere	X		X		X						X					X	X					X	X	X	X	X	X	X					
		Study the structure and dynamics of the Jovian magnetosphere, including processes that generate Jupiter's aurora	Determine the coupling of magnetosphere/ionosphere/atmosphere					X												X								X	X							
		Characterize the spatial distribution and temporal variability of minor atmospheric species to understand Jupiter's origin and present state	Determine the bulk abundance of water in the deep atmosphere; Determine the 3-D concentrations of the condensable gases water and ammonia and disequilibrium species								X						X						X			X				X	X					
		Characterize Jupiter's clouds and hazes and the processes that maintain them	Determine the height, composition, optical thickness, and particle size distribution of clouds and hazes; Determine the concentrations of condensable atmospheric gases								X			X			X											X		X	X					
		Understand the processes that maintain the hot thermosphere	Characterize the vertical structure of the thermosphere and its spatial and temporal variability; Determine the properties and fluxes of vertically propagating waves; Characterize the atmosphere-magnetosphere interaction, including the contribution of aurorae to the thermal structure of the upper atmosphere; Determine the latitudinal variation of solar-energy absorption and thermal radiation								X			X											X		X			X	X					
		Study the temperature and energy balance of the planet to improve our understanding of the relative roles of internal and solar heating in controlling the structure and dynamics of the atmosphere	Determine the global, 3-D temperature structure from the thermosphere to the upper troposphere; Determine the dynamical contributions to the latitudinal energy transport											X			X									X	X			X						
		Determine the processes that maintain the jet streams, polar vortex circulations, large vortices, quasi-quadrennial oscillation, and planetary-scale waves such as the hot spots, equatorial plumes, and slowly moving thermal features	Determine the wind speeds, temperatures, and variability of atmospheric features; Determine the latitudinal momentum and heat fluxes of waves and eddies; Characterize the existence, horizontal wavelengths, and speeds of small-scale atmospheric waves to constrain the vertical stability structure (Brunt-Vaisala frequency) of the upper troposphere; Determine the concentrations of condensable atmospheric gases											X			X									X	X			X		X	X			
		Characterize the morphology, spatial distribution, and role of thunderstorms and small-scale waves and eddies in driving the large-scale circulation	Determine the occurrence frequency, locations, pressures, and temporal evolution of thunderstorms; Determine the occurrence frequency, locations, amplitude, spectrum, and depth of lightning; Determine the latitudinal momentum and heat fluxes of waves and eddies					X			X			X			X				X				X			X								
Magnetosphere	Understand the magnetospheric environments of Jupiter, its moons and their interactions	Understand the structure and circulation of the middle and upper atmosphere	Determine the global, 3-D temperature structure, radiative heating rates, and wind speeds from the thermosphere to the upper troposphere																					X	X		X									
		Establish internal structure of icy moons including presence and properties of putative conducting layers, measurement of higher harmonics and secular variations of Ganymede's magnetic field and set limits on intrinsic magnetic fields for Europa and Callisto	Investigate and confirm presence of a conducting layer at Ganymede and deeper conducting layers by monitoring steady and time-varying magnetic configurations; Investigate response of local magnetospheric plasma, energetic particle, and ionospheric environment at Ganymede to changing total and induced magnetic fields; Investigate and confirm presence of a conducting layer at Europa and Callisto and deeper conducting layers by monitoring steady and time-varying magnetic configurations; Investigate response of local magnetospheric plasma, energetic particle and ionospheric environment at Europa and Callisto to changing magnetic fields.	X	X																															
		Investigate the magnetic field, particle populations, and dynamics of Ganymede's magnetosphere.	Investigate the magnetopause to establish spatial distribution of reconnecting field lines and to characterize the spatial distribution and temporal distribution of reconnection, including possible intermittency of reconnection; Investigate Ganymede's magnetospheric structure, in particular the spatial structure and energy distributions of particle populations, including time variability in response to external Jovian magnetospheric perturbations; Investigate the generation of Ganymede's aurora; Investigate the modification of surface composition and structure on open vs. closed field line regions.	X	X	X		X			X					X											X									
		Determine the effect of the Jovian magnetosphere on the icy moons. Understand effects of the moons on the magnetosphere and Jupiter's auroral ionosphere.	Investigate the magnetic field, plasma, energetic particle, electromagnetic, and dust distribution in the Jovian magnetosphere, at the jovicentric orbits of the moons, including spatial and temporal variations; Investigate the changes of magnetospheric properties (the magnetic field, plasma, energetic particle, electromagnetic, and dust environments) in the near vicinity of the moons in order to establish effects of the magnetosphere on the moons and to characterize the moons as sources of gas and dust tori. Investigate effects of direct magnetospheric plasma, energetic particle, solar UV, and interplanetary dust interactions with the moon surfaces & atmospheres, and associated temporal variations; Investigate the coupling of the moons with the low altitude magnetosphere and the Jovian atmosphere, including formation processes of the satellite footprint and wake aurora in the Jovian polar atmosphere to understand the electrodynamic circuit connecting them	X	X	X					X				X												X									
		Understand the contributions of Io to the composition, and to the transient and periodic dynamics, of the Jovian magnetosphere	Investigate the relationship between temporal variations of volcanic activity on Io, the Io torus and the magnetosphere; Determine the composition of the plasma torus and iogenic neutrals.		X								X																							
Satellites	Understand the mechanisms responsible for formation of surface features and implications for geological history, evolution, and levels of current activity	Study the global dynamics of the Jovian magnetosphere including processes that generate the planetary aurora. Identify internal particle sources, acceleration processes, transport and loss processes that shape and drive the Jovian magnetosphere. Understand injection events in the inner magnetosphere.	Identify locations and activity levels for sources of major and minor plasma ions; Investigate internal transport acceleration and loss processes that shape and drive the Jovian magnetosphere and produce observed local time asymmetries; Investigate the phenomenon of energetic particle injection in the inner magnetosphere; Investigate magnetospheric and solar wind energy sources and dynamics for the Jupiter planetary aurora; Investigate the important boundary layers of the magnetosphere (Bow shock, magnetopause, plasma sheet boundary layer, high energy particle radiation belt boundaries, equatorial plasma disk)	X	X			X				X							X																	
		Io-Understand heat balance, tidal dissipation, relationship to volcanism, and the coupling of its thermal/orbital evolution to that of the icy satellites	I-Determine regional and global heat flow; I-Determine regional and global time-varying topography/shape											X							X															
		Io-Monitor Io's active volcanism for insight into its geological history and evolution, and the mechanisms of surface changes	I-Perform long-term and high-temporal-resolution monitoring of volcanic activity; I-Determine global distribution of volcanic activity and styles; I-Characterize crustal recycling of volatiles; I-Determine eruption temperatures (implications for superheating); I-Determine local, regional, and global topography					X						X		X	X															X	X			
		Io-Understand Io's surface geology, including the relationships between volcanism and tectonism, erosion and deposition processes	I-Determine distribution of geologic structures; I-Characterize distribution and transport of volatiles; I-Determine regional and global topography; I-Characterize morphology and structure of geologic features; I-Perform surface monitoring for change detection					X						X	X	X		X			X															
		Europa--Understand geologic history, potential for current activity, and the implications for Jupiter's satellite system	E-Determine distribution of geologic structures; E-Determine differences in crater morphology and cratering rates over time and between satellites; E-Constrain past non-synchronous rotation; E-Search for evidence of current activity through surface monitoring for change detection, thermal anomalies, plumes									X			X	X								X												
		Europa--Understand heat balance and tidal dissipation	E-Determine regional and global heat flow; E-Determine regional and global time-varying topography/shape														X							X									X			
		Europa--Understand the processes responsible for the observed geologic features and as analogs for surface geology of other icy satellites	E-Characterize morphology and structure of geologic features; E-Understand compositional variations and role in formation mechanisms; E-Determine regional and global topography and relationship to surface features; E-Determine the role of regolith formation and mass wasting in the modification of surface features													X	X	X				X											X	X		
		Europa--Search for evidence of recent activity (e.g., thermal anomalies; the presence of short-lived species; the absence of radiolytic products such as H2O2; chemical disequilibrium).	E-Search for changes in surface heat flow by mapping regolith thermal and thermophysical properties, and performing long-term monitoring of changes; E-Identify and map accumulation of radiation products and compounds which are unstable to radiation; Monitor long-term changes in abundances of these materials						X						X	X	X							X												
Europa--Characterize suitability of surface for future lander missions	E-Evaluate surface structure, characteristics and properties at local scales (spatial scales of centimeters)												X	X																						

SCIENCE THEME	GOALS	OBJECTIVES	INVESTIGATIONS	INSTRUMENT TYPE																															
				Magnetometer	Plasma EPD	PWS	HIC	UV Imager	UV Imaging Spectrometer	UV Hyperspectral Imager	Spectrometer	EUV Imaging Spectrometer	Med-Res Imager	Hi-Res Visible Imager (color)	Super Hi-Res Imager	Stereo Imager	VIS-NIR Hyperspectral Imager	VIS-NIR Imaging Spectrometer	Visible Spectrometer	Visible Polarimeter	IR Imager	IR Imaging Spectrometer	Mid-IR Spectrometer	Far-IR Imaging Radiometer	Thermal Imaging Spectrometer	Thermal Imager	Thermal Hyperspectral Imager	Radio	X-ray Imager	Sub-millimeter Sounder	Microwave Radiometer	LIDAR	Laser Altimeter	Ice Penetrating Radar	SAR
Satellites (continued)	Understand the mechanisms responsible for formation of surface features and implications for geological history, evolution, and levels of current activity (continued)	Ganymede--Understand geologic history, potential for current activity, and the implications for Jupiter's satellite system	G-Determine distribution of geologic structures; G-Determine differences in crater morphology and cratering rates over time and between satellites; G-Constrain whether non-synchronous rotation has occurred in the past; G-Search for evidence of current activity through surface monitoring for change detection, thermal anomalies, plumes						X			X		X	X	X																	X		
		Ganymede--Understand the processes responsible for the observed geologic features	G-Characterize morphology and structure of geologic features; G-Determine regional and global topography and relationship to surface features; G-Understand compositional variations and role in formation mechanisms; G-Determine the role of regolith formation and mass wasting in the modification of surface features									X	X		X						X												X	X	
		Ganymede--Understand heat balance and tidal dissipation	G-Determine regional and global time-varying topography/shape; G-Determine regional and global heat flow											X																					
		Callisto--Understand geologic history and implications for Jupiter's satellite system	C-Determine differences in crater morphology and cratering rates over time and between satellites; C-Identify and map distribution of other geologic structures											X	X																		X		
		Callisto--Understand the processes responsible for the observed geologic features	C-Characterize morphology and structure of geologic features; C-Determine the role of regolith formation and mass wasting in the modification of surface features; C-Determine regional and global topography and relationship to surface features; C-Understand compositional variations and role in formation mechanisms										X	X	X							X											X		
	Determine the surface compositions and implications for the origin, evolution and transport of surface materials	Io-Understand the volatile component of Io's crust and its behavior	I-Characterize volatile cycle: document composition, physical state, distribution, and transport of surface volatiles; I-Determine roles and rates of sublimation, sputtering, and radiation darkening						X								X					X													
		Io-Understand the silicate component of Io's crust	I-Identify compositions (including the source(s) of the 1.0- and 3.915-μm bands) and physical characteristics (e.g., particle size, porosity) of silicates; I-Determine distribution of silicates; I-Search for compositional variability among silicates												X		X																		
		Europa--Understand composition, physical characteristics, distribution, and evolution of surface materials	E-Identify bulk material compositions, grain size, porosity, crystallinity, and physical state; E-Map distributions of different materials, including radiolytic materials (e.g. SOx, O3, H2O2, OH, O2), and document variability over a range of timescales; E-Determine origin and evolution of non-ice materials, including the role of geologic processes; E-Characterize volatile cycle: document composition, physical state, distribution, and transport of surface volatiles, e.g. sublimation						X	X				X												X	X								
		Europa--Determine if and how material is interchanged between surface and ocean	E-Profiling of thermal, compositional, and structural horizons; E-Perform coordinated overlapping topographic, compositional, and thermal measurements to assess diagnostic geologic and compositional interrelationships						X					X	X		X									X	X						X		
		Ganymede--Understand composition, physical characteristics, distribution, and evolution of surface materials	G-Identify bulk material compositions, grain size, porosity, crystallinity, and physical state; G-Map distributions of different materials, including radiolytic materials (e.g. SOx, O3, H2O2, OH, O2), and document variability over a range of timescales; G-Determine origin and evolution of non-ice materials, including the role of geologic processes; G-Characterize volatile cycle: document composition, physical state, distribution, and transport of surface volatiles, e.g. sublimation						X	X							X									X									
		Callisto--Understand composition, physical characteristics, distribution, and evolution of surface materials	C-Identify bulk material compositions, grain size, porosity, crystallinity, and physical state; C-Map distributions of different materials, including radiolytic materials (e.g. SOx, O3, H2O2, OH, O2), and document variability over a range of timescales; C-Determine origin and evolution of non-ice materials, including the role of geologic processes; C-Characterize volatile cycle: document composition, physical state, distribution, and transport of surface volatiles, e.g. sublimation											X				X								X									
		Determine the compositions, origins, and evolution of the atmosphere, including transport of material throughout the Jovian system	Io-Understand the sources (volcanism, sublimation, surface sputtering) and sinks (freezing out, plasma pickup/sputtering, thermal escape) of atmospheric components	I-Determine column densities of atmospheric/plume species across the globe and document correlations with plumes, geologic features and local albedo variations; I-Perform long-term and high-temporal-resolution monitoring of atmosphere, plumes, limb-glow, and equatorial spots; I-Monitor Io torus; I-Determine the composition, distribution and physical characteristics (grain-size, crystallinity) of volatile materials on the surface, including SO2 frost										X					X																
	Io-Understand the temporal, spatial, and compositional variability of the atmosphere		I-Perform long-term and high-temporal-resolution monitoring; I-Determine column densities and compositions of atmospheric/plume species across the globe; I-Determine temperatures of gas in plumes and atmosphere											X				X				X													
	Europa--Understand the sources (sublimation, surface sputtering) and sinks (freezing out, plasma pickup/sputtering, thermal escape) of atmospheric components		E-Determine column densities of atmospheric species across the globe; E-Perform long-term and high-temporal-resolution monitoring of atmosphere in context of plasma bombardment and potential endogenic variations; E-Determine the composition, distribution and physical characteristics (grain-size, crystallinity, physical state) of volatile materials on the surface; E-Investigate sputtering processes at high latitudes as compared with lower latitudes						X			X	X				X																		
	Europa--Understand the temporal, spatial, and compositional variability of the atmosphere		E-Determine column densities, compositions and temperatures of atmospheric species across the globe											X				X																	
	Ganymede--Understand the sources (sublimation, surface sputtering) and sinks (freezing out, plasma pickup/sputtering, thermal escape) of atmospheric components		G-Determine column densities of atmospheric species across the globe; G-Perform long-term and high-temporal-resolution monitoring of atmosphere in context of magnetospheric variations; G-Determine the composition, distribution and physical characteristics (grain-size, crystallinity, physical state) of volatile materials on the surface; G-Investigate sputtering processes at high latitudes as compared with lower latitudes						X			X					X																		
	Ganymede--Understand the temporal, spatial, and compositional variability of the atmosphere		G-Determine column densities, compositions and temperatures of atmospheric species across the globe						X								X																		
	Callisto--Understand the sources (sublimation, surface sputtering) and sinks (freezing out, plasma pickup/sputtering, thermal escape) of atmospheric components		C-Determine column densities of atmospheric species across the globe; C-Perform long-term and high-temporal-resolution monitoring of atmosphere in context of plasma bombardment variations; C-Determine the composition, distribution and physical characteristics (grain-size, crystallinity, physical state) of volatile materials on the surface; C-Investigate sputtering processes at high latitudes as compared with lower latitudes						X			X					X																		
	Callisto--Understand the temporal, spatial, and compositional variability of the atmosphere		C-Determine column densities, compositions and temperatures of atmospheric species across the globe						X								X																		
	Determine how the components of the Jovian system operate and interact		Determine the structure and particle properties of the Jovian ring system	Determine the size distribution in each ring component; Determine the 3-D structure Jovian ring system; Determine the composition of the rings and embedded moons; Complete a comprehensive search for small inner moons of Jupiter, down to a size of 100 m																															
Interiors	Determine the interior structures and processes operating in the Galilean Satellites in relation to the formation and history of the Jupiter system and potential habitability of the moons.	Characterize the formation & chemical evolution of the Jupiter system	Place bounds on the orbital evolution of the satellites; Determine the sizes and states of the cores of the moons.	X																						X		X							
		Determine the presence and location of water within these moons.	Determine the extent of differentiation of the three icy satellites; Establish the presence of oceans; Characterize the extent and location of water (including brines) in 3D within Europa, Ganymede and Callisto; Determine the thickness of the ice layer for all Icy Satellites	X											X											X		X				X	X		
		Characterize the operation of magnetic dynamo processes in the Jovian system and their interaction with the surrounding magnetic field	Globally characterize Ganymede's intrinsic magnetic field and search for temporal variability in the field; Characterize the interaction of Ganymede's magnetosphere with Jupiter's magnetosphere; Monitoring of Jupiter's magnetic-field environment, with the goal of searching for changes in the intrinsic Jovian field and characterizing plasma processes in the Jovian magnetosphere	X	X		X	X																											
		Identify the dynamical processes that cause internal evolution and near-surface tectonics of all four moons	Determine the extent of differentiation of all four satellites; Characterize the near-surface tectonic and volcanic processes and their relation to interior processes	X											X	X		X								X		X				X	X	X	

of how trace constituents are distributed throughout Jupiter's atmosphere, particularly in the stratosphere where there is a dearth of information on any details of its thermal structure, composition and circulation. Little is known about the thermal or compositional structure of the atmosphere at spatial scales below some 3000 km, which is the limit of large Earth-based telescopes in the mid-infrared.

2.2.1.2 Goals and Objectives

High-resolution, long-term (multi-year) imaging of the clouds will revolutionize our understanding of Jupiter's cloud-layer meteorology. JSO will yield unprecedented insight into key questions such as: What are the relative roles of deep convection and cloud-layer turbulence in powering the jet streams that dominate Jupiter's dynamics? What are the sources of cloud-layer turbulence—thunderstorms, baroclinic instabilities, or other processes, how do they vary in latitude and time, and what is their role in driving the circulation? Do small eddies pump momentum up-gradient into the jets, thereby helping to maintain the jets, as has been tentatively observed at some latitudes on both Jupiter and Saturn from Cassini data (Salyk et al., 2006; Del Genio et al., 2007)? How do compact vortices (of which the Great Red Spot and Ovals are but the largest examples) interact with the jets—do they contribute to jet pumping, or do they instead rob energy from the jets (Vasavada and Showman, 2005; Showman et al., 2006)? What are the processes that determine the vertical structure of the atmosphere, including the fact that the jet streams decay with height in the upper troposphere and lower stratosphere? How do the cloud-layer dynamics change during Jupiter's well-known multiyear climate cycles, several of which have ~3–5-year periods that may allow them to be documented by the JSO mission? Global sampling that spans a wider time interval would provide a revolutionary database to use in assembling these sorts of climate statistics. JSO can address the above questions with high-resolution imaging that, via cloud tracking, allow the zonal (east-west) and meridional (north-south) velocities to be obtained. In addition to addressing the above questions, this database could allow measurement of the mean-meridional velocity

at the cloud level for the first time, which would provide very important constraints on the circulation (including the deep-vs.-shallow forcing issue). Observations at resolutions of 10 km are sufficient for these measurements, but they should be done at multiple levels (using, for example, continuum and methane and/or near-ultraviolet filters) in order to measure vertical shear. Lower resolution observations will miss some of the finest-scale features, such as individual convective clouds, but a higher priority is placed less on resolution than a consistent global set of measurements over time. Measurements of lightning in individual convective cells at this resolution will also constrain the energetics of the atmosphere at depth (Borucki and Williams 1986; Little et al., 1999).

Measurements of thermal emission and reflected sunlight ([Fig. 2.2-1](#)) will also characterize the detailed meridional variability of the energy balance of the atmosphere (continuing initial work begun with Voyager), and provide a detailed picture of stratospheric structure and dynamics. Coupled measurements of the velocity and temperature fields with resolutions of 100 km or better will measure the poleward eddy heat flux. Measurements of temperature profiles with 100 km or better resolution in the nadir direction and 25–50 km toward the limb will provide, using the thermal wind (shear) equation, the means to determine the variability of winds with altitude. A long-term database of such observations will, when coupled with modeling, allow an unprecedented look at the structure of stratospheric jets, the magnitude, geometry, and time-variation of the stratospheric mean-meridional circulation, and the mechanisms that cause jet acceleration and deceleration. They will also characterize the properties of a variety of thermal waves. This includes small-scale gravity and Rossby waves, the ~4-year cycle of low- and mid-latitude stratospheric waves known as the Quasi-Quadrennial Oscillation (QJO, Leovy et al., 1991), and the altitude dependence of slowly moving thermal waves which are uncorrelated with cloud features.

Stratospheric thermal monitoring could also allow the detection for the first time of the tides raised on Jupiter by the Galilean

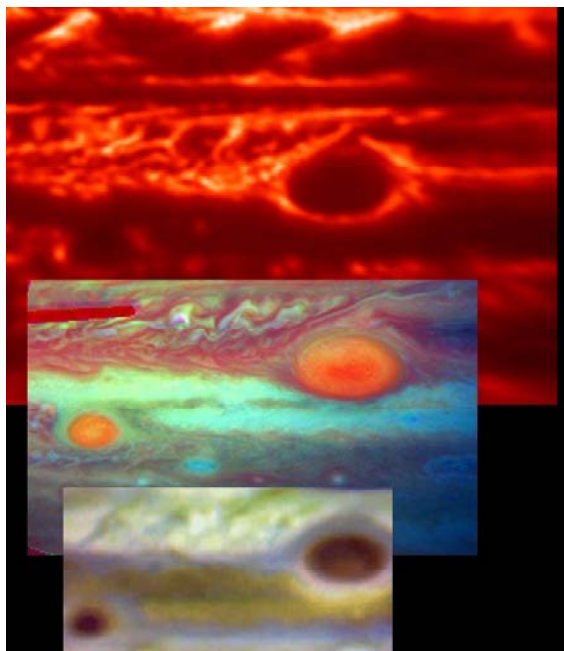


Figure 2.2-1. A portion of Jupiter in April 2006, showing the Great Red Spot and its new “Little Red Spot” revealed by remote sensing over a broad spectral range. Top: 5- μm thermal radiance showing temperatures of cloud tops, with warmest layers indicating thermal emission from 3–5 bar pressure levels (NASA Infrared Telescope Facility). Middle: 3-color (ultraviolet, green, infrared) composite of Hubble Space Telescope’s Advanced Camera for Surveys, showing regions of highest altitude clouds in red, medium-level clouds in light green and deepest clouds in dark blue/brown. Bottom: false color composite of 10.3- μm (NH_3 gas), 13.1- μm (400-mbar temperature), and 8.9- μm (NH_3 ice cloud) distribution (European Southern Observatory, Very Large Telescope).

satellites, particularly Io; it is the dissipation of these tides that drives the satellites into the Laplace resonance and thereby causes the intense volcanism and tectonism on Io and Europa (and potentially Ganymede in the past). Although the dissipation mechanism remains poorly understood, a favorable hypothesis suggests that the tides trigger global-scale waves that propagate upward into Jupiter’s stratosphere, where they deposit their energy. Binning of JSO’s climate database over the known tidal periods and wavelengths may allow the thermal signature of these waves to be detected and their amplitudes inferred; this could shed light on the

dissipation mechanisms and constrain Jupiter’s tidal Q value. This example, which illustrates the tight interrelationship among Jovian atmospheric dynamics, satellite orbital evolution, and satellite geology, underscores the powerful synergism enabled by a system observer like JSO.

Measurements of the distribution of water and para- H_2 (e.g., Gierasch et al., 2004) from the top of the troposphere to the several-bar level will constrain their roles in providing energy to Jupiter’s dynamical engine. Measurements of minor constituents that are condensates, such as water and ammonia, and disequilibrium chemicals (phosphine, carbon monoxide, arsine, silane, germane, and para- H_2) will provide tracers of vertical motions in the atmosphere over different vertical provenances.

Measurement of the vertical distributions of stratospheric constituents, such as the hydrocarbons, recombinant products of methane photolysis, will provide fundamental constraints on atmospheric chemistry. Their vertical and meridional distribution will determine the rate of transport in the stratosphere, as well as their role in radiative heating and seasonal forcing (Moses et al., 2005). Measurements of both tropospheric and stratospheric thermal and abundance properties near the pole over time will determine the relative roles of dynamics and seasonally-forced radiation in maintaining Jupiter’s cold and hazy polar vortices (Vincent et al., 2000; Porco et al., 2003). Measurement of H_2O , CO and CO_2 as a function of latitude and time will constrain the external source of oxygen, most probably water ice, delivered to the upper stratosphere, distinguishing among comets, interplanetary dust, as well as ring and satellite systems as the origin. A merely slow degradation of these abundances would, on the other hand, provide weight to the argument that they were all delivered at the time of the Comet Shoemaker-Levy 9 fragment impacts. The characterization of the altitude and lateral distribution of photochemical hazes will also provide fundamental clues to their origin and the meridional dependence of transport in the stratosphere. Their distribution is important to our understanding of the details of solar energy deposition in the atmosphere.

Global and regional properties of clouds and their lifetimes will also provide strong constraints on dynamical processes in Jupiter's atmosphere. Correlation between cloud properties (size, color and albedo) and their changes over time with changes of environmental temperatures and constituent abundances will supply for the first time sufficient evidence to begin to determine what types of gas abundance or phase changes are responsible for major changes in Jupiter's cloud properties. These afford a fundamental clue for the origin of their various colors. Up to this point, only changes in major properties have been observable, such as the development of Jupiter's newest red spot (e.g., Simon-Miller et al., 2006). The detection of ammonia, ammonium hydrosulfate and water ice signatures will provide significant clues to the size and strength of significant updraft regions in the atmosphere. Resolutions as high as 10 km provide the capability to examine individual storms (Porco et al., 2003).

The sharp decline of hydrocarbon abundances at the top of the stratosphere has been cited as the reason for a sharp rise of temperatures with height. But Jupiter's thermosphere is hotter than can be explained by radiative equilibrium. A primary goal is to determine the source of its heating. A leading candidate is transfer of energy by upwelling waves (Yelle et al., 1996). JSO will measure thermospheric temperatures and energy deposition by waves simultaneously. Other credible heat sources for the upper atmosphere are (1) heating by energetic magnetospheric particles (Ajello et al., 2005; Bhattacharya et al., 2005), and (2) joule dissipation of auroral currents, though the latter is limited to high latitudes (Yelle and Miller, 2004). It is difficult to measure the temperature of the atmosphere at these altitudes by thermal emission, and measurements by radio and stellar occultations will be important, both for characterizing the thermospheric temperature profile as well as upwelling waves.

Another major candidate for synoptic observations making a major advance in our understanding is the area of interactions between the charged and neutral atmosphere. Aurorae in the ultraviolet, visible and near infrared are well documented (Clarke et al., 2004), as are X-ray emissions (Elsner et al.,

2005a,b) and auroral-related heating in the polar stratosphere. We do not know what accounts for the detailed spatial structure observed in the three main auroral regions (i.e., the satellite flux tube footprints and associated tails, the main oval resulting from co-rotation breakdown and its kinks, and the region inside the main ovals where the flares occur). Nor do we know how and where these regions map to source regions in the magnetosphere (i.e., do the flares map to pulsating reconnection regions at the dayside magnetopause as has been suggested, or to somewhere down the flanks or in the magnetotail)? What are the precipitating particles in each region and how (and where) are they accelerated (i.e., electrons that produce the UV and H_3^+ auroras versus O and S ions that produce the x-ray aurora)? What accounts for the major timescales seen for variability in the different regions (i.e., very rapid changes (10–100 sec) in the polar region flares, hours in the dawn storms of the main oval, and years or longer in the basic shape of the main oval)? How are the auroras connected with the thermal infrared hot spots? Is auroral heating just conducted down to the homopause where it is radiated away by hydrocarbons? If so, what is the timescale and would there be a phase lag with respect to the short-term variability in emissions? How are the auroral aerosols formed? Synoptic observations of these phenomena are needed in the X-ray, ultraviolet, visible (night side), near infrared (for H_3^+ auroras) and mid-infrared (methane and other hydrocarbon enhanced emission) together with the magnetic field to begin making progress on these questions.

Finally, JSO's five year long stay in the Jovian system will allow it to address the longer-term, temporal variability of these atmospheric phenomena.

2.2.2 The Jovian Magnetosphere

2.2.2.1 Background

Among planetary magnetospheres, Jupiter's magnetosphere is unique because of its vast spatial extent (Khurana et al., 2004; Cooper and Khurana, 2005) and its strong internal magnetic field. At distances beyond $\sim 20 R_J$, the field is distended by a rapidly rotating heavy ion population and the rotating system carves a gargantuan cavity out of the solar wind. The size of the system is emphasized

here because it establishes both the spatial and the temporal scales (many R_J and hours to days) of the internal dynamics. It takes 5 hours for the solar wind to flow almost 100 R_J from the nose of the magnetosphere to the terminator and days for it to flow along the lengthy magnetotail.

Jupiter's magnetosphere differs from Earth's not only because of the scales relevant to dynamical processes but also because the solar wind is not the dominant controlling factor. Of at least equal importance are internally driven instabilities that must be characterized if one is to achieve a physical understanding of the magnetosphere. For example, in the magnetotail region, events with some of the same magnetic and plasma signatures associated with substorms at Earth have been observed, but it remains uncertain whether they are driven by reconnection with the solar wind or are internally controlled.

Closer to the orbits of the Galilean moons, the properties of the magnetosphere are sensitive to local plasma sources and to coupling with Jupiter's upper atmosphere. The Io torus is presumed to be the dominant plasma ion and neutral atom source (Thomas et al., 2004; Takahashi et al., 2005), but other moons, e.g., Europa for Na (Leblanc et al., 2005), may contribute distinctively through atmospheric and surface interactions (Johnson et al., 2004) to minor ion and isotopic composition of the local magnetosphere. The Galileo spacecraft found significant changes from month to month in field and plasma properties as it passed through roughly the same magnetospheric regions. It remains uncertain whether such changes arise from changes in external conditions or time-varying sources of plasma such as might be caused by changing volcanic activity at Io.

Local perturbations of the field and plasma environments by the moons are of major interest in the search for induced magnetic fields (Kivelson et al., 2004) and for interpretation of surface composition data in terms of magnetospheric particle interactions and resultant changes in surface chemistry (Johnson et al., 2004). Energetic particles are accelerated with the magnetosphere and interact both with the moons (Johnson et al., 2004) and the spacecraft in ways that drive the science objectives. Decreasing electron and

other particle fluxes between the orbits of Europa and Ganymede (Jun et al., 2005), and reduced fluxes within the Ganymede magnetic field and at Callisto (Cooper et al., 2001), changes the moon surface interactions and also impacts spacecraft operations. Dispersive signatures of impulsive injection of energetic particles (Krupp et al., 2004) have been observed both in Jupiter's magnetosphere and Saturn's. The mechanisms of particle injection, acceleration, transport, and loss require much better understanding to model these interactions and dynamic processes.

2.2.2.2 Goals and Objectives

Despite the invaluable data acquired by the various spacecraft that have explored the Jupiter system, much remains to be learned about Jupiter's magnetosphere, largely because of the extended time in orbit required to "catch" activity. Long dwells at different radial distances, local times, and latitudes within the magnetosphere are essential to acquire the data needed to understand the processes through which plasma is transported and accelerated in our only example of a vast, rotation-dominated magnetosphere. JSO will spend years orbiting the planet, and will be instrumented to monitor magnetospheric dynamics at changing local times and radial distances in the near equatorial regions and will provide the measurements needed to characterize the system.

A key challenge is to assess whether the solar wind contributes significantly to the transport and acceleration of Jovian magnetospheric plasma. We know that solar wind shocks modify aurorae and radio emissions, but the mechanisms that produce the observed effects are uncertain. Some light can be cast on this matter by monitoring changes in Jupiter's polar aurorae during initial approach to the Jupiter system while JSO is still making measurements in the solar wind. In Jupiter's inner magnetosphere, transport is thought to be dominated by flux tube interchange (whose existence has been established but whose properties remain unexamined), but additional processes must be acting to produce the very dynamic energetic particle injection events that were identified in the Galileo particle data.

The JSO tour design offers many opportunities for in-situ measurements in the

magnetotail region, where events with some of the features expected for reconnection have been observed. As noted above, it remains uncertain to what degree the reconnection is internally controlled. Even the spatial distribution of reconnection events has not been fully established and JSO will fill in some of the gaps. Global changes in the magnetospheric configuration can be inferred from in-situ measurements of shifts in position for boundary layers such as the equatorial plasma sheet, trapping boundaries for energetic particles, and the Jovian magnetopause, and from remote monitoring of Jovian auroral structures. Long-term monitoring with JSO in-situ and remote measurements will provide abundant opportunities to investigate global responses of the Jovian magnetosphere to changing conditions.

The JSO mission, designed to monitor volcanoes while recording magnetospheric behavior, should provide insight into the source of internally driven long-period temporal variations. Europa has been identified from earth-based telescopic observations as a net source of sodium gas, and more sensitive in-situ and remote compositional measurements with JSO can determine the contributions of Io, Europa, and potentially other moons to minor species abundances of the magnetospheric plasma. With sufficiently capable plasma and energetic particle instrumentation on JSO, it will be possible for the first time in the Jovian system to measure the isotopic markers of plasma origin for differing isotopic fractionations from solar wind, Jupiter atmospheric, Io volcanic, and moon sputtering sources. Near the moon sources, these isotopic fractionation measurements could probe internal geochemical processes, including limits on astrobiological contributions in the case of Europa.

Although JSO will encounter the farthest reaches of the Jovian system, beyond 100 R_J only on its early orbits, the field and plasma dynamics measured at these large distances will give evidence of the processes through which plasma introduced into the system near Io is lost to the solar wind. Plasma instrumentation capable of measuring plasma flows and the anisotropic pressure will be examined for evidence of the nature of plasma on reconnecting flux tubes in order to assess

the relative importance of internal and external drivers of magnetotail reconnection. Evidence that flux tubes participating in reconnection are linked to the solar wind would suggest some external control, but if the plasma is found to be that of the middle magnetosphere, it will suggest that the outward pressure of centrifugally accelerated plasma dominates the dynamics.

Inside of 50 R_J , where JSO will spend most of its time, lies a region that is less dynamic than the more distant magnetosphere but well suited for monitoring long term temporal variations of the system. Most JSO orbits will remain in this region during the Jupiter phase of the mission. Fields and particle instrumentation in uninterrupted operation can detect significant changes on time scales ranging from minutes to days. Long-term variations can be monitored in conjunction with changing solar wind properties (partially reflected in Jovian auroral activity) and with changes in volcanic activity at Io (monitored with spacecraft imaging) to establish the dominant sources of variability, and to clarify further how the magnetosphere operates. The long term monitoring capability is also well suited to unraveling the mystery of the injection events.

Large-scale spatial variations in plasma and energetic particle fluxes and abundances are best surveyed during passes through the inner and outer magnetosphere. By mapping the particle flux, magnetic field, and ephemeris data into appropriate magnetospheric coordinates JSO can determine the most likely source regions for specific ion species and the parameter for diffusive acceleration and transport from these sources. Compositional analysis for trace element species, and rare isotopes of major species, can be carried out with the maximal ion abundance statistics afforded during these periods. Since magnetospheric corotation and dispersive drifts rapidly spread the ionized species escaping from the moons in longitude, even distant crossings of the moon drift shells can be used to investigate moon contributions to magnetospheric composition.

Close encounters with all four Galilean moons provide the opportunity to compare interactions between each moon and its local magnetospheric environment before the

mission focus shifts primarily to Ganymede and remote observations from that moon's locale. Whereas the magnetospheric cruise segments described above survey the jovian orbital environments of the moons, the close flybys reveal the perturbed magnetospheric and near-surface environments in the immediate vicinity of each moon. Multiple flybys of each moon can variously probe the upstream, flank, and wake regions with respect to corotational plasma flow and the polar regions. For the icy moons these flybys expand the coverage of the induced and intrinsic magnetic field perturbations from the initial measurements of Galileo. Higher capability instrumentation for plasma composition will enable direct measurements of pickup ions from ionization of escaping atmospheric and sputtered surface neutral atoms. The pickup ion abundances can be used to infer surface composition, in the case of surface sputtering from identifiable locations correlated to surface geologic structures also analyzed by remote sensing instrumentation.

JSO will thoroughly characterize the auroral and magnetospheric activity before and after each flyby, so that specific variances from other flybys can be understood in the context of ongoing changes in global activity. Transients in Io torus activity will change ion loading of the magnetospheric plasma sheet with anticipated effects on the local magnetospheric environment for a moon flyby. Multiple flybys of Ganymede in advance of capture into orbit around it will characterize the variability of energetic particle fluxes that may be of concern for subsequent orbital operations.

2.2.3 Io Torus

2.2.3.1 Background

Io's lower SO₂ and S₂ atmosphere is derived ultimately from its volcanoes. The upper atmosphere is composed primarily of S and O, products of the lower atmosphere. Exospheric ions and atmospheric neutrals escape; neutrals are ionized through charge exchange and electron impact. Once ionized, the ions are picked up by the corotating planetary magnetic field to form a torus that completely surrounds Jupiter (Saur et

al., 2004; Thomas et al., 2004) and are radially transported and accelerated to higher energies (Krupp et al., 2004) within the magnetosphere of Jupiter.

The Jupiter-Io system is complex and interconnected (**Figure 2.2-2**). The mass loss from Io is generally thought to be 1 ton/sec. This is a large amount of material that affects the Jupiter system to varying degrees. Approximately two-thirds of the mass removed from Io is ejected out of the Jovian system via charge-exchange processes on short timescales. For the remaining material, the mean residence time for torus ions is ~25-80 days. Radial transport feeds heavy ions produced near Io into the rest of Jupiter's magnetosphere and most of the phenomena exhibited by Jupiter's magnetosphere depend on these ions. Iogenic ions affect the other icy satellites (especially Europa) by surface sputtering deposition into the surfaces (Johnson et al., 2004). This expansion of plasma into the middle magnetosphere is a significant mass loss process for the torus. Charge exchange (and subsequent ballistic escape) is also an important mechanism and leads to an observable cloud of neutrals which extends out to more than 400 R_J from Jupiter. Neutral species in the torus (Thomas et al., 2004; Takahashi et al., 2005) are generally

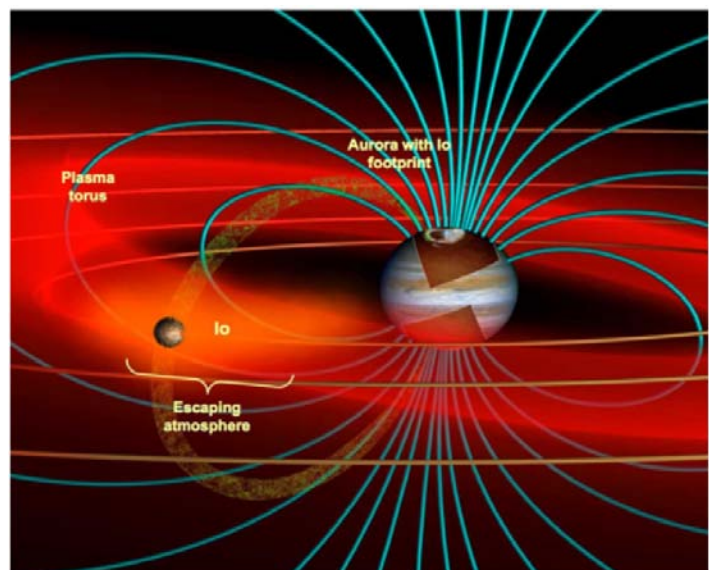


Figure 2.2-2. Diagram showing the complex interaction between Io and the Jupiter magnetosphere. Specific components for study are the Io Torus, Io flux tube and its footprint on Jupiter (J. Spencer, SWRI).

present in a cloud that does not extend all the way around Jupiter but is focused on Io and stretches ahead of Io in its orbit, largely constrained to the inner part of the orbit. Electron impact ionization and charge exchange with torus plasma are significant loss processes on timescales of a few hours. As a result, the observed distributions of the neutral clouds are dependent upon the spatial distribution of the torus plasma. The amount of ionization that takes place near Io compared with distant ionization is an outstanding question. Processes that are not well understood distribute the plasma radially and lead to a non-uniform spatial distribution of plasma, both in density and temperature. Finding the cause of the longitudinal structure within the torus is an important goal.

Remote observations of torus emissions reveal that the structure is variable on many different timescales. Most of the processes producing this variability are poorly understood, although there are clues to their nature. Some are probably related to features of Jupiter's magnetosphere while others are almost certainly related to variations in the source. Given that the highly time-variable volcanic activity may contribute significantly to Io's atmospheric structure, the latter might appear obvious. However, it has proved difficult to show a clear, unambiguous link between the two phenomena. Timescale variations on the order of < 10 hr have been suggested for the torus, possibly as short as 5 hr.

Many of the significant Io torus measurements have come from the Pioneer 10 UV instrument, the Voyager Plasma Science (PLS) and UVS instruments, HST, EUVE, Galileo UVS, and Cassini UVIS. These are important observations, but are essentially snapshots of a dynamic system. JSO will play a key role in its long-term studies. Correlations among the following phenomena can be made through long-term monitoring: auroral intensity (footprint) (especially through FUV measurements), torus brightness (especially through EUV-FUV measurements), and Io volcanic activity (especially through IR measurements). The Cassini flyby revealed tantalizing correlated variabilities in these phenomena (namely between auroral and torus brightnesses), but lacked the resolution and

coverage needed to identify causes and effects (Ajello et al., 2005; Clarke et al., 2004; Pryor et al., 2005).

2.2.3.2 Goals and Objectives

Major issues and questions exist to be studied by JSO. For instance, the influence of Io's atmosphere on the system isn't clear: do volcanic gases translate directly from the atmosphere to the torus, or does the atmosphere act as a buffer between the volcanoes and the rest of the system? The plasma torus is variable on temporal and spatial scales—are changes in the torus ultimately driven by volcanic and atmospheric variability? Does the plasma torus in turn affect Io's atmosphere (e.g., by sputtering)? How does plasma production depend on Io's volcanic activity? Are Jovian magnetospheric processes driven primarily by internal (Io) or external (solar wind) forces? Finding the cause of the longitudinal structure within the torus is also an important goal.

JSO observations at EUV (60–110 nm), FUV (110–190 nm) and NUV (190–350 nm) wavelengths are critical for studying the torus and Io's atmosphere, as well as Jupiter's aurorae and the Io footprint. Infrared measurements of Io are significant for correlative studies with volcanic activity. Io torus measurements will ideally be made on scales of $0.1 R_J$ (~7150 km); day-long campaigns will take place (ideally every week or so, throughout the mission) wherein torus measurements are made every 1–2 hours, interleaved with Io measurements and auroral observations.

2.2.4 Galilean Satellites—Surfaces and Interiors

Four goals are defined for surveying the surface composition and geology of the satellites of the Jovian system. These will be accomplished through multiple flybys, distant observations during the main Jovian tour, and orbit around Ganymede:

- Understand the mechanisms responsible for formation of surface features and implications for geological evolution and levels of current activity.
- Determine the surface compositions and implications for the origin, evolution and transport of surface materials.
- Determine the compositions, origins, and evolution of the atmosphere, including

transport of material throughout the Jovian system.

- Determine how the components of the Jovian system operate and interact.

Interior science focuses on acquiring data that will aid in understanding the large-scale structure of each satellite, processes occurring in the near-surface, and the manifestation of interior activity in the surface geology. A single overarching goal is established for JSO interior science:

- Determine the interior structures and processes operating in the Galilean Satellites in relation to the formation and history of the Jupiter system and potential habitability of the moons.

Voyager and Galileo have provided our primary knowledge of satellite geophysics (see reviews in, for example, Showman and Malhotra, 1997; Schubert et al., 1986, 2004; and Kivelson et al., 2004). Close Galileo flybys past Io, Europa, Ganymede and Callisto provided observational constraints on second-degree gravitational harmonics, which, with the assumption of hydrostatic equilibrium, allowed the moments of inertia of each body to be inferred. Magnetometer observations allowed inferences on the existence of internal oceans and on the interactions of each moon with the surrounding Jovian magnetosphere and its plasma. Detailed imaging of portions of each surface provided constraints on near-surface tectonics.

Our understanding of the subsurface structure and surface compositions of the Jovian moons are affected by magnetospheric interactions. Jupiter's rotation imposes periodic changes of the Jovian magnetic field at Europa, Ganymede, and Callisto that induce electrical currents within any conductive subsurface layers and perturb the magnetic fields near these moons (Kivelson et al., 2004). Long-term measurements of the field are required to separate oceanic induced fields from other sources of magnetic perturbations near Ganymede. Records of the magnetic field perturbations over many Jovian rotation periods will also probe the deeper interior conducting structures of Ganymede. These data will also facilitate attempts to detect possible secular change in the internal dynamo. Surface composition on all three icy Galilean moons is apparently influenced by

magnetospheric interaction (Johnson et al., 2004), since sulfate hydrates concentrate on the trailing hemisphere of Europa (which is exposed to the flow of plasma), surface reflectivity changes across the open/closed magnetic field boundary on Ganymede, and CO₂ concentrates on the trailing hemisphere of Callisto. Since Io volcanic gas emissions and Io torus processes are the dominant source of magnetospheric plasma, correlative monitoring of Io and torus activity is essential to modeling of the moon-magnetosphere interactions.

2.2.4.1 Io

2.2.4.1.1 Background

Io, the innermost of the large Galilean satellites of Jupiter, is a rocky body roughly 1,820 km in radius. It has an average density of 3,530 kg m⁻³, suggesting a primarily silicate, structurally differentiated interior (McEwen et al., 2004). A 4:2:1 Laplace resonance between Io, Europa, and Ganymede as they orbit massive Jupiter maintains slight eccentricities in their orbits, leading to tidal flexing of the order of ~100 m at Io's surface, generating the heat that powers Io's global volcanism (Yoder and Peale, 1981). Galileo's equatorial and polar flybys of Io support the inference that Io's degree-2 static response is in hydrostatic equilibrium (Anderson et al., 2001); this state is also supported by the satellite's tidally and rotationally distorted shape. Nash et al. (1986), Showman and Malhotra (1997), McEwen et al. (2004), Lopes and Williams (2005), and Moore et al. (2007) provide thorough reviews of our understanding of Io.

Galileo data indicate the presence of extensive moon-plasma interactions near Io but appear to rule out a strong intrinsic dipolar magnetic field at Io. Io's moment of inertia inferred from Galileo, $0.377 MR^2$ (where M and R are the satellite mass and mean radius, respectively), suggests that the satellite is differentiated into a metallic core and silicate mantle (Anderson et al., 2001). Io is thought to have a large Fe-FeS core, whose radius is slightly less than half that of Io and whose mass is 20% of the moon. The evident lack of an intrinsic magnetic field despite two polar flybys by the Galileo spacecraft suggests that Io's silicate mantle is currently experiencing sufficiently strong tidal heating to prevent cooling and therefore convective dynamo

activity in Io's putative iron core (Weinbruch and Spohn 1995).

The mantle of Io appears to undergo a high degree of partial melting (~5-20% molten; Moore, 2001) that produces mafic to ultramafic lavas dominated by Mg-rich orthopyroxene, suggesting a compositionally undifferentiated mantle. Silicate volcanism appears to be dominant at most of the observed hot spots, although secondary sulfur volcanism may be important in some areas. The high heat flux inferred from long-term thermal monitoring of Io exceeds 2 W/m^2 and indicates that Io is by far the most volcanically active solid body in the solar system (Nash et al., 1986; Veeder et al., 2004; McEwen et al., 2004; Lopes and Spencer, 2007) (**Fig. 2.2-3**). Despite the high heat flux, the existence of numerous mountains up to 18 km tall indicates that the lithosphere is at least 20–30 km thick, rigid and cold away from volcanic heat sources, and composed mostly of silicates with some sulfur and sulfur dioxide (SO_2) components (e.g., Carr et al., 1998; Schenk and Bulmer, 1998; Turtle et al., 2001; Jaeger et al., 2003). The thick lithosphere can only conduct a small fraction of Io's total heat flux, and several researchers have suggested that Io loses its heat primarily via magmatic transport through the lithosphere (O'Reilly and Davies, 1981; Carr et al., 1998; Moore, 2001). Io's rapid resurfacing rate (Io has no known impact craters) requires a gradual subsidence of its lithosphere, which could cause a compressional lithospheric environment that may help to explain the formation of Io's numerous mountains (Schenk and Bulmer, 1998).

The surface of Io is composed of five primary types of material: bright plains, paterae (caldera-like, volcano-tectonic depressions), lava flow fields, massive tectonic mountains, and diffuse deposits (of five different varieties). No impact craters of any size have been identified, attesting to the dynamic nature of Io's volcanism, which results in rapid resurfacing (Geissler, 2003). Silicate, sulfur, and sulfur dioxide materials interact in a complex and intimate way, resulting in three major eruption styles similar to: a) Hawaiian compound inflationary flow fields, b) major, explosive, high-temperature outbursts, and c) periodically overturning lava

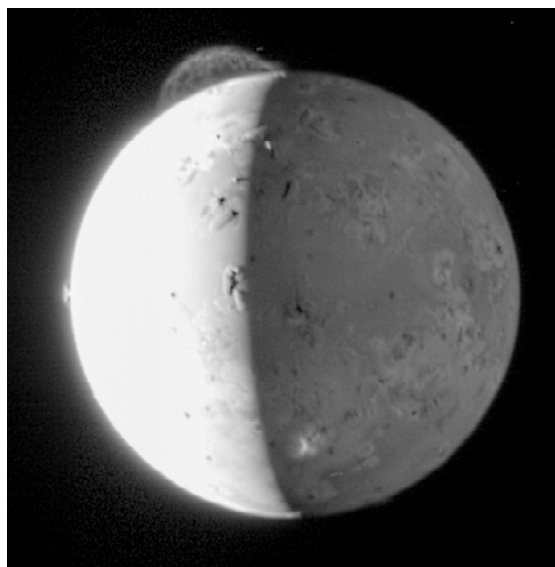


Figure 2.2-3. Volcanic plumes on Io, as imaged by the LORRI instrument on NASA's New Horizons spacecraft on February 28, 2007, at a distance of 2.5 million kilometers (35 R_J). Top: 290-kilometer high plume from the polar volcano Tvashtar, showing detailed structure; left: 60-kilometer symmetrical plume from the volcano Prometheus, which has been active during all spacecraft flybys. Long-term observations by JSO, from much closer to Io, will reveal more information about Io's active volcanism. Credit: NASA/JHU/APL, Planetary Photojournal PIA09248.

lakes. There are also two major varieties of volcanic plumes, Pelean, or central vent plumes, and Promethean, or flow front plumes. Key discoveries during the Galileo era include: 1) the detection of high-temperature volcanism ($\geq 1300^\circ\text{C}$, consistent with mildly superheated mafic to slightly ultramafic magmas); 2) the detection of both S_2 and SO_2 gas in Ionian plumes; 3) a relationship between mountains and paterae, namely that many paterae may be formed as magma preferentially ascends along tectonic faults associated with mountain building; 4) lack of detection of an intrinsic magnetic field, and 5) a new estimate of global heat flow. Volcanism on Io feeds a patchy and variable atmosphere, in which sulfur, oxygen, and sodium become ionized to form Io's plasma torus, neutral clouds, and aurorae. Sublimation of SO_2 frost is also a source of Io's thin atmosphere; the relative contributions of sublimation and volcanism to the

atmosphere are not well understood. Electrical current flows between Io and Jupiter and produces auroral footprints in the Jovian atmosphere. Near the ionospheric end of the Io flux tube, accelerated electrons interact with the Jovian magnetic field and generate decametric radio emissions (Lopes and Williams, 2005).

There is an apparent paradox between Io's potentially ultramafic volcanism (suggestive of a primitive, compositionally undifferentiated mantle) and the widespread intensity of the volcanism on Io (which, at the current rate, would have produced a volume of lava ~40 times the volume of Io over the last 4.5 Ga, resulting in differentiation and consequent eruption of more silicic materials). The resolution of this paradox requires either that Io only recently (geologically) entered the tidal resonance and became volcanically active, or that recycling of Io's lithosphere is sufficient to prevent extreme differentiation (McEwen et al., 2004).

2.2.4.1.2 *Goals and Objectives*

The volcanism paradox described above is one of many important issues about Io that will be addressed by JSO. The overall science goals for Io include understanding the mechanisms responsible for the formation of its surface features, determining the surface compositions and the implications for the origin, evolution and transport of surface materials; and determining the compositional and temporal evolution of the Ionian atmosphere. JSO will accomplish these goals through a variety of measurements focused on these science objectives: a) Understanding Io's heat balance and tidal dissipation; b) Monitoring Io's active volcanism for insight into the mechanisms of surface changes; c) Understanding Io's surface geology, including the relationships among volcanism, tectonism, erosion and deposition processes; d) Understanding the silicate and volatile components of Io's crust; and e) Understanding the sources and sinks of atmospheric components and their temporal, spatial, and compositional variability. Long-term studies from a spacecraft in the Jovian system will help to address current questions about the origin and geologic evolution of Io. Since this moon is a dominant source of plasma for the Jovian magnetosphere,

measurements of trace ion composition in the Io torus and throughout the magnetosphere may reveal more details of the internal composition.

The Galileo mission has provided strong evidence that Io is differentiated into a metallic core and silicate mantle. Additional gravity data that would be acquired by tracking of the JSO spacecraft on flybys of Io will place more stringent constraints on interior structure. New discoveries are likely, e.g., gravity anomalies similar to that detected by Galileo on a Ganymede flyby. Determination of Io's pole position and changes in the location of the pole with time might be possible with high resolution imaging; these observations would also constrain the satellite's shape and, thus, internal structure. It might also be possible to determine any secular acceleration of Io in its orbit through the combination of Doppler tracking and high-resolution imaging. Knowledge of whether Io's orbit is expanding or shrinking would be of enormous significance in understanding the satellite's evolution, as well as that of the system. Heat flow determinations through thermal imaging by JSO would augment the Earth-based observations and place important constraints on theories of tidal dissipation in Io and on the satellite's internal structure and thermal and orbital evolution and those of its sibling Galilean satellites.

2.2.4.2 *Europa*

2.2.4.2.1 *Background*

Europa is a primarily silicate body, with a mean density of about 3000 kg/m^3 . Galileo gravity data indicate a moment of inertia of 0.346 MR^2 (Anderson et al., 1998, Schubert et al., 2004). Three-layer models constrained by plausible compositions suggest that Europa contains an outermost H_2O layer 100–200 km thick, an intermediate silicate rock mantle, and a metallic iron core. The most plausible models have a metallic core of 30–50% of Europa's radius, and a silicate mantle density of $3000\text{--}3500 \text{ kg/m}^3$ (Anderson et al., 1998; Schubert et al., 2004).

Magnetometer data from several Galileo flybys provide evidence that Europa exhibits an inductive magnetic response to Jupiter's time-variable magnetic field; this response is most easily explained by the presence of a

conductive salty ocean within Europa's interior (Kivelson et al., 2000, 2004; Zimmer et al., 2000). In contrast, the conductivity of solid ice and rock is too low, a hypothetical metallic core is too far below the surface, and the European ionosphere is insufficiently conductive to explain the data. The inferred induction response indicates that the ocean must be within ~200 km of the surface, and if it has the salinity of Earth's oceans it must be at least ~10 km thick (Zimmer et al., 2000).

Studies of Europa's long-term evolution, morphology of craters on its surface, and formation of specific landforms suggest that Europa's ice shell is between 10 and 30 km thick, although values as small as ~3 km and >50 km have also been proposed (Greeley et al., 2004b; Pappalardo et al., 1999). The paucity of impact craters indicates a relatively young surface with a nominal age as low as 50 million years (Zahnle et al., 2003); it is therefore possible that Europa remains geologically active today (Schenk et al., 2004).

Numerous types of endogenic geologic surface features are present on Europa (see reviews in Malin and Pieri 1986 and Greeley et al. 2004b). Dark, mottled terrain dominates the trailing hemisphere and is present elsewhere as well. Ridges are the most ubiquitous landform seen at Europa; they most commonly occur as double ridges. Their lengths vary and can extend up to many hundreds of kilometers. The origin of the double ridges is under debate and several models of their formation have been proposed, each of which have different implications for the presence and distribution of liquid water. Wedge-shaped pull-apart bands and strike-slip faults provide evidence about the original configuration of the ice before surface movement. Lenticulae, along with larger chaos regions and smooth dark plains, make up Europa's mottled terrain (Figure 2.2-4) and

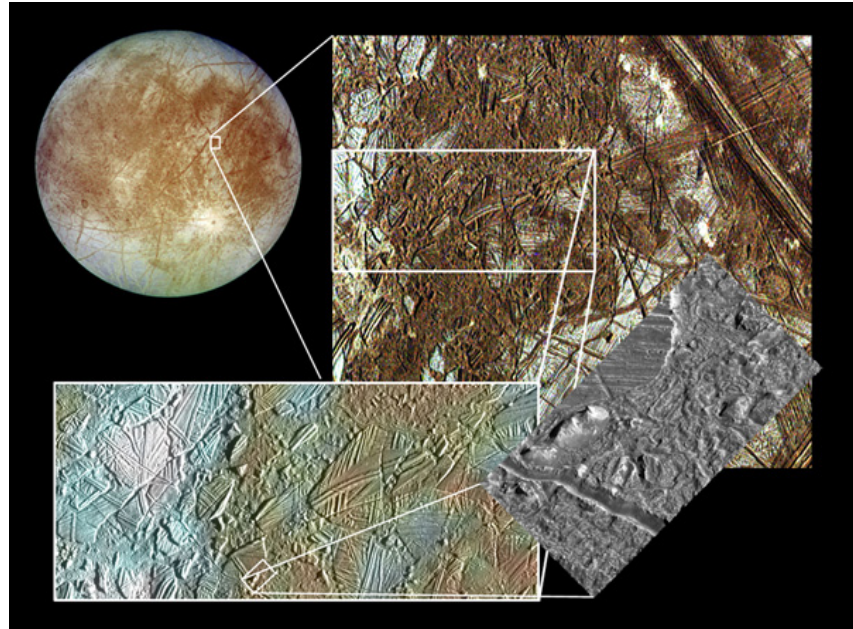


Figure 2.2-4. The Conamara Chaos region of Europa at a variety of scales, as imaged by the Galileo spacecraft (NASA/JPL/ASU).

could be the result of diapirism (Pappalardo et al., 1998a). Many formation models for these surface features suggest the presence of liquid water, or warm ductile ice, at the time of their formation (e.g., Greeley et al., 2004b, 2000). The largest impact structures are consistent with, although they do not require, the presence of a liquid water interior. However, the morphologic progression exhibited by impact craters of increasing diameter seems to indicate that the solid ice shell must have been at least 10 to 20 km thick at the times and locations of complex-crater formation (Moore et al., 2001; Schenk et al., 2004).

In addition to ice, Europa's surface contains considerable amounts of hydrated minerals, suggested to be either salts, sulfates, carbonates and/or sulfuric acid (McCord et al., 1999; Carlson et al., 1999); these materials are closely associated with the mottled/chaotic terrain, which is also visibly darker than surrounding, more water-ice-rich regions.

Europa orbits at 9.4 R_J and its surface is considerably affected by charged particle bombardment. With no appreciable atmosphere or magnetosphere to shield the surface, plasma bombardment serves primarily to alter the surface chemistry by delivering Iogenic species such as sulfur and by sputtering the native surface water ice and breaking the chemical bonds, allowing for the

formation of new species (Johnson et al., 2004). The trailing hemisphere is darker than the leading hemisphere at UV-IR wavelengths, likely as a result of the stronger effect of corotating plasma bombardment (Johnson et al., 2004), but higher concentrations in association with surface fractures could have internal sources (Greeley et al., 2004b).

A thin molecular oxygen atmosphere has been detected and sparse Hubble Space Telescope observations suggest a temporal and/or spatial variability in the thin atmosphere (McGrath et al., 2004). Potential sources of the oxygen gas are direct sputtering of water ice by magnetospheric ions and the complex oxidant chemistry produced mostly by ionization from penetrating electrons and protons. High-density phase oxygen is detected from visible absorption spectroscopy of the trailing hemisphere, possibly from oxygen trapped with other gases in clathrates (Hand et al., 2006), and another strong oxidant, hydrogen peroxide, is present in icy regions of the leading hemisphere (Johnson et al., 2004).

2.2.4.2.2 *Goals and Objectives*

The Galileo mission has provided strong evidence that Europa is differentiated into a metallic core, silicate mantle, and liquid water/ice crust. However, there is a need to confirm beyond doubt that there is a liquid water ocean beneath Europa's icy surface as well as the depth to the top of the ocean and its thickness. The additional magnetic and gravity field data that would be acquired by the JSO magnetometer and tracking of the spacecraft on flybys of Europa will place more stringent constraints on interior structure including the depth and thickness of the ocean. With JSO it might also be possible to directly detect the top of the ocean using the ice-penetrating radar on flybys of the satellite. New discoveries are anticipated, e.g., gravity anomalies similar to the anomaly detected by Galileo on a Ganymede flyby. With several flybys dispersed broadly over Europa's orbit around Jupiter, the gravity and topographic signatures of the eccentricity tidal response might be measurable in the Doppler tracking and laser altimeter data. This would provide a limited, independent means to detect an ocean. Determination of Europa's pole position and changes in the location of the pole with time

(Bills, 2005) might be possible with high resolution imaging on multiple Europa flybys; these observations would also constrain the satellite's internal structure. It might also be possible to determine any secular acceleration of Europa in its orbit through the combination of Doppler tracking and high-resolution imaging—knowledge of whether Europa's orbit is expanding or shrinking would be of enormous significance in understanding the satellite's evolution.

JSO will investigate Europa's geologic history by imaging during flybys to map regions that have not previously been observed at regional resolutions and for comparison to Galileo and Voyager data. Atmospheric monitoring and searches for current activity will be carried out using stellar occultations at UV wavelengths throughout the mission. Evidence for current activity will also be sought using thermal imaging on Europa's darkside. Topographic measurements will be made during the flybys using altimetry, and radar swaths will investigate sub-surface geologic structures during closest approach. Hyperspectral imaging from UV through IR wavelengths will be carried out during the flybys and at other parts of the tour, to determine the composition, distribution and physical characteristics of surface materials.

2.2.4.3 *Ganymede*

2.2.4.3.1 *Background*

Ganymede is the solar system's largest satellite and exceeds Mercury and Pluto in diameter. The surface of Ganymede can be broadly separated into two geologically distinct types of terrain—bright and dark (Shoemaker et al., 1982; McKinnon and Parmentier, 1986; Pappalardo et al., 2004). Dark terrain covers 1/3 of the surface and is dominated by impact craters with a variety of morphologies. Dark terrain is ancient, perhaps nearly primordial, and appears similar to the surface of Callisto (Prockter et al., 1998). In addition to craters, dark terrain also displays hemisphere-scale sets of concentric troughs termed furrows, which are probably the remnants of vast multi-ring impact basins (e.g., Valhalla on Callisto), now broken up by subsequent bright terrain tectonism.

Bright terrain forms a global network of interconnected lanes, breaking the dark terrain into isolated patches. Within the bright terrain

is an intricate patchwork of smooth bright material and material with closely-spaced parallel ridges and troughs, termed grooves (**Figure 2.2-5**). The grooves are dominated by extensional tectonic features, and morphologically have much in common with terrestrial rift zones (Parmentier et al., 1982; Pappalardo et al., 1998b). Bright terrain exhibits the full range of extensional tectonic behavior, from wide rifting, to narrow rifting, to possible examples of crustal spreading (much like the smooth bands on Europa). Though the ultimate driving mechanism behind groove formation is still unknown, there are many intriguing possibilities that may be tied to the internal evolution of Ganymede and the history of orbital evolution of the Galilean satellite system.

Ganymede's surface composition is dominated by water ice of varying grain sizes (McKinnon and Parmentier, 1986). Near the poles, there is a pronounced boundary between frosty polar caps and the rest of the surface. This surface boundary appears to follow the magnetospheric boundary between open and closed field lines (Khurana et al., 2007), and provides a unique opportunity to examine differences in space weathering processes on the same surface under different conditions.

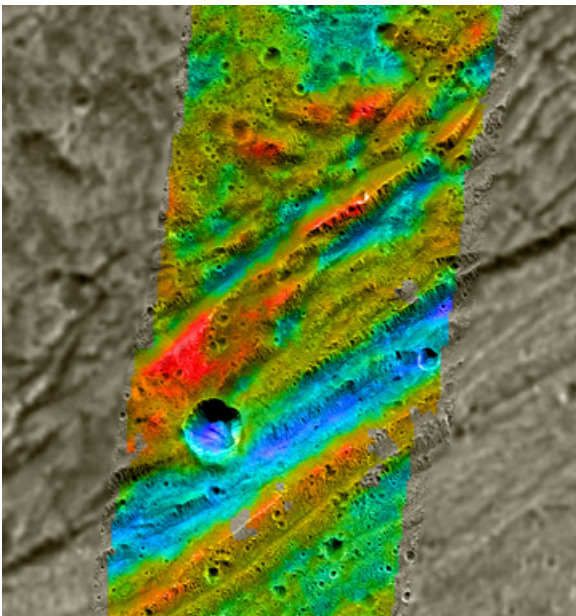


Figure 2.2-5. High-resolution topography overlaid on image of Ganymede's surface acquired during Galileo's G28 orbit. Red is high, blue is low. (NASA/JPL/Brown U.)

Outside of the polar caps and toward the equatorial regions, there are also dark non-ice materials on the surface, which may be hydrated brines similar to those on Europa. Other minor constituents of Ganymede's surface include CO₂, SO₂, and some sort of tholin material exhibiting CH and CN bonds (McCord et al., 1998). There is also evidence for trapped O₂ and O₃ in the surface, as well as a thin molecular oxygen atmosphere, with auroral emissions concentrated near the polar cap boundaries (McGrath et al., 2004), but there are yet no ionospheric indications from Galileo radio occultation data of an equatorial atmosphere. To the extent that surface composition may reflect magnetospheric irradiation effects that depend on the intrinsic magnetic field, global distributions of some species may inform us on age and variability of the present magnetic configuration.

Analysis of Galileo data from several close flybys indicate that Ganymede's moment of inertia is 0.31 MR², which is the smallest measured value for any solid body in the solar system (Anderson et al., 1996). Three-layer models, constrained by plausible compositions, indicate that Ganymede is differentiated into an outermost ~800-km thick ice layer and an underlying silicate mantle of density 3000–4000 kg/m³. A central iron core is allowed, but not required, by the gravity data. The existence of Ganymede's magnetic field, however, supports the presence of such a metallic core. Galileo gravity data also indicate that Ganymede has internal mass anomalies, possibly related to topography on the ice-rock interface or internal density contrasts (Anderson et al., 2004; Palguta et al., 2006).

Galileo magnetometer data provide tentative evidence for an inductive response at Ganymede, which again suggests the presence of a salty internal ocean within 100–200 km of Ganymede's surface. However, the inference is less robust than at Europa and Callisto, because the existing flyby data are equally well explained by an intrinsic quadrupole magnetic field (superposed on the intrinsic dipole), whose orientation remains fixed in time, rather than an induced dipole (Kivelson et al., 2002). Additional flybys by a future spacecraft are needed to resolve this ambiguity. The Ganymede surface is more

cratered and ancient than Europa's, consistent with a much thicker outer shell of solid ice. Although Europa shows stronger geologic and magnetic manifestations of a subsurface ocean, potentially (along with Ganymede) fulfilling the liquid water requirement we associate with life on Earth, the intrinsic magnetic field of Ganymede offers an alternative astrobiological parallel to Earth in partial protection of the equatorial surface and low-altitude orbital environment from magnetospheric irradiation. Importantly for potential long-term extensions of the Ganymede orbiter phase of this mission, this intrinsic field deflects much of the magnetospheric particle flux away from portions of low-altitude orbits within the region of dipolar field lines.

Magnetometer data acquired during several close flybys show that Ganymede has an intrinsic magnetic field strong enough to generate a mini-magnetosphere embedded within the Jovian magnetosphere (**Figure 2.2-6**) (Kivelson et al., 1996). A model with a fixed Ganymede-centered dipole superposed

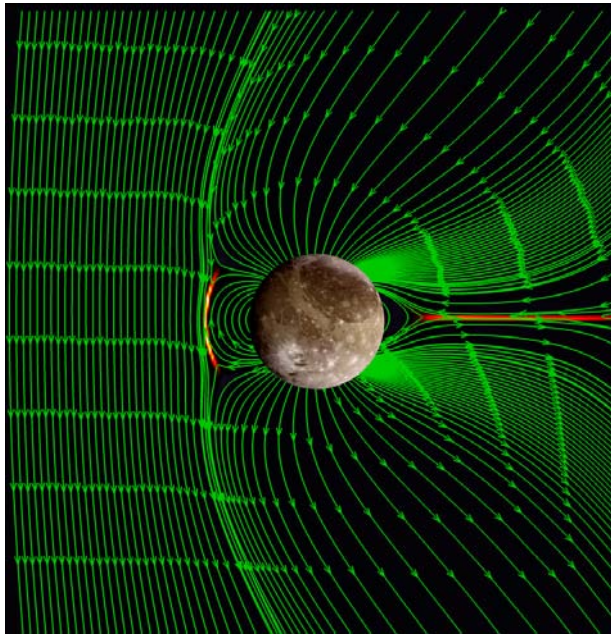


Figure 2.2-6. *Ganymede's magnetosphere, simulated by X. Jia, UCLA, 2007. Field lines are green; current perpendicular to B is represented by color variation. Note intense currents flow both upstream on the boundary between Jupiter's field and the field lines that close on Ganymede, and downstream in the reconnecting magnetotail region.*

on the ambient jovian field provides a good first-order match to the data and suggests equatorial and polar field strengths of ~ 719 and 1438 nT, respectively; these values are 6–10 times the 120-nT ambient jovian field at Ganymede's orbit. Detection of numerous electromagnetic and electrostatic waves and measurements of energetic particles close to Ganymede confirm the inference of a magnetosphere. The most plausible mechanism for generation of Ganymede's intrinsic field is dynamo action in a liquid-iron core. Dynamo action in a salty ocean is unlikely because unrealistically large convective velocities of ~ 1 m/sec are required to trigger a dynamo; in contrast, the required velocities in the core are only $\sim 10^{-5}$ m/sec (Schubert et al., 1996). Remnant magnetization in the uppermost layers of Ganymede's silicate mantle is also a possible explanation for the intrinsic magnetic field, but to magnetize these layers, Ganymede must have exhibited strong dynamo action in the past (with field strengths at least ~ 30 times the present value). In addition, such an explanation would require unrealistically high levels of silicate magnetization. Whether or not Ganymede's intrinsic field has secular variation like that of Earth cannot be determined from the presently available data, but primary and potentially extended orbital mission measurements by JSO would be valuable in attempting to set limits on this variation.

Ganymede's magnetosphere is one of the most important targets for exploration by the JSO. This unique magnetosphere within a magnetosphere is of particular interest because it exists in a parameter regime that can be studied in no other known magnetospheric system. The pressure in the surrounding plasma is dominated by magnetic pressure, a situation described as being a low β plasma. (Near the Earth, the solar wind plasma β is close to 1.) The flow upstream of the magnetosphere is sub-Alfvénic and sub-magnetosonic, so there is normally no bow shock upstream in the flow. The diversion of flow and the interaction with the upstream plasma is mediated by magnetohydrodynamic waves, with some contribution from interaction with ions newly produced from neutrals sputtered off of Ganymede (such ions

are referred to as pickup ions). The upstream field rocks back and forth about a mean direction opposite to Jupiter's spin axis and the upstream flow conditions change very slowly. The intrinsic field of Ganymede at the upstream boundary of the magnetosphere is nearly antiparallel to the average upstream field. These conditions are of particular interest for the study of magnetospheric reconnection because of the near constancy of the upstream conditions. At the upstream boundary of the terrestrial magnetosphere, where reconnection is well studied, it is often found to occur intermittently in bursts of limited spatial extent referred to as flux transfer events or FTEs. What is not known is whether the bursty nature of the reconnection process results from fluctuations in the solar wind or rather from some intrinsic non-linearity in the process. At Ganymede, with relatively steady upstream conditions, it will be of great interest to look for signatures of reconnection, seeking to understand both temporal and spatial behavior of the boundary process.

Within the magnetosphere, transport will differ from that familiar at the earth. In an intrinsic magnetospheric coordinate system whose symmetry is relative to the direction of the corotating Jovian plasma, there is no effect of rotation. This means that flows are likely to flow over the polar cap (where fluxes of energetic particles have unimpeded access to the surface), down to the mid plane and to flow back upstream near the equator on paths that are energy dependent, running into Ganymede for low energy particles, but drifting around it for relatively high energy particles. The nature of this transport remains rather poorly understood. The coupling of the magnetosphere to Jupiter's upper atmosphere calls for field-aligned currents to flow.

2.2.4.3.2 Goals and Objectives

In all magnetospheric studies, the properties of the plasma within which the magnetosphere is embedded must be monitored, so the mission design calls for elliptical orbits that extend outside

of the magnetosphere in order to monitor, even if intermittently, the slowly changing ambient conditions which do affect the interaction. It is even possible that for some encounters near the center of the Jovian plasma sheet, the external plasma flow will become supermagnetosonic and one would be able to examine the formation of a trans-sonic shock.

The planned tour will monitor the configuration of the magnetosphere using data from both fields and particle instruments. **Figure 2-2-7** shows that as a spacecraft enters the region of closed magnetic flux tubes, abrupt change of particle distributions give unambiguous evidence of the local magnetic configuration, providing key support for models of the magnetic environment. Both fields and particle instrumentation will reveal signatures of changing magnetic configuration and rapid flows that characterize reconnection. The presence of bursty reconnection and its possible periodicity will be assessed by the combined instrumentation.

Low altitude circular polar orbits are optimum for the assessment of the internal magnetic field and its variability. To lowest order, the normal to the spacecraft orbital plane remains fixed in inertial coordinates while Ganymede moves in its orbit,

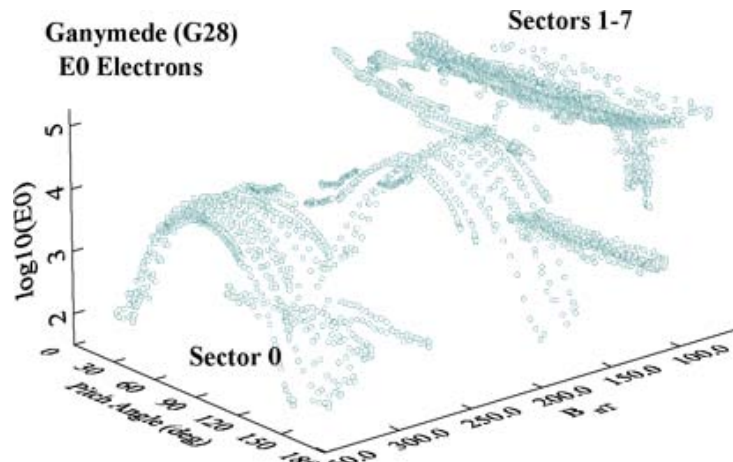


Figure 2.2-7. Fluxes of 10 keV electrons as a function of pitch angle (angle between particle velocity and the magnetic field) along Galileo's trajectory near and within the Ganymede magnetosphere. Flat distributions at lower B are found outside the magnetosphere. The transition to pancake distributions (peak intensity at 90 deg) occurs on entry into the closed dipolar field region. (From Energetic Particle Detector data of the G28 flyby of the Galileo Orbiter, J. F. Cooper, unpublished data, 2006.)

maintaining a fixed orientation relative to Jupiter. This implies that in a Ganymede-fixed coordinate frame, the spacecraft orbit precesses, with a full rotation occurring in one orbital (synodic) period. Every 3.5 days, the orbit will have come close to every point of the surface. Such complete coverage is ideal for establishing the internal magnetic multipole moments of Ganymede. A low altitude orbit lies below most of the currents flowing in the external plasma, thus implying that the internal sources of field perturbations can be well established. In order to measure the inductive response and establish or disprove the existence of a conducting layer close to the surface, one needs to measure the magnetic field near Ganymede over weeks or months and calculate from these measurements the power at a range of frequencies. The relative power and relative phases at different frequencies can, in principle, establish the thickness and the electrical conductivity of a putative liquid water layer. This is a fundamental objective of the JSO mission.

Low altitude orbits will cross the auroral region and provide valuable input for interpreting Ganymede's aurorae, known from Hubble measurements to arise in regions closely analogous to the auroral zones at earth. Evidence of strong acceleration by field-aligned electric fields will contribute to understanding both the Ganymede aurorae and the source of the glows that have been identified at the Jupiter end of the Ganymede flux tube. These orbits will allow investigation of close interactions between the magnetospheric energetic particles and the irradiated surface of Ganymede within a few scale heights of any tenuous atmosphere arising from products of these interactions. The surface origin points of pickup ions from surface sputtering can be resolved to some degree with ion trajectory measurement, so that the orbital ion measurements can be directly traced to surface geochemical composition and interaction processes. Lower altitude measurements also allow searches for heavier molecular ions sputtered off the surface by energetic heavy ionogenic ions penetrating through the otherwise protective intrinsic field.

With its mix of old and young terrain, its ancient impact basins and fresh craters, its various landscapes dominated by tectonics, volcanism, or slow degradation by space weathering, Ganymede serves as a type example for understanding many icy satellite processes throughout the outer solar system. Understanding this largest and most typical example of an icy satellite surface will give us insight into how this entire class of worlds evolves differently from the terrestrial planets. JSO provides the most ideal platform for studying Ganymede, and the powerful combination of topography, subsurface radar profiles, and high-resolution global imaging and spectroscopy will offer the best data set to understand how its surface has formed and evolved. For example, the role of volcanism in modifying the surfaces of icy satellites is an outstanding question about which little is truly understood. Like many other icy satellites, there is ambiguous evidence for cryovolcanic processes modifying the surface of Ganymede. Given the physical constraints in getting cryovolcanic melt up to the surface of an icy satellite (Showman et al., 2004), the abundance of cryovolcanic deposits gives us insight into the structure and functioning of icy satellite interiors. It would be very important to learn whether cryovolcanism is widespread or rare in the formation of bright terrain on Ganymede, and by extension what its role is in the many similar features seen on other icy satellites in the solar system. Another outstanding question on Ganymede is the driving mechanism behind the origin of the grooved terrain on its surface. Has Ganymede's surface been pulled apart by tidal forces, internal convection, and/or phase changes in its interior? What are the relative roles of tectonism and cryovolcanism in the resurfacing events that formed the grooved terrain? Because grooved terrain analogous to that on Ganymede exists on many other icy satellites, understanding the processes that occurred on Ganymede will inform our understanding of resurfacing mechanisms on icy satellites generally. As a final example, craters are found on Ganymede in a huge variety of sizes, degradation states, interior structures, and stages of modification by viscous relaxation, and as such form a basis for understanding different crater forms in icy surfaces throughout the solar system.

JSO will determine the presence and location of water within Ganymede, characterize Ganymede's magnetic field, identify the processes that cause internal evolution and near-surface tectonics of Ganymede, and place constraints on Ganymede's long-term evolution. To do so, JSO will establish the extent of internal differentiation, determine whether Ganymede has an ocean and the thickness of the ice shell, characterize the distribution (if any) of near-surface water contained within the ice shell, and characterize near-surface tectonic/volcanic processes that have operated in the past. These objectives will be satisfied by globally mapping the magnetic field and gravity field down to few-hundred-km scales, globally mapping the topography at km scales, characterizing the gravitational and altimetric amplitudes of the time-variable tide, determining the pole position and its time variation, globally mapping (via radar) near-surface structural/compositional horizons, global imaging the surface at high resolution, characterizing the intrinsic and induced magnetic field signatures, constraining the internal heat flow using global thermal IR mapping at a range of geometries relative to the Sun, and searching for changes over time to determine whether Ganymede is active now.

By entering a high-inclination, low-altitude, near-circular Ganymede orbit, JSO will globally map the spatial structure of Ganymede's near-surface magnetic field at scales of a few hundred km and determine the temporal variation of this field on time scales from days to years. This revolutionary data set will allow the determination of whether Ganymede has an induced field (as opposed to an intrinsic quadrupole field) and allow the induction signature, if any, to be distinguished from any spatial and temporal variations in the intrinsic field.

Although induction signatures are expected primarily at the Jovian rotational (~10 hour) period, JSO will also determine whether Ganymede exhibits induction at additional periods (e.g., that of Ganymede's 7-day orbit). This data set will also allow determination of whether Ganymede's intrinsic magnetic field contains small-scale spatial structure (down to scales of a few hundred km) and/or temporal variations. Such information would be

invaluable in constraining our understanding of dynamo processes in planetary interiors.

Likewise, the close circular orbit will allow characterization of Ganymede's global gravity and topography signatures at scales of several hundred and ~1 km, respectively. The gravity field will allow detailed mapping of small-scale mass anomalies known to exist from Galileo, refinement of the global (degree-2) internal structure, including the moment of inertia and degree of hydrostaticity, and, using gravity/topography correlations, determination of whether the near-surface is flexurally or isostatically supported, which places crucial constraints on geological processes.

Mapping of Ganymede's atmosphere and aurorae will be accomplished during flybys as well as during the orbital phases. Such observations will be a key component in understanding the atmospheric composition, as well as the spatial and temporal heterogeneities of the magnetic field.

Note that several of the baseline goals and objectives, including complete global magnetic field and gravity mapping at several-hundred-km scales, require a low-altitude, high-inclination, near-circular Ganymede orbit; flybys and dynamically available elliptical orbits are insufficient for this purpose. Other objectives (e.g., using radar to search for internal horizons including the base of the ice shell) can be achieved with an elliptical Ganymede orbit or flybys, but these objectives are much better satisfied with a low-altitude, high-inclination circular orbit. Still other objectives (e.g., global high-resolution imaging) can be achieved solely from flybys, as long as the flybys are sufficiently numerous, low in altitude, and diverse in geometry.

2.2.4.4 Callisto

2.2.4.4.1 *Background*

Callisto, as the outermost large satellite of Jupiter, is the least affected by tidal heating, the least differentiated, and offers an "endmember" example of satellite evolution for the Jovian system (see reviews in McKinnon and Parmentier, 1986; Showman and Malhotra, 1999; and Moore et al., 2004). Accordingly, fully understanding its internal structure, geologic history, compositional evolution, impact cratering history, and radiolysis of its surface are important to

understanding the evolution of the Jovian satellites.

Galileo gravity data plus the assumption of hydrostatic equilibrium suggest that Callisto's moment of inertia is $0.355 MR^2$, indicating that Callisto has a partially differentiated structure containing an ice-rich outer layer less than 500 km thick, an intermediate ice-rock mixture with a density near 2000 kg/m^3 , and a central rock/metal core (Anderson et al., 1998). However, if Callisto's degree-2 gravity structure is not hydrostatically balanced, then Callisto could be more or less differentiated than indicated above. This could have major implications for our understanding of satellite formation. Pre-Galileo models suggested that Ganymede and Callisto can form from debris in a proto-jovian disk in $\sim 10^4$ years; however, for Callisto to remain undifferentiated, Callisto's formation time must have exceeded 10^6 years (Canup and Ward, 2002; Mosqueira and Estrada, 2003).

Galileo magnetometer data indicate that, like Europa, Callisto has an inductive magnetic response that is best explained by an internal salty ocean within 200 km of the surface (Khurana et al., 1998; Kivelson et al., 1999; Zimmer et al., 2000); properties of the ice phase diagram strongly suggest that the ocean on Callisto (and Ganymede) lies ~ 160 km below the surface. Maintaining an ocean in Callisto today either requires stiffer ice rheology than is generally assumed (to slow down the convective heat loss) or existence of antifreeze (ammonia, salts) in the ocean. However, reconciling partial differentiation with the existence of the ocean is difficult: some portion of the uppermost ice layer must remain at the melting temperature to the present day, while the mixed ice-rock layer must never have attained the melting temperature.

The surface geology of Callisto is dominated by impact cratering and subsequent endogenic and exogenic modification processes, with scant evidence of tectonism or other signs of "active" geology (e.g., Greeley et al., 2000) (Fig 2.2-8). There is a dearth of smaller craters compared to Ganymede, suggestive of a size-dependent destruction mechanism. Large-scale mass wasting is extremely effective on Callisto and may be augmented by loss of subsurface volatiles

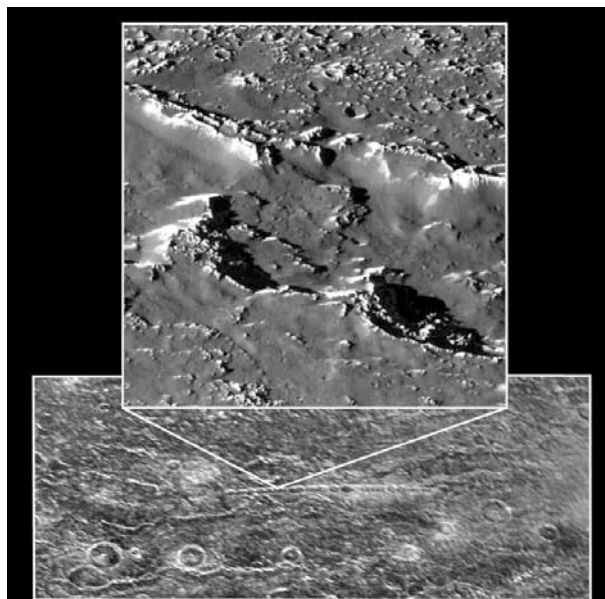


Figure 2.2-8. Galileo images of catena (crater chain) on Callisto. Note the dearth of small craters in the inset (NASA/JPL).

(Moore et al., 1999), with slump-like deposits of nonice materials observed at the base of cliffs. This nonice material probably originates from the sublimation of ice from the ice/dirt country rock and is unconsolidated with a thermal inertia of about $1.5 \times 10^4 \text{ erg cm}^{-2} \text{ s}^{-1/2} \text{ K}^{-1}$ (Spencer, 1987). Callisto, like the other icy Galilean satellites, has an unusual radar signature, being 7 times brighter than a terrestrial planet at 3.5 and 13 cm, and bright but less so, at 70 cm (Ostro et al., 1992). There is no leading/trailing difference in its radar reflectivity and the circular polarization is consistent with coherent backscattering from a high radar-albedo scattering surface.

The surface composition is bimodal, being water ice and an unidentified nonice material, with a number of additional trace constituents detected in the nonice material. The water ice is crystalline and ubiquitously large-grained (> 50 microns) except at the poles where finer-grained ice is also found (Hansen and McCord, 2004). The visible color of the nonice material is similar to C-type asteroids and carbonaceous chondrites. The icy and nonice materials are discretely mixed as segregated patches, though the icy material itself is likely an intimate mixture of ice and the nonice material. The trace materials detected in the nonice material include: CO_2 , a C-H band, CN, SO_2 , and possibly SH (Carlson et al., 1999; McCord et

al., 1998). They may be present in the ice as well although they would remain undetected via remote sensing because of the low reflectance of large-grained ice at the wavelengths where these materials are spectrally active. The carbon dioxide is detected as an atmosphere and is non-uniformly dispersed over the surface being present everywhere, but concentrated on the trailing hemisphere and being more abundant in morphologically-fresh impact craters than in surrounding terrain (Hibbitts et al., 2002). This hemispheric asymmetry is similar to that for sulfate hydrates on Europa and is also suggestive of externally induced effects by corotating magnetospheric plasma (Cooper et al., 2001).

Callisto's CO₂ atmosphere was first detected by Galileo NIMS (Carlson et al., 1999). The ionosphere (Kliore et al., 2002) appears to be present only when the trailing hemisphere is illuminated by the Sun, suggesting that sputtering produces the neutral atmosphere, which is subsequently ionized by solar UV. No emission features were detected by HST at FUV wavelengths that would be a result of electron excitation and dissociation of CO₂ (Strobel et al., 2002) and it was suggested that the interaction between the ionosphere and Jupiter's magnetosphere effectively reduces the electron impact induced emission rate.

2.2.4.4.2 *Goals and Objectives*

The JSO mission will enable planetary scientists to address most of the questions regarding Callisto that remain unanswered from the Voyager mission and to answer several new questions that discoveries by the Galileo spacecraft have raised. Investigations that JSO can carry out to help understand these processes include: determining the distribution of impact craters on Callisto's surface via high-spatial resolution global imaging, imaging mass wasting events via high-spatial resolution global imaging, characterizing the Jovian and the parasitic Callistoan magnetospheres to better understand the extent and depth of the globally conducting layer discovered by Galileo, better determining the internal distribution of mass to more fully understand the process of differentiation on large icy satellites, measuring energetic particle fluxes and energies over a long duration and over several different time

periods to more fully understand the role of radiolysis on the surface composition of icy satellites, and globally mapping the composition of the surface via UV-IR reflectance to better understand the relative influences of primordial composition, geologic processes, and radiolysis. Stellar occultations will be performed to measure Callisto's atmospheric species in absorption. These are issues which, when addressed for Callisto, will shed considerable light on similar processes that occur on the other icy Jovian satellites, other icy satellites, and perhaps on outer solar system bodies in general. Thus, understanding Callisto as a member of the Jovian satellite family is important for our understanding of processes that may operate throughout the outer solar system.

2.2.4.5 Jupiter's Rings

2.2.4.5.1 Background

In contrast to Saturn's ring system, the Jovian rings are tenuous, comprising the main ring, the halo, and the gossamer rings (e.g., Burns, 2004). The main ring extends about 0.1 R_J from the orbit of the moon Adrastea toward the orbit of Metis, and is < ~30 km thick. Immediately inside the main ring lies the halo, which is about 12,500 km in thickness and is thought to have had the inclinations of its constituent particles increased by interactions with Jupiter's magnetic field. Outside the main ring lie gossamer rings, one immediately interior to Amalthea, another interior to Thebe, with more material lying outside Thebe's orbit. It is estimated that the lifetime of the ring particles is less than or equal to about 10³ years, therefore an ongoing source of ring particles is required to replenish the rings. Since the rings are reddish in color, as are Adrastea and Metis, it is plausible to suppose that they are formed from dust eroded from the moons, perhaps along with a component from Io.

2.2.4.5.2 Goals and Objectives

The JSO mission will determine the structure and particle properties of the Jovian ring system in three dimensions, and over different timescales, using a combination of imaging and spectroscopy. Compositional measurements of embedded moons and rings will be compared, and a comprehensive search will be made for new inner Jovian moons as small as 100 m in diameter.

2.2.4.6 Small Satellites

2.2.4.6.1 Background

At the time of writing, Jupiter is known to have a total of 59 small moons in addition to the large Galilean satellites. Four of the small satellites Metis, Adrastea, Amalthea and Thebe lie inside the orbit of Io, and appear related to the Jovian rings, while the remaining small moons lie outside the orbit of Callisto (e.g., Burns, 2004; Jewitt et al., 2004). The largest small satellite is Amalthea, at ~270 km in its long dimension, and the combined mass of all the small satellites is only about 1/1000 that of Europa. Amalthea has a surprisingly low density—Doppler data from the Galileo spacecraft yields a mass of $857 \pm 99 \text{ kg/m}^3$, lower than the density of water. These data suggest that Amalthea is porous and composed primarily of water ice, and thus may have formed in a cold part of the solar system rather than in its present position (Anderson et al., 2005). The small outer moons are in orbits that are highly inclined and eccentric—some are even retrograde—implying that they may be the remnants of captured asteroids.

2.2.4.6.2 Science goals and objectives

The JSO mission may have opportunities during the outer parts of the tour to image some of the small satellites. Imaging and spectral observations will be acquired to investigate the shapes, compositions, and bombardment histories of these bodies, and to ascertain whether they formed in situ, or elsewhere in the solar system.

2.3 Scientific Advancement Achieved by JSO

The figure of merit to judge the level of science advancement is to evaluate the degree to which JSO will build upon and increase the state of knowledge relative to previous missions. Based on the defined science measurements and potential modes of operation (e.g., multiple satellite flybys, orbiting Ganymede, etc), the ability for each science theme to generate significant new results is assessed.

Jovian Atmosphere. Understanding the composition and dynamics of the Jupiter atmosphere will provide new insight into the interworkings of a gas giant planet and, by analogy, have implications for extra-solar planetary systems. From a historical perspective, data on atmospheric dynamics

have been limited to concentrated observations widely spaced in time. Specifically, the first detailed analysis was performed using flyby data from the Voyager spacecraft ([Figure 2.3-1](#)). These data were acquired at a spatial scale (100s of km) not previously known, but as a flyby the temporal coverage was necessarily restricted. Similarly, the fly-throughs of the Cassini and New Horizons spacecraft were also restricted in temporal coverage. In contrast, the orbiting Galileo mission was a long-term observer, but due to its limited down-link capability, was restricted to intermediate temporal coverage at a relatively high spatial scale (30–40 km). JSO will combine both high-temporal coverage with high-spatial resolution—one to two orders of magnitude greater than previous missions to address both global (planet-wide dynamics) and targeted objectives (e.g., individual thunderstorms). As the Juno mission will be returning data during the period when JSO will be on its way to Jupiter, it will be possible to follow-up on Juno discoveries in a timely fashion.

Magnetosphere. The ability to perform long-term observations of the Jupiter magnetosphere environment will form a basis to understand broad system interactions ([Figure 2.3-2](#)). Designing a mission to sample various aspects of the magnetosphere from bow-shock to magnetotail will provide a deeper understanding of magnetospheric phenomena including Jupiter-satellite interactions and Jupiter-sun interactions.

The study of the internally generated Ganymede magnetic field makes *in situ* observations in orbit around this satellite an imperative. By spending up to two years in Ganymede orbit, separated into one year in a highly elliptical orbit and a second year in a close circular orbit, will allow an understanding as to how the Jupiter and Ganymede fields are convolved followed by a detailed investigation of the structure and variability of the Ganymede field.

Strategically planned flybys of Io, Europa, and Callisto will allow the search for any potential internally generated Io magnetic field and provide additional information related to the induced fields at Europa and Callisto—constrained only by a limited number of Galileo flybys.

Satellites. The advancement in satellite surface science (composition, geology and tectonics) can be characterized as a function of image resolution and surface coverage ([Figure 2.3-3](#)). Beginning at the broadest scale, imaging at 10s of km provides global information on the distribution of landforms, physiography and compositional variation. Like previous missions, JSO will be able to readily achieve imaging at this scale.

The next important spatial scale for observations is ~1 km, which provides information on individual landforms, tectonic zones and other structures. It will be possible to map the entire surface of Ganymede at this scale, far exceeding coverage from previous missions. For the remaining Galilean satellites, the overall percent surface coverage will be comparable to that achieved by Galileo. However, JSO will be able to build on the Galileo data set by targeting flybys to cover parts of the satellites not previously imaged at this resolution.

Regional-scale processes can be addressed at the ~100-m pixel scale. The Galileo regional coverage ranged from ~1% (Io) to 5% for the other large satellites. In comparison, areas of note for JSO are 100% coverage of Ganymede and over 20% coverage of Europa (assuming 6 flybys), exceeding Galileo by 100 times.

Finally, local-scale processes such as individual faults, lava flows, “ice rafts” and

mass-wasting can be studied with data with 10s of meter spatial scale. The limited flybys of Io will provide surface coverage comparable to Galileo but targeted at features not previously observed or used to revisit sites where significant surface change has occurred. JSO will be able to provide 100x more data of Europa and map the entire surface of Ganymede at the local scale.

Interiors. The link between surface geology and interior structure is important to understanding the overall geologic histories of the satellites. During satellite flybys, radio tracking will enable better understanding of low-order gravity signatures, and radar sounding and altimetry will provide unique samples of upper crustal structure and quantitative morphology. The greatest science advancement will be made in Ganymede orbit ([Figure 2.3-4](#)). Global topography will be achieved along with maps of subsurface structure to provide a clear three-dimensional view. As the resolution of gravity anomalies is approximately equal to the orbital altitude (~200 km), it will be possible to study mechanisms of regional-scale compensation, in conjunction with topographic information. Combining both gravity and magnetosphere data will bring new insight to be achieved into models for the generation of planetary dynamos.

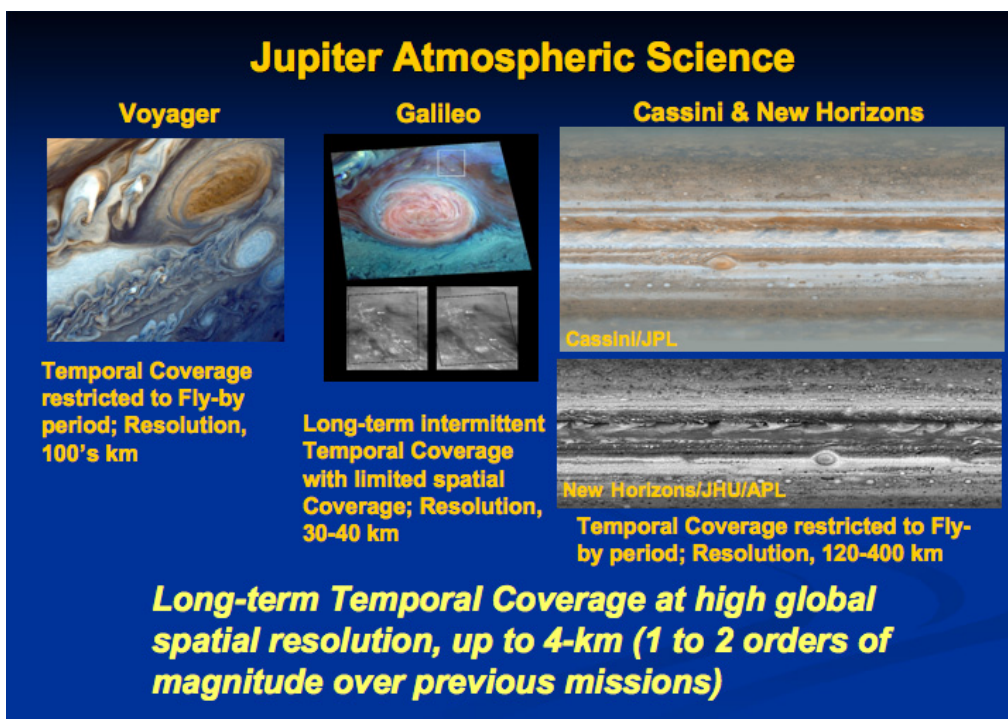


Figure 2.3-1. The JSO mission will provide for long-term monitoring of the Jovian atmosphere with temporal sampling of hours to years and spatial scales 1-to 2-orders of magnitude greater than previous missions.

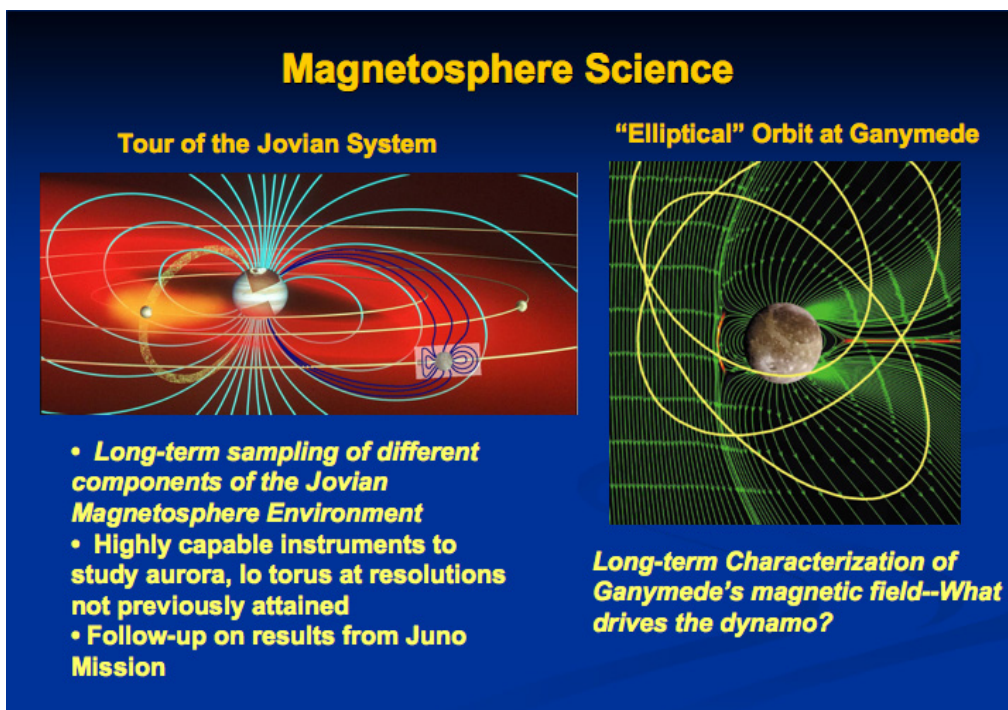


Figure 2.3-2. The long-term nature of the JSO mission will allow sampling of the various parts of the Jovian magnetosphere. Elliptical orbits of Ganymede for a year will provide insight into the interaction of the Jupiter field and that generated by this planet-sized moon.

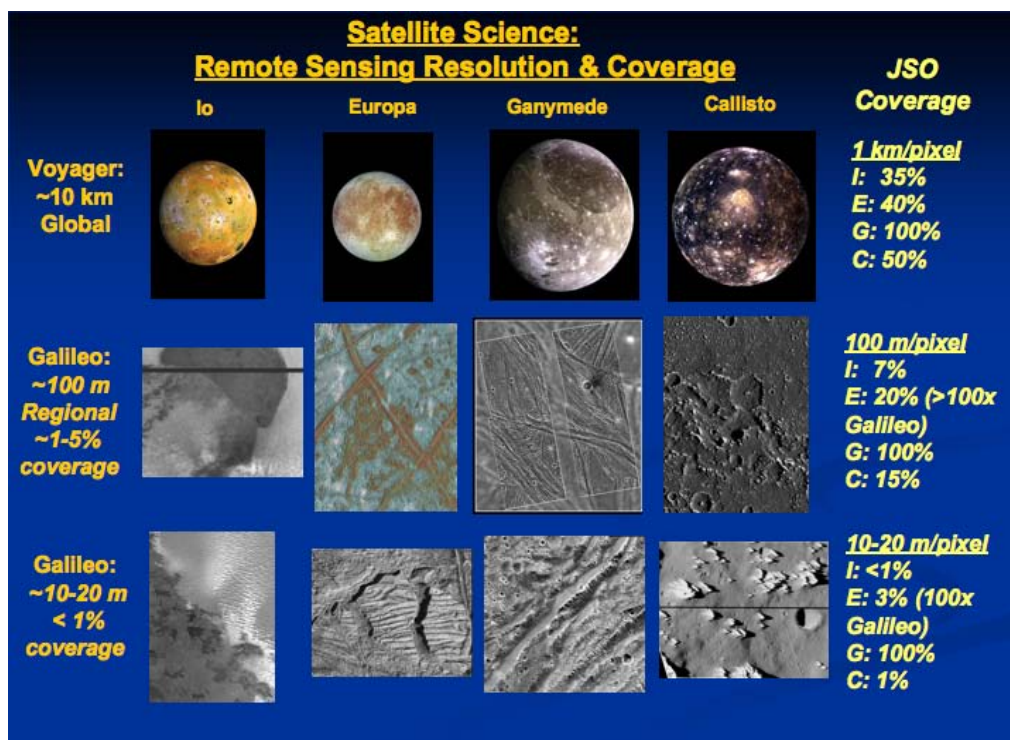


Figure 2.3-3. Remote sensing observations of the Galilean satellites will provide information on geologic processes from global to local scales and either meet or significantly exceed the surface coverage obtained by previous missions

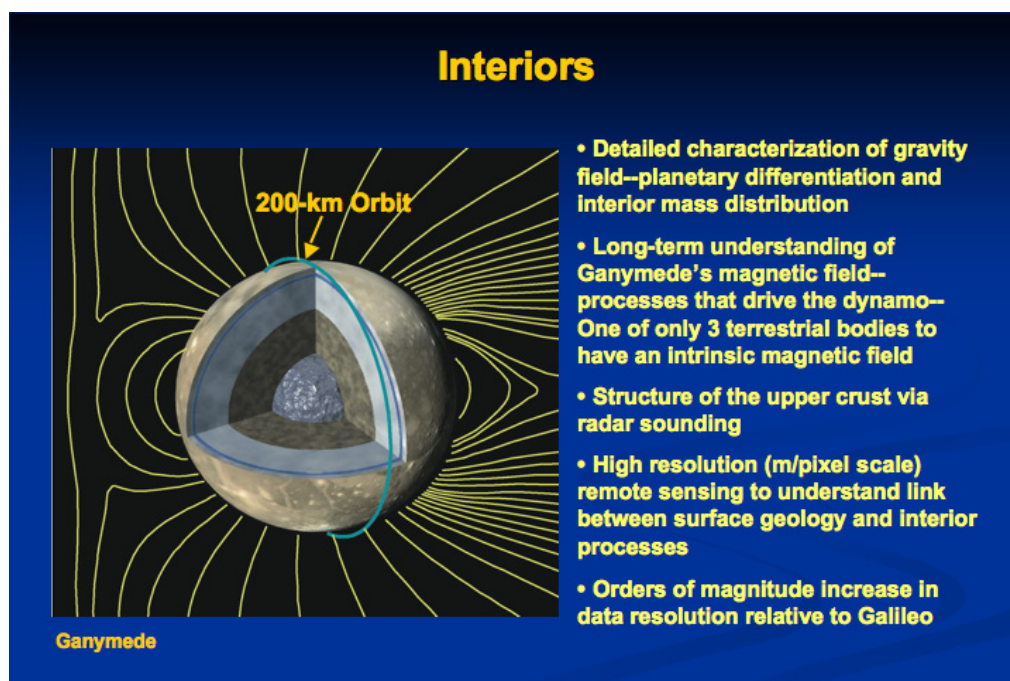


Figure 2.3-4. A low circular orbit will provide the opportunity to collect significant new data on Ganymede's internal structure and allow three-dimensional geophysical analysis from the upper crust and surface to the deep interior.

3.0 MISSION ARCHITECTURE ASSESSMENT

The study guidelines called for a two-phase process for completing this report. Phase I was a survey of possible architectures that would meet the science goals and objectives, and then a downselect to at most two mission concepts. In Phase II, those surviving mission concepts would be developed into implementation concepts.

3.1 Discriminating Architectural Elements

At the beginning of Phase I the JSO team established a list of discriminating mission architecture elements ([Figure 3.1-1](#)). A thread connecting these elements would constitute a mission architecture.

The study guidelines limited the launch vehicle (LV) option space to the Atlas V family and the higher performing, albeit higher cost, Delta IV-H.

Four classes of interplanetary trajectories from Earth to Jupiter were considered. The trade among them generally is flight time versus mass performance, with direct trajectories having the shortest flight time, ΔV -Earth Gravity Assists, such as what Juno is using, that have higher mass capability but take longer than the direct. The $V^kE^mM^nGA$ (multiple Venus, Earth, Mars Gravity Assists) trajectories have the longest flight times and highest mass performance; the Venus-Venus-Earth Gravity Assist trajectory is a special member of this class.

The trade between chemical versus Solar Electric Propulsion (SEP) is mass performance versus flight time and complexity.

The trade between Radioisotope Thermo-electric Generator (RTG) and solar power is the risk of not being able to acquire sufficient plutonium versus the higher mass and/or lower solar power output at the distance of Jupiter.

It was recognized that some of the science objectives may be best satisfied with a detachable payload. Some of the options are a dedicated spinning sub-satellite for fields and particle experiments; a Jupiter atmospheric deep probe, or a dedicated Ganymede lander for in-situ measurements. The science requirement to continue to conduct Jupiter system science while at Ganymede necessitates an optical system with a significant aperture. A half-meter size aperture such as the HiRISE camera on MRO is considered a lower

bound in terms of mass and cost with good heritage. A one-meter size aperture is considered the upper bound in terms of mass for a monolithic primary mirror design similar to the Spitzer Space Telescope. For a 1.5-meter aperture, a multi-segmented aperture and active control may help reduce the mass but with increased complexity.

There are three options for the final destination: with the main spacecraft remaining in Jupiter orbit, or captured into an elliptical Ganymede orbit, or captured into a circular Ganymede orbit. The trade among them is mass performance versus satisfying the diversity of Jupiter system science. Published literatures have indicated that orbits around Ganymede above 40° inclinations are unstable, so the trade is between reduced orbit maintenance and operational risk versus reduced observational coverage of Ganymede using a lower inclination orbit.

3.2 Preliminary Mission Architectures Selection

A simple inspection of [Figure 3.1-1](#) suggests that there are more than a thousand architectures that could be considered, far more than was possible during this study. The team quickly narrowed down the number of architectures to a manageable, yet promising set by making the following selections:

- a) A VEEGA type trajectory with flight time of 5 to 7 years was selected for the baseline. Together with a 5-year presence at Jupiter, a 12-year mission life sets the upper limit on qualification and power degradation.
- b) Chemical propulsion was selected to be the baseline. SEP may provide higher mass performance but would have high implementation (e.g., qualification for 12 year mission) and mission (e.g., operational complexity and harsh environment) risk. In addition, the maneuvers during the tour and the orbit insertion maneuvers (JOI, GOI) require a high thrust system due to their time criticality. This would require a separate chemical subsystem, thus reducing the mass benefit but significantly increasing system complexity.
- c) RTGs were selected to be the baseline power source. Study guidelines allow

Launch Vehicle	Interplanetary Trajectory	Propulsion	Power Source	Number of S/C	Aperture	Final Destination
Atlas V 551	VEEGA	Chemical	RTG	Single	~ 0.5 m	Jupiter Satellite Tour
Delta IV-H	Direct	SEP	Solar	+Probe	~ 1 m	Ganymede Elliptical Inclination < 40°
	ΔV -EGA			+Sub-Satellite	~ 1.5m	Ganymede Elliptical Inclination > 40°
	V ^E M ⁿ GA			+Lander		Ganymede Circular

☒ Element options considered in detailed tradeoffs
☐ Element options eliminated early due to high cost, risk, or complexity

Figure 3.1-1. JSO Discriminating Architectural Elements

up to 8 MMRTGs, which would provide about 800 W of power at the end of mission. Supplying such power using solar cells at Jupiter would require panels of about 100 m², which would create a challenge to maneuver the panel and still provide stable pointing for the telescope. The MMRTG was selected for its maturity and heritage as compared to the ASRG. In addition, reliability and environment impact (magnetic and vibrational) of the ASRG was a concern.

- d) A Ganymede lander would be ideal for compositional measurements of surface materials and seismometry. Unfortunately, soft landing on an airless body would require a massive propulsion system to provide deceleration and attitude control that would otherwise be provided by an aeroshell and parachute. Hard landing would require the system to survive loads of thousands to tens of thousands of g's. Without attitude control, the system must be designed to be crushable in any orientation during impact. Based on the technical difficulty and the available mass, the lander option was eliminated.

The JSO team adopted the Europa spacecraft scaling model that allows for rapid calculations of available payload mass given launch vehicle, launch energy, total ΔV , power source and telecom capability. Through a series of brainstorm discussions and rough order magnitude scoping of available payload mass, the team quickly narrowed down to 11

mission architectures based on the remaining 4 key discriminating elements (Figure 3.2-1).

3.3 Intermediate Mission Architectures Selection

The SDT evaluated these 11 architectures according to the 4 major science themes so as to narrow down to 4 architectures for detailed study. Table 3.3-1 shows the science rating of each architecture. In all cases, a “Galileo-like” tour of the Jupiter system is included prior to the final destination. Each architecture was rated on a scale of 0 to 1 by each theme group as to how well its science could be achieved. In addition to the science merit, technical viability and mission complexity were factored in the down-select. The following briefly described the considerations associated with each of the elements eliminated.

3.3.1 Jovian Tour

Early on in the evaluation process, the SDT determined that mission types that solely toured the Jovian system had low merit. Although such missions would allow a significant number of visits to each satellite, the expected science return was only incrementally better than from the Galileo mission and would not sufficiently address the highest priority objectives.

3.3.2 Sub-Satellite

A dedicated spinning sub-satellite would be optimal for fields and particles science, whereas, remote sensing, radar, and altimeter would require a 3-axis stabilized spacecraft. The concept would be to release the sub-satellite prior to Ganymede orbit insertion, thus reducing the amount of propellant needed

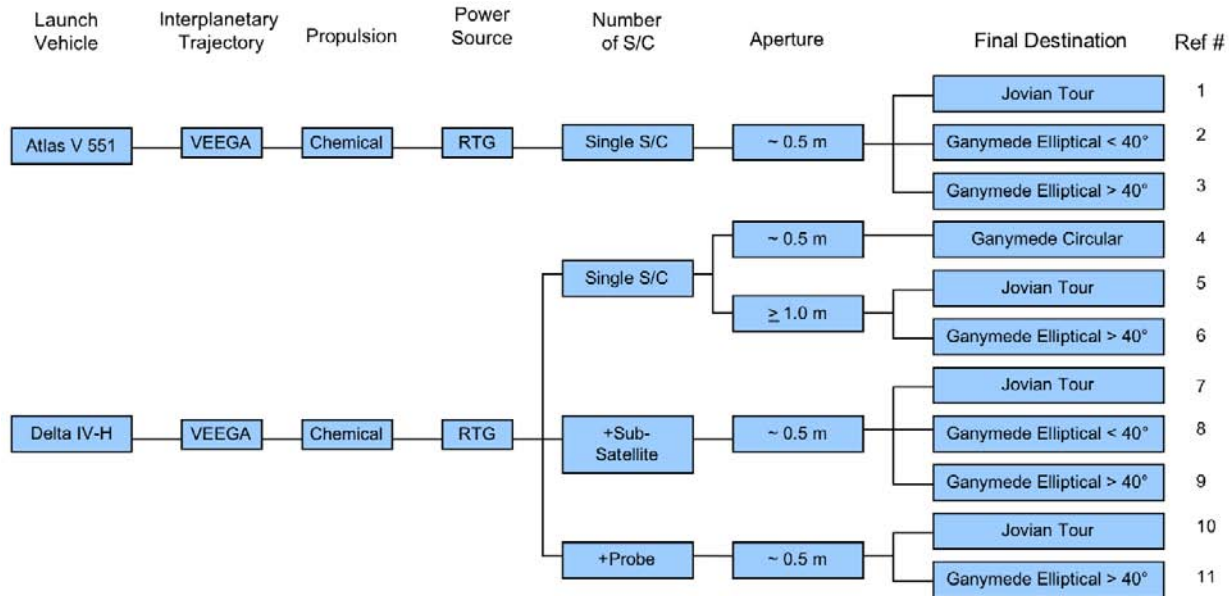


Figure 3.2-1. Mission Architecture Selection

for capture into Ganymede orbit. Given the scaling model, an initial estimate of the mass available for the sub-satellite is approximately 300 kg. To duplicate a fully functional spacecraft for the harsh Jovian environment for only 300 kg was deemed extremely difficult. This option was consequently eliminated.

3.3.3 Low Inclination (< 40°) Orbit

The high inclination orbit received higher science rating when compared to low inclination because of better coverage of high latitude regions of Ganymede. In addition, the mission design team discovered the existence of stable elliptical orbit at inclinations of up to 60°. Therefore, orbits < 40° in inclination were eliminated from further consideration.

3.3.4 Intermediate Four Architectures

Given the considerations above, four mission architectures remain.

- 1) Ganymede elliptical orbit with inclination > 40° on an Atlas V with a 50-cm optic—expected to be lower bound on cost (reference number 3 in [Table 3.3-1](#))

- 2) Ganymede highly inclined low-altitude circular orbit on a Delta IV-H with 50-cm optic—provides significant mission flexibility and high science coverage (reference number 4 in [Table 3.3-1](#))
- 3) Ganymede elliptical orbit with inclination > 40° on a Delta IV-H with 1.0-m optic—provides the most remote sensing capability (reference number 6 in [Table 3.3-1](#))
- 4) Ganymede elliptical orbit with inclination > 40° on a Delta IV-H with a Jupiter Deep probe would extend Galileo probe atmospheric in-situ science and measure composition and dynamics (reference number 11 in [Table 3.3-1](#))

3.4 Final Mission Architectures Selection

A high fidelity, detailed design of the four architectures was performed using the JPL Team-X concurrent engineering team. The resulting design and cost were further evaluated against the science measurements to be achieved.

The following describes the selection criteria and the rationale for eliminating two of the architectures.

Table 3.3-1. Science assessment of potential JSO mission types and the ability to achieve significant new understanding of the Jupiter system

Reference #	Atlas V 551	Delta IV-H	Architectural Elements			SDT Rating				Architecture Selectability Rationale
			Mission Design	Spacecraft Configuration	Optics	Int.	Sat.	Mag.	Atmo.	
1	X		Jovian Tour	Orbiter	~ 0.5	0.25-	0.50+	0.33	0.75	Science priorities addressed only modestly
2	X		Ganymede Elliptical Orbit Inclination < 10°	Orbiter	~ 0.5	0.50	0.50	0.50	0.50+	Science priorities addressed only modestly
3	X		Ganymede Elliptical Orbit Inclination > 40°	Orbiter	~ 0.5	0.75	0.50	0.75	0.33	Good System Science at potential lower cost
4		X	Ganymede Circular Orbit Inclination > 85°	Orbiter	~ 0.5	1	1	1	0.75	Significant advancement in Icy body geophysics
5		X	Jovian Tour	Orbiter	≥ 1.0	0.25-	0.66	0.33	0.75+	Science priorities addressed only modestly
6		X	Ganymede Elliptical Orbit Inclination > 40°	Orbiter	≥ 1.0	0.75	1	0.5	0.75+	Significant remote sensing science return
7		X	Jovian Tour	Dual Spacecraft - 1) Orbiter 2) F&P spinning subspacecraft	~ 0.5	0.75	0.75+	1	0.75	Complex Architectural elements 2 spacecraft
8		X	Ganymede Elliptical Orbit Inclination < 10°	Dual Spacecraft - 1) Orbiter 2) F&P spinning subspacecraft	~ 0.5	0.50	0.75	0.75	0.75	Complex Architectural elements--2 spacecraft
9		X	Ganymede Elliptical Orbit Inclination > 40°	Dual Spacecraft - 1) Orbiter 2) F&P spinning subspacecraft	~ 0.5	0.75	0.75	1	0.50	Complex Architectural elements--2 spacecraft
10		X	Jovian Tour	Dual Spacecraft - 1) Orbiter 2) Jupiter Deep Probe	~ 0.5	0.50	.75-	.75-	1	Minimal satellite interior science
11		X	Ganymede Elliptical Orbit Inclination > 40°	Dual Spacecraft 1) Orbiter 2) Jupiter Deep Probe	~ 0.5	1	1	0.75	1	Significant advancement in Jupiter interior, Atmospheres & Satellite Science

	Potential mission architectures
	Architectures selected based on science rating for further analysis
	Architecture eliminated based on noted rationale

0.75-1.0	Very Good-Excellent
0.50-0.75	Good Very Good
0.25-0.50	Fair-Good
0.0-0.25	Poor-Fair

3.4.1 Cost Comparison

Figure 3.4-1 shows the relative cost of the 4 architectures evaluated. Architecture 1 with the Atlas LV and the elliptical orbit at Ganymede is the lowest cost mission. Its cost is normalized to one with an uncertainty bar of -10% to +20%. The cost difference between architecture 2 and architecture 1 is mainly from the LV and the payload that is twice as much. The cost difference of architecture 3 from architecture 1 is mainly from the LV, similar payload as architecture 2, plus 1-m size optics. The cost difference for architecture 4 from architecture 1 is from the LV, similar payload as architecture 2, plus the probe.

3.4.2 Optical System Aperture

The science to be achieved by optical remote sensing must build and expand upon that achieved by Voyager, Galileo, Cassini, and New Horizons. In terms of satellite science, all previous missions have provided compositional information at the ~10-km scale. The next level at which an advancement in science knowledge can be achieved is ~1 km (regional to global-scale processes—major physiographic and structural/tectonic features). Data sets at the 1 km scale were collected by the Voyager and Galileo spacecraft, but do not provide complete global coverage of each satellite. This suggests that a JSO optical system with an aperture of at least 0.5 m is needed (see Table 3.4-1). The next leap in

understanding, at the local to regional scale (individual faults, localized compositional anomalies, etc.), necessitates ground samples at the 10's of meters scale. To achieve this from a spacecraft at Ganymede would require an optic with a diameter equivalent to ~4 meters (**Table 3.4-1**). Such a large telescope would dominate the JSO payload and shift the balance from system science to that dominated primarily by remote sensing. Although such a system would provide important data on, Io, Europa, and Callisto, its usefulness in orbit at Ganymede (especially a 200-km circular orbit) would be limited. From a 200-km orbit, the raw surface pixel scale is ~3 cm. However, significant smearing due to spacecraft motion would not allow useful data at this scale to be collected.

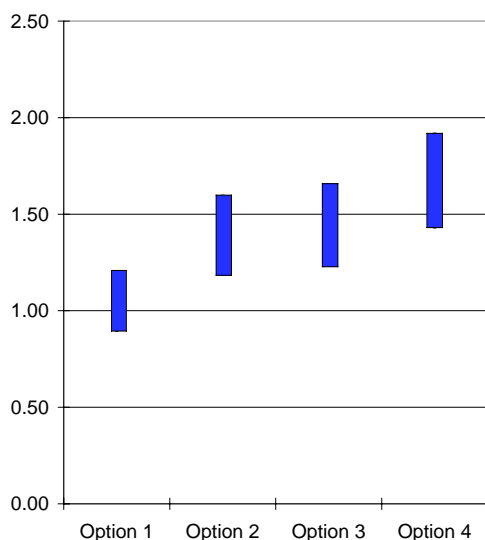


Figure 3.4-1. Cost Comparison

Like satellite science, understanding the structure and dynamics of the Jupiter atmosphere will employ remote sensing techniques. Previous missions have monitored the Jupiter atmosphere at scales of 30- to 40-km (Galileo) and 100- to 400-km (Voyager, Cassini, New Horizons). For a 0.5 m optic, pixel samples would be ~1.0-km. Global maps of Jupiter could potentially be achieved at the 4-km scale, providing a one-to-two order of magnitude improvement over previous missions. This allows exploration of Jupiter at a level not previous achieved and provides significant new insight into the structure and dynamics of the atmosphere.

Table 3.4-1. Visible Image Resolution as a Function of Optics Diameter

Target	Best Resolution (m/pixel)*	Optics Diameter (m)
Io	1550	0.25
	775	0.50
	390	1.00
	195	2.00
	130	3.00
	95	4.00
Europa	960	0.25
	480	0.50
	240	1.00
	120	2.00
	80	3.00
	60	4.00
Callisto	1950	0.25
	975	0.50
	485	1.00
	245	2.00
	160	3.00
	120	4.00
Jupiter	2400	0.25
	1200	0.50
	600	1.00
	300	2.00
	200	3.00
	150	4.00

*Assumes a visual wavelength of 0.5 microns at minimum distance between Ganymede and target.

The trades between the size of an optical system, the number and types of instruments flown and the ability to achieve a circular orbit around Ganymede are fundamental to achieving overall Jupiter system science. Keeping in mind the overarching goals of the mission, the Science Definition Team closely evaluated remote sensing systems in the 0.5- to 1.0-meter range and the potential advancement in knowledge with a larger optical system. The team concluded that achieving a close circular orbit around Ganymede was necessary and would provide significantly new science return and that expending payload mass for propellant to do so was an equitable trade. To achieve important satellite science, an imaging optic with substantial capability is needed. By having a mission design that allows multiple fly-bys of Io, Europa, and Callisto, an optic of 0.5 m is adequate. This trade also allows for the inclusion of other significant remote sensing and fields and particles instruments

that might not be included otherwise. Relative to satellite science, such a payload will provide significant new Jupiter atmospheric science. In addition it allows for the inclusion in the payload of other capable instruments (e.g. Thermal Spectrometer with a 0.5-m aperture) that are important for studying Jupiter.

To summarize, a highly capable remote sensing payload has the potential to shed new light on questions regarding the formation, composition and evolution of Jupiter and its satellites. To accommodate such a system and still achieve Ganymede orbit requires the trade between a close circular and an elliptical orbit at a lower inclination (subsequent analysis has shown that a 60° inclination orbit can be attained). Relative to a circular orbit, the elliptical orbit significantly compromises both the magnetosphere and interior science (both having an inverse radial dependence on resolution). The desire to address local-scale geologic processes makes a 1.0-m optical system highly desirable. However, placed in the context of overall Jupiter system science, its accommodation would require significant mass resources resulting in the elimination of other, non-remote sensing instruments and drive JSO to a be a predominately remote sensing mission. The SDT concluded that the trade should be made between optics size and the number of fly-bys of each satellite. That is, if it is possible to have a sufficiently large number of satellite fly-bys (> 2 for Io and > 6 for Europa and Callisto) a smaller optic (i.e., 50-cm) coupled with many satellite visits should equalize science return relative to a larger optic without a large number of fly-bys.

3.4.3 Jupiter Deep Entry Probe

One of the highest-priority science objectives for Jupiter is to determine the fraction of Jupiter's mass that is oxygen, dominated by its hydrogenated form: water (H_2O). This characteristic is the best-known indicator of the mechanism by which elements heavier than hydrogen and helium were delivered to Jupiter during its formation, a major process associated with formation of our planetary system as a whole. Currently the best avenue for making this determination is to measure the "deep abundance" of water at Jupiter, i.e. the fraction of the atmospheric mix of gases that is water deep below the visible clouds, where "weather" processes such as

condensation and cloud formation no longer affect that fraction. Usually this fraction is expressed in terms of the fraction of oxygen in the sun's mix of gases. If Jupiter's oxygen fraction were twice that of the sun, it would be said to be "twice solar"; other such elements, such as nitrogen and carbon, are treated similarly. There are other science objectives to be addressed in Jupiter's middle and upper troposphere, but the oxygen fraction is the most important one.

As designed, the Galileo Probe was to make this measurement. Jupiter atmospheric models at that time indicated that the base of the water cloud, below which the water abundance should be the deep abundance, might be as deep as the 10 bar level, so the probe was designed to reach 20 bars, which it did. Unfortunately nature and chance conspired against Galileo, and the location in Jupiter where it descended was most decidedly unrepresentative of Jupiter's normal atmospheric structure. It entered a "5 micron hot spot", a locale of intense atmospheric downwelling that plays havoc with the usual abundance profiles of heavier species such as water and ammonia. At the lowest levels it reached, the probe was just beginning to detect water, and the measured water abundance was still increasing at the time the probe stopped functioning, strong evidence that it had not reached the portion of the atmosphere representative of the deep abundance of water.

More complex models, generated subsequent to the Galileo Probe mission, include such atmospheric dynamics. Researchers disagree somewhat, but most now advise that to ensure measuring deep-abundance air at Jupiter, a probe must reach the 100 bar level. They also expect oxygen and nitrogen abundances about 5 times solar, though they caution that they could be as much as 10 times solar.

Reaching the 100 bar level at Jupiter is possible but is certainly not an easy task. Temperatures at that level are expected to be 650 to 680 K, nearly as high as the surface of Venus. At those pressures and temperatures a cooled (possibly by phase-change material) pressure vessel is a necessity, a much heavier descent module structure than the Galileo Probe's vented, uncooled descent module. Radio communications from those depths are

also challenging, since the water and especially ammonia overhead absorb radio signals. Given the capabilities of radio systems available for Galileo-like Jupiter probe applications, at the “sweet spot” frequencies around 1.35 to 1.4 GHz, and given 5 times solar oxygen and nitrogen abundances, the deepest a probe could expect to reach and still transmit a useful signal is less than 70 bars. If the abundances are 10 times solar, the limiting depth is much shallower. The primary problem is that a Galileo-like, single-element probe’s radio system must address simultaneously the problems of atmospheric attenuation and attenuation due to the large distance from the probe to the receiving asset. This problem might be overcome by a two-element probe that maintains one element higher in the atmosphere, where overhead absorption is much less severe, and a deep element that relays its data to the shallow element only a few hundred km away. The deep-to-shallow link is relieved of the need to fight the large distance to the ultimate receiving asset, and the shallow-to-ultimate-receiver link is relieved of the atmospheric attenuation problem. Such probe architectures have not yet been seriously studied for a flight project so their TRL is low, and the need to use them undoubtedly adds to the estimated probe system mass and adds risk to the mission.

The desire to follow-up on the Galileo probe results is very compelling. The science to be returned by a potential JSO deep probe must be assessed in light of a number of factors. First, the science questions to be addressed by the probe must be well defined. There is currently debate in the Jupiter atmospheric science community regarding the depth (100 bars or possibly more) needed to achieve a conclusive and robust water measurement. The range of depths has significant implications as to how to design the probe. Second, and linked to the first issue, the Juno Mission will just be starting to return critical water abundance data needed for design at the time when the manufacture of the JSO probe should be nearly complete. Finally, the JSO mass available for a probe is sufficient for the inclusion of a single probe. Since targeting a probe at Jupiter must be accomplished well before JOI, the specific atmospheric environment that it will enter

cannot be predicted. Like the Galileo probe, there is a risk of entering an anomalous region and compromising the science return. Therefore, the design of the probe needs to have a better understanding of the science requirements on depth along with the need for Juno results for design constraints.

3.4.4 Selection Criteria

The selection criteria to arrive at the final two architectures were based on science, cost, risk, and other intangibles.

Table 3.4-2 shows the relative qualitative scoring of these factors for the four architectures using a star rating scale, 4 being the highest.

Table 3.4-2. Comparative Rating of the Intermediate Architectures

		Option 1	Option 2	Option 3	Option 4
Science		○○	○○○○	○○○	○○○○
Cost		○○○○	○○○	○○○	○○
Risk	Mission	○○○○	○○○○	○○○○	○○
	Development	○○○○	○○○	○○	○
	Technology	○○○	○○○	○○	○
Intangibles		○○	○○○	○○○	○○
		19	20	17	12

The science merit was evaluated as described in §3.3, 3.4.3, 3.4.4, and is shown in **Figure 3.3-1**.

The cost rating is based on the relative cost comparison from §3.4.1.

Risk ratings are separated into 3 areas. Mission risk is associated with potential operations failure due to system or mission operations complexity, or operating in an unknown environment. Based on the discussion of the deep probe option in §3.4.3, it was given a 2-star rating compared to the other architectures. Development risk is associated with complexity of interfaces and number of elements that are required for integration and test. Architecture 1 is the simplest. Architecture 2 is more risky than 1 because of the larger suite of instrumentation. Architecture 3 is more risky because of the large optics and potential shared focal plane of multiple instruments. Architecture 4 is more risky with the addition of the deep probe. Architectures 1 and 2 are similar in technology readiness with concern mainly in the re-design of rad-hard electronics and sensors. Architecture 3, with optics equal or better than

1 m class, is more risky because of the need to reduce mass either by using lightweight material or a segmented mirror with active control. Architecture 4 has significant technology challenges as discussed in §3.4.3.

The “intangibles” ratings take into account factors that may not be covered elsewhere. They include factors such as public excitement, science community support, proper timing of results of other missions. Architectures 2 and 3 were ranked higher in public excitement and community support as compared to architecture 1 because of innovation (e.g., mission design in architecture 2, Hubble going to Jupiter in architecture 3). Architecture 4 was down graded because Juno results would not have been available at the time needed for the probe design as discussed in §3.4.3.

As a result of the above considerations, architectures 1 and 2 (reference numbers 3 and 4) were chosen for the next level of detailed design.

3.4.5 Final Two Architectures

The two architectures selected for detailed study both assume a Jupiter tour with JSO ultimately achieving orbit at Ganymede. To demonstrate that viable and robust missions can be carried out, it must be shown that significant observations can be made using launch vehicles with different capabilities. Because a magnetosphere sub-satellite is not a viable option (§3.3.2), the SDT determined that a single orbiter that first spends a year in an intermediately inclined (60°) orbit to sample both the external Jupiter field and the Ganymede field (to understand how they are convolved) followed by a second year in a highly inclined ($> 85^\circ$) low-altitude circular orbit will achieve most of the required objectives. The circular orbit is also ideal for gravity measurements, high resolution remote sensing and other system science. This architecture has the most capability and is the JSO “Baseline” mission. Because the second architecture relies on a smaller, less capable, launch vehicle, compromises in the ability to achieve the science are required. The major difference between the two architectures is that the second does not provide a close circular orbit at Ganymede. It is instead restricted to an intermediately inclined elliptical orbit. Because of this, there is a significant

degradation to the gravity and the magnetosphere data while objectives for Jupiter atmosphere and satellites remain relatively unaffected. This second architecture is designated the “Descoped” mission.

In addition, the SDT also re-examined the notional payload for the two architectures prior to the down select to arrive at a more balanced and more optimized payload suite that is consistent with the two final architectures and with the available mass and power.

4.0 MISSION CONCEPT IMPLEMENTATION

4.1 Mission Architecture Overview

The JSO mission is composed of 3 segments: launch, flight, and ground, as shown in [Fig. 4.1-1](#).

The launch segment is composed of the launch vehicle and the launch site. For the baseline JSO mission, the launch vehicle is the Delta IV-H. The Delta IV-H is the most capable LV of the Delta IV family. The first stage and the two strap-on boosters use cryogenic propellants (liquid oxygen and liquid hydrogen). The 5-m diameter second stage also uses cryogenic propellants. The composite fairing is 5 m in diameter and 19.8 m long. For planetary missions, the Delta IV-H is launched from the Eastern Range (ER) in Florida. The Space Launch Complex (SLC) of the ER, designated SLC-37, is located at Cape Canaveral Air Force Station (CCAFS).

The flight segment, also known as the spacecraft, is composed of the bus and the

payload. The bus is made up of subsystems including telecommunication, thermal, propulsion, structures and mechanisms, power, attitude and articulation control, command and data handling, and flight software. Section 4.4 provides a detailed description of the bus. The planning payload for the baseline mission has nine notional instruments. The high resolution camera and the VIS-NIR spectrometer share a 50-cm aperture front optics. The remaining are the medium-resolution stereo camera, laser altimeter, UV and thermal spectrometers, radar, magnetometer, plasma spectrometer/energetic particle detector. Radio science is conducted through the telecommunications subsystem using dual Ka- and X-band frequencies. §4.2 provides more detailed description of the payload.

The ground segment is composed of the Deep Space Network (DSN), the Flight Operations Center (FOC), and the Science Operations Center (SOC). The DSN is operated out of JPL and includes 3 Deep Space Communications Complexes (DSCC) located

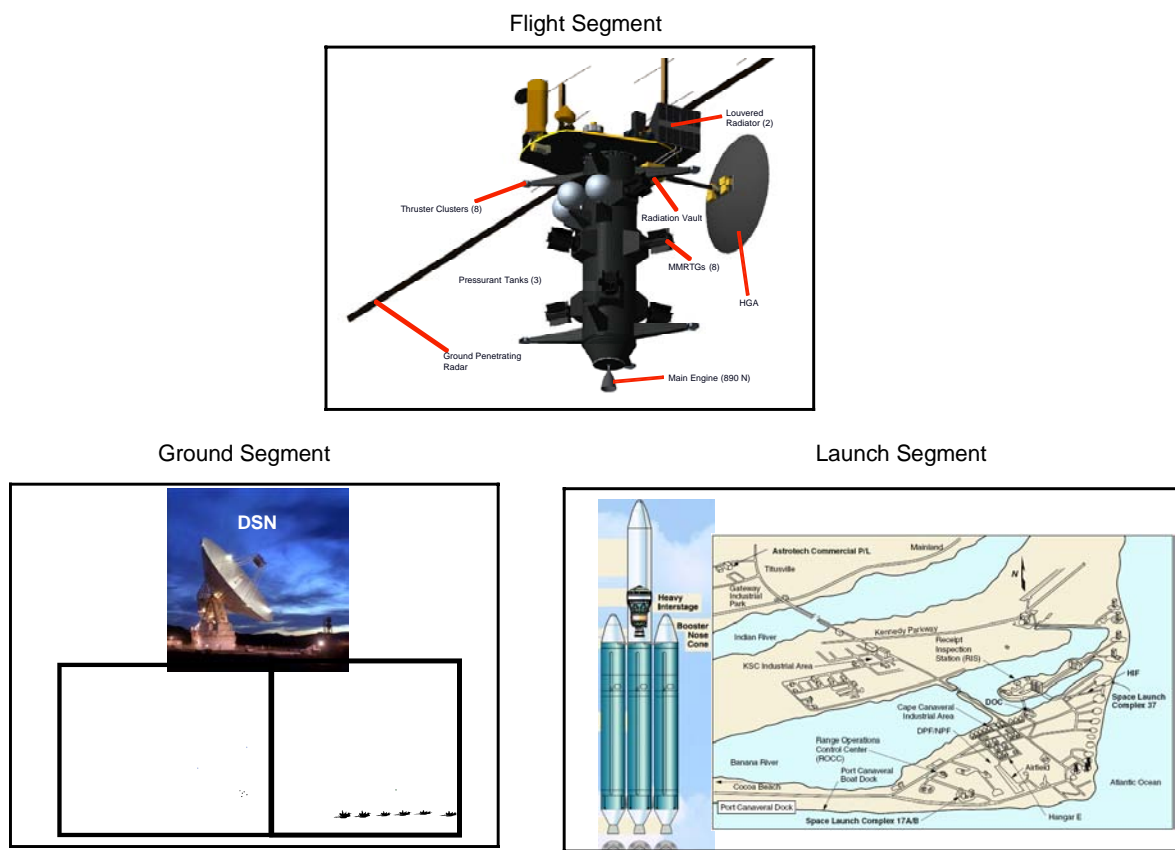


Figure 4.1-1. JSO Mission Architecture

near Madrid, Spain; Goldstone, California; and Canberra, Australia and provides global coverage of deep space missions. Each complex has several 34m antennas and one 70m antenna. It should be noted that while the 70m antennas currently do not have Ka-band capability that is assumed in this report, that assumption is consistent with the study guidelines which state that such capability will be available in 2015. The FOC located at JPL is composed of the Deep Space Operation Center (DSOC) and a dedicated Mission Support Area (MSA) that house the flight operations teams. Depending on the implementation of operations, additional MSAs can be established at other NASA centers, universities, or industrial partners. The SOC is envisioned to be a dedicated science operations facility at or near JPL that would house science instrument teams during critical and intense activities that require close coordination among the flight operations teams and other instrument teams. Instrument command generation and telemetry analysis capabilities will be established at the instrument teams' home organizations.

This mission architecture is typical of deep space missions and will be the basis of organizing the project team responsibilities and systems performance flow-down and interfaces.

4.2 Science Investigation

The measurement requirements discussed in §2.2 are formulated to achieve the best overall Jupiter System science. The JSO instrument complement (notional instruments for each measurement are provided in Foldout 1) must have the capability and flexibility to collect useful data in distant observation mode, flyby-mode and elliptical and tight circular orbit around Ganymede. In this section, we discuss key implementation drivers from each of the science theme areas.

Jupiter Atmosphere

Data to evaluate various aspects of the Jupiter atmosphere requires a long temporal baseline and the ability to make observations on the frequency of hours to years. During the course of the JSO mission, both routine observations and dedicated campaigns will be carried out. Ample opportunities for Jupiter observations will be available during the "long arcs" between satellite flybys along with the

elliptical and circular Ganymede orbits. The instrument complement required to carry out these science goals consists primarily of a VIS-NIR hyperspectral remote sensing package along with a thermal spectrometer and UV spectrometer.

Magnetosphere Science

Achieving the goals of magnetosphere science necessitates measurements of fields and particles to be made throughout the mission. Noteworthy are the need for measurements at a range of local times and radial distances and continuity of data in order to describe the time variability of the Jupiter system. As the JSO orbit evolves subsequent to JOI, the tail petal will rotate into the magnetotail, a critical region for understanding the temporal changes of the system. Instrument performance requires magnetic cleanliness of 0.1 nT at the sensor location, and knowledge of spacecraft orientation to 0.1°.

During flybys of Io, Europa, and Callisto, fields and particles data will be collected to (1) assess any potential internal Ionian field, (2) Characterize Europa's internal field to better constrain the presence of a subsurface ocean and (3) Characterize the induced field at Callisto and constrain its potential subsurface ocean. To address these objectives, continuous measurements are needed throughout the flyby period.

The Ganymede science phase of the mission provides the opportunity to understand the internal processes by which this satellite generates its intrinsic magnetic field in the following ways:

1. The one year, inclined (60°), elliptical orbit will facilitate sampling of the Jovian field and the Ganymede field nearly simultaneously, to understand how they are convolved;
2. The elliptical orbit allows sampling of the fields from various geometries;
3. The one year, highly inclined (>85°), low-altitude (~200 km), circular orbit samples the environment at both open field and closed field lines.

Satellite Science

Spacecraft and environmental constraints drive the overall implementation approach to achieving the satellite science goals. The

general structure of science observation activities after JSO is captured into Jupiter orbit fall into three areas, (1) non-encounter portions of the Jovian Tour, the long arcs between satellite flybys, (2) flyby of a satellite and (3) Ganymede orbit—both at moderate-inclination ($\sim 60^\circ$) elliptical and low-altitude (~ 200 km) high inclination ($>85^\circ$) circular orbit. Because Ganymede is the only satellite that will be orbited, it is necessary to have a sufficient number of flybys of the other satellites ([Table 4.2-1](#)) to achieve the greatest amount of surface coverage possible. To optimize the science return, robust satellite observations need to be accommodated during all phases of the mission. The ability to achieve significant surface coverage by the remote sensing payload necessitates an optical system with an aperture of at least 50 cm. This accommodates longer-term observation periods while on approach to flybys and during the outer portion of the elliptical orbit around Ganymede, addressing system science objectives such as Io and Jupiter atmosphere monitoring. In addition, for all remote sensing science instruments, it will be necessary to acquire co-registered, simultaneous or near-simultaneous observations. While in orbit at Ganymede, the spacecraft can be slewed from nadir to acquire observations of the other satellites and Jupiter.

Operations in Ganymede orbit must take into account potentially divergent requirements from visible imaging, to assess geology and morphology, and NIR hyperspectral

imaging for composition. The former typically prefers the spacecraft to be at a late afternoon ($\sim 4:00$ PM) orbit while the latter will achieve its best data in an early afternoon ($\sim 1:30$ PM) orbit. A compromise is to place JSO in an approximately 2:30 PM orbit that is as near to sun-synchronous as possible for uniform illumination. The best global coverage of Ganymede requires a high-inclination ($>85^\circ$) circular orbit. If it is not possible to achieve a circular orbit, an elliptical orbit with an inclination no less than 60° should be able to address an acceptable portion of the science objectives. Since the elliptical orbits' argument of periapse will circulate, it should be possible to view the polar regions to achieve near-global coverage, albeit at somewhat more oblique geometries. Combining an elliptical orbit with a large optical system, should allow for the acquisition of global maps at 10s to 100s of meter spatial scales for local and regional geologic studies.

Near repeating orbits are needed to perform imaging, spectroscopy, and thermal mapping, with the last necessitating day-night repeat coverage. Observations of atmospheric emissions and their time-variability, and of stellar occultations, require near-continuous observations near the satellite's limb. For quantitative morphology and processing of radar data a global digital terrain model from altimetry must be generated. As the Ganymede orbit phase will last for two years, a dedicated campaign to acquire a topography map will be carried out early on along with samples of

Table 4.2-1. Discriminating Science Requirements on Mission Design Implementation

Science Theme	Tour	Encounter	Ganymede Orbit
<u>Satellite Science</u>			
Io	Dedicated observing campaigns; temporal Monitoring	≥ 2 at low altitude (100-200 km)	Dedicated observing campaigns
Europa		≥ 6 at low altitude (100-200 km); globally distributed	Dedicated observing campaigns
Ganymede			Global coverage, high inclination ($>85^\circ$ orbit)
Callisto		≥ 6 at low altitude (100-200 km); globally distributed	Dedicated observing campaigns
Rings & Small Satellites	Dedicated observing campaigns		Dedicated observing campaigns
<u>Interiors</u>		All satellites at low altitude (100-200 km); globally distributed	High inclination ($>85^\circ$); low altitude (100-200 km); circular orbit
<u>Magnetosphere</u>	Sample different parts of the Jovian magnetosphere environment	Dedicated observing campaigns	Elliptical orbit to sample both Ganymede and Jovian field; High inclination ($>85^\circ$); low altitude (100-200 km); circular orbit
<u>Jovian Atmosphere</u>	Dedicated observing campaigns		Dedicated observing campaigns

radar profiling. Extensive radar profiling will be performed during the latter part of the mission.

Interior Science

To probe the interior of the satellites, gravity measurement requirements dictate multiple low altitude (100 to 200 km) flybys of Io, Europa and Callisto. As flybys are performed throughout the mission prior to Ganymede orbit insertion, each geometry must ideally be planned such that the closest approach point covers a different latitude and longitude distributed globally about each satellite. When placed in orbit around Ganymede, the requirements of both gravity and altimetry necessitate a low-altitude (100 to 200 km) circular orbit with an inclination greater than 85°. This allows broad global coverage and the ability to constrain some of the higher-order components of the gravity field (e.g., anomalies associated with impact basins). Such orbits also provide crossover points for altimetry and, when combined with knowledge of the spacecraft's orbital position to high accuracy via two-way Doppler, enable measurements of tides at the meter scale. Gravity measurements require long (greater than 12 hours), unperturbed (no spacecraft thrusting or momentum wheel desaturation) arcs for high-precision measurements to be achieved. Ground tracks should not repeat, to provide for a dense network of data points. The constraints described for the gravity measurements provide concurrently highly desirable orbits for characterizing the internal magnetic fields of the moons.

Like measurements for gravity and altimetry, probing the upper crusts of the satellites with Ground Penetrating Radar (GPR) requires low altitude (below 2000 km, with optimum at ~200 km) flybys. Similarly, while in orbit at Ganymede, useful data can be acquired in an elliptical orbit when the spacecraft is below 2000 km. A low altitude, 200 km circular orbit will provide the best GPR data. During the Ganymede orbit phase of the mission, a global altimetry map will be used in conjunction with the GPR data to model ground clutter.

4.2.1 Planning Payload

The JSO planning payload consists of seven remote sensing instruments, and two space physics instruments. In addition, two radio

science investigations, one for gravity and one for probing atmospheres, use the bus' telecom system's X- and Ka-band signals. The radio science-gravity investigation uses the two-way Doppler for accurate orbit reconstruction in support of geophysical objectives. The radio science-atmospheres investigation uses a USO and a one-way, dual-frequency downlink to investigate the atmospheric structure of Jupiter and the rarified atmospheres of the Galilean satellites.

The detailed science measurement requirements trace to a broad set of instrument types (see [Foldout 1](#)). The selection of the baseline architecture allows a refinement and down-selection to a notional suite of nine instruments plus the radio science investigations ([Table 4.2-2](#)). The subsequent part of this section discusses the science payload in detail.

4.2.2 Payload Accommodation

The remote sensing portion of the payload needs to view in the nadir direction when in orbit about Ganymede. The bus provides an adequate mounting volume of up to $\sim 1 \times 1 \times 1$ m for the science payload on the nadir-facing deck. The optical remote sensing instruments will need a conical clear field of view with at least a 10° half angle centered about the nadir direction.

The science payload is expected to have sensors that need to be cooled to as low as 80 K for proper operation while dissipating perhaps 300 mW of heat. Cooling to this level can be accomplished via a passive radiator mounted so as to view in a direction away from the Sun and away from Ganymede at all times.

The remote sensing instruments will require spacecraft pointing control to better than or equal to 0.4 mrad and stability to 2 μ rad over 0.5 s. Pointing reconstruction to 80 μ rad is also required.

The severe radiation environment at Jupiter will present challenges for the science instruments. The predicted radiation dose at the end of the JSO mission is 1.8 Mrad behind 100 mils of aluminum shielding. Sensors and supporting electronics will need to be shielded. The most mass-efficient approach to providing shielding is to upgrade required parts' radiation tolerance to 300 krad and to house as much of the instrument electronics as can be

Table 4.2-2. JSO Baseline Planning Payload Resource Requirements

Mission Option 2: Example Main S/C Payload, Delta IV H, High inclination, Low altitude Circular Ganymede Orbit						
Instrument/Investigation	CBE Mass (kg)	CBE Power (W)	Native Rate (Mbps)	Date Reduction Factor (at Instrument)	Rate to C&DH (Mbps)	Notes
High-res Camera (HRC)	70	95	126	3	40	IFOV = 2.0 μ rad, 50-cm aperture, f/8, 10-color filter wheel
VIS-NIR Hyperspectral Imager System (VHS)			3500	89	40	0.4–5 μ m, 2 nm spectral resolution from 0.4 to 0.9 μ m, 4 nm spectral resolution 0.9 to 2.5 μ m, 10-nm spectral resolution from 2.5 to 4.8 μ m, 1 nm spectral resolution from 4.8 μ m to 5 μ m, IFOV 10 μ rad, three spectrometers, 640x480 HgCdTe array, SNR >300, shared 50-cm foreoptics with camera, f/5.33
Medium-res Stereo Camera (MRC) (per camera)	20	20	25	3	8	IFOV = 20 μ rad, 6-cm aperture, f/6, monochromatic, near-simultaneous stereo capability
UV Spectrometer (UVS)	15	10	12	100	0.12	0.06–0.35 μ m range, <0.3-nm spectral resolution, IFOV <1 mrad
Thermal Spectrometer (TS)	43	26	32	3	11	7 - 500 μ m, imaging FTS, IFOV <250 μ rad, 50-cm aperture
Ground-Penetrating Radar (GPR)	36	45	30	100	0.30	Profiling of thermal, compositional, and structural horizons, ice penetration between 0.1 and 3 km at 10-m vertical resolution and between 2 and 30 km at 0.1 km vertical resolution, 0.1 km horizontal resolution, wavelengths of 10–30 cm, globally distributed measurements
Laser Altimeter (LA)	15	21	0.012	1	0.012	Time-dependent globally-distributed topography to 1-m vertical accuracy, horizontal resolution <1 km along the ground track, range up to 2000 km altitude
Magnetometer (MAG)	4	2	0.004	1	0.004	Vector magnetic field to accuracy <0.1 nT, 0.05-s time resolution including low-altitude globally distributed passes over each satellite
Plasma Spectrometer/Energetic Particle Detector (PS/EPD)	25	15	0.002	1	0.002	Plasma composition, moments and differential directional fluxes for energetic charged particles (protons, electrons, ions) at eV to MeV energies, 1–30-s time resolution, elemental mass, energy, and angle distributions
Radio Science – Gravity Investigation	-	-	-	-	-	Uses the telecom system, for X-/Ka-band two-way coherent Doppler and range measurements
Radio Science – Atmosphere Investigation	-	-	-	-	-	Uses the telecom system's radio signal to probe Jupiter and satellite atmospheres during occultations of Earth. USO included as part of telecom system for one-way frequency stability
Total	228	234	-	-	-	

distanced from the sensors in a central shielded vault. The payload design includes such a vault with space for up to the equivalent of 24 6U cards.

The downlink data rate from JSO at Jupiter will typically be ~600 kb/s at the worst-case range to Earth, station elevation angle, etc. (see §4.5) and as high as 1600 kb/s at minimum range and maximum DSN elevation angle. At this lower rate, and assuming outages of ~40% of an orbital period for occultations by Ganymede when in the 200 km circular orbit, the downlink data volume for science will be about 9 Gb per 8-hr DSN pass.

This data volume limit places severe constraints on the return from high-data-rate instruments. High data reduction factors on the raw data rates of some likely instruments will need to be applied through compression and/or editing, and the highest data rate instruments will have stringent duty cycle limitations. Representative data acquisition scenarios are presented in §4.5. The observing scenarios during close encounters and when in orbit about Ganymede are expected to include continuous observing with the fields and particles instruments but only periodic bursts of data collection for the rest of the

instruments, except that the laser altimeter will also operate continuously when in the 200-km circular orbit phase. The laser altimeter and ground-penetrating radar will only work at close range (assumed < 2000 km) and may be able to operate continuously when below this range during satellite flybys and near periapsis in the elliptical orbit about Ganymede. The remote sensing instruments will typically obtain data in frames or cubes targeted to specific features of interest. Single-frame plus single-cube coverage of such features by all remote sensing instruments will be limited to a few targets per day. For distant observing with the spectrometers, the S/C will need to be able rock slowly and smoothly to provide the second spatial dimension of the spectrometer cubes (40 μ rad/s to 9 mrad/s with rate stability to < 10% of the commanded rate). Care will need to be taken in the S/C ACS implementation to provide the capability to execute such scans without exciting unacceptable modes due to the boom appendages. A fallback position would be to have the spectrometers all include internal scan mirrors in their designs, but this approach is not the baseline.

The science observing scenarios are described in §4.5. In general, the space physics instruments will be operated continuously starting no later than 6 months prior to Jupiter arrival. During Jupiter approach and the initial two-year Jupiter tour, the remote sensing instruments will concentrate on obtaining Jupiter atmospheric measurements, monitoring Io's volcanic activity, and obtaining global scale, multispectral coverage of the Galilean satellites. Some high-resolution observations, including use of the laser altimeter and ground-penetrating radar, will be obtained during close satellite flybys. Global-scale multispectral coverage of limited segments of the satellites will be possible during approach to and/or departure from such flybys. After entering the elliptical orbit about Ganymede, additional high-resolution coverage (including laser altimeter and ground-penetrating radar) of selected targets on Ganymede will be possible from low-altitude periapsis passes. During the more distant portions of each orbit, global multispectral mapping of Ganymede at improved resolution will be obtained and continuing observations of Jupiter, Io, and

other Jovian system bodies will be made. For the baseline mission's circular 200-km altitude orbit phase, the emphasis will be on detailed gravity and magnetic field mapping, laser altimeter measurements of the global shape, and ground-penetrating radar coverage along with continued high-resolution multispectral coverage of selected targets of interest using the remote sensing instruments.

Throughout the course of the Ganymede orbital phases (including the circular orbit period), extensive remote sensing instrument power cycling will be required. S/C power limitations do not permit all the instruments to be operated at 100% duty cycle for extended periods (i.e., longer than ~5 hours). The average power available for remote sensing instruments (including GPR and LA) will be < 50% of their normal operating power levels. Instruments will need to have reduced-power modes into which they can be switched thousands of times without incurring damage due to thermal cycling.

To achieve the Ganymede geophysical objectives connected with characterizing the subsurface ocean and the overlying icy shell, the spacecraft orbit must be reconstructed to an accuracy of 1 m in the radial direction. To achieve this level of accuracy, adequate levels of Doppler tracking (dual frequency is preferred) are required, and thruster firings must be restricted to not more than one per 24 hours for at least the first two Ganymede days in low orbit.

Table 4.2-2 presents the estimated resource requirements for each instrument and for the total payload.

Radiation shielding is a common concern for all instruments. Detailed design work in these areas is beyond the scope of the present study but is needed for specific instruments as they are conceived and proposed. The allocated masses presented here are estimates based on analogous instruments on previously flown missions with consideration of the mass needed for radiation shielding. Detailed descriptions along with specific issues for each instrument follow.

4.2.3 Instrument Descriptions

High-res Camera + VIS-NIR Hyperspectral Imager

The notional High-res camera+VIS-NIR Hyperspectral Imager System (HRC+VHS)

employs a shared 50-cm aperture f/8 telescope feeding a camera and a 3-arm spectrometer. The two instruments share the focal plane. The telescope is a 3-mirror anastigmat design, which provides a wide enough field of view (FOV) to allow both instruments to share the focal plane

The High-res Camera (HRC) has an IFOV of $2.0 \mu\text{rad}$ yielding a pixel footprint on the surface of 0.4 m from a 200-km orbit. For imaging at this high resolution from a low circular orbit, a pushbroom imager with a wide swath is best. However, the HRC also serves as the prime imaging instrument for observing Jupiter, Io, and other distant objects in the Jupiter system during the Jovian tour. In this mode, a framing camera is more desirable. We envision an HRC system that uses a 2048×2048 CCD or CMOS array. The detector needs to be cooled to $\sim -80^\circ\text{C}$ for adequate signal-to-noise (SNR) performance. A radiation shield around the detector and its co-located electronics (~ 1 cm of tantalum, mass of ~ 1 kg) will be required to ensure adequate SNR performance whenever the spacecraft is inside roughly the orbit of Europa. The rest of the electronics can be located remotely in a shielded vault. While the notional HRC employs FPGAs, they will be replaced by radiation-hard ASICs if necessary. The HRC includes a 10-color filter wheel. A block diagram for the HRC is shown in **Figure 4.2-1**.

In the 200-km orbit with nadir viewing, the FOV will move one image line in 0.23 ms; adequate SNR can be achieved for integration times this short only for a broadband clear filter with binning of perhaps 5×5 pixels. Full-resolution unbinned panchromatic images require integration times of ~ 10 ms and can be obtained without smear only for more distant observations or by using S/C attitude scans to provide target motion compensation. Color imaging will require integration times of perhaps 100 ms and will be possible for distant or target-motion-compensated observations or by binning perhaps 15×15 pixels in the 200 km orbit. Images are read out in < 0.4 s to allow contiguous single-color coverage along track in the 200-km orbit and to minimize radiation noise when close to Jupiter. With 12-bit encoding, the raw output data rate is 126 Mb/s. Real-time data reduction by a factor

of ~ 3 is envisioned internal to the instrument via lossless compression. The data then are transferred to the bus C&DH with an output data rate of ~ 40 Mb/s. The HRC will have similarities to the MRO HiRISE, Deep Impact HRI, and Cassini NAC cameras.

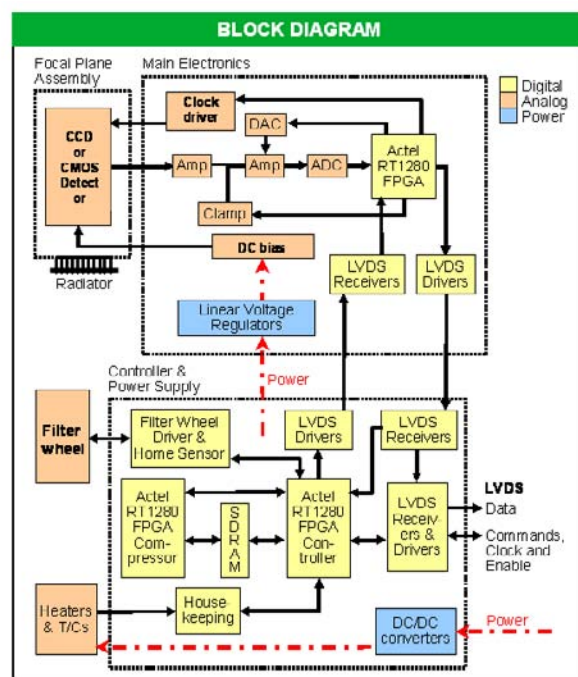


Figure 4.2-1. HRC Block Diagram

The VIS-NIR hyperspectral (VHS) portion of the instrument has its slit located alongside the camera detector in the focal plane of the shared telescope. A set of relay optics provides a 1.5:1 magnification resulting in an effective spectrometer focal ratio of f/5.33. A set of dichroic beamsplitters separates the incoming beam to feed 3 spectrometer arms covering $0.4\text{--}2.5 \mu\text{m}$, $2.5\text{--}4.8 \mu\text{m}$, and $4.8\text{--}5.3 \mu\text{m}$. Each spectrometer uses a $640 \text{ spectral} \times 480 \text{ spatial}$ HgCdTe detector array. Not all of the spectral pixels are used in the two longer wavelength spectrometers; a total of 1380 spectral channels is output. The detectors have $27\text{-}\mu\text{m}$ square pixels, which results in an IFOV of $10.1 \mu\text{rad}$ and a swath width of 4.86 mrad . The detectors need to be cooled to $\sim 80\text{K}$ for adequate SNR performance. A passive radiator provides the required cooling for both the spectrometer and camera detectors. Radiation shielding around the three spectrometer detectors and their associated electronics will be similar to that used in the HRC. The radiation shield for each detector is estimated

to require 1.3-cm thick tantalum with a mass of 2 kg. The signal-chain electronics co-located with the detectors also require shielding of 0.5-cm thick tantalum with a mass of 0.5 kg for each. A block diagram of the VHS is shown in [Figure 4.2-2](#).

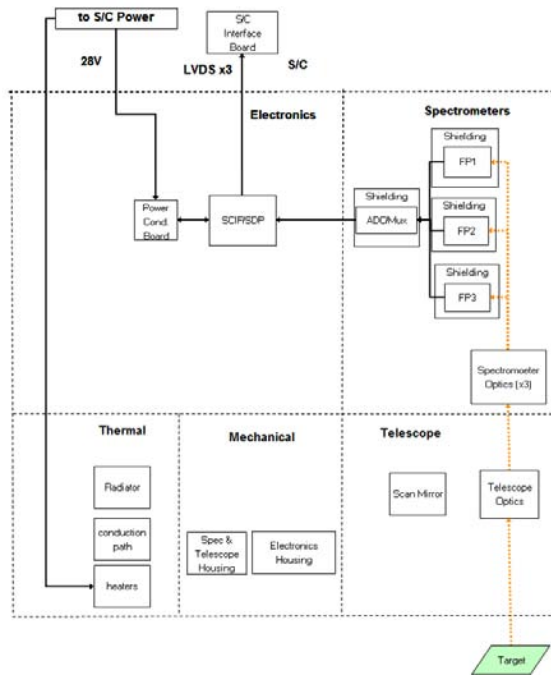


Figure 4.2-2. VHS Block Diagram

For viewing distant targets, integration times of a few 10s of seconds will provide adequate SNR at the full spatial and spectral resolution capabilities of the instrument. In the 200 km orbit with nadir viewing, the projected slit will move one IFOV in 1.1 ms; adequate SNR can be achieved across the spectral range only by accepting degraded spectral resolution (~ 10 nm) and reduced spatial resolution ($\sim 8 \times 8$ pixel binning). With 12-bit encoding, the raw full-resolution output data rate is 3.5 Gb/s. Real-time data reduction by a factor of ~ 100 are envisioned internal to the instrument via editing, binning, summing, and compression. Any number of spatial and spectral editing/summing modes could be included. The data then are transferred to the bus C&DH with an output data rate of ~ 40 Mb/s. More distant observations or those obtained with slower scanning rates can have longer integration times and lower data rates. The VHS will have similarities to the Chandrayaan M³ spectrometer.

Medium-Res Camera

The notional Medium-res Camera (MRC) has an IFOV of $20 \mu\text{rad}$ yielding a pixel footprint on the surface of 4 m from a 200 km orbit. The f/6 optics have a 6-cm aperture. To provide context coverage for the HRC images and the imaging spectrometers, a swath width of 8 km from 200-km altitude is desired; therefore, a detector with 2048 pixels across track is warranted. Radiation shielding is similar to that described for the HRC. The MRC is limited to a single panchromatic band to keep the data volume acceptably low. The baseline includes twin MRC optics viewing fore and aft along track with $\sim 30^\circ$ separation angle to obtain stereo images of a given target area on the same orbital pass and thus with the same lighting geometry (alternatively, a two-position forward/aft steerable mirror, with stereo obtained on repeated ground tracks, could be used). The block diagram for the MRC is the same as that for the HRC shown in [Figure 4.2-1](#), except that the MRC has dual optics and camera heads for stereo.

Because the MRC will be used to make distant observations during the orbital tour and in the elliptical orbit about Ganymede, it is envisioned as a framing camera. In the 200-km circular orbit, orbital motion moves a nadir pixel by its dimension in 2.3 ms. Adequate SNR can be achieved for integration times this short for a broadband clear filter. Frames taken every 4 seconds will provide continuous coverage along the ground track of the 200-km orbit. Images are read out in < 2 s to minimize radiation noise when at or inside the orbit of Europa. Assuming 12-bit encoding, the raw instrument output data rate is 25 Mb/s from each camera. Real-time data reduction by a factor of 3 is envisioned via compression. The data are then transferred to the bus C&DH with an output data rate of 8 Mb/s from each camera. The MRC will have similarities to the Stardust NAVCAM, the Dawn Framing Camera, the pushbroom Mars Express HRSC, and Chandrayaan Terrain Mapping Camera.

Laser Altimeter

The notional Laser Altimeter (LA) is a diode-pumped Nd-YAG laser transmitting at $1.064 \mu\text{m}$ and including a sensing telescope and time-of-flight sensing electronics. Its range precision is ~ 10 cm. The baseline design includes a 5-spot cross pattern of 0.25 mrad

diameter spots. Each 3-ns pulse produces 200 μJ of energy. Pulses will be transmitted at a rate of 30 Hz. Its output data rate is 12 kb/s. Any data reduction via compression/editing/summing is expected to be done in the S/C computer.

Shielding is anticipated for most sensitive components, including detectors and electronics. While the notional LA employs FPGAs, they will be replaced by radiation-hard ASICs if necessary. The fiber optics in the lasers will require an active mitigation approach such as photobleaching to anneal out radiation-induced color centers [Ott, 1998]. The LA is similar to the Mars Global Surveyor's Mars Orbiter Laser Altimeter

(MOLA) instrument, the Near Earth Asteroid Rendezvous' Laser Rangefinder (NLR; **Figures 4.2-3 and 4.2-4**), and the Lunar Orbiter Laser Altimeter (LOLA) for the Lunar Reconnaissance Orbiter.

Ground-Penetrating Radar

The notional Ground-Penetrating Radar (GPR) is a dual-frequency sounder (nominally ~ 5 MHz with ~ 1 -MHz bandwidth and ~ 50 MHz with ~ 10 -MHz bandwidth). The higher frequency band is necessary to provide high spatial resolution (footprint and depth) for studying the subsurface above 3-km depth at high (10 m) vertical resolution. The low-frequency band is designed to penetrate into the deep subsurface at a depth of up to 30 km

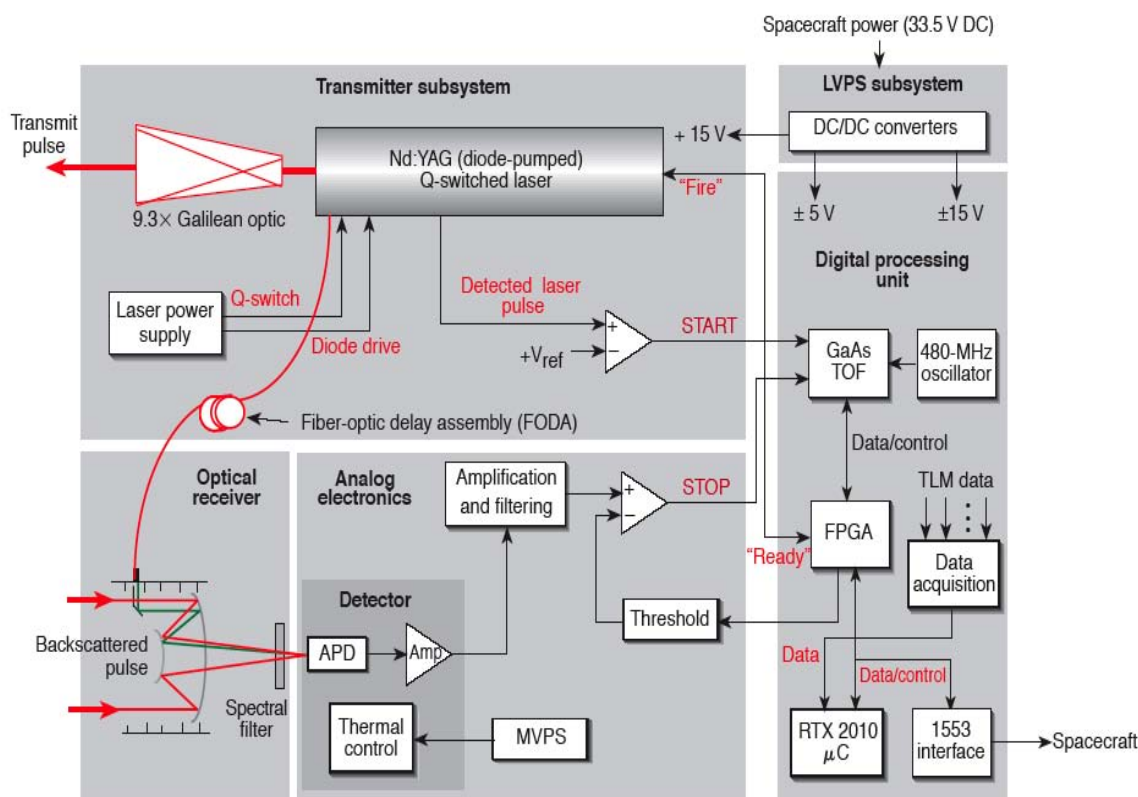


Figure 4.2-3. Block diagram of the NEAR Laser Rangefinder, a similar type of instrument to what would be flown on JSO. The five subsystems of the NLR instrument consist of the transmitter subsystem, the low-voltage power supply (LVPS), the optical receiver, the analog electronics, the digital processing unit. Gray areas indicate these subsystems. Red lines indicate optical signals (laser light). Thresholding is used both to start the time-of-flight (TOF) counters (START) and to stop the same counters (STOP). APD = avalanche photodiode; μC = microcontroller; FPGA = field-programmable gate array; MVPS = medium-voltage power supply; TLM = telemetry data [from Cole, 1998]. The physical decomposition of the subsystems is indicated by the grey boxes. The "Detector" cannot be separated from the Optical Receiver. The other subsystems may be separated for radiation shielding [from Cole, 1998].

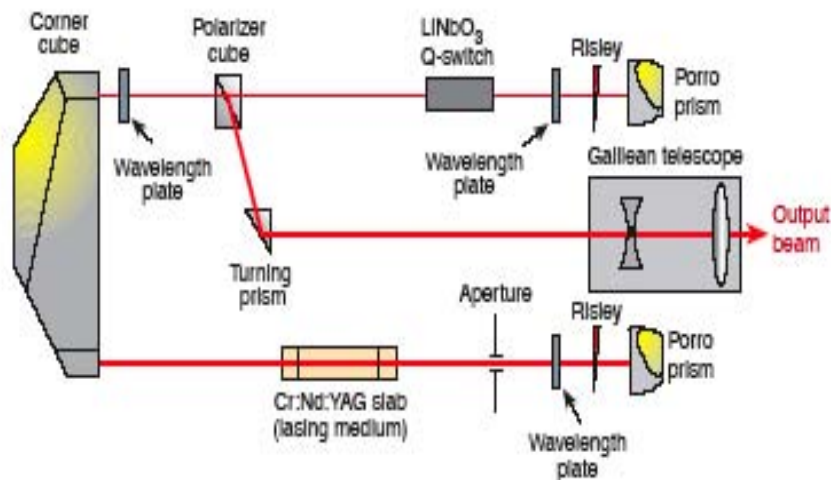


Figure 4.2-4. Optical Schematic from the NEAR Laser Rangefinder. NLR laser resonator cavity configuration is a polarization-coupled U-shaped cavity design. The CR:ND:YAG zigzag slab is side-pumped by a diode laser array to optimize conversion efficiency [from Cole, 1998].

(and a vertical resolution of 100 m). This band is necessary to mitigate the risks posed by the unknown subsurface structure both in terms of unknown attenuation due to volumetric scattering in the shallow subsurface and thermal/compositional boundaries that may be characterized by brine pockets. Additionally, the low-frequency band is less affected by the surface roughness that can attenuate the reflected echo and clutter noise. However, because the low-frequency band is vulnerable to Jupiter noise when operating on the Jovian side of the moon, it is necessary to increase the radiated power compared to space-flight hardware currently deployed for subsurface studies of Mars.

The instrument will use a dual antenna system with a nadir-pointed 50-MHz Yagi array with a backing element that also serves as a dipole antenna for the 5-MHz system. Because this instrument is a depth sounder with variable vertical resolution, there is no FOV requirement. The GPR Functional Block Diagram is shown in **Figure 4.2-5**. The transmitter matching network box #2 is located close to the antenna box. The digital electronics and receiver are located in box #1, which could be in a remotely located shielded vault. The two boxes can be combined to save mass if needed.

256 Mbits of internal non-volatile memory is envisioned. The GPR will rely on its own processing capability. Range compression,

pre-summing, Doppler filtering, data averaging, and re-sampling are done internal to the instrument to reduce its normal output data rate to ~280 kb/s. Unless a radiation hard FPGA is developed, an ASIC will be required for the digital subsystems; such an ASIC development has been included in the baseline cost estimate.

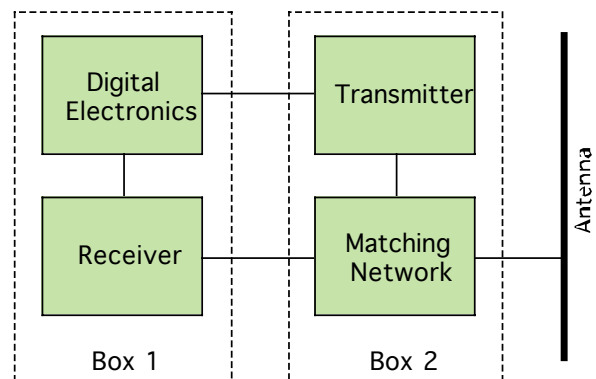


Figure 4.2-5. GPR Functional Block Diagram

Electromagnetic interference must be considered in the S/C design from the start. These requirements need to flow down to all S/C and science subsystems. Special care must be taken in shielding cables and other subsystems. Space-qualifiable parts that can be radiation hardened to 1 Mrad are currently available.

There are essentially two operating modes for the GPR. Because the global surveying mode is achieved with onboard processing and the deeper targets will benefit from better

relative sampling along track, both the shallow high-resolution and deep low-resolution surveys (i.e., < 3 km depth targets at 10 m resolution and < 30 km depth targets at 100 m resolution, respectively) will have similar power consumption and data rates of ~45 W and ~280 kb/s, respectively (noting that the deeper targets will benefit from better relative sampling along track). Radar tracks will be restricted by data volume limitations to less than 30 min per orbit in the low-orbit phase. During flybys and in the elliptical orbit, the GPR is only useful at ranges < 2000 km. Standby power will be ~20 W for the non-operating portions of the orbits. When the GPR is off for extended periods, 10 W is needed for heaters. A second mode capable of capturing short bursts of raw radar data (~30 seconds at 30 Mb/s producing a post-processing swath ~20 km long) will also be available for targeted surveys using full power for several minutes, producing ~900 Mb of data.

The GPR will have similarities to the Mars

Advanced Radar for Subsurface and Ionosphere Sounding (MARSIS) instrument on Mars Express and the Shallow Radar (SHARAD) instrument on the Mars Reconnaissance Orbiter (MRO).

Thermal Spectrometer

The notional Thermal Spectrometer (TS) is envisioned to be based on Cassini CIRS heritage (see [Figure 4.2-6](#)). It has a spectral range of 7–40 μm (with a goal of extending the longwave sensitivity up to 500 μm). Spectral resolution of 0.5 cm^{-1} is achieved using a pair of Fourier Transform Spectrometers (FTSs), one for the mid-IR and one for the far-IR. Its f/6 telescope has a 50-cm aperture and is passively cooled to ~170K. The Mid-IR spectrometer includes two 1 × 10-pixel HgCdTe detector arrays one of which covers the 7–9- μm range and the other that covers the 9–17- μm range. The IFOV of these detectors is 250 μrad . These detectors are passively cooled to ~80K. A detector radiation shield of ~1 kg is included. An internal blackbody calibration source is provided with a flip

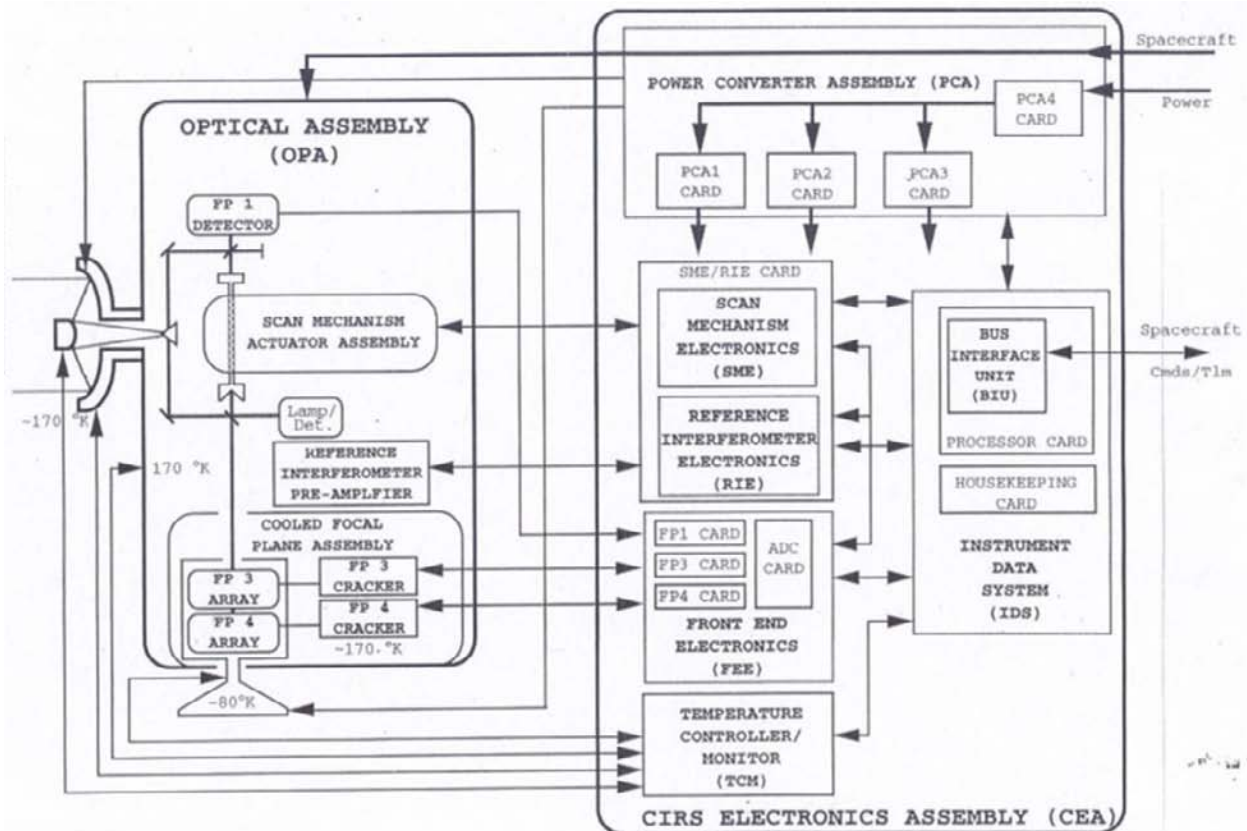


Figure 4.2-6. Thermal Spectrometer Block Diagram

mirror to direct the Mid-IR beam to the calibration source. The Far-IR spectrometer uses a single thermopile detector with a FOV of 4.3 mrad and running at the 170K telescope and housing temperature.

The integration time for one pixel of smear is 28 ms from a 200 km orbit. With data encoded to 16 bits/pixel, the raw data rate is 32 Mb/s. Data compression of 3:1 is applied internal to the instrument. Data summing can be done to improve SNR or reduce data rate. Except for detector preamps and thermal control sensors, the TS electronics are located in a separate enclosure from the optics and detectors where they are shielded adequately against radiation damage.

Magnetometer

The notional Magnetometer (MAG) is a fluxgate magnetometer similar to those flown on several other missions including Galileo at Jupiter. It comprises two DC magnetic sensors mounted on a 10-m boom, one at the tip and the other about half way out from the spacecraft. Fluxgate instruments rely on the hysteresis effect found in ferromagnets. Two solenoids with ferromagnetic cores wound in opposite directions are driven with a sufficiently high frequency (several kHz) current to drive them into saturation. The difference field between these coils is sensed by a third coil, which sees a second harmonic of the primary field. This second harmonic field is rectified and smoothed and is directly

proportional to the background field. The rectified field is exceptionally linear and is digitized using A/D converters. Newest magnetometers use the sigma-delta technique to digitize the signal using a single bit A/D converter and over-sampling. The sigma-delta magnetometers are exceptionally radiation hardened. A block diagram of the MAG is shown in [Figure 4.2-7](#).

The highest cadence rate required is 32 vectors/s to measure the ion cyclotron waves near Ganymede. The expected field range over the whole mission is 0–1000 nT. The magnetic field of the spacecraft at 5-m distance along the boom must be < 0.1 nT with a variation of < 0.03 nT.

The sensor is mounted at the end of the boom and has no active electronics. The magnetometer electronics will be housed in the spacecraft vault. The baseline MAG is capable of data processing and requires two electronics cards. It incorporates a CPU and internal RAM (< 2 MBytes) for data processing and burst mode. The baseline instrument can manage I/O and data processing and limited storage (to avoid blackouts at critical times). The output data rate is 2 kb/s per sensor (uncompressed).

The dual magnetometer design reduces two types of risks. First, the dual magnetometer is able to quantify and therefore separate the internal field from the spacecraft from the background field. Secondly, if one magnetometer were to fail, the second one would still be able to fulfill the science role if

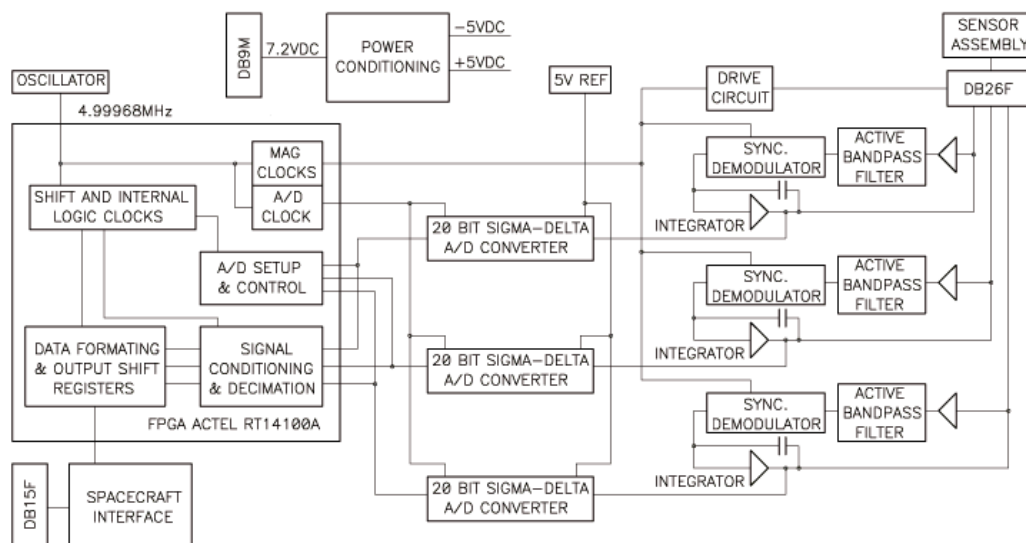


Figure 4.2-7. MAG Block Diagram

calibrations are performed in space to assess the spacecraft generated magnetic field.

Fluxgate magnetometers can easily withstand the high radiation environment of JSO. Sensors should have no problems with radiation since they have no active parts. Radiation hardened versions of all processing parts, including ADCs, opamps, analog switches, and discrete transistors, are available and will allow the construction of a magnetometer that can withstand > 300 krad without shielding.

The fluxgate sensors suffer from small but measurable drifts in their zero levels. On a non-spinning spacecraft such as for JSO, these can be measured in the solar wind by utilizing the rotational nature of the interplanetary magnetic field. Calibrations from the measured field will need to be performed once a week. Continuous data at a resolution of 1 s or better is required. Once inside Jupiter's magnetosphere, slow spacecraft spins around two orthogonal axes will be required to determine offsets. These should be performed roughly once every week. In the primary Ganymede Orbit phase, the calibration frequency could be reduced to once every month.

The MAG has similarities to instruments flown on Galileo, Polar, Fedsat, and Space Technology 5 (ST5).

Plasma Spectrometer/Energetic Particle Detector

The notional Plasma Spectrometer/Energetic Particle Detector (PS/EPD) will measure the energy and electrical charge of particles such as electrons and protons that the instrument encounters. It will determine the flux of ions as a function of mass per charge, and the flux of ions and electrons as a function of energy per charge and angle of arrival relative to the instrument. PS/EPD will measure particles with energies up to MeV levels and will determine moments of the local plasma field as well as its composition.

The instrument consists of three sensors: an electron spectrometer, an ion beam spectrometer, and an ion mass spectrometer. A motor-driven actuator rotates the sensor package to provide wide-angle scanning. The electron spectrometer consists of a collimator feeding an electrostatic analyzer. The collimator geometry and particle detectors at various positions are used to determine the direction of

the incoming electrons. Angular resolution is 20°. Variable commandable electric potentials applied in the analyzer discriminate between incoming electron energies.

The ion beam spectrometer consists of a hemispherical electrostatic analyzer having two conductive hemispheres of slightly different radius mounted concentrically one within the other with a small gap between the two surfaces. The electric field in the gap selects the range of energy per charge and angular direction that ions are allowed to have in order to pass through the analyzer. Energy spectra are taken by stepping the analyzer potential through a set of spaced values. Three apertures spaced 30° apart allow particles to enter the analyzer. Channel electron multipliers produce an output pulse of about 10^8 electrons for each entering ion.

The ion mass spectrometer provides species-resolved measurements of the flux of positively charged atomic and molecular ions as a function of energy/charge and aperture entry direction. It uses a toroidal electrostatic analyzer to discriminate energy/charge and to define a narrow field of view ($12^\circ \times 20^\circ$) combined with a time-of-flight (TOF) mass spectrometer to determine mass/charge and other species-resolving data. Particles exiting the electrostatic analyzer enter the TOF spectrometer after being accelerated and passing through thin carbon foils. An electric field then directs the particles to a set of microchannel plate (MCP) detectors. The time of flight between passing through the carbon foils and reaching the MCP is related to the mass per charge for a given particle.

The PS/EPD will operate continuously within the Jovian system. The instrument is mounted on the bus so that the various sensors view the highest flux directions of incidence over part of the orbit. For example, it would optimally view into the ram over Ganymede's trailing hemisphere as often as possible.

All event processing and data compression are performed by the instrument processor; output is formatted as packets and sent to bus C&DH. The output data rate is 2 kb/s. The PS/EPD is expected to operate continuously at Jupiter.

The instrument data processing unit manages the acquisition and onboard data processing and controls sensor and actuator

motor functions. Instrument engineering data are monitored and reported. High-voltage power converters provide the necessary voltages to the various instrument components. The electronics and the sensors are shielded by 100 mils of WCu (density 15.85 g/cm³); this is the same as the Juno design, and will permit use of available parts good to ~200 krad. Additional spot shielding may be needed around the detectors. This design assumes the electronics are not housed in the common vault.

The notional PS/EPD has similarities to the Cassini Plasma Spectrometer.

Ultraviolet Spectrometer

The notional UV spectrometer (UVS) comprises a 2-D CODACON detector with simultaneous spectral and 1-D spatial coverage capabilities. The UVS will be capable of measuring atmospheric and surface composition and atmospheric density through stellar occultations, limb scans, and surface imaging.

The UVS has three channels, covering the Extreme UV (55–110 nm), Far UV (110–190 nm), and Near UV (190–350 nm) wavelength ranges. A high-speed photometer is aligned with the telescope-spectrographic channels. Images are made by scanning the slit, using the motion of the spacecraft. Stellar occultations are performed by pointing the UVS boresight at a star (via instrument articulation) and tracking the star as the spacecraft's motion along its trajectory causes the star to pass behind the limb of the satellite. The detector format is 1024 spectral × 64 spatial pixels. Each of the 64 spatial pixels is 1 mrad (× ~0.75 mrad). A 1-min swath performed in 200 km orbit will cover an area 200 m wide × 100 km long, for one of the 64 pixels.

To obtain full spatial resolution on the surface of Ganymede in the 200-km orbit, frames will need to be acquired every 85 ms. Assuming 16-bit encoding, the raw uncompressed full-resolution data rate would be 12 Mb/s. Substantial editing, binning, and compression will be accomplished internal to the instrument. During global mapping at 200 km, the output data rate will be reduced to 120 kb/s by using a combination of such techniques.

Prior to launch, the instrument will be calibrated in the laboratory in manners similar

to UV instruments on past missions. The post-launch interplanetary phase will be important for performing stellar calibrations to check instrument behavior with time. Observations of objects such as the Moon and asteroids will aid calibration and testing of data processing techniques.

The UVS has similarities to the Cassini Ultraviolet Imaging Spectrometer (UVIS).

Radio Science

The planning payload includes provision of a dual-frequency (X and Ka band) transponder in the spacecraft telecommunications system, providing 2-way coherent Doppler tracking and range measurements required for orbit reconstruction in support of geophysics (and navigation). Noise in the Doppler measurements is dominated by line-of-sight plasma effects in the solar wind and the Earth's ionosphere. Having multiple frequencies (X- and Ka-band) permits the best job of removing these adverse effects, yielding improvement over the 0.1 mm/s (30-s integration time) provided by X-band tracking alone. The telecom system also includes a USO for use during atmospheric occultation measurements.

4.3 Mission Design Overview

The baseline mission design calls for launch on a Delta IV 4050H-19 from CCAFS/KSC onto a VEEGA (Venus-Earth-Earth Gravity-Assist) trajectory to Jupiter. After performing a 3-year tour of the Jovian System the spacecraft enters an “elliptical” 3-body orbit around Ganymede. After 1 year in that orbit it transfers to a 200-km polar, circular orbit of Ganymede. [Table 4.3-1](#) gives a detailed description of these mission phases and their durations.

The JSO mission design is particularly interesting in both its Jovian system science-rich tour and for its innovative orbital phase. The orbital phase makes use of a stable, high-inclination, “elliptical” Ganymede orbit. This orbit is strongly perturbed by Jupiter and, as a result, precesses around Ganymede. Additionally, the perturbations drive large, periodic changes in altitude (see [Figure 4.3-2](#)). This variation gives a diverse sampling of Ganymede's magnetosphere and the perturbed Jovian field outside of Ganymede's magnetosphere.

4.3.1 Interplanetary Trajectory

The current design uses a January 2017 VEEGA trajectory to Jupiter (see [FO-2A](#)). However, the spacecraft is designed to make use of any of several VEEGA trajectories that launch between 2015 and 2022. These trajectories range in flight time from 5.5 years to 7.1 years.

[Table 4.3-2](#) shows a subset of VEEGA trajectories available in 2016–2022. Of these, the January 2017 VEEGA is used as the baseline for the spacecraft design. Therefore, the spacecraft can launch on any of the VEEGA trajectories in this table.

It should be noted that the Europa Explorer (EE) Mission Study is using the 2015 VEEGA. Because JSO is not quite as well developed as EE, 2016 was the earliest launch year considered in this mission design analysis. It is also worth noting that the 2016 trajectory shown in [Table 4.3-2](#) actually arrives after the baselined 2017 trajectory and would only be a reasonable choice if the extra mass delivered is needed.

For the 2017 VEEGA, the 21-day launch period starts on Dec. 24, 2016 with a C_3 ranging from 9.3 to 10 km²/s². Over the launch period, the Deep Space maneuver (DSM) ranges from 258 to 264 m/s.

Table 4.3-1. Mission Phase Definition and Description

Phase	Activity	Duration
Interplanetary	Launch and Early Operations: Begins with the launch countdown. Activities include initial acquisition by the DSN, checkout and deployment of all critical spacecraft systems and a potentially large maneuver to clean-up trajectory errors from launch vehicle injection	1 month
	Cruise: Activities include engineering and science checkouts, calibrations and maintenance, Venus and Earth gravity assist flyby science operations, potential asteroid flyby target-of-opportunities, trajectory correction maneuvers, and operations readiness testing.	5–7 years
	Jupiter Approach: Activities include final preparations, training, and ORTs for all mission elements in preparation for JOI and Jovian moon flybys, and an optical navigation campaign to determine satellite ephemerides prior to pre-JOI lo flyby.	6 months
Jovian Tour (3 years)	JOI & Capture Orbit: Starts with lo flyby just hours prior to JOI at 4 RJ and then a 6-7 month initial capture orbit with a perijove raise maneuver at first apojoove to counter solar perturbations	9–12 months
	lo Sub-tour: Starts at 2nd lo encounter, total of three lo encounters during lo Sub-tour, characterized by low Jupiter (i.e., high radiation) periapses and moderately-large orbits	
	EGC Sub-tour: Starts at first satellite encounter after last lo encounter. ~19 Europa, Ganymede, and Callisto encounters including extensive Jupiter system science data acquisition.	18–21 years
	Ganymede Approach: Starts after last Callisto encounter and includes the final four flybys of Ganymede and large maneuvers leading up to GOI and Ganymede orbit.	~6 months
Ganymede Science	<u>Elliptical Orbit</u> Starts with GOI. Includes high-altitude Ganymede observations, periodic lo and Jupiter monitoring, and high resolution Ganymede observations when @ low altitude	1 year
	<u>Circular Orbit</u> 200 km altitude, near-polar, circular Ganymede orbit. Continuous high resolution Ganymede observations	1 year
Extended Ganymede Science	Spacecraft could continue in Ganymede orbit for an extended mission as allowed by funding and spacecraft health and propellant.	
Disposal	Orbit will naturally impact Ganymede at spacecraft end of life	

Table 4.3-2. VEEGA Trajectories

Launch mm/dd/yyyy	Arrival mm/dd/yyyy	TOF years	Launch C_3 km ² /s ²	DSM V km/s	Arrival V_∞ km/s
01/01/2015	07/24/2021	6.56	12.6	0.07	6.30
06/12/2015	07/4/2021	6.07	14.1	0.21	6.20
09/13/2016	10/08/2023	7.07	11.6	0.07	6.17
01/03/2017	09/11/2022	5.65	10.0	0.26	6.09
09/28/2018	10/06/2025	7.02	13.4	0.00	6.19
03/22/2020	02/24/2026	5.93	9.8	0.03	5.56
05/24/2021	03/22/2028	6.83	12.8	0.00	5.73

Table 4.3-3 details the 2017 VEEGA trajectory used for the interplanetary trajectory design.

Table 4.3-3. 2017 VEEGA Trajectory [middle of Launch period case]

	Date (Jupiter's closest approach and Io Flyby)	Alt	Vinf
	ET/SCET	km	km/s
Launch	03-Jan-2017		3.0
Venus	27-Apr-2017	1693	4.8
Earth	14-Jan-2018	3136	7.9
Earth	09-Apr-2020	300	9.6
JOI	11-Sep-2022		4.6

4.3.1.1 Jupiter Approach and Capture

Prior to the Jupiter Orbit Insertion (JOI) the spacecraft performs a flyby of Io to reduce its orbital energy relative to Jupiter. Three hours after this flyby the 660 m/s JOI maneuver captures the spacecraft into a large, 6–7 month orbit. At apojove of this orbit a 165 m/s Perijove Raise (PJR) maneuver is used to raise periapsis and reduce the Io V_{∞} at the next encounter from 15.1 km/s to 10.5 km/s.

4.3.1.2 Jovian Tour

JSO performs a three-year tour of the Jupiter system (see **FO-2C**). During this tour, science observations of the Galilean satellites, and Jupiter's atmosphere and magnetosphere

are conducted. Jovian Tour is comprised of three principal sub-phases: Io Science Sub-tour, EGC (short for Europa-Ganymede-Callisto) Sub-tour, and the Ganymede Approach. Exceeding the science requirements defined by the SDT, the mission plan calls for 4 flybys of Io, 6 flybys of Europa, 11 of Callisto, and 7 of Ganymede prior to the Ganymede Science phase.

The reference tour for JSO (**FO-2C** and **Table 4.3-4**) should be viewed simply as a proof-of-concept. It is expected that the actual tour that would ultimately be designed may differ in many ways from this example, depending on the eventually agreed-upon scientific, engineering, and programmatic constraints. In responding to the study assumptions, this reference tour for JSO has a deterministic ΔV of 110 m/s and an estimated statistical ΔV cost of 60 m/s, well within the 200 m/s budgeted for the tour. It has not been optimized for science beyond simply counting the number of flybys for each moon.

During the Io Sub-tour, JSO performs three flybys of Io, resulting in a total of four counting the one prior to JOI. This requires the spacecraft to have low Jupiter periapses that

Table 4.3-4. Encounters During JSO's Representative Jovian Tour

Encounter	Body	Date ET/SCET	Alt km	V_{∞} km/s	Period days	Inclination deg	Rp R _J
I0	Io	11-Sep-2022	500	15.1	---	8.4	4.0
I1	Io	7-Feb-2023	208	10.5	53.1	11.9	5.1
I2	Io	1-Apr-2023	100	10.6	40.2	11.0	5.0
C1	Callisto	10-May-2023	500	9.3	50.0	6.2	5.5
C2	Callisto	29-Jun-2023	200	9.3	56.4	0.2	5.7
I3	Io	26-Aug-2023	100	6.9	35.5	0.2	5.8
C3	Callisto	2-Oct-2023	660	8.7	50.1	1.3	6.8
C4	Callisto	21-Nov-2023	210	8.8	83.6	0.3	7.9
E1	Europa	12-Feb-2024	376	7.1	49.5	0.4	8.2
C5	Callisto	3-Apr-2024	649	8.2	78.2	0.3	9.5
E2	Europa	18-Jun-2024	600	5.4	56.8	0.4	9.2
E3	Europa	14-Aug-2024	400	5.6	39.1	0.4	9.1
E4	Europa	22-Sep-2024	100	5.6	26.3	0.3	8.9
G1	Ganymede	18-Oct-2024	487	8.0	17.1	0.2	7.9
C6	Callisto	7-Nov-2024	1940	6.3	20.6	0.4	9.3
E5	Europa	25-Nov-2024	156	4.3	17.8	2.2	9.2
E6	Europa	13-Dec-2024	100	4.3	21.3	0.1	9.3
C7	Callisto	1-Jan-2025	237	6.4	31.1	0.1	11.6
G2	Ganymede	2-Feb-2025	1242	6.2	19.2	0.2	10.7
C8	Callisto	20-Feb-2025	100	5.6	25.1	5.7	12.9
C9	Callisto	11-Apr-2025	323	5.6	31.4	0.2	14.3
G3	Ganymede	15-May-2025	2850	3.7	21.5	0.2	13.9
G4	Ganymede	6-Jun-2025	298	3.7	11.9	0.9	12.6
C10	Callisto	13-Jun-2025	100	2.8	16.7	8.4	18.3
C11	Callisto	30-Jun-2025	661	2.8	13.8	0.2	14.8
G5	Ganymede	17-Jul-2025	100	2.0	14.2	0.1	14.8
G6	Ganymede	31-Jul-2025	100	1.9	10.6	0.2	14.4
G7	Ganymede	20-Aug-2025	1562	1.3	8.8	0.9	14.3
G0I	Ganymede	24-Sep-2025	200	---	---	---	---

go deep into the radiation belts, resulting in a larger dose per encounter than for the later stages of the mission.

EGC Sub-tour

The EGC Sub-tour uses gravity-assists to raise the Jupiter periapse out of the highest radiation environment to the less severe environment near Europa and eventually out to the relatively benign environment near Ganymede.

During this sub-phase, science flybys of Europa and Callisto are emphasized since Ganymede is the focus of the later orbital phase. The EGC-Sub-tour also gradually reduces the energy of the spacecraft with respect to Ganymede by making the spacecraft's orbit as similar to Ganymede's orbit as possible. **FO-2C** shows an example tour that starts with large, very eccentric orbits. By the end of the EGC Sub-tour, the orbits are near-Hohmann transfers between Callisto and Ganymede.

Ganymede Approach

The Ganymede Approach starts after the last Callisto flyby of the EGC Sub-tour. The goal of the Ganymede Approach is to lower the spacecraft's energy with respect to Ganymede to reduce the cost of the Ganymede Orbit Insertion (GOI) maneuver. This is done by making JSO's orbit more circular and more

like that of Ganymede. This phase consists of 2–4 Ganymede flybys with several relatively large maneuvers (20–100 m/s) in-between to keep periapse near the orbit of Ganymede.

4.3.1.3 Ganymede Science

Following the tour, the spacecraft performs an approximately 200 m/s Ganymede Orbit Insertion (GOI) maneuver to enter into a large “elliptical” orbit around Ganymede. The spacecraft leaves this orbit after a year and enters a 200 km, nearly polar circular orbit for the last year of the prime mission.

Ganymede Elliptical Orbit

This “elliptical” orbit is a 24-hour, dynamically stable, albeit non-Keplerian, 3-body orbit that spends time in both the Jupiter and Ganymede spheres of influence. This orbit is highly perturbed by Jupiter, resulting in variability of the periapsis and apoapsis distance over an approximately 42-day cycle (see **Figure 4.3-2**). It varies from a 64° inclined, almost circular 9,000 km by 10,000 km orbit to a 44° inclined 200 km by 19,000 km eccentric orbit. This orbit has been numerically verified to be stable for 1 year without any obvious secular trends in energy or eccentricity and may be stable for much longer. **FO-2D** illustrates this orbit in a sun-fixed frame and shows the groundtrack coverage of this orbit achieved after one year.

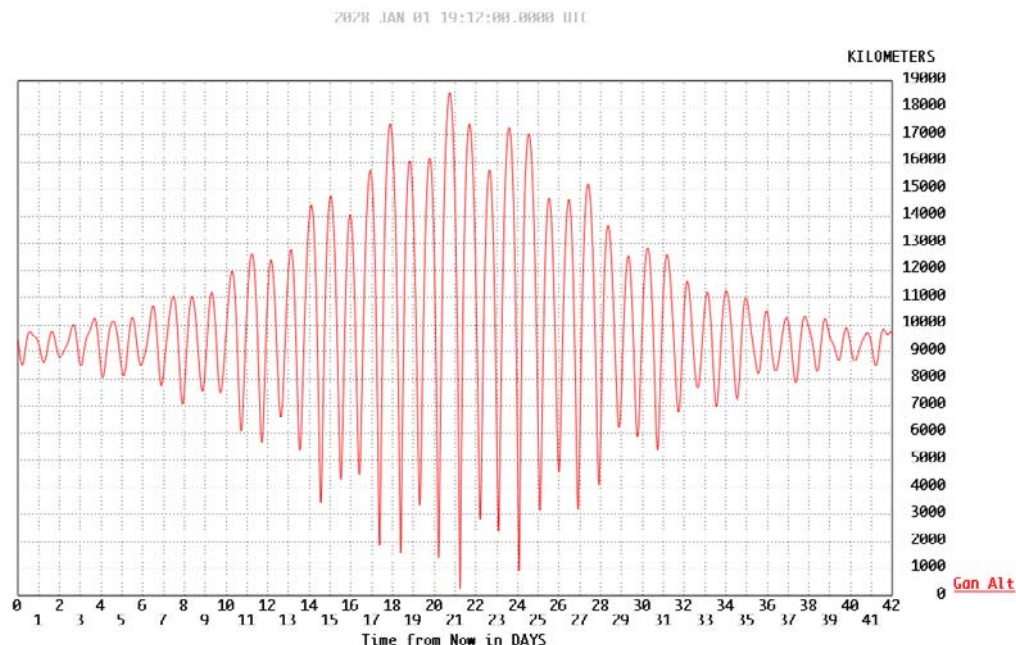


Figure 4.3-2. Altitude of Elliptical Orbit Fluctuates Periodically

Ganymede Circular Orbit

After 1 year in the “elliptical” orbit, the spacecraft enters a 200 km, 95° inclined circular Ganymede orbit. This circular orbit is unstable but controllable, requiring only 40 m/s of orbit maintenance ΔV over 1 year.

The circular orbit may be sun-synchronous (shown in **FO-2E**) or the project may choose

to vary the solar beta angle to see the surface at a variety of solar phase angles. **FO-2E** shows the groundtrack coverage achieved after one Ganymede day.

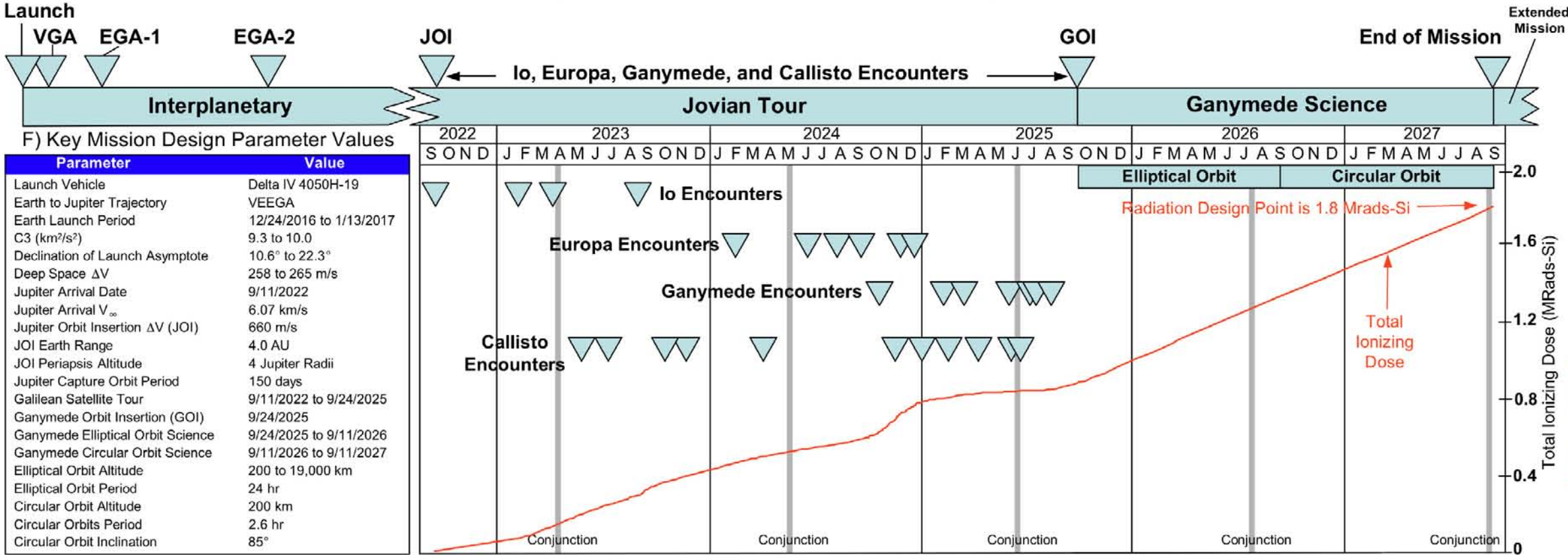
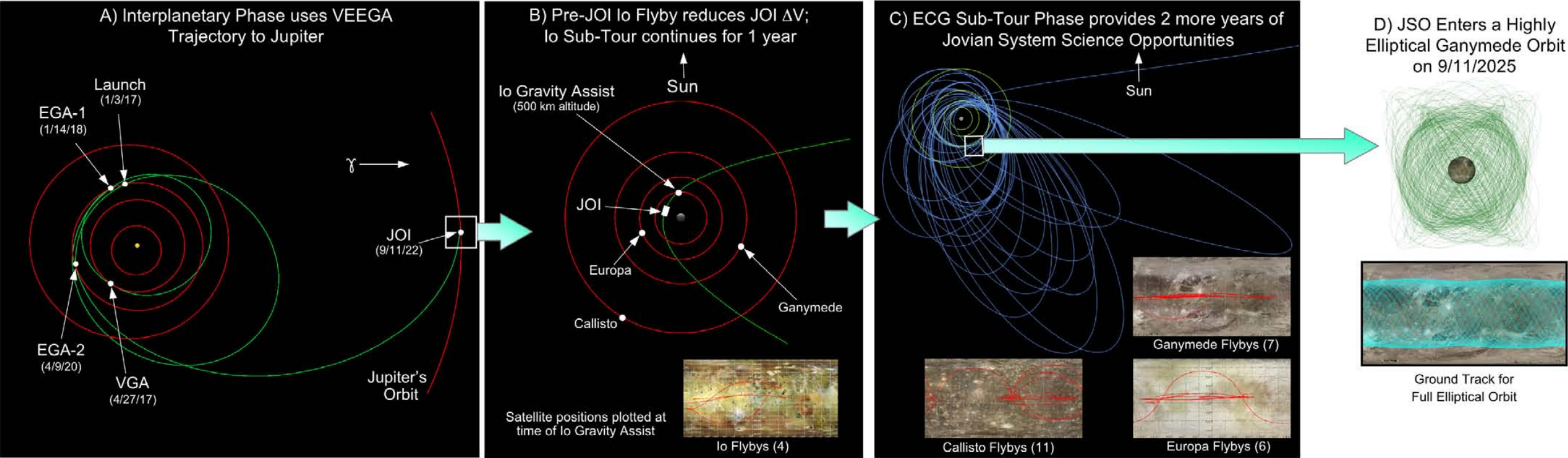
4.3.1.4 Mission ΔV

Table 4.3-5 shows the mission ΔV allocations.

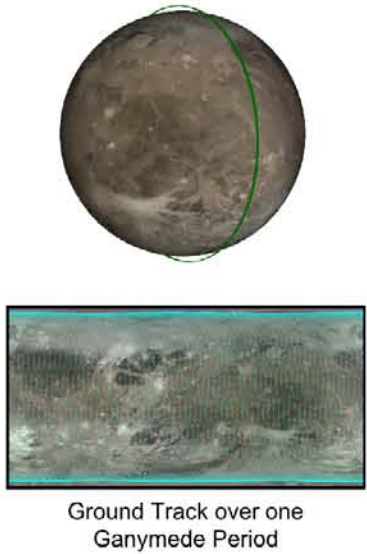
Table 4.3-5 Baseline Mission Delta V

Activity	ΔV [m/s]	Description
Launch Injection Correction	30	Correct launch vehicle injection errors.
Earth Biasing	50	Bias of aimpoint of both Earth flybys away from planet. Will be integrated with other TCMS.
DSM	265	Deep Space Maneuver. If other interplanetary trajectories in Table 4.3-2 are used, this will be lower.
Interplanetary TCMS	20	Many small statistical maneuvers
JOI	660	Jupiter Orbit insertion (at 4 R_J)
PJR	165	Perijove Raise Maneuver for Io Sub-tour
Tour	200	Jovian Tour estimate from I1 to Last Callisto flyby (C11).
Ganymede Approach	200	Deterministic maneuvers to reduce energy relative to Ganymede (from G5 to GOI)
GOI	200	Ganymede Orbit Insertion
Orbit Maintenance (elliptical)	25	Groundtrack control
Plane Change	230	Plane-change to 95-deg orbit
Circularization	620	Transfer to 200 km orbit
Orbit Maintenance (circular)	40	Groundtrack control
TOTAL	2705	

JSO Studies the Jovian System Through Close Flybys and Long-range Monitoring With In-Depth Study of Ganymede via Elliptical / Circular Orbits



E) JSO Enters a 200 km Circular Ganymede Orbit on 9/11/2026 (Descope Option)



4.4 Bus Design and Development

4.4.1 Spacecraft Overview

The JSO spacecraft is a redundant, 3-axis stabilized spacecraft powered by radioisotope power systems (RPSs) and rechargeable batteries for peak load periods (see [Figure 4.4-1](#)). The spacecraft attitude is controlled by reaction wheels (RWAs) during fine pointing for science, and by small 0.7 N thrusters for higher pointing rates and desaturating the RWAs. The 2.75 m HGA is 2-axis articulated to allow for Earth communications while the instruments are nadir-pointed during science observations. The baseline design has 9 instruments (for both fields and particle and remote sensing), plus radio science-gravity and radio science-atmospheres investigations that use the telecommunications subsystem. The 8 MMRTGs provide 778 W of electrical power at the end of mission (EOM). Redundant Li-ion batteries provide for spacecraft modes that require higher power loads than can be provided for by the RPSs alone, such as main engine maneuvers and satellite flybys (encounters).

The command and data handling architecture includes a fully redundant system based on the RAD 750 computer that performs

selected science functions and the engineering functions, including hot swapping during critical events such as launch and JOI. Redundant 150 MB mass memory is available for engineering data storage and a separate 9.6 Gb solid-state recorder (SSR) is available for science data storage. Both types of data storage use non-volatile chalcogenide memory (CRAM).

These subsystems, as well as the rest of the bus subsystems, are further described in later sections. [Foldout 3](#) is the spacecraft system block diagram.

Configuration

The driving requirements on the JSO spacecraft configuration are: 1) the large propulsion tanks; 2) radiation vaults to protect sensitive electronics; 3) eight MMRTGs; 4) the 2.75-m diameter, articulated HGA; 5) a 10 m long magnetometer boom; 6) a 30-m tip to tip ground penetrating radar antenna; and 7) a Narrow-Angle Camera that includes a 50-cm primary mirror. Flight-proven bus construction methods and techniques using carbon fiber composites will be used for mass-efficient layout of load paths. [Figure 4.4-2](#) shows a view of the instrument deck.

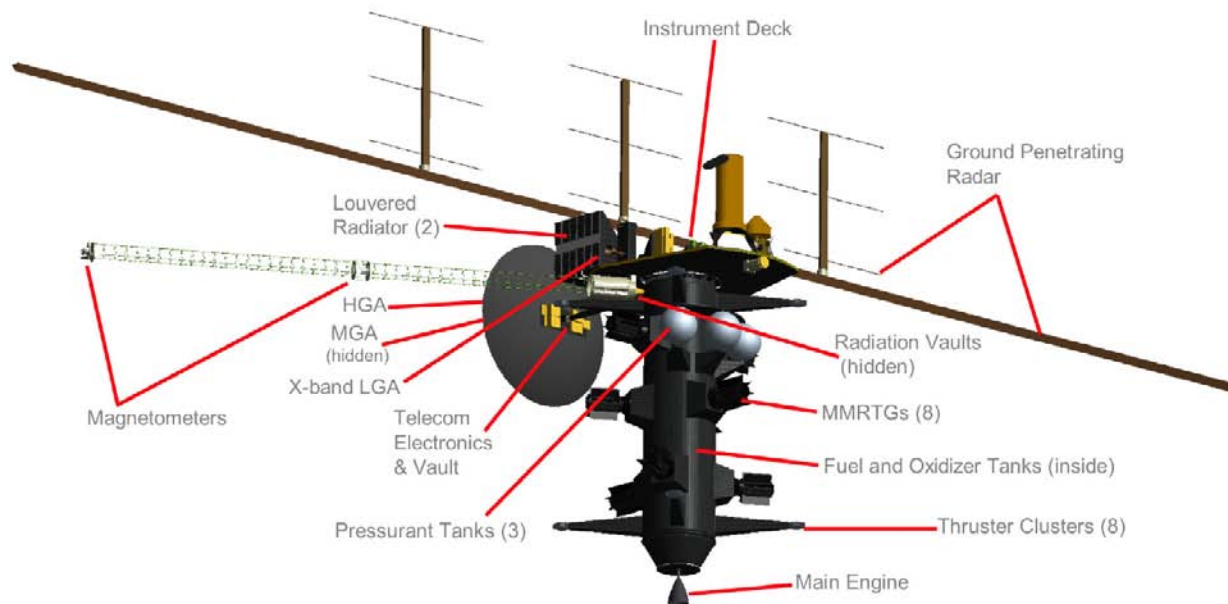
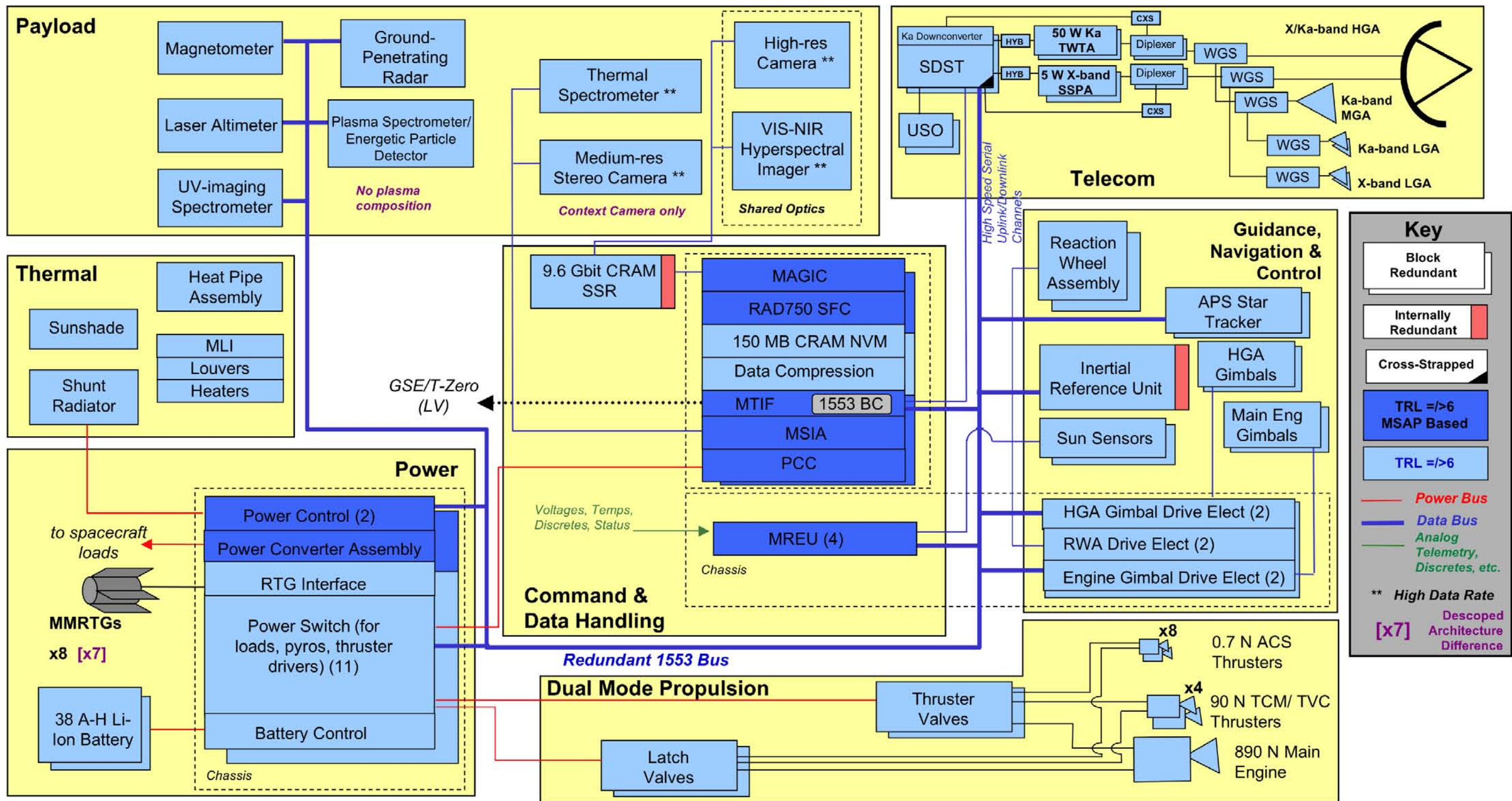


Figure 4.4-1. JSO Spacecraft



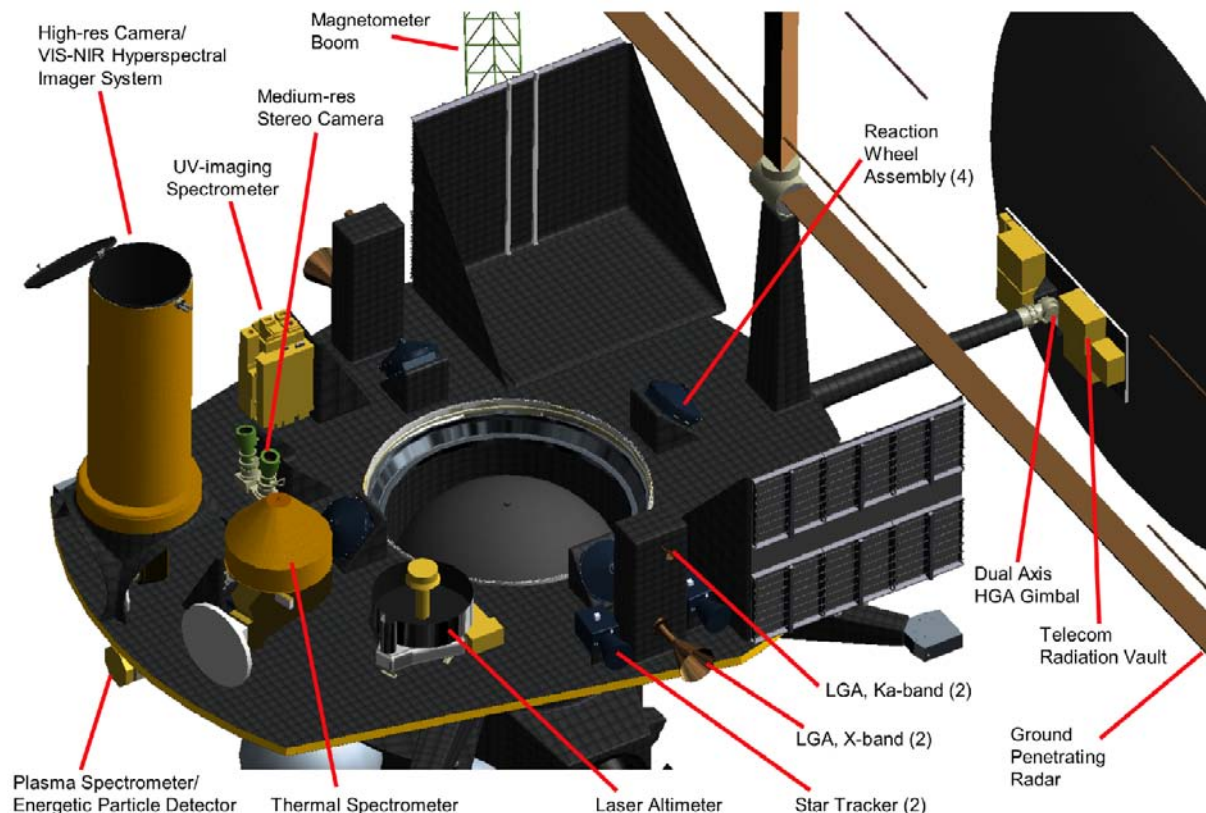


Figure 4.4-2. Instrument Deck

4.4.2 Systems Design Approach

Overview

The design approach is to leverage, where appropriate, from JPL heritage hardware and software designs such as JPL's institutional avionics product line (Multi-mission System Architectural Platform, MSAP), Juno and Cassini propulsion systems, various JPL mission telecom systems, and MSL's MMRTG. Due to the long life and harsh radiation environment, it is envisioned that circuits will be new (with upgraded parts and new analyses) but the basic architecture can be inherited.

Three specific cross-cutting areas are especially challenging for this mission: radiation, long-life, and fault protection. As the JSO design evolves, system engineering trades across these areas will represent an ongoing effort that will keep the team focused on producing an efficient, robust design. Additional discussion regarding these efforts appears in the following subsections.

4.4.2.1 Radiation

Radiation Environment

JSO is exposed to severe radiation environments of high-energy electrons, protons, and heavy ions trapped in Jupiter's magnetosphere; electrons and protons due to Earth's radiation belt; protons and heavy ions from the Sun; and protons and heavy ions due to galactic cosmic rays (GCR). Of these radiation sources that the spacecraft must deal with, the dominant contributor is the trapped particles in Jupiter's magnetosphere.

JSO's radiation environment is divided into three mission segments: interplanetary, tour, and Ganymede orbit. The radiation dose from launch to JOI is overwhelmed by the effects by the dose while at Jupiter so the focus of this study's analysis is on the tour and Ganymede orbit environments. The radiation dose during the 730-day Ganymede Science phase is calculated assuming the spacecraft is at Ganymede's distance from Jupiter but without regard to any influence of Ganymede itself. Since it is expected that Ganymede will

provide a net shielding benefit, this calculation is conservative.

The JSO spacecraft is designed to handle the extreme radiation environment of the Jovian system using a multi-level approach consisting of radiation tolerant parts and electronic designs, shielding, and a mission design that lessens the duration in extreme environments. The total predicted ionizing dose as a function of aluminum shielding thickness for JSO mission is shown in **Figure 4.4-3**. Shown without margin, JSO will receive

1.84 Mrad (Si) behind 100-mil Al spherical shell of shielding. Of this, 0.91 Mrad (Si) occurs during the launch to GOI and 0.93 Mrad (Si) during Ganymede orbiting segment of 730 days.

Figure 4.4-4 shows the dose accumulation as a function of time behind a shielding thickness of 100 mils of aluminum.

Driving Requirement

A key driving requirement that governs the JSO radiation shielding approach is the radiation capability of the semiconductor

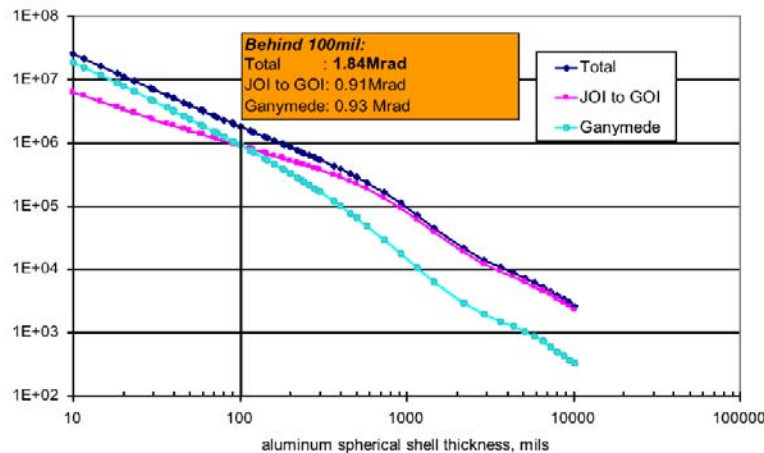


Figure 4.4-3. JSO Dose Depth Curve

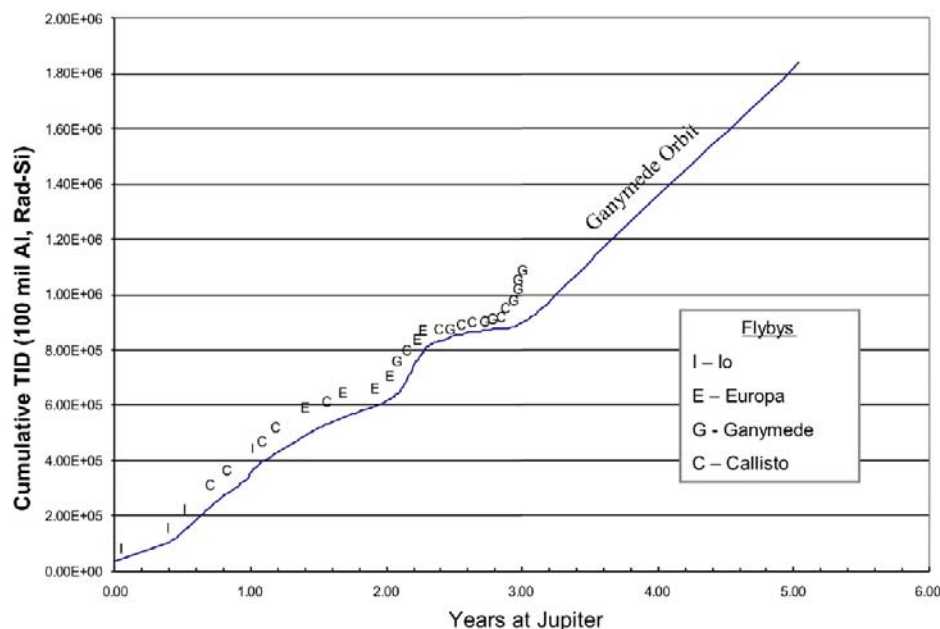


Figure 4.4-4. Dose vs. Time for JSO Mission

Table 4.4-1. Radiation Vaults Component Breakdown for the Baseline Mission

Baseline Architecture											
Subsystem	Components	krad (RDF 1)	# of Units	L (cm)	W (cm)	H (cm)	Volume	Type of Shielding Technique/Comments	Shielding Material	mass (kg)	
Telecom	SDST X-up/X&Ka down	300	2	42.2	46.0	20.2	39234.2	Enclosed Shielding, added 5 cm to height for cable connections. All MGA and HGA hardware are on the back of the HGA, LGA hardware is on spacecraft	75%W-25%Cu	68.6	
	USO, 1E-12		2	15.2	15.2	20.2	4700.9			8.5	
	Ka-band TWTA, RF-50W		2	20.3	15.2	15.2	4694.7			8.6	
	X-Band sspa, RF-5W		2	17.8	12.7	15.2	3423.2			6.9	
	Waveguide Transfer Switch (WGTS)		5	5.1	5.1	15.2	391.2			4.5	
	Coax Transfer switch		2	2.5	2.5	6.0	38.8			1.1	
	Hybrid Coupler		2	5.1	5.1	7.5	193.5			0.4	
	x4 Multiplier		2	2.5	2.5	7.5	48.6			0.5	
ACS	Sun Sensors	600	4	7.6	4.5	6.1	208.6	Enclosed Shielding, added 5 cm to height for cable connection.	75%W-25%Cu	13.3	
	Star Camera Head		4	11.5	11.5	15.0	1983.8			1.1	
	IMUs		2	26.7	17.3	16.4	7575.3			4.6	
	Reaction Wheel	1000	4	31.6	15.9	20.9	10501.0		6U Chassis Vault Shielding, Held in CDS's MREU Chassis, 6U Cards	Aluminum	4.9
	Rad-hard Reaction Wheel Electronics		2								0.2
	Rad-hard Gimbal Drive Electronics (HGA and Main Engine)		4								0.5
CDS										38.5	
	MSAP Chassis 203x272x204	300	2	25.2	22.9	27.9	16089.1	6U Chassis Vault Shielding, 6U cards	75%W-25%Cu	11.2	
	Rad-hard RAD750 (6U 200MHz) w/256MB SRAM (NR)		2							Holds 8 cards	0.9
	Rad-hard 6U C-RAM card for JSO mission (NR)		2								0.9
	Rad-hard MTIF Card (6U) for JSO mission (NR)		2								0.9
	Rad-hard SIA Card (6U) for JSO mission (NR)		4								1.9
	Rad-hard MAGIC Card (6U) for JSO mission (NR)		2								0.9
	Data Compressor co-processor card (NR)		2								0.9
	Rad-hard PCC DC-DC Converter: 5 V, 3.3V and +/-12V (NR)		2								0.9
	MREU Chassis		1	25.2	24.8	27.9	17461.4			Holds 10 cards (will hold the 6 ACS cards)	5.8
	Rad-hard Analog/Discrete MREU (NR)		4								1.9
	CDS Backplane: MSAP Backplane		2							6U Chassis Vault Shielding, 6U cards	0.9
	Rad-hard 9.6 Gbit SSR for JSO Mission (NR)		1	25.2	26.9	27.9	18940.0			Hold 11 cards	5.9
	Memory Card		8							6U Chassis Vault Shielding, 6U cards	3.8
	Controller		2								0.9
Power Supply	1						0.5				
Instruments										28.2	
	Chassis	300	3	25.2	22.9	27.9	16089.1	6U Chassis Vault Shielding, 6U cards	75%W-25%Cu	16.8	
	High-res monochrome camera		3								1.4
	VIS-NIR hyperspectral imager		3								1.4
	UV spectrometer		2								0.9
	Thermal spectrometer		3								1.4
	Laser altimeter		3								1.4
	Magnetometer		1								0.5
	Plasma spectrometer/ energetic particle detector		2								0.9
	Medium-res stereo camera		3								1.4
Ground-penetrating radar	4									1.9	
Propulsion									13.5		
Power	Pressure Transducer	100	12	13.3	3	3	119.7	Enclosed Shielding	75%W-25%Cu	13.5	
	Chassis	2000	1	25.4	57.4	27.9	40414.7	6U Chassis Vault Shielding, 6U cards	Aluminum	No additional shielding needed	
	Load Switching*		10								Holds 26 cards
	Thruster Drivers		4								
	Pyro Switching		2								
	Converters*		2								
	Shunt Regulators		4								
	Battery Control*		2								
	RTG Interface Card		2								
Total Mass									162.0		

devices, sensors, optical devices, and materials. The number of components that needed to be shielded also drives the radiation shielding mass. The required design factor for the program is 2 for all of the hardware. The Radiation Design Factor (RDF) is defined as:

$$RDF = \frac{\text{Radiation_resisting_capability_of_Part}}{\text{Radiation_environment_present_at_Part}}$$

Devices with a total ionizing dose (TID) capability of less than 150 krad are evaluated at an RDF of 3.

Table 4.4-1 lists the components in the primary and secondary radiation vaults that require radiation protection, their radiation capabilities, the mass of the radiation vault, and the dimensions. C&DH has a total of 31 6U boards. As can be seen in the table, all components but the pressure transducers will be upgraded to have TID tolerance of 300 krad or higher. This is a significant difference from previous approaches, such as Juno where the parts were accepted at current TID tolerances (typically for Mars-like environments), and

provide a mission-enabling mass savings for the increased TID environment expected for JSO.

The mass of the chassis is not included in the radiation vault mass.

Preliminary Shielding Thickness Calculation

The shielding analysis for this concept study used a simple radiation mass model, which consists of a spacecraft, an electronic box, a PWB, and an electronic package. With this radiation mass model served as a baseline, required extra shielding thicknesses are calculated using either aluminum or tungsten-copper as shielding material to bring down dose level to 50 krad, 100 krad, 150 krad, 300 krad, and 500 krad when RDF of 2 is included. **Table 4.4-2** shows the baseline radiation mass model description and **Table 4.4-3** lists the required shielding thicknesses calculated based on input specified in **Table 4.4-4**.

Table 4.4-2. Baseline Radiation Mass Model Description

Model Component	Model Description
Spacecraft	40-mil eq. Al thickness hollow cylinder
Electronic Box	60-mil Al wall thickness
PWB	A 62-mil graphite slab
Electronic Package	20-mil Al solid sphere simulating device package

Table 4.4-3. Required Electronic Box Extra Shielding Thickness

Part Radiation Level	Aluminum Extra Shielding Thickness, mils (to be added to electronic box)	W-Cu Extra Shielding Thickness, mils (to be added to electronic box)
To use 100-krad part (shielded to 33 krad)	990	130
To use 200-krad part (shielded to 100 krad)	600	80
To use 300-krad part (shielded to 150 krad)	441	60
To use 600-krad part (shielded to 300 krad)	192	30
To use 1Mrad part (shielded to 500 krad)	60	9

There were two approaches taken in designing the radiation vaults. One approach was to hold the electronics 6U cards in chassis and then add additional shielding to the chassis and individual 6U cards. The second approach was to enclose the stand-alone electronics and hardware in shielding. The shielding mass for the stand-alone components can be estimated using the following equation with the calculated shielding thickness.

$$\text{Shield Mass (g)} = \text{density} \times [(L + 2 \times \Delta t) * (W + 2 \times \Delta t) * (H + 2 \times \Delta t)] - (L * W * H)$$

where

- L, W, and H are the electronic box's length, width, and height.
- Density is 2.7g/cm³ for aluminum, and 15.5g/cm³ for tungsten-copper (W-Cu).

Five cm was added to each height dimension of the components to account for connectors and harness routing.

Δt = shielding thickness in cm, shown in **Table 4.4-3** (value depends on part radiation

capability).

JSO used scaling factors to scale down the 6U card and chassis mass results that Europa Explorer calculated previously. Europa Explorer used the Monte Carlo method to determine how much additional mass had to be added to both end plates of a chassis and each 6U slice in a chassis to protect to 1 Mrad, 300 krad, 200 krad, and 100 krad. JSO scaled these masses for JSO's components. The scaling factors used were based on the shielding thickness calculations for aluminum from the Radiation Dose Depth Curve for both JSO and EE. For each dose level, the ratio of JSO's aluminum shielding thickness to EE's aluminum shielding thickness was taken and multiplied by the Monte Carlo Mass values EE determined. These results were then used to size the radiation vault mass for the chassis and 6U cards. **Table 4.4-4** shows the algorithm used to determine JSO radiation vault mass and what values EE used. The shielding mass breakdown of each component is shown in **Table 4.4-1**. The total radiation vault mass for the baseline mission is 162 kg.

Role of System Engineering and Management for Radiation Design

Radiation requires a system-level response. System engineering the radiation design involves defining the environment, designing for that environment and mitigating residual risk due to uncertainties. Defining the environment includes defining the lifetime requirements, modeling the environment, and designing the trajectory to lessen radiation. Designing for the environment encompasses parts capability and testing, configuration and layout, and modeling for radiation transport mechanism and shielding. Mitigating residual risk covers prioritizing science collection, designing fault protection, and developing contingency plans to ensure graceful system degradation and margin adequacy. All these must be done concurrently by performing trade studies and risk analysis to optimize the design and to manage margins.

Table 4.4-4. JSO and Europa Explorer 6U and Chassis Mass Algorithm

TID RDF 1	JSO		EE		Material
	6U Both End Plates (kg)	6U Shielding Each Slice (kg)	6U Both End Plates (kg)	6U Shielding Each Slice (kg)	
100 krad	12.4	2.1	13.8	2.3	75% W – 25% Cu
200 krad	5.2	0.9	5.1	0.85	75% W – 25% Cu
300 krad	3.9	0.6	3.6	0.59	75% W – 25% Cu
1 Mrad	0.9	0.2	1.2	0.2	Aluminum

Processes and products, and radiation experts will be in place to enable a good radiation design. The specific approach is to:

- appoint a Deputy Project Manager for Radiation Development (DPMR), reporting to the Project Manager (PM) to manage resources aimed at resolving radiation development issues
- appoint a Deputy Project System Engineer for Radiation (DPSE) reporting to the Project System Engineer (PSE) to lead the Radiation Systems Team comprised of system engineers, configuration and shielding engineers, parts and materials specialists, and mission designers ;
- add trained radiation system engineers at the Project, Spacecraft, Payload, instrument and subsystem levels, to address system issues related to environment, parts, material, shielding, fault protection and operations, with access to area experts supporting all aspects of developments including science instruments and vendor activities;
- engage the Mission Assurance organization early in the Project lifecycle (Pre-phase A) to document and communicate the radiation requirements and design guidelines and to understand the systems trades;
- utilize radiation technical working groups to work day-to-day issues such as requirements, trades, modeling and plans;
- initiate a Radiation Advisory Board early in the Project lifecycle consisting of scientists and practitioners independent of the project who will periodically review the project's approach to radiation tolerant design, risks and mitigation strategies, and advise the Project Manager;
- provide frequent communication of new issues and insights about radiation to all staff;
- leverage from existing processes developed in programs outside NASA or develop new engineering processes as needed to handle radiation issues to enable a highly reliable system such as interfaces between structural models and shielding models and radiation-hard by design techniques; and
- develop and distribute Radiation and Planetary Protection Design Guidelines, an

Approved Parts and Materials List and a formal Radiation Control Plan to all staff (including potential instrument providers prior to instrument AO release) early.

Radiation system engineering is an ongoing process that emphasizes system optimization: trading implementation options with performance risk.

Project management has ultimate responsibility for all radiation aspects of the mission and delegates the day-to-day activities to the DPSE. The DPSE will work technical issues closely with the PSE, the Mission Assurance Manager (MAM), Payload System Engineer, Project Scientist (as the representative of the science teams) and the DPMR in trading off between technical and programmatic margins such as consumables, budget and schedule. The Radiation Advisory Board will interact and report to the PM as an advisory panel regularly.

There will be many trade studies performed in Phases A and B to determine the best radiation mitigation design aspects. Technical trades between trajectory design, shielding design, component rad-hardness, fault protection design and autonomy will need consideration. Designing for the Jupiter radiation environment requires significant time for a system level design approach, circuit design and analysis, parts procurement and testing and verification and validation. These and other approaches need to be adequately assessed during the early phases of the project. All of these intricate trades involve significant schedule, cost and risk implications and therefore must be considered early and across the project.

4.4.2.2 Fault Protection

Given the duration of the mission and the one-way light time from the Jovian system, autonomy is needed to handle the flight system safety issues. As such, a system of monitors and responses will mitigate, isolate, and recover from off-nominal behaviors if encountered during the mission. It is common design practice for onboard fault protection algorithms to halt normal operations and place the flight system into a safe configuration, awaiting ground response, when they detect a potentially unsafe condition. An exception to this is when a flight system is executing a time critical operation, such as an orbit insertion.

In line with this philosophy but taking into account the particular radiation effects from a Jupiter mission, JSO's fault protection design will include transient recovery. In many fault situations it can be assumed initially that an anomaly is a radiation induced transient, and the response could be to reset the affected equipment and continue the mission. A hardware reset could be attempted first, followed by a power cycle if necessary. An anomaly that does not clear after resetting will be treated as a hard failure. Hard failures will wait for a ground response.

JSO's fault protection design is based on an underlying architecture consisting of:

- Lower-level fault protection that is built into the hardware-control software modules
- Performance-level fault protection that consists of a series of performance monitors that examine and respond to specific subsystems for performance deviations or fault indications
- System-level fault protection that is made up of system-level utilities and contingency mode executives

All fault monitors and responses can be individually enabled or disabled by command or configuration file.

Assumptions, Guidelines and Constraints, Key Driving Requirements

The technical approach for the concept system design used the following assumptions and guidelines:

- Use technology and instruments that currently exist or are under development and are planned for qualification early during the JSO project lifecycle.
- Use only MMRTG due to limited study time and knowledge of other power options. Use of ASRGs not precluded, and would need further study.
- Launch vehicle accommodations by the Delta IV-H used for the baseline design.
- The mission radiation design dose (referenced to 100 mil aluminum shell) is 1.8 Mrad, which must be tolerated with a RDF of at least 2
- The required ΔV is 2705 m/s
- Assume DSN 70m-equivalent Ka band or equivalent—not currently available but consistent with HQ study guidelines

- 12 year mission life

4.4.2.3 Resource Margin Summary

Mass

The JSO spacecraft mass totals and margin are shown in **Table 4.4-5**. Each element on the spacecraft is catalogued with a current best estimate (CBE) and contingency based on its heritage. Total of the CBE plus its contingency provides the maximum expected value (MEV). Current JSO design shows contingencies averaging about 27% of the total CBE. With the launch vehicle capability (M_{launch}) of 7810 kg for the JSO reference mission, the $M_{\text{propellant}}$ is 4775 kg and the $M_{\text{s/c}}$ allocation is 3010 kg providing a system margin of $M_{\text{s/c}}$ allocation – MEV = 523 kg, or 21% margin. Together, the contingency and system margin provide 1051 kg over the current best estimate (CBE), exceeding JPL's design principles for a > 30% contingency+margin over the $M_{\text{s/c}}$ allocation, (which is $3035 \times 30\% = 910$ kg).

Table 4.4-5. Mass Summary

Jupiter System Observer 2007-07-10 Systems Comparison	Baseline Architecture (kg)		
	CBE (kg)	Cont. (%)	CBE+ Cont. (kg)
Payload			
Instruments	228	36%	310
Bus			
Attitude Control	51	31%	67
Command & Data	49	37%	67
Power (non-MMRTG)	54	30%	70
MMRTGs	376	5%	395
Propulsion	356	28%	454
Structures & Mechanisms	448	30%	582
Cabling	125	30%	163
Telecom	58	20%	69
Thermal	53	28%	67
Bus Total	1569	23%	1934
Radiation Vault	162	50%	243
Spacecraft			
Spacecraft Dry Mass	1959	27%	2487
Propellant & Pressurant			4775
Wet Mass			7262

Mass (kg)		
System Margin *	21%	523
Spacecraft Dry Mass Allocation		3010
Launch Vehicle Adapter (LV side)		25
Launch Vehicle Capability	Delta IV 4050H-19	7810

* Margin = Remaining LV Mass/Spacecraft Dry Mass (CBE+Cont)

Power

The power margins are summarized in **Table 4.4-6**. Each assembly is catalogued by its various power states, including: off, standby, reduced power active modes, fully powered active modes. A blanket contingency of 30% is assumed for each assembly. The primary source of power is from the

8 MMRTGs, which provide 843 W at the end of the Interplanetary phase (L+7 years), 803 W at the end of the Jovian Tour phase (L+10 years) and 778 W at the end of the Ganymede Science phase (L+12 years).

In addition to the 30% contingency in each of the modes, there is positive power margin in all steady-state modes.

Two modes require more power than is put out by the MMRTGs. These high power loads are for the main engine maneuvers when the

C&DH is in hot swap mode and the satellite flyby encounter mode when science desires to maximize the number of instruments that can be turned on while downlinking realtime and recording the rest on the SSRs. The number of these events will total well below 100, and the depth of discharge of the battery (only 1 battery is assumed for this analysis) will be well below the 70% as guidelineed in JPL's design principles.

Table 4.4-6. Power Summary

	Mode 1	Mode 2	Mode 3	Mode 4	Mode 5	Mode 6	Mode 7	Mode 8	Mode 9
Baseline Architecture	Power	Power	Power	Power	Power	Power	Power	Power	Power
Subsystem	(W)	(W)	(W)	(W)	(W)	(W)	(W)	(W)	(W)
	Launch	Cruise	Critical Mnv	Jupiter System Tour	Encounter Mode	Ganymede Circular (Sci/RS/Tel.)	Ganymede Circular (Science)	Fault Recovery	Safe Mode
<i>Power Mode Duration (hours)</i>	<i>8</i>	<i>24</i>	<i>1.5</i>	<i>24</i>	<i>6</i>	<i>24</i>	<i>8</i>	<i>1</i>	<i>indefinite</i>
Payload	0	40	40	66	185	76	126	45	45
C&DH	89	89	140	103	121	113	113	68	68
ACS	31	87	97	87	87	94	87	87	87
Telecom	107	112	112	112	112	154	112	112	112
Propulsion	58	58	217	10	58	10	10	90	52
Thermal	9	15	15	15	15	15	15	58	58
Power	38	50	73	51	67	57	57	53	50
Bus	331	411	654	378	460	444	394	468	427
TOTAL (W)	331	451	694	444	645	520	520	513	472
Total with Contingency (30%) *	430	586	902	577	838	676	676	667	614
Available Power, (W)**	944	843	843	803	803	778	778	778	778
Net Power Margin (W)	514	257	-59	226	-35	102	102	111	164
Battery Energy Used (W-Hr)			88			210			
DoD (%), one battery			8%			19%			

* Blanket 30% contingency is applied conservatively; many assembly uncertainties are understood better than 30%.

** Power computed for end of BOM (mode 1), 7 years (modes 2, 3), 10 years (modes 4, 5), and 12 years (modes 6-9).

4.4.3 Subsystem Descriptions

Structures and Mechanisms

The approach to JSO's structures design on was driven by an aggressive plan to minimize mass. To reduce mass, graphite-epoxy composite honeycomb is used throughout as primary structure, with Aluminum and Titanium alloy fittings distributed as necessary. Independent calculations were performed to gain confidence in the feasibility of mass reductions given the specific spacecraft configuration. For the 3-axis stabilized spacecraft, a minimal balance mass of 17 kg is calculated.

The spacecraft layout comprises a stack of the following modules: (1) a propulsion module that includes the propellant tanks, pressurant tanks, all thrusters, the main engine assembly, and the associated structure. Additionally, the MMRTGs and the reaction wheels are mounted to this module and (2) the instrument platform assembly that comprises a flat deck housing the instruments, bus equipment, radiation vaults, and telecom equipment. The spacecraft is configured such that the instrument platform is located near the launch vehicle separation interface in order to reduce the spacecraft CG distance from the launch vehicle PAF. There is a short conical structure that is a transitional adapter cone just

above the launch vehicle adapter. This cone also supports the propellant tanks used to stand the instrument platform off of the PAF to accommodate the Narrow Angle Camera and Ground Penetrating Radar instruments. A Cassini SuperZip™ separation device is used to support and separate the spacecraft from the launch vehicle.

The 8 MMRTGs are mounted in groups of 2 or 3 in planes that are distributed along the length of the propulsion module structure. Thruster modules are arranged in 2 planes to provide attitude control authority in 6 degrees of freedom

The instruments are mounted in a fixed configuration on a graphite epoxy honeycomb panel that forms the Instrument Platform. This arrangement facilitates the co-alignment of many of the instruments and allows the Attitude Control equipment (star trackers and inertial reference units) to determine the instrument pointing knowledge to < 0.25 mrad. The platform is connected to the main propellant core structure via 6 radial fin and post flexures. The flexures prevent distortion of the platform by any distortions induced in the propulsion module structure. Twin heat pipes are employed to dissipate the heat from the instruments electronics in the radiation vaults to 2 opposed radiators around the periphery of the instrument deck panels that are mounted to the instrument platform

The propellant tanks are not load carrying. The material and construction of these tanks follow conventional practice for Titanium alloy. There is no clear opportunity to reduce mass by making the tanks load-carrying as there is a significant number of individual items that require mounting to this core structure and subsequently requiring local strengthening of the support points. Using the carbon fiber composite tube to distribute point loads was determined to be more mass efficient.

Placement of the MMRTGs facilitates thermal management of the propulsion system and instruments in a similar manner to the Cassini spacecraft. The MMRTG mounts are designed to radiate heat from the base of the MMRTGs to a cocoon-like MLI enclosure of the propulsion module.

The magnetometer boom mass is scaled up to 10 m long from a 5 m long unit made by

Northrop-Grumman and is deployed shortly S/C separation from the launch vehicle. The boom section diameter remains approximately 0.25 m, which is adequate for the 3 kg tip mass of the magnetometer. The first mode of the deployed boom is expected to be greater than 0.2 Hz, a frequency acceptable to ACS. The structural frequency of the ground penetrating radar is predicted to be above 1 Hz which is also acceptable to the ACS subsystem.

The HGA boom is estimated to be approximately 1.5-m long, 2.3-cm diameter, with a 2-mm thick wall. It is constructed of graphite-epoxy. A pyro-actuated spring driven hinge, mounted on the instrument deck, deploys the boom shortly after S/C separation from the launch vehicle. Another pyro device releases the HGA from its mounting stowage location on the propulsion module.

The mass of cabling is estimated by conservatively using 7% of the dry Maximum Expected Value (CBE+contingency) of the rest of the spacecraft.

JSO will use the 1575-F PAF launch vehicle adapter, which requires an additional 25 kg above the standard PAF carried in the Delta IV-H performance. This mass stays with the launch vehicle and is accounted for in the mass summary [Table 4.4-5](#).

Telecommunications

The Telecom subsystem provides two-way communications, including telemetry, two-way Doppler, ranging, and Δ DOR at both X- and Ka-band, and commanding at X-band. A Ka-band carrier-only uplink capability is provided for the Radio Science – Gravity investigation.

The high data rate link is sized at a range of 6.5 AU. Scenario analysis shows that a 600 kb/s downlink data rate is sufficient to meet the science objectives. The link assumes a 70m-equivalent capability at Ka-band. The spacecraft also supports a low-rate data link during safe mode and critical events (e.g., JOI and launch).

The Ka-band pointing accuracy requirement is 0.07° (1.2 mrad). An autotrack system (monopulse) using an X-band uplink from the DSN may be used depending on trades performed during Phase A. The nominal frequency scheme is to use an X-band uplink with a Ka-band downlink.

The Ka-band uplink is achieved with a Ka to X-band downconverter, also known as a translator. The JSO mission leverages on the Ka-band carrier-only design that is being developed for the Juno mission. This effort feeds into the design for the Ka-band downconverter along with the existing X-band downconverter design.

A block diagram of the telecom subsystem is shown in [Figure 4.4-5](#) and additional details are in [Appendix D](#).

Significant features of the telecom design include the following:

- Redundant, cross-strapped 50-W Ka-band traveling wave-tube amplifiers (TWTAs),
- Redundant, cross-strapped X/X/Ka Small Deep Space Transponders (SDSTs), each with a Ka-band downconverter,
- Redundant 5-W X-band solid state power amplifiers (SSPAs) for Radio Science-Gravity investigation,
- One 2.75-m X/Ka HGA,

- One Ka-band transmit MGA for emergency downlink,
- Two X-band transmit/receive low-gain antennas (LGAs)
- Two Ka-band transmit LGAs
- Two ultra stable oscillators (USO) for radio science occultations
- The X-band link can only be operated with the HGA and 2 X-band LGAs, but the Ka-band link can be operated with HGA, MGA, or Ka-band LGAs.

To minimize transmit circuit losses and simplify the design, part of the telecom hardware that is needed for the HGA and MGA is mounted on the back of the HGA, in a radiation vault, which reduces the loss between the output of the high-power amplifiers and the HGA. It is also desirable to minimize the loss between output of the Ka-Band TWTAs and the LGAs for improved link performance during safe mode and critical events. All of the links are designed for a

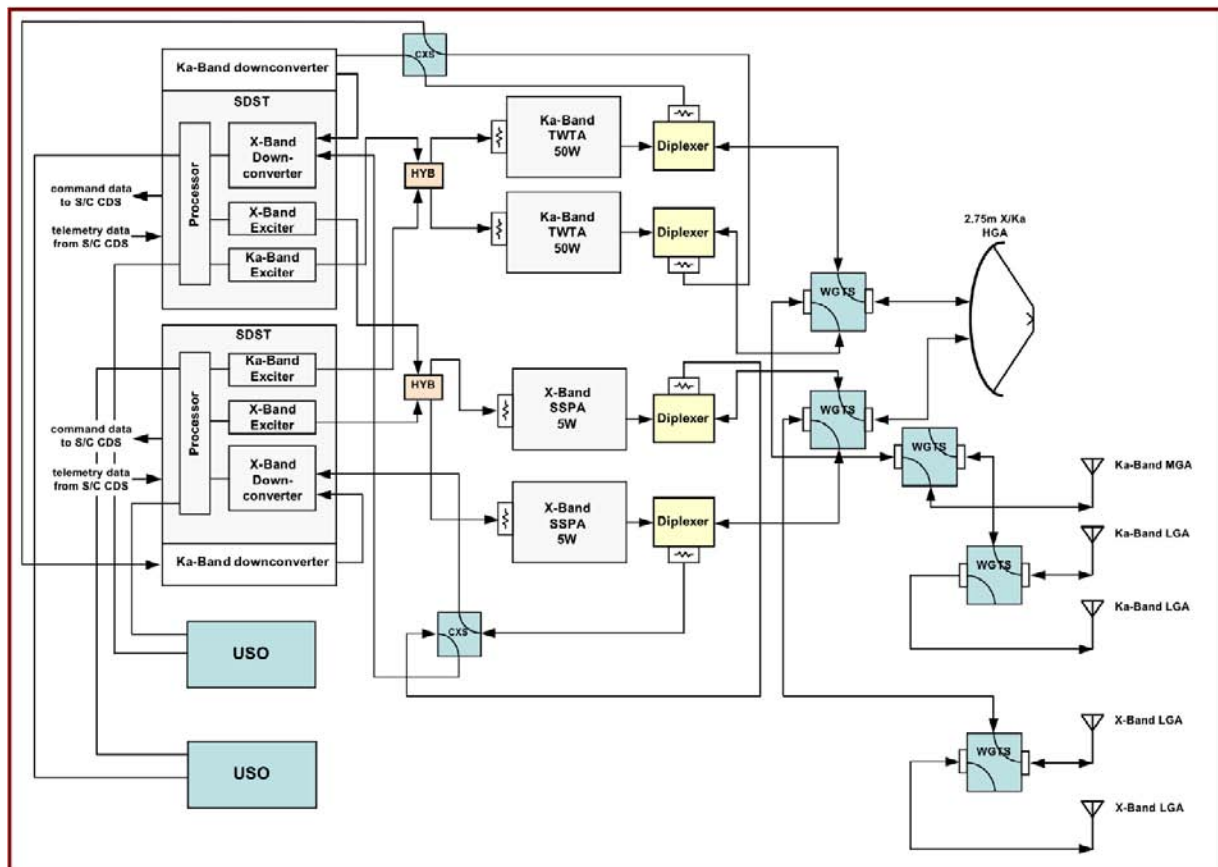


Figure 4.4-5. JSO Telecom Block Diagram

downlink frame error rate (FER) of $1\text{E-}4$. The uplink bit error rate (BER) is $1\text{E-}05$. All links have a minimum margin of 3 dB.

For the Radio Science–Gravity investigation, the X and Ka-band signals are routed through the HGA. The Ka-band uplink is downconverted to X-band and sent to the SDST, which then generates a coherent Ka-band downlink signal.

A USO is provided in the telecom subsystem to support instrument timing and for occultation measurements. In this case, a USO signal is used as the frequency reference for X-band and Ka-band downlink carrier signals.

The X-band downconverters are cards in the SDST. Their mass and power are bookkept with the SDST.

On hourly time-scales, the downlink rate varies as a function of Jupiter hot body noise and higher elevation angles at DSN sites. JSO expects to take advantage of the actual capability on an orbit-by-orbit basis.

The high rate link uses a rate $1/6$ turbo code (Frame length 8920) and assumes 90% weather model statistics. Low rate safe mode links use a rate $1/2$ turbo code (Frame length 1784). A link budget for both architectures is shown in [Table 4.4-7](#).

The design uses heritage components except where modification is required to address key issues such as radiation. The HGA is based on the MRO 3 m design. The Ka-band TWTA is a modification of the MRO 35 W Ka-band TWTA, and the X-band 5 W SSPA is a smaller version of the MER 17 W X-band SSPA. The Ka-band downconverter requires redesign for its engineering development. It is based on the effort done for Juno and the existing SDST design.

Command and Data Handling

The design approach for the C&DH subsystem provides a low-risk, high inheritance solution to meet the mission performance, environmental, and reliability requirements.

The C&DH architecture is based on JPL's Multi-mission System Architecture Platform (MSAP) technology that was developed to provide a data processing solution for a broad array of spacecraft needs. While the primary architectural elements remain unchanged from

the standard MSAP product, allowing the direct inheritance of software modules for hardware interfaces, the logic components will be replaced with rad-hard ASIC implementations of the FPGA designs. This approach enables a low risk development path for a high radiation tolerant data processing system and minimizes the amount of shielding required for reliable operation in the JSO environment.

In addition to the existing MSAP designs, JSO will develop three C&DH components specific for the mission requirements. These include a Data Compression Board to handle the throughput of science data, a Non-Volatile Memory board for storing FSW images and engineering data, and a Solid State Recorder.

The NVM and SSR memory components are based on Chalcogenide RAM (CRAM) technology that has been developed by BAE Systems. The phase-change CRAM memory elements are inherently radiation hard. The substrates for the CRAM elements will be fabricated on BAE's rad-hard foundry, offering a true rad-hard non-volatile memory solution. Engineering models of the CRAM components are available now as 4-Mb devices with 16 Mb available in time for JSO.

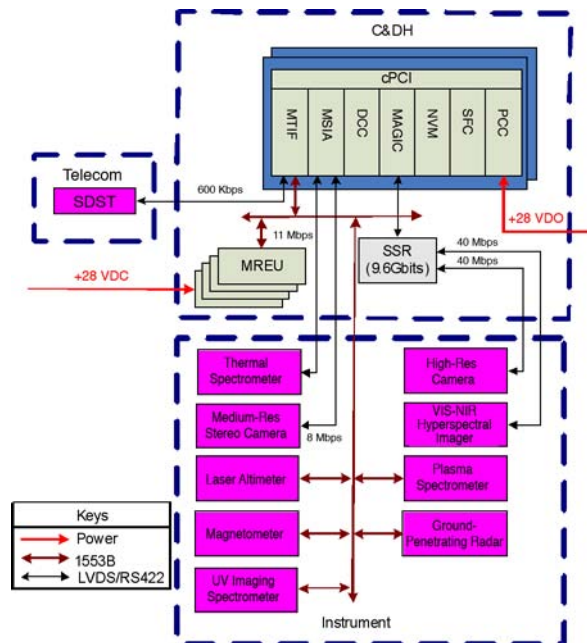
The C&DH subsystem is a dual string, block redundant architecture. The top-level block diagram of the JSO C&DH architecture is shown in [Figure 4.4-6](#).

Each C&DH string consists of the following components:

- **Space Flight Computer (SFC)** board is a BAE Systems RAD750 processor board with a 132-Mhz clock rate, 256-KB EEPROM memory for storing the initial boot-loader program, and a 256 MB of SRAM for software execution.
- **RADHard Non-Volatile Memory (NVM)** board contains 150 MB EDAC-protected NVM based on Chalcogenide RAM (C-RAM) technology for storing FSW images and engineering data.
- **RADHard MTIF** board that provides redundant telecommunication interfaces to the SDST, the MIL-STD-1553 bus controller, dual-string arbitration for fault protection, and Tz umbilical interface.

Table 4.4-7. Telecom Link Budgets

Link Budget Table					
Link	Nominal Uplink	Emergency Uplink	High Rate TLM Downlink	Emergency Downlink	Cruise Downlink
Transmit Antenna	DSN 34m	DSN 70m	2.75m Ka-Band HGA	Ka-Band MGA	2.75m Ka-Band HGA
Transmit Antenna Articulation	2 axis	body fixed	2 axis	body fixed	2 axis
Transmit Antenna Gain, dBi	66.9	72.8	57.4	19.2	57.4
Pointing Accuracy, deg	0.01	0.01	0.07	5	0.07
Pointing loss, dB	-0.1	-0.1	-1.04	-0.9	-1.04
Transmit Power, W	20000	20000	50	50	50
Frequency Band	X-Band	X-Band	Ka-Band	Ka-Band	Ka-Band
Frequency, MHz	7183	7183	32050	32050	32050
Range	6.5 AU	6.5 AU	6.5 AU	6.5 AU	6.5 AU
Receive Antenna	X-Band HGA	X-Band LGA	70m equivalent	70m equivalent	34m
Receive Antenna Gain, dBi	44.4	7.7	84.8	84.8	78.8
Pointing Accuracy, deg	0.07	20	0.002	0.002	0.002
Pointing loss, dB	-0.05	-1.2	-0.2	-0.2	-0.2
System Noise Temp, K	370	370	89	89	90
Ranging On/Off	On	Off	Off	Off	On
Data Rate	2000	7.8125	600000	10	20000
Coding	None	None	Turbo 1/6, 8920	Turbo 1/2, 1784	Turbo 1/6, 8920
Margin	13.8	7.6	3.4	3.5	11.7

*Figure 4.4-6. C&DH Architecture*

- **RADHard MSAP System Interface Assembly** board provides 4-channel LVDS/RS422 serial interfaces to instruments with 8 Mbps transfer rate per channel, and a 20 Mbits EDAC-protected SRAM for download data buffering.
- **RADHard MAGIC** board provides interfaces to the sensors and actuators in the ACS subsystem.
- **RADHard Data Compressor Card (DCC)** collects high rate science data compresses science data and offloads the SFC.

- **RADHard MSAP Remote Engineering Unit** has dual MIL-STD-1553 interfaces and over 120 analog channels and discrete I/Os for collection of spacecraft engineering telemetry. It also contains timer functions. Four MREUs are used in the JSO architecture.

- **RADHard PCC** board provides regulated 28V power to all cPCI boards.

The Solid State Recorder provides 9.6 Gbits of non-volatile CRAM memory for storing science data. The SSR design includes internal redundancy internal interfaces rather than block redundancy to allow the total available memory to be accessed between the primary and secondary CDH strings without the need for cross-strapping. To accomplish the internal redundancy, it contains dual controller boards, dual power supplies and EDAC-protected data boards.

The C&DH subsystem provides three separate paths to interface with the nine instruments based on the instruments data rates (**Table 4.2-2**) and volumes:

1. Very high-speed instruments, the High-Res Camera (40 Mbps) and the VIS-NIR hyperspectral imager (40 Mbps) are connected to the SSR directly via a dedicated point-to-point LVDS high-speed serial bus;
2. High-speed instruments, the Thermal Spectrometer (11 Mbps) and the Medium-Res Camera (8 Mbps) are interfaced with the MSIA through

a point-to-point LVDS high-speed serial bus;

3. The remaining five low-speed instruments are connected to the C&DH by the standard 1553 bus.

During science data collection, data from the very high-speed instruments are processed by the Data Compression Card and stored into the SSR directly without support from the main system computer. The design of the DCC allows the compression of science data to be enabled or disabled as needed.

Data from high-speed instruments are processed by the system computer through the Data Compression Card and then stored in the SSR. Data from low-speed instruments are collected through the MSIA board and stored in the SSR. For transmission of the data to the ground, the MTIF retrieves the stored data from the SSR, encodes the data and then send it to the SDST via point-to-point LVDS interface.

Flight Software

Highly reliable software for mission-critical applications is essential for this long-life, highly visible mission. JPL has established a set of institutional software development and acquisition practices as well as design principles that apply to mission-critical and mission-support software. These practices conform to the NASA Procedural Requirements for Software (NPR 7150.2) and are an integral part of the JPL FPP and DPP. In addition, the JPL organizations that will be responsible for the management and development of the JSO mission critical software will be certified at CMMI Level 2 which has been shown to correlate strongly with reduced defects and improved cost and schedule performance.

A significant portion of the FSW effort will be inherited from JPL's MSAP development activity. This flight-proven software design provides high test and operational flexibility to accommodate science and engineering needs, autonomous fault recovery, and in-flight software updates. In addition to the flight software itself, other inherited products reduce development cost and risk including: documentation, the development environment (configuration management, test harnesses and scripts) for delivered functionality. Further, the

MSAP simulation test environment includes the simulation for the MSAP supported hardware. The Operating System and sequencing machine will be the same as for MSAP. It is assumed that 30% of JSO's code would be inherited from MSAP.

Software is written in "C" or C++ using the VxWorks operating system. C&DH FSW functions and software units include:

- Allocation and management of onboard computational resources for all engineering and science processing needs
- Performance of memory management of command sequences and science data
- Command receipt verification and validation
- Performance of self-test
- Gathering and reporting of health/safety status at the subsystem and spacecraft level
- Hosting of onboard autonomy necessary to recover the spacecraft from anomalies
- Interfacing with all science instruments
- Execution of attitude control maneuvers, using precision pointing for attitude control
- Performance of data acquisition and processing of attitude sensors information.

ACS FSW software units and functions are described below:

- Control spacecraft attitude
- Manage spacecraft modes (Acquisition, Coarse/Fine Science, Thruster Control, RWA Control)
- Manage thrust vector control
- Acquire data acquisition and processing of data from Sun sensor, IRU, star tracker, reaction wheels, and thrusters
- Control actuator commands to HGA, reaction wheels and thrusters
- Propagate s/c ephemeris
- Compute & manage system momentum
- Estimate state vector
- Detect and correct ACS faults
- Perform orbit adjusts
- Provide redundant data set management

A functional block diagram of the software subsystem is shown in [Figure 4.4-7](#).

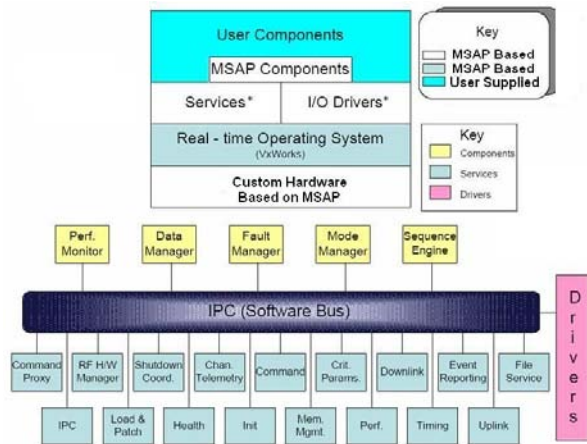


Figure 4.4-7. Software Functional Block Diagram

Assumptions:

- MSAP real-time executive to provide multi-tasking, scheduling, intertask communication, interrupt, and exception handling (via VxWorks)
- External communication bus operation and arbitration used.
- Capability to perform cold and hot start of the C&DH exists.
- Very high data management complexity. CCSDS packetization along with internal data packet distribution and significant onboard storage and organization. Need to do complicated data management for large numbers of instruments with summed high data rate and high data volume with limited on-board memory.
- State data is collected and distributed on board.
- The Boot (initial program load) and the flight software initialization modules are inherited from MSAP but requires some level of re-engineering and full re-testing to work for the JSO mission. A moderate re-engineering effort is required for those MSAP modules that interface with the radiation-hardened avionics set.
- Data compression is done in hardware not software.
- The Data Handling/CCSDS Data formatter is a custom hardware build.
- The Solid State Recorder (SSR) is a custom board whose software interfaces mimics those of the Seakr SSR. The custom made

onboard solid state recorder is used for data management

- Stability requirements are tighter than the pointing requirements

Attitude Control

The vehicle is 3-axis stabilized using reaction wheels for fine pointing control and thrusters to unload excess angular momentum accumulated by the wheels. Stellar inertial attitude determination is used to provide accurate knowledge of spacecraft attitude reference axes. The baseline includes rad-hard star camera heads and rad-hard gyros. Star processing is done within the main computer. The sun-safe mode uses the gyros and rad-hard sun sensors for attitude determination.

Pointing requirements are driven by a high-resolution imager with a 4 mrad FOV and a 2- μ rad IFOV. The pointing accuracy requirement is to point the imager boresight to within 0.4 mrad (3σ , zero-to-peak), which is one tenth of the FOV. In comparison, the requirement for pointing the boresight of the HGA is to within 1.2 mrad (3σ , zero-to-peak). The requirement for twist about the boresight is significantly looser, because of the narrow FOV and is not a driver.

The pointing knowledge requirement is to limit uncertainty to less than 40 pixels of the high-resolution imager. This corresponds to boresight knowledge to within 80 μ rad (3σ , zero-to-peak). The requirement for knowledge of twist about the boresight is significantly looser because of the narrow FOV and is not a driver.

The pointing stability requirement is to limit smear for the high-resolution imager to less than one pixel over an exposure time of up to 0.5 seconds. This corresponds to per-axis pointing stability within $\pm 4 \mu$ rad/sec (3σ , zero-to-peak). Alternatively, the accumulated angle error due to smear acting over 0.5 seconds would be less than $\pm 2 \mu$ rad (3σ , zero-to-peak).

Near closest approach during worst-case flybys, tracking a point on the target would require a slew rate of as much as 6 degrees/second. Massive Hubble-class reaction wheels (48 kg each) would be needed to support fine pointing control in this case. Since imaging during flybys is a secondary objective this goal did not drive the Attitude Control Subsystem (ACS) design. Reaction wheels in the baseline (10 kg each) are sized to support

Ganymede orbital science with ample margin and can also provide the capability for fine pointing control at rates as high as 1 degree/second, for slews about the principal axis with the least inertia.

For those flybys where the target angular rates exceed the capability of the reaction wheels, imaging near closest approach will be taken on a best-effort basis. Use of thrusters could rotate the vehicle faster than the reaction wheels could. Thruster firings may induce jitter that would degrade image quality. Future, detailed analysis would be needed to determine the pointing stability achievable using thrusters.

Because the detection of the tidal signature requires an orbit reconstruction with a radial error of 1–2 m, residual ΔV must be minimized during the Ganymede Science phase and so the 0.7 N thrusters are coupled and redundant.

For spacecraft attitude control during the science phase, a redundant set of four reaction wheels are configured in a pyramid configuration that is optimized to meet the momentum and torque requirements for the mission while minimizing power usage. All four wheels are nominally in operation at the same time, so that the wheels' speeds are biased well away from zero in order to minimize bearing wear and to avoid stiction during zero crossings.

Each wheel is a rad-hard version of the Honeywell HR14 reaction wheel, configured to provide up to 50 Nms and up to 0.1 Nm per wheel. Rad-hard wheel drive electronics that are able to survive up to 1 Mrad are going to be developed for this mission.

The wheel drive electronics boards would be housed in the vault, as opposed to within each wheel.

Honeywell HR14 wheels have been flight proven on a number of earth orbiting missions including missions with long (e.g., 10 year) design life. Each wheel can be configured for momentum capability ranging from 20 to 75 Nms.

Very precursory analysis was performed to size the RWAs. While in orbit around Ganymede, there will be a gravity gradient torque, the magnitude of which will depend on how the vehicle is oriented relative to Ganymede. The long axis of the vehicle will

orient toward nadir. In that case, gravity gradient torque is lessened and momentum accumulated due to gravity gradient torque does not drive wheel sizing.

A very preliminary estimate is that the vehicle will have principal axis inertias of about 20,000 kg-m² about two transverse axes and 6,000 kg-m² about its long axis. If the vehicle is oriented with its long axis perpendicular to nadir while in orbit around Ganymede, then reaction wheels would need to cancel orbital angular momentum about the long axis. The orbit period for a circular orbit at 200 km altitude will be about 2.5 hours, and the orbital angular velocity will be about 0.04 degrees/second. In that case, the reaction wheels will need to cancel about 4 Nms of angular momentum.

A slew at 1 degree/second about the vehicle's long axis would require a set of reaction wheels able to store at least 105 Nms. Including a 30% margin to allow for control authority while slewing, the wheels would need to store 136 Nms. Suppose the vehicle were to carry a pyramid of four reaction wheels, and suppose that the spin axis of each wheel were canted 45 degrees away from the pyramid's axis of symmetry that passes through the apex. Then, the angular momentum capability along the symmetry axis would be 2.8 times the capability of a single reaction wheel. Four wheels with 50 Nms momentum capability would yield a total capability of 140 Nms along the symmetry axis, enough to support a slew at 1 degree/second about the vehicle's long axis.

Future analysis of the impacts on pointing from the deployed ground penetration radar antenna and to a less extent, the magnetometer boom is recommended, but not expected to be a significant problem.

In view of the above preliminary analyses, an HR14 wheel configured to store up to 50 Nms of angular momentum was selected as a reasonable placeholder for mass, power, and cost. If it turns out that greater momentum storage capability is needed, an HR16 can be configured to store up to 150 Nms.

For spacecraft maneuvers, the 90-N thrusters are configured as four pairs with both thrusters in a pair providing thrust in the same direction. Only one thruster in a pair is used at a time; the other thruster is for redundancy.

During main engine burns using the 890 N engine, four 90-N thrusters provide pitch and yaw control. Roll control is provided by a subset of the sixteen 0.7 N thrusters. During smaller ΔV maneuvers, the 90-N thrusters are off-pulsed to provide pitch and yaw control, and a subset of the sixteen 0.7 N thrusters are used to provide roll control.

The proposed configuration for the main engine and 90-N hydrazine thrusters is shown in **Figure 4.4-8**. The arrows in the figure indicate the direction of thrust. The X, Y, and Z axes are for reference in this discussion and do not necessarily agree with other coordinate frames mentioned in this report.

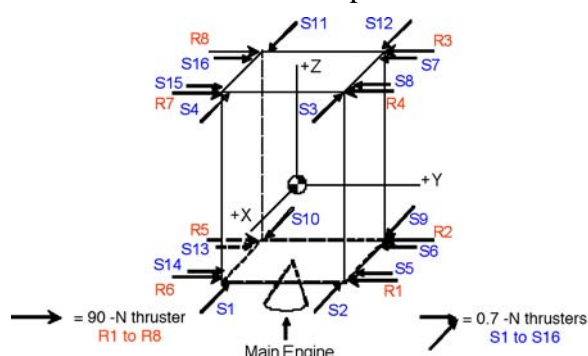


Figure 4.4-8. Propulsion System Configuration

The sixteen 0.7 N minimum impulse thrusters (MIT) are configured to provide couples during unloading of reaction wheel momentum. They also provide couples for control about the Z axis during ΔV burns. The sixteen MIT thrusters would be implemented as two strings of eight. Each string would provide couples. One string would include thrusters S1, S3, S5, S7, S9, S11, S13, and S15. The other string would include thrusters S2, S4, S6, S8, S10, S12, S14, and S16. **Table 4.4-8** indicates how couples would be achieved with either string.

Table 4.4-8. Thruster Couples

Axis of Couple	Primary Pair	Secondary Pair
+X	S7, S13	S8, S14
-X	S5, S15	S6, S16
+Y	S1, S11	S2, S12
-Y	S3, S9	S4, S10
+Z	S3, S11 or S7, S15	S2, S10 or S6, S14
-Z	S1, S9 or S5, S13	S4, S12 or S8, S16

To minimize disturbance torque during main engine burns, the line of thrust from the

main engine should be directed through the center of mass (CM) of the vehicle.

Because the CM of the vehicle will have some misalignment with the vehicle centerline, and the main engine thrust will also be slightly uncertain, the line of thrust will not be exactly aligned with the centerline. With a gimballed main engine, the misalignment will be largely mitigated.

The two-degrees of freedom gimbal mechanism for the main engine uses closed-loop control to vary the gimbal angles so that the thrust will pass through the CM. The control system will actively vary the line of thrust by small angles as needed to provide control torque about the two transverse axes. Control torque about the vehicle's long axis will be generated using some of the sixteen MIT thrusters; propellant needed has been included for that function.

Galileo Avionica currently has a rad-hard version of its AA-STR star tracker that was developed for Bepi-Colombo. (The TRL for this model is 6 or higher.) This has an Active Pixel Sensor (APS) focal plane based on CMOS technology. Similar focal planes have shown good performance (e.g., very little increase in dark current) after exposure to a total dose of 300 krad behind 100 mils of aluminum. Tests on APS detectors suggest that the technology can be designed to survive a total dose as large as 10 Mrad behind 100 mils of aluminum. The pre-amp used to boost the signals from the AA-STR camera head must be rad-hard as well. APS sun sensors are baselined for initial acquisition post launch and safe mode operations. Solar cell-based sun sensors can be an alternative choice and can be studied in the future.

The Litton Scalable Space Inertial Reference Unit (SSIRU) contains a redundant set of four hemispherical resonating gyros (HRGs). These are "wine glass" gyros made of a crystalline material that is robust to radiation. Cassini is currently flying Litton HRGs in an earlier version of this inertial reference unit. The commercially available SSIRU has redundant power supplies, redundant processing electronics, and is fully internally cross-strapped. Rad-hard electronics for the box need to be developed.

Stellar inertial attitude determination would make use of a Kalman filter to blend

measurements from the gyros and star tracker to provide a continuous estimate of spacecraft attitude.

In a high radiation environment, there could be many false star indications and relatively few persistent true stars in the focal plane. Software algorithms to filter out the false stars and identify the true stars will be a key development to operate in JSO's radiation environment.

Well-calibrated HRG gyros are used to propagate attitude for hours at a time without star updates, while still meeting pointing requirements. So, while the vehicle is operating in a high radiation environment with numerous false star indications, such as at JOI and the Io encounters, the Kalman filter is tuned to rely more heavily on gyro measurements and less on star updates.

The radiation environment is much less harsh while in orbit around Ganymede than at Io or Europa, consequently, there will be fewer false star indications and more frequent true star updates. Then, the Kalman filter is tuned to rely more heavily on star updates and less on gyro measurements.

Propulsion

The dual mode design for JSO uses a hydrazine/nitrogen tetroxide bipropellant main engine ($I_{sp} = 325$ s) for major ΔV requirements, and hydrazine catalytic monopropellant thrusters ($I_{sp} = 225$ s) for minor ΔV requirements, roll control, and attitude control backup. [Figure 4.4-9](#) shows the propulsion subsystem schematic. The final design for a Class A system may add pyro ladders and other components specific to the expected major propulsion events, and consistent with Cassini propulsion system design. The driving requirements on the propulsion subsystem are a wet spacecraft mass of 7810 kg and a ΔV budget of 2705 m/s with additional fuel (hydrazine) for RCS.

The dual mode design uses a two-axis gimballed, Aerojet-Redmond 890 N High Performance Apogee Thruster (HiPat) main engine for major ΔV events. It was developed for a DoD program and will be qualified in 2009. The design is a scaled up version based on the 450 N HiPat thruster currently qualified and in service. The 450 N HiPat is a design based on improvements from the engine on Cassini. The main engine is centerline

mounted and not redundant (due to low probability of failure—the same as the Juno mission).

Dual mode propulsion has not previously been flown for outer planetary missions, but is a well-understood technology proposed for Juno and other deep-space missions. The fuel tank is shared between the main engine and the monopropellant thrusters. The design has dual seat valve inlet, with upstream latch valves to the thrusters, which allow added reliability to cut off fuel flow in the event of a thruster leak. The dual-mode system is kept at near-constant pressure via a helium pressurant assembly. Isolation during the long interplanetary phase is provided by pyro-valves. When not isolated, the propellant temperatures are maintained below that of the feed system to prevent cryo-pumping through the feed system. While cryo-pumping is not a major concern for reliability, this strategy prevents a failure mechanism associated with unwanted leaking of the pressurant system. The dual-mode feed system completely isolates the oxidizer from the fuel, eliminating concerns for unexpected fuel/oxidizer contact (the suspected Mars Observer failure).

The HiPAT engine is used for six events totaling 244 minutes of firing. The JOI orbit insertion burn of 76 minutes exceeds the current qualified single thrust duration of 30 minutes but is not expected to be an issue since it is at steady state and the risk of a longer duration are very low. Work for qualifying this engine has been included in the cost estimate.

Eight Aerojet MR-107P 90 N (20 lbf) monopropellant engines provide for smaller trajectory correction maneuvers (TCMs) and for thrust vector control when the HiPAT engine is firing. Total operational time for the 90 N thrusters is 176 minutes. The 90 N thrusters are side pointing at the corners of the spacecraft and are off-pulse controlled for pitch and yaw. The eight thrusters are fully redundant. The throughput and cycle qualifications are well above JSO needs. Dual catalyst bed heaters are warmed for 60 minutes prior to planned operation.

The sixteen, monopropellant, 0.7 N MITs provide for de-saturation of the reaction wheels, roll control, and for backup attitude control with pure couples for functional

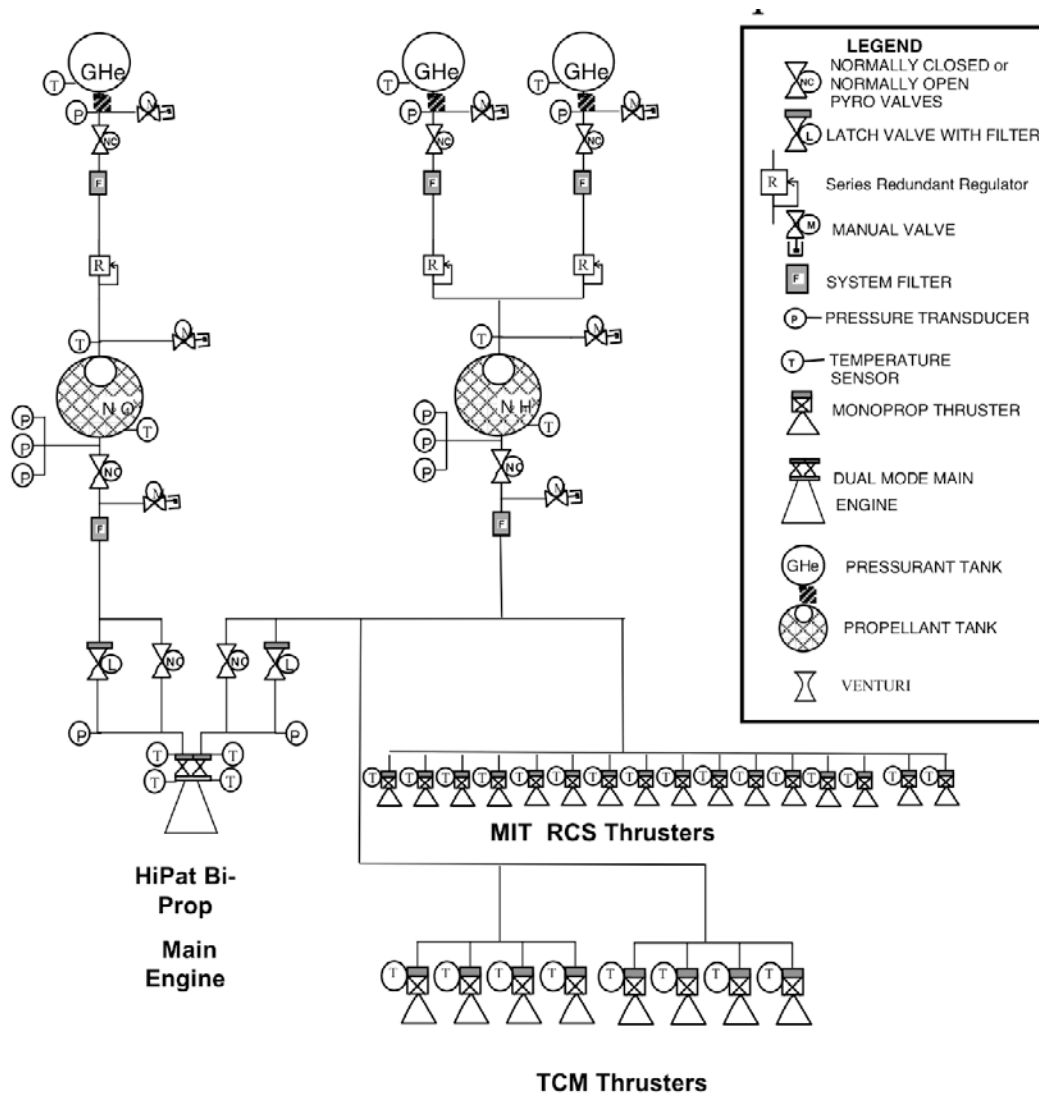


Figure 4.4-9. Propulsion Subsystem Schematic

redundancy with the reaction wheels. Their small impulse bit of one milli-Newton-second allows for highly accurate spacecraft attitude and pointing control. They are not yet space qualified but have completed development and have been tested in a space-like environment. Qualification for these valves is included in propulsion subsystem costs.

One hydrazine (fuel) tank and one oxidizer (MON-3) tank provide the propellant storage. Fuel and oxidizer are stored in monolithic titanium tank with spherical ends and a cylindrical center section. The diameters are 48.9 inches (1242 mm) based on the ATK/PSI operations 80456-1 propellant tank used for MRO. Using tanks that have the same diameter as a previous mission results in

significant cost savings in tooling and manufacturing. Both tanks would need to be rated for a higher maximum operating pressure of 340 psia to allow the HiPat main engine to achieve its specific impulse. Therefore a single qualification for both tanks (done on the longer hydrazine tank) is needed and included in the costs.

A surface tension PMD, probably very similar to the MRO 80456-1 tank (if not identical) would be used inside the tanks to ensure no gas is drawn into the propulsion system.

Custom composite overwrapped pressure vessels (COPVs) with aluminum liners store helium pressurant for the spacecraft. The tank designs are well within recent COPV design

experience with the diameter being a key design parameter. There are a total of three pressurant tanks: two fuel pressurant tanks and one oxidizer pressurant tank, so that the three are approximately the same size and can be bought as the same tank (even if that makes the fuel pressurant tanks slightly over sized). The pressurant tanks are near-spheres with a diameter of 0.71 m and the same length but elliptical heads.

Power

The Power Subsystem provides power using 8 MMRTGs for the baseline with a predicted end of mission power capability of 778.5 W. A fully redundant 38 Ahr Li-Ion battery is used for energy storage to handle the peak power during main engine maneuvers and satellite flybys during the Jovian Tour. The design utilizes a regulated power bus with the operating point adjusted to track the peak power point of the MMRTGs throughout the life of the mission. The regulated power bus (22–36 Vdc) is capable of delivering 1440 W under peak load conditions. The power subsystem concept is illustrated in [Figure 4.4-10](#)

4.4-10. The battery connects to the power bus via bi-directional converters, which provide charge and discharge control.

Each MMRTG can deliver 125 W each at beginning of life (BOL). For the JSO study, the MMRTG power level was derated to 118 W each at Beginning of Mission (BOM) to account for the time interval (which can be on the order of years) between when each MMRTG is fabricated by the Department of Energy and when the generators are actually launched. The MMRTG is currently under development and is the baseline power source for the Mars Science Laboratory due to launch in 2009. The MMRTG has a degradation rate of approximately 1.6% per year leaving approximately 778.5 W at the end of the 12-year mission for all MMRTG units. A performance summary and illustration of the MMRTG is shown in [Figure 4.4-11](#).

Two 38-Ahr Li-Ion batteries were selected due to the high energy density (~100 W-hr/kg) and the relatively benign radiation degradation. Both Li-Ion and Super Ni-Cd batteries have been radiation tested and are environment. The cell size and cell protection

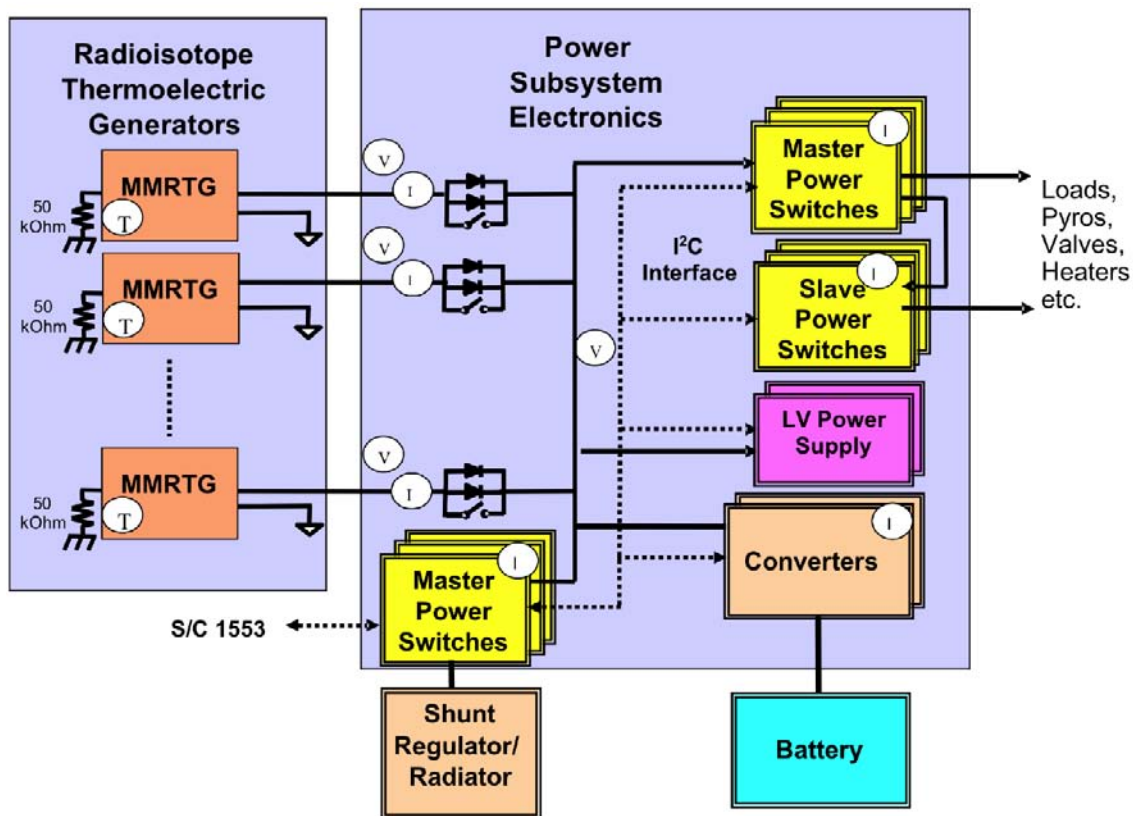


Figure 4.4-10. Power Subsystem Block Diagram

MMRTG Characteristics	
Power/unit, W (BOM)	118
Duration from BOM to EOM, yrs	12
Power Degradation Rate/year	1.6%
Power/unit, W (EOM)	97.3
Mass, kg	44
#GPHS Modules	8
Thermal Power, Wth	2000
Specific Power, W/kg (BOL)	2.8
Conversion Efficiency, %	6.3%
T_{hot} , °C	635
T_{cold} , °C	208
Rad. Sink Temperature, K	4
Redundancy	Built-in

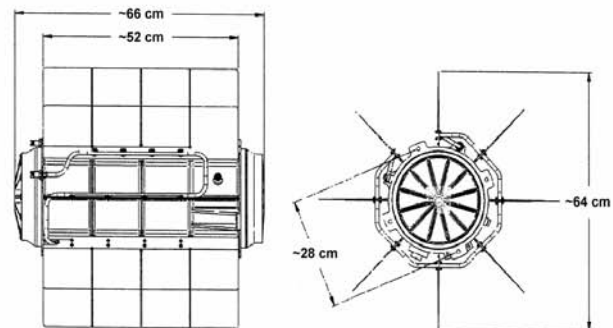
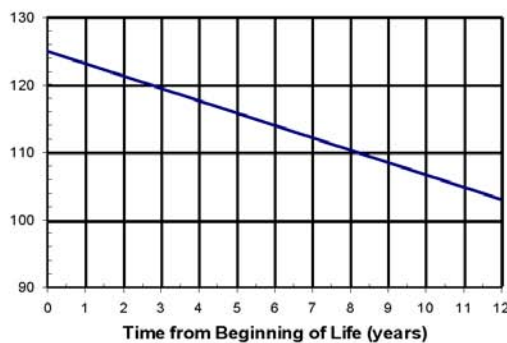
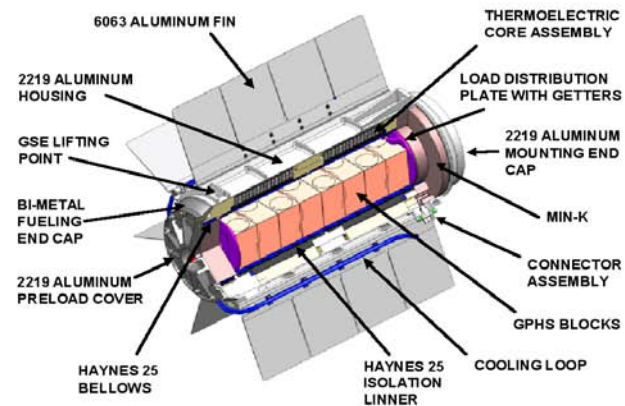


Figure 4.4-11. Performance and Configuration of the MMRTG

for the Li-Ion batteries are considered in the point design power electronics. The depth-of-discharge for the battery is limited to 70% for < 100 cycles on the battery. If a lower depth of discharge was desired, both batteries could be used. **Table 4.4-6** shows the battery margin and DOD for all the power modes.

The power subsystem electronics are based on radiation-hardened X2000 technology that has been verified to the 1 Mrad total dose level. Development of critical chips has been completed along with TRL 6 radiation testing. MMRTG power is provided through a fault tolerant interface to a single, power bus similar to the Cassini design. The power bus regulation (22–36 Vdc) combines the use of the shunt regulator, which is sized for the BOL power from the MMRTGs, with the bi-directional power converter, which is used to control the charge and discharge of the battery. The power electronics chassis (**Table 4.4-9**) performs MMRTG and battery management, pyro and valve drivers and various switching functions. The power electronics boards are fully redundant. The power model also uses

relatively lightly populated boards (fewer switch functions per board), which gives higher switch count than a more densely loaded board. This is a lower risk solution. COTS conversion technology is being used along with the MCM-HDI (Deep Architecture (DA)) switching technology. Some of the benefits to the smart switch technology is it has over current protection and soft start over voltage protection.

Thermal

Driving requirements on the thermal design are primarily from: 1) the VEEGA trajectory where the incident solar energy varies from about twice the incident energy at the Earth for the Venus gravity assist to about 4% of the incident energy at the Earth at Jupiter, 2) accommodating the MMRTGs, 3) cooling radiation vaults housing the electronics that will run very warm, while 4) minimizing electrical power for heaters.

The design utilizes both passive and active thermal control elements. The passive elements are multilayer insulation (MLI), thermal control surfaces (films and paints),

Table 4.4-9. Power Electronics Suite

Card/Slice Units	Total NA	Mass/Unit (Kg) CBE	Total Mass W	Power/Unit W	Total Power W
Shunt Regulator	4	0.8	3.2	2	8
Battery Control Slice	2	0.8	1.6	2	4
Load Switching	10	0.9	9	2	20
Thruster Drivers	4	0.9	3.6	2	8
Pyro Switching	2	0.9	1.8	2	4
RTG Interface Card	2	1	2	2	4
Power Converter Assembly	2	1.1	2.2	5	10
Backplane	2	1.4	2.8	1	2
Chassis	1	8.39	8.39	0	0

thermal conduction control (In this case thermal conduction isolation to minimize thermal heater power requirement), thermal radiators, and thermal louvers. The active thermal control elements are electric heaters, control thermostats, temperature sensors, and variable conductance heat pipes.

The electronics for this mission are encased in several radiation vaults to protect them from the radiation environment at Jupiter. This means that all the electric dissipation is in the vaults. To reject the thermal energy generated, the energy is transported from the internal elements from the vaults to a thermal heat rejection system using heat pipes. For this design, the thermal rejection system is a thermal collector plate in each vault, with a thermal transfer system to the rejection system, which in this design is a variable conductance heat pipe system. This heat pipe system is connected to a 2.5 m² thermal radiator, which has a view to space. Mounted on the thermal radiator are two thermal louvers to control the temperature of the vault by varying the thermal rejection capability of the radiator. The thermal radiator also functions as the shunt radiator. It is sized so that it can dump most of the electrical energy that the MMRTGs generate when all power is off to the spacecraft. In order to accommodate the bus during the Venus gravity assist, a sun shade provides thermal blockage.

The Propulsion subsystem is relatively large and requires significant thermal design. The tanks are covered with MLI, and use RTG waste thermal energy to keep the temperature of the propellants above their minimum allowable temperatures. There are two propellant tanks, one fuel, one oxidizer, and three pressurant tanks. The fuel and oxidizer tanks are enclosed in a mechanical support cylinder, and are covered with MLI. The mechanical support cylinder is covered with

MLI as well. The pressurant tanks are mounted outside the mechanical support cylinder, and are covered with MLI. The outer layer of MLI around the mechanical support cylinder is doubled layered with a stand off to protect against micro-meteroids. The MLI layer on the inside of the stand off has 5 layers and the MLI on the outside of the stand off has 20 layers. The stand off distance is on the order of 10 to 30 cm depending on MLI location on the spacecraft. Electric heaters and RHU's are used on the propellant lines and valves. Electrical heaters are used where RHU's are impractical (e.g., along certain parts of the propellant lines). RHU's are used on the thruster clusters.

The MMRTGs are carried on a support ring, and the mechanical design has addressed their field of view requirement. Thermal energy from the MMRTG's is transferred to the propellant tanks with IR transfer devices. The thermal balance in the propellant tank system is maintained by controlling the thermal energy transfer to space with thermal radiators and thermal louvers. The Cassini spacecraft uses this approach.

Thermal control for the instrument interface is a thermally isolated interface (both radiatively and conductively) and provides a thermal interface temperature control of -20 to +35°C.

Temperature sensors are placed to provide engineering data for the spacecraft. Most of the cabling is inside the vehicle. The cabling that is outside the vehicle is covered with MLI.

4.4.4 Verification and Validation

JSO will verify and validate the mission system to ensure it meets specifications and is capable of accomplishing the science objectives. A combination of system analysis, modeling and simulation tools, engineering development unit hardware and testbeds, flight

software testbeds utilizing simulations and engineering model (EM) hardware, spacecraft functional/environmental testing (Assembly, Test and Launch Operations, ATLO) and readiness tests will be used.

Simulation Capability

A high fidelity model-based simulation capability (S-Sim) is baselined for flight software test and verification. The plan includes having the first S-Sim version available to support the first flight software release and continue on with expanded capability in support of testing of subsequent flight software builds. The simulation environment will be available on all software development and test workstations (full software simulators). These simulators will be built to allow for interchangeability between software models and hardware EMs later in the “hardware-in-the-loop” testbeds in such a way that is transparent to the flight software, allowing the use of the same test scripts whenever the testbed models are interchanged with EMs.

In addition to the simulation capability described above, JSO will have 2 dual string testbeds. The Mission System Testbed (MSTB) is a high-fidelity testbed that is dedicated to system V&V, Flight Software fault tests, mission system tests, and ATLO support. Earlier in the V&V plan, the dual string testbed functions as 2 single string testbeds for subsystem level 4 V&V. These testbeds will include the C&DH, AACS, power, telecom and harness subsystems. Only the Mission System Testbed (MSTB) will have hardware versions of the engineering subsystems; they will be simulated on the other testbeds.

The testbeds provide a high fidelity environment for development and for verification and validation. They will include the Ground Data System (GDS) hardware and software as well. The EM versions of all spacecraft engineering subsystems and instruments pass through the testbeds for integration and interface verification. No flight units are required to flow through the testbeds unless there have been major modifications from the EM, although the testbeds can support flight hardware integration if needed. S-Sim will be used for Verification and Validation (V&V) that can off-load the

hardware-in-the-loop testbeds as well as using the EM integration effort to help enhance evaluation of model fidelity. The S-Sim interfaces and procedures will be compatible with those of the hardware testbeds. The testbeds will also be used to train test analysts to support ATLO testing as well as to support ATLO procedure development and anomaly investigation. All flight software versions will be verified on the testbeds prior to being loaded onto the Spacecraft in ATLO or in operations.

ATLO and I&T Approach

The JSO system integration and test (I&T) approach is modeled after the Cassini ATLO effort as these two missions share a great deal of similarity in complexity and design. JPL’s 25-foot thermal vacuum chamber will be utilized for system thermal vacuum testing with two planned tests, one using the solar simulator and one without the solar simulator. The JSO GDS will be used in all the functional and performance tests to allow for end-to-end data flow testing and tools suites validation. Operational Readiness Tests (ORTs) will be performed to assess the infrastructure and team’s ability to execute the operational phases of the mission.

A Developmental Test Model (DTM) will be built that will effectively be the EM for the spacecraft structure. The DTM is used to alleviate the schedule impact of the flight unit. The DTM will be used to do static and modal testing which allows the flight unit to be integrated in parallel. In addition, the DTM is used to do fit checks and cable or mass mock-ups. This model will also be used as a fit check “trailblazer” at the launch site to ensure that the procedures and processes for integration of the RPSs with the spacecraft are compatible and streamlined during the launch preparations.

The ATLO schedule and I&T plan will be developed early. This process is designed to provide verification of the spacecraft design and workmanship by subjecting the spacecraft to a demanding series of functional, operational, and environmental tests. Initial assembly begins with delivery of the spacecraft primary structure, the propulsion subsystem and the electrical cable harness. Each electrical subsystem undergoes vibration, thermal, pyroshock, Electromagnetic

Compatibility/Interference (EMC/EMI) and magnetics testing/characterization, and potentially sterilization processing prior to delivery to ATLO. Each subsystem with electrical functionality is integrated using assembly plans and test procedures that ensure mechanical and electrical safety and which have been verified in the testbed. Once all of the subsystems are safely integrated and fully functional at the bus level, the payload is integrated with the spacecraft forming a complete spacecraft. A preliminary Incompressible Test List is generated by Project Critical Design Review (CDR) and approved by System Integration Review to identify and assure that all critical testing is performed on the spacecraft prior to launch. To ensure that a complete and comprehensive system-level test program is provided, ATLO V&V is augmented with payload simulators, engineering models and the DTM.

The JSO team will maintain a rigorous formal program for testing flight hardware at all levels of assembly (“Test as you fly”). Electrical testing includes component interface tests, spacecraft functional tests, DSN compatibility tests, instrument interface verifications, performance tests and environmental tests. All electrical test procedures are verified on the testbed prior to being run on the spacecraft. Similarly, all flight software versions are run through the testbeds before being uploaded onto the spacecraft in ATLO.

The JSO environmental test program consists of a comprehensive system level test program that ensures that the spacecraft has been verified to operate in the expected environments of the mission. At the subsystem or assembly level, all flight hardware will be tested to acceptance levels and durations if there has been a preceding qualification test or to protoflight levels and durations if no qualification unit was available. System level environmental tests include system level acoustics, vibration and shock, thermal balance, and thermal vacuum. The system level EMC/EMI and magnetic cleanliness verification is performed via modeling of the assembly and subsystem level testing performed prior to ATLO. Modal surveys are also performed to validate the spacecraft structural model. Functional tests are repeated

after each environmental test to ensure that the test effects have not degraded system performance. Post-environmental tests also facilitate verification of any modification to flight software or flight sequences.

All flight engineering subsystems are required to track powered-on time and are required to accumulate 1000 hours (goal 2000 hours) prior to launch. Flight engineering spares are required to accumulate 500 hours (goal 1000 hours). Instrument electronics are required to accumulate 500 hours prior to launch and functional testing is performed prior to and immediately after shipment to verify that the shipment did not adversely effect its performance.

The RPSs will be delivered separately to the launch site by the DoE. The RPSs will be test fitted to the spacecraft to ensure adequate mechanical and electrical functionality. They will then be removed and stored until final integration on the launch pad.

The last steps for the spacecraft prior to launch are: final electrical testing, propellant loading, integration with the launch vehicle, and RHU and RPS integration.

4.5 Operational Scenarios

4.5.1 Overcoming the Challenges of Operating in the Jovian System

Jupiter and its vicinity present a challenging and hazardous environment for operating any science mission. Operational scenarios provide a means to collect and return the science data needed to meet all of JSO’s mission goals in the primary science mission.

Some components commonly used for spacecraft data systems such as high-speed, high-density memory components are not sufficiently robust for use by JSO. Lower density memory components can be used, but mass memories of reasonable size and power consumption have relatively low data storage capacity. Mass memories of ~9.6 Gb can be reasonably accommodated in the JSO spacecraft design. Given a few operational constraints commonly encountered in past missions, such memories can support daily data volumes approximately equal to their capacity. These constraints include: near real time data compression and downlink encoding, no data retransmission, and scheduling one DSN pass per day.

The JSO science operations scenario is designed to obtain comprehensive measurements of the major Jovian system bodies during the Jupiter Approach sub-phase and the Jovian Tour phase. Remote sensing observations of Jupiter, the Galilean satellites, and the rings will be obtained. These observations will serve to extend the currently available coverage from Voyager, Galileo, Cassini, and New Horizons in spectral range, spectral resolution, spatial coverage, spatial resolution, and time sampling. They will allow monitoring of the state of Jupiter's atmosphere and its circulation and of Io's volcanic activity. Particles and fields measurements by the space physics instruments will characterize the state of the Jovian magnetosphere.

More detailed observations of the Galilean satellites and their environs will be possible during the 20+ close flybys that comprise the tour. These flybys will permit remote sensing coverage at higher resolution over regional to global scales as well as very high-resolution samples of limited areas. Near closest approach, the ground-penetrating radar and laser altimeter will return signals allowing measurements of the satellites' surfaces and subsurfaces along the closest approach ground track as well as characterizing the performance of these instruments so their utility can be optimized during the later Ganymede orbital phase. The solid-state recorder (SSR) memory will be filled during each close encounter. The magnetometer and plasma spectrometer/energetic particle detector will characterize the magnetospheric interactions with the satellites and permit improved measurements of their intrinsic and induced magnetic fields.

After the Jovian Tour lasting about 3 years, the JSO mission will enter orbit about Ganymede. This orbit is described in more detail in §4.3.1.3. Due to limited knowledge of the Ganymede gravity field and Jupiter's gravitational perturbations, initial orbits will likely need maintenance every week to few weeks. In the first weeks in Ganymede's orbit, Doppler data will increase knowledge of the Ganymede gravity field rapidly, and initial orbit parameters will be adjusted accordingly. A lower circular, high-inclination orbit will be designed for improved geophysical measurements. Orbit maintenance interruptions to science operations should decrease in

frequency over the course of the Ganymede orbital phase.

During the low periapsis passes, high-resolution measurements of Ganymede along the ground track can be made, and the SSR will be filled. At intermediate altitudes, SSR playback takes place. In the apoapsis period, global-scale mapping of Ganymede is obtained (in stereo) and distant monitoring of other Jovian system bodies is conducted.

After one year in the elliptical orbit, the spacecraft will transfer to a $\sim 95^\circ$ inclined, 200 km altitude circular orbit. From this orbit, precise gravity and magnetic field determination and altimetry can be used to constrain the interior and surface shape of Ganymede and their variations throughout its tidal cycle. High-resolution coverage of targets of particular science interest on Ganymede can be obtained with the ground-penetrating radar and at wavelengths spanning from UV to far-IR, with visible coverage in stereo for the baseline mission.

Several previous planetary missions have met similarly aggressive science goals in challenging environments with similar operations scenarios. [Table 4.5-1](#) shows a comparison of operational mission characteristics for other in-family previous planetary missions.

In the 5 years of the primary JSO science phase, complete color and stereo maps of the Galilean satellite surfaces are obtained, altimeter and ground-penetrating radar profiling observations cover the globe of Ganymede, and more than 50,000 synergistic multi-instrument targeted observations are obtained for monitoring Jupiter, Io, and the rings and of high priority sites on the Galilean satellites.

4.5.2 Mission Overview

Operational scenarios have been devised for each JSO mission phase based on mission priorities. As shown in [Table 4.5-1](#), the primary mission duration is up to 12 years. Up to 7 years are allocated for the Interplanetary phase and five years for Jupiter system science operations. Following JOI, the mission will undertake a series of gravity assist flybys of the Galilean satellites Io, Ganymede, Callisto, and Europa to explore the Jovian system and finally to reduce the propellant requirements to enter orbit at Ganymede. The gravity assist

Table 4.5-1. Comparison of Operational Mission Characteristics*

Mission Comparison	JSO	Cassini	MRO	MGN	MER
Mission Phase Durations					
Interplanetary Cruise	84 months	84 months	7 months	14 months	7 months
Primary Science	60 months	48 months	26 months	9 months	3 months
Number of Instruments	9	12	8	4	6
On-board Data Storage	9.6 Gb	2 Gb	160 Gb	2 Gb	256 Mbytes
Downlink Data Rate	600 kb/s	14–165 kb/s	700–4000 kb/s	270 kb/s	128 kb/s
Daily Data Volume	17–50 Gb	2 Gb	70 Gb (avg)	13 Gb	0.3 Gb
Primary Mission Data Volume	30 Tb	2.5 Tb	50 Tb	3.5 Tb	0.03 Tb
DSN Tracking	7–21 tracks/week	8 tracks/week	18 tracks/week	21 tracks/week	2 ODY relays/day
Science Planning: Execution Cycle:					
Approach & tour -	26 wk: 4 wk	26 wk: 4 wks	2 wk: 2 wks	2 wk: 1 wk	1 day: 1 day
Ganymede orbit -	4 wk: 2 wks				

*Galileo was not included here due to its HGA failure and the consequent difficulty of making meaningful comparisons

flybys and other aspects of the Jovian Tour trajectory represent opportunities for close and far observations of the Galilean satellites and Jupiter. GOI begins a 2-year primary Ganymede science phase, which completes the primary mission. When the spacecraft becomes non-operational or when it runs out of propellant for orbit maintenance, the spacecraft will de-orbit and crash into Ganymede within weeks to months.

Summary of Operations Scenarios by Mission Phase

After launch, the mission focus will be on the checkout and characterization of the spacecraft. The radar antenna, MAG boom, and HGA are deployed. For the first month of operations, the mission will rely on continuous tracking with 34 m DSN stations. The first trajectory correction maneuver (TCM) will be needed to remove launch injection errors. Real-time-initiated commanding will predominate during this early period to provide flexibility to respond to unknowns. A transition to sequence-initiated commanding will occur as the transition to cruise completes.

The cruise sub-phase encompasses the gravity assist flybys of Venus and Earth, which are needed to add the necessary energy to the trajectory to reach Jupiter. Each gravity assist will be used to checkout and characterize all instruments and flyby operating processes and tools. During quiet periods of cruise the operations and supporting teams will be testing and training on the tools and processes to be used for the Jupiter system science and Ganymede science operations.

Cruise sequences will last one to two months during quieter periods, and will last one to two weeks near the Venus and Earth flybys. DSN tracking will be normally twice per week with 8-hour 34 m passes. Tracking will increase to nearly continuous levels in the weeks surrounding major maneuvers and gravity assist flybys.

After the final Earth gravity assist flyby, the mission operations and science teams and operations centers will begin preparation for arrival at Jupiter and will deploy and test final flight and ground software. While all critical activities for JOI and science operations at Jupiter will have been tested pre-launch, final updates based on post-launch experience and new capabilities will be deployed, and testing and training will be performed to assure mission readiness. DSN tracking will increase to nearly continuous levels in the two months prior to JOI to support navigation and the first Jupiter system observations.

In the Jovian Tour phase, the spacecraft will make routine and frequent observations of Jupiter and its environment. There will be opportunities to observe Io, Ganymede, Callisto, and Europa during more than 20 close flybys in this phase. Nearly as many opportunities exist as well to observe Jupiter from less than 1 million kilometers, and Io, Europa, Ganymede, and Callisto from less than 500,000 km. Flybys are 1 to 2 months apart early in this phase, becoming a week or less apart as the tour ends.

While the spacecraft is in Jupiter orbit during the tour, each Jupiter closest approach

typically happens within a day or two of a satellite gravity assist flyby or encounter. Orbits with gravity assist flybys have additional DSN tracking coverage scheduled. The Jupiter opportunities are well distributed across the tour, facilitating observation of changing phenomena that span the length of the 3-year tour. There are opportunities to collect Jupiter system science in the weeks between encounters. **Table 4.5-2** summarizes the number and characteristics of the Jupiter observing, gravity assist encounter, and non-targeted observing opportunities during the tour.

Several feasibility level analyses were conducted to explore the usefulness of the JSO system for scientific measurements during gravity assist encounters. Ground speeds, altitudes, and lighting conditions vary drastically for flybys. Furthermore, to effectively use some of the instruments, spacecraft slews may be needed. SSR capacity is the primary constraint to encounter data collection but is less so for non-targeted encounters and Jupiter observations.

Operations team sizes increase by the end of the tour to support activities in the reduced time between flybys and to prepare for Ganymede operations. The final month prior to GOI will focus on setting up the geometry for GOI. Science operations in this sub-phase will be reduced in complexity in favor of navigation activities. Early Jovian Tour sequences will last one to two months with special short term sequences developed for encounters.

DSN tracking will be normally one 8-hour 34 m pass per day with additional 70 m DSN passes scheduled around close flybys. Tracking will increase to nearly continuous

levels in the month prior to GOI to support final navigation targeting and prepare for Ganymede science operations. Continuous 70 m DSN tracking will be scheduled for the first month in Ganymede orbit to support the required improvement in gravity field determination and unique new opportunities for Ganymede science. Tracking will be reduced to two 70 m passes per day for months 2 and 3 in Ganymede orbit followed by one 70 m pass per day after that. When the orbit is circularized at 200 km altitude, the same increased tracking coverage pattern will be implemented for the first 3 months in the lower orbit. DSN coverage is summarized in **Table 4.5-3**.

The Ganymede Science phase is 24 months long. Data acquisition and return scenarios are detailed in §4.5.3.6 and 4.5.3.7. Data collection scenarios are defined depending on the type of orbit (elliptical vs. circular) and the level of DSN tracking planned (1, 2, or 3 passes per day). The SSR is used to buffer data taken between DSN passes, when the Earth is occulted, or at higher rates than the real-time downlink can support.

Science data collection includes continuous fields and particles data throughout the Jovian Tour and Ganymede Science phases. Remote sensing observations will be planned to take advantage of desirable geometric opportunities. Altimetry and radar sounding will be restricted to times when target distances are below ~2000 km. Targeted data acquisitions comprising GPR profiles and remote sensing coverage will be collected. Lists of targets to be acquired via onboard targeting software will be developed and uplinked to the spacecraft every 2 weeks. Quick-look data processing, mapping assessment, and target

Table 4.5-2. System Science Observing Opportunities

	Opportunities	Ranges (km)	Phase angles (deg)	Ground Speeds (km/s)
Jupiter	9 23	290,000 – 500,000 500,000-1,000,000	5° - 60°	
Encounters				
<i>Callisto</i>	11	100 – 1940	30° - 170°	2.8 – 9.3
<i>Europa</i>	6	100 – 600	60° - 170°	4.3 – 7.1
<i>Ganymede</i>	7	100 – 2850	10° - 170°	1.3 – 8.0
<i>Io</i>	4	100 – 500	60° - 140°	6.9 – 15.1
Non-Targeted Encounters				
<i>Callisto</i>	2	230,000 – 400,000	40° - 150°	
<i>Europa</i>	8	78,000 – 490,000	50° - 140°	
<i>Ganymede</i>	7	24,000 – 410,000	5° - 160°	
<i>Io</i>	8	110,000 – 480,000	10°-70°	

Table 4.5-3. DSN Coverage

Phase	Sub phase	Duration	DSN Coverage hours/day	Sub-net	Activity Summary
Interplanetary	Launch and Early Operations	1 months	Continuous	34m	Flight system characterization, calibrations, maintenance, housekeeping, and cruise science
	Cruise	Up to 83 months	8 twice a week, except: 1) Continuous +/- one week @ Venus and Earth gravity assists 2) Continuous for two days @ tracking data cutoff for TCMs		
	Jupiter Approach	2 months	Continuous	70m equivalent	Optical Navigation, Jupiter imaging
Jovian Tour	JOI and Capture Orbit	7 months	8 during cruise, 24 during encounter day and within +/-2 days around perijove	70m equivalent	Continuous fields and particles, Mapping activities for target satellites, GPR and altimetry when altitude < 2000 km Io monitoring, Jupiter atmospheric monitoring Close satellite flybys for gravity assists
	Io Sub-tour	23 months			
	EGC Sub-tour				
	Ganymede Approach	6 months	Continuous in last month prior to GOI		
Ganymede Science	Elliptical Orbit	1 year	Continuous for 1st month 16 over next 2 months 8 over last 9 months	70m equivalent 34m (Ka) for radio science	Fields and particles science – 24/7 High-resolution global mapping of Ganymede, selected targets
	Circular Orbit	1 year	Continuous for 1st month 16 over next 2 months 8 over 9 months 8/day Ka for 1 st month		Fields and particles science – 24/7 GPR, Altimetry, Gravity map, Mag map Selected high-res targets

selection processes will all be undertaken continuously during the Ganymede orbit phase with new sequences being uplinked every 2 weeks. Downlink data rates will be determined for each sequence based on the conditions for Earth range, DSN elevation angle, and Jupiter radio (hot body) noise for each pass. These variable data rates increase the average data volume returned by nearly 50% over traditional methods. In the first month of each Ganymede orbit phase, one 34 m DSN station will be scheduled each day to allow 2-way Ka-band Doppler tracking for gravity science.

Spacecraft Operability Features

The JSO spacecraft is comprised of a bus and a payload of 9 science instruments and two radio science investigations. The payload list, operational needs, and data rates are shown in [Table 4.2-2](#). The details of the spacecraft design are in §4.4. The radio science investigations use the bus' telecom system

The bus features a C&DH with a redundant RAD750 flight computer and a stand-alone SSR with 9.6 Gigabits allocated to science data collection. The C&DH hardware and flight software are capable of providing the needed data reduction and downlink encoding at near real-time rates for the low-rate instruments. But the highest data rate instruments must have real-time data reduction and compression capabilities built in.

The telecommunications subsystem features a 50-W Ka-band telemetry system and a 5 W X-band carrier-only transponder for gravity science. The Ka-band telemetry rates are 600 kb/s at 6.5 AU for 70 m DSN elevation angles of 20 degrees (and 90% weather). The C&DH subsystem and the SDST together provide for modulation and encoding (Reed-Solomon and Turbo) of telemetry. Data rates for science data return will range from 600 kb/s up to nearly 1800 kb/s under the best range and elevation angle combinations at

70 m stations. The detailed scenarios described here are all based on the worst-case 600-kb/s capability, which provides a return of ~15 Gb per 8-hr DSN pass. **Figure 4.5-1** illustrates the JSO information flow.

The spacecraft will typically be continuously nadir pointed while in the low, circular Ganymede orbit and during much of the elliptical orbit period. This orientation allows the payload to observe the surface continuously and to monitor the local environment from a consistent attitude. The HGA will be pointed to Earth continuously via a 2-axis gimbal. Pointing accuracy is at least 1.2 mrad for the HGA and 0.4 mradians for the instruments.

Mission Design

The cruise trajectory, Jovian tour trajectories, and Ganymede science orbits are described in §4.3. One Ganymede orbit, or ganysol, is 7.155 days in duration. Ganymede is occulted from the Earth by Jupiter for ~3.6 hours every ganysol.

To satisfy the science objectives, the science orbit at Ganymede will initially be elliptical to permit global mapping along with gravity and magnetic field determination.

Requirements for improved geophysical measurements and observing selected targets on Ganymede at high resolution lead to the requirement for a low-altitude (~200 km), near-circular, high-inclination orbit with consistent day-to-day lighting. In this low orbit there will be ~9 orbits per day, and ground-track speeds will be ~1.77 km per second.

For a 200 km altitude orbit, the orbit period is 2.6 hr, and occultations by Ganymede can last up to 37% of the time depending on the orientation of the orbit. The primary constraints on the orbit orientation are the required inclination and nodal phase angle. The orbit inclination is 95 degrees, which maintains the local true solar time of the node at ~4:00 pm.

Mission Operations System

The Mission Operation System (MOS) is comprised of all hardware, software, networks, facilities, people, and processes used to operate the spacecraft. The MOS includes project-specific elements, i.e., GDS and flight teams, elements shared with other projects, i.e., DSN and related services, and those parts of the science teams that are used in the operations of the spacecraft.

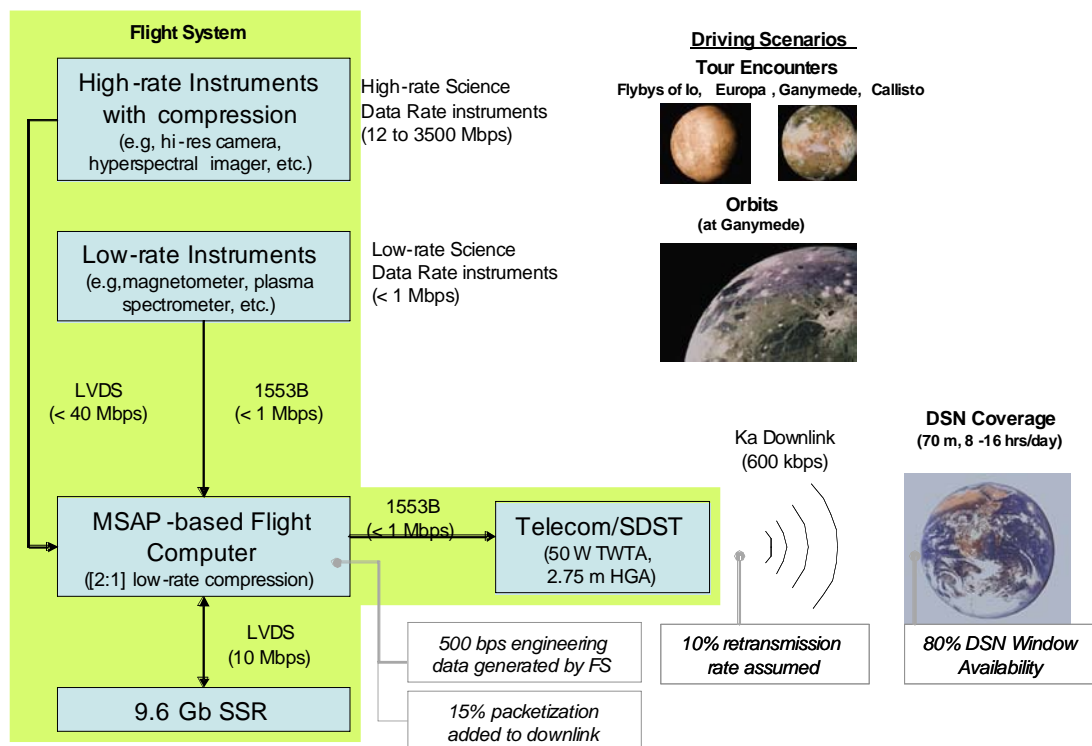


Figure 4.5-1. JSO Information Flow

The MOS functional elements include mission and science planning, sequencing and command processing, telemetry and tracking data processing, data management and archiving, science data processing, navigation, mission monitoring and spacecraft analysis, and infrastructure support.

Most of the MOS functions planned for JSO use standard implementations and practices. Per the study guidelines 70 m equivalent support is assumed to be in place. Another MOS issue that deserves special attention is that of long-term experience retention. The most challenging activities requiring the highest degree of technical flexibility occur at least 5 years after launch. While several methods for retaining domain and test knowledge will be needed, one method planned is that of regular and intensive training. Training activities will be planned at regular intervals and will include post-launch training activities and ORTs for each gravity assist encounter, the first Io flyby, JOI, GOI, and Ganymede science campaigns. Specially designed challenges and spacecraft anomaly resolution exercises will be needed to keep specialized knowledge fresh and accessible.

4.5.3 Science Data Acquisition Scenarios

4.5.3.1 Interplanetary

Science calibrations will be conducted periodically during cruise. Low-rate fields and particles may be gathered continuously during this phase. All science instruments will be exercised during the Venus and Earth gravity assist encounters consistent with thermal and other constraints.

4.5.3.2 Jupiter Approach Strategy

The MAG and PS/EPD space physics instruments will be operated continuously. The remote sensing instruments will concentrate on making Jupiter atmospheric measurements, monitoring Io's volcanic activity, and obtaining global-scale, multispectral coverage of the Galilean satellites. Full rotation maps of Jupiter will require continuous DSN tracking periods of at least 10 hours duration.

4.5.3.3 JOI & Capture Orbit Strategy

The space physics instruments will operate continuously. The emphasis of the remote sensing instruments will be on global multispectral mapping during the Galilean

satellite encounters. Around JOI, it is expected that science observations will have to be included in a critical sequence to minimize any risk to accomplishing JOI successfully. Therefore, there is likely to be little to no flexibility from plans derived perhaps 6 months in advance. In addition, power for the instruments may be restricted due to added propulsion system needs. Because of downlink data rate limitations, the spatial resolution of full global maps of Jupiter will be limited to no better than ~4 km/pixel; this resolution is obtained at approximately Callisto's orbit roughly 1.5 d before JOI.

4.5.3.4 Jovian Tour Strategy

After the JOI & Capture Orbit sub-phase during the periods between close satellite encounters, the remote sensing instruments will continue to monitor Io and Jupiter's atmosphere. As on approach, telemetry can support global maps of Jupiter at up to 4 km/pixel resolution when DSN passes of 10 hours or greater are available. To meet the science requirement of hourly monitoring of Io, some special telemetry passes may need to be scheduled if this monitoring is to extend longer than 8 hours at a stretch. This period of the mission is likely to be the prime time for Jupiter and Io monitoring, since once the spacecraft enters Ganymede orbit, the competition for limited downlink resources by other science objectives will be greater. Opportunities for global-scale multispectral mapping of the Galilean satellites will occur, particularly during fortuitous non-targeted satellite flybys. MAG and PS/EPD will remain operating continuously.

4.5.3.5 Satellite Encounter Strategy

Satellite encounters are defined here to be the time period within ± 3 hours of closest approach to a targeted satellite. This time duration is limited by the added power draw required to operate all the instruments simultaneously and the bus battery capacity. Given the bus telecom capability and the SSR data storage limitations, a typical encounter might return about 17.6 Gb of data. This downlink volume is primarily constrained by the SSR data storage limit, since there is ample time between encounters to return data recorded near closest approach.

For purposes of quantifying the amount of science return from a typical encounter, standard science data quanta have been defined. Since the LA and GPR are limited to close-range operation, we have assumed that each operates for 800 s near closest approach, during which time the LA will generate 10 Mb of data and the GPR will generate 240 Mb. For the remote sensing instruments, the quantum chosen is a data set for which each instrument generates spatial coverage in a square whose height is equal to its cross-track swath width. For the spectrometers, full spectral coverage is obtained over this spatial frame yielding a standard spectral cube for each spectrometer. For the MRC used in stereo, a stereo pair of frames is assumed. Modest levels of data compression (or editing or summing) are assumed for each instrument except the VHS, which must reduce its data in real-time internal

to the instrument by a factor of 100. The remote sensing standard data quanta are summarized in [Table 4.5-4](#), and the overlapping FOVs for the various remote sensing instruments in such a data quantum are shown in [Figure 4.5-2](#).

The encounter strategy, shown schematically in [Figure 4.5-3](#), is to begin with an empty SSR and a fully charged battery. The MAG and PS/EPD run 100% of the time. The LA and GPR run for 800 s around closest approach. These four instruments collect 380 Mb of data during the encounter period. The remaining 17.2 Gb of capability per encounter is used to return remote sensing data. This data volume corresponds to 149 remote sensing quanta. These remote sensing frames or cubes can be used in a wide variety of ways including regional-scale mapping and high-resolution targets. [Figure 4.5-4](#) summa-

Table 4.5-4. Standard Remote Sensing Data Quanta

Instrument	Cross-track spatial pixels	Along-track spatial pixels	Spectral (or stereo) channels	Bits/pixel	Compression factor	Data Volume (Mb)
HRC	2048	2048	1	12	4	12.6
MRC (stereo)	2048	2048	2	12	4	25.2
VHS	480	480	1350	12	100	38
UVS	64	64	1024	12	3	17
TS	32	32	2800	16	2	23
Total						115.8

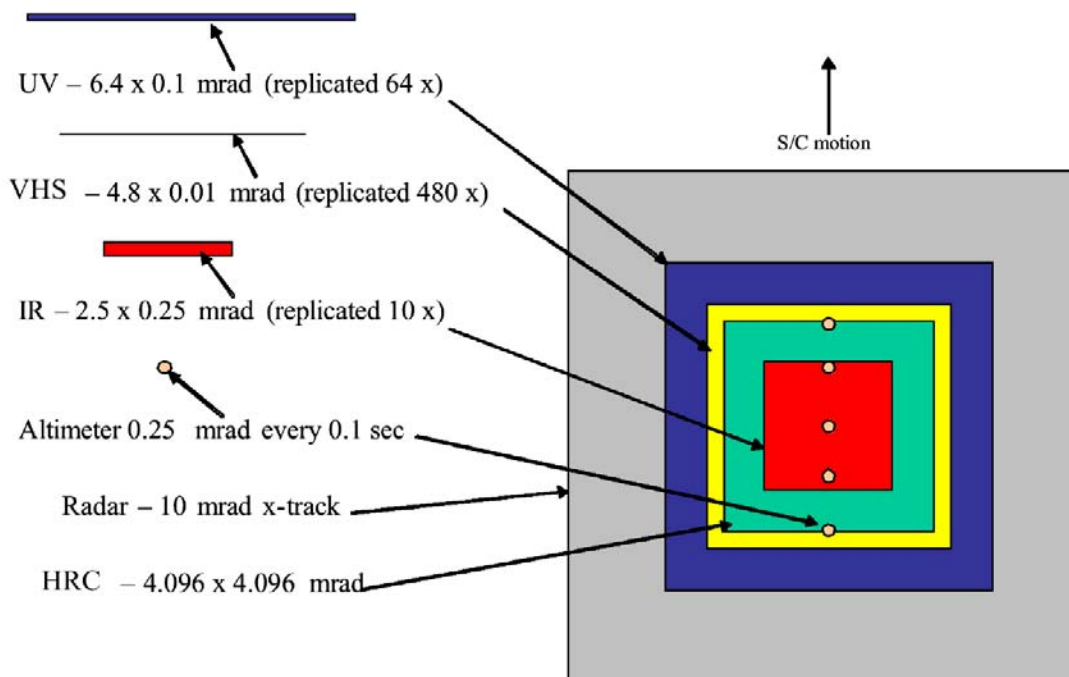


Figure 4.5-2. Overlapping FOVs of standard remote sensing quantum. The MRC FOV is 10× larger than that of the Hires FOV and is not shown here.

izes the number of standard data sets that can be obtained for each remote sensing instrument over the course of the JSO tour. The numbers for each satellite scale directly with the number of close flybys of each during the tour.

Global-scale color and spectral coverage will be obtained on either side of the close encounter period (within a few days of closest approach, but not within a few hours). The best-resolution areas for global coverage for each satellite will be restricted by the available encounter geometries. The encounter geometries at each satellite are determined by the orientation of the line of apsides of the spacecraft orbit about Jupiter relative to the Sun direction, the perijove altitude (i.e., how far inside of a satellite's orbit the spacecraft orbital perijove is), and whether an encounter is pre- or post-perijove. **Figure 4.5-5** shows the sub-spacecraft ground tracks on the Galilean satellites for the sample JSO tour. Note that the approach and departure points (the end points of each ground track) are clustered at low latitudes and within fairly narrow longitude bands. The approach and departure points, along with the solar illumination at the time of a given encounter, restrict those regions that can be globally mapped well during the tour.

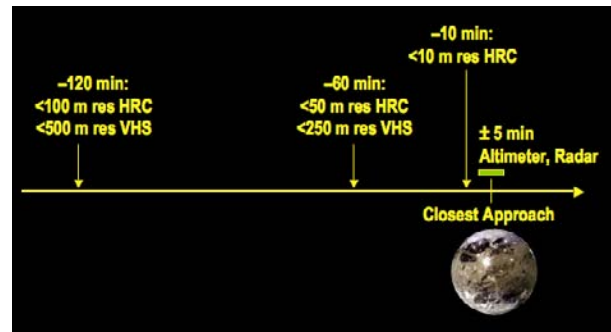


Figure 4.5-3. Schematic showing remote sensing activities for the period three hours prior to satellite closest approach during a flyby. Note that subsequent to this period, samples of high quality science data can still be acquired.

Table 4.5-5 summarizes the types of observations that will be taken as a function of time from encounter on a typical flyby (the times in parenthesis in **Table 4.5-5** are for a less typical slow flyby of Ganymede during the end game portion of the tour) and the areal coverage possible at each resolution over the course of the tour for each satellite.

4.5.3.6 Elliptical orbit strategy

The contents of the science observing scenarios during the elliptical orbit phase (**Figure 4.5-6**) are limited by the downlink

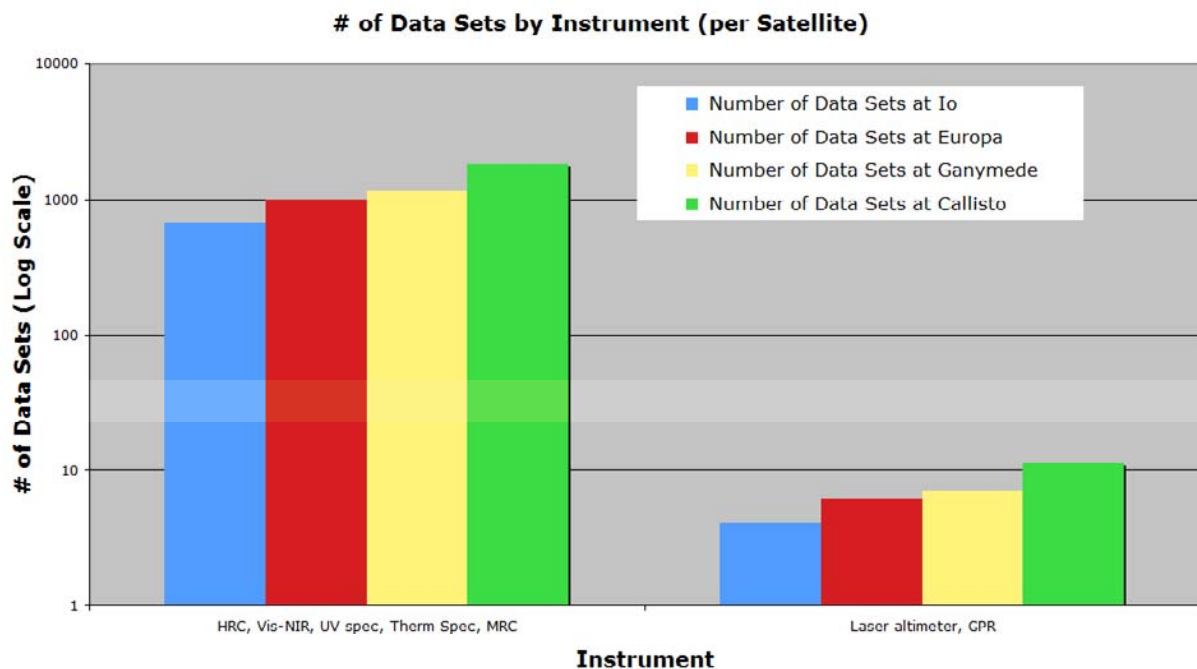


Figure 4.5-4. Number of standard remote sensing data sets that can be returned during the tour for each Galilean satellite.

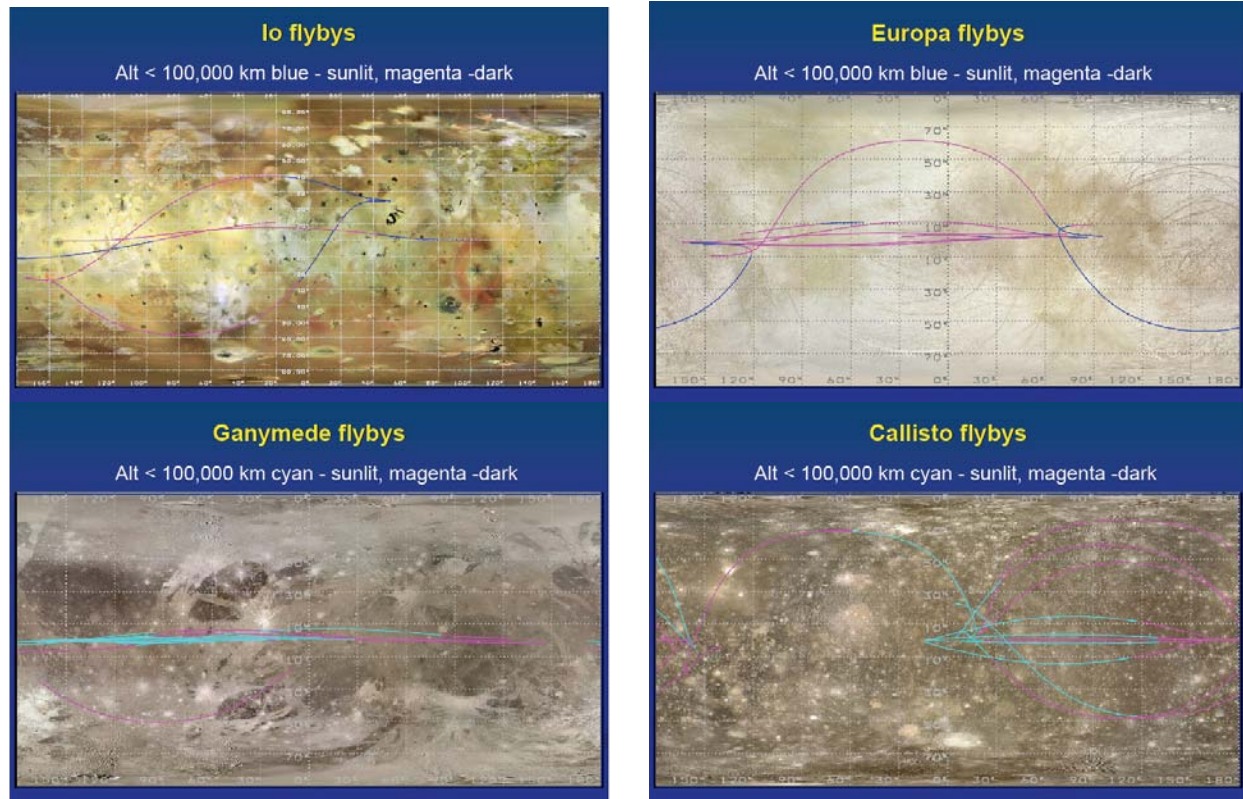


Figure 4.5-5. Ground Tracks of JSO Encounters.

Table 4.5-5. Representative Encounter Coverage vs. Resolution

Time	Activity	Comments
Periapse +/- 5 minutes (or +/- 25 minutes)	Altimetry Radar Flux tube measurements High Resolution obs Gravity measurements	Time interval for HiRes @ (<5m) ranges from @ 5 to 50 minutes. This is much shorter for the altimeter and radar, which have an altitude limitation of ~2000 km
+/- 10 (60) minutes	<10 meter HiRes	For first reference to ur % global coverage: Europa: 0.5%, Ganymede: 1.2%, Callisto: 0.9%
+/- 22 (100) minutes	<20 meter HiRes <100 meter VNIR	Europa: 2.7%, Ganymede: 5.1%, Callisto: 1%
+/- 60 (260) minutes	< 50 meter HiRes < 250 meter VNIR	Europa: 21%, Ganymede: 40% Callisto: 7.9%
+/- 120 (500) minutes	< 100 meter HiRes < 500 meter VNIR	Europa: 400% Ganymede: 760%, Callisto: 94% (> 100% implies multiple bands)
+/- 250 (1000) minutes	< 200 meter HiRes < 1000 meter (VNIR)	Europa: 2680% Ganymede: 5075%, Callisto: 980%

Note that wide-area coverage will be possible only of limited locations

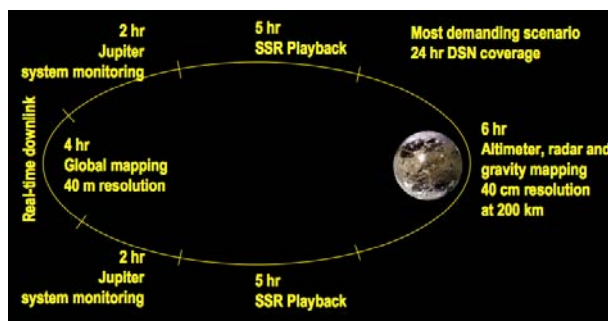


Figure 4.5-6. Schematic showing activities during Ganymede elliptical orbit. For the circular phase, the activities are scaled and adjusted to meet the need of the science plan.

data return capability. During the first month in orbit when 24 hours a day of DSN tracking is planned, excellent gravity and magnetic field determinations can be made. The improvement to our knowledge of Ganymede's gravitational field will help in predicting the evolution of future orbits and planning trajectory corrections. This period also provides the best opportunity for acquiring high-resolution global maps of Ganymede in a single color. Global coverage at 40 m/pixel can be achieved at a cost of 54 hours of downlink time. With an allocation of 4 hours of downlink per day to this objective, the first map can be completed in two weeks. When the periapsis altitude of the elliptical orbit is low (below ~3000 km), the observing strategy around periapsis will be similar to that of a flyby during the tour. For the 6 hours around periapsis, real-time data will be returned, and the SSR will be filled with science data. Downlinking the data from the SSR will take about 5 hours. During the remaining 9 hours of each orbit, Jupiter system science observations could be made and downlinked. **Table 4.5-6** presents some useful spatial resolution values for the remote sensing instruments for various types of observations

Table 4.5-6. Instrument Resolution (per pixel) vs. Altitude in Elliptical Orbit

Instrument	HIRES	VNIR	UV	IR
IFOV (urad)	2	10	100	250
Apoapse @ 20000 km (meters)	40	200	2000	5000
Periapse @ 1000 km (meters)	2	10	100	250
Altitude @ 200 km (meters)	0.4	2	20	50
Io from Ganymede (meters)	1,296	6,484	64,840	162,000
Europa from Ganymede (meters)	798	3,991	39,910	99,775
Callisto from Ganymede (meters)	1626	8,130	81,300	203,250
Jupiter from Ganymede (meters)	1,997	9,986	99,860	249,638

while in the elliptical orbit.

During the second and third months in the elliptical orbit when 16 hours of DSN tracking per day is planned, high levels of data return can continue during which additional global maps in multiple colors and with the spectrometers can be obtained. A collaborative global spectral map will require about 300 hours of downlink time to complete taking ~80 days of elliptical orbit time. Jupiter system monitoring will be reduced as tracking time is reduced.

After the third month when DSN tracking is reduced to 8 hours per day, not only will Jupiter system science monitoring be severely curtailed, but real-time periapsis science data collection will also be reduced. **Figure 4.5-7** shows the number of standard remote sensing data sets that can be acquired per elliptical orbit for the three levels of DSN tracking. **Figure 4.5-8** shows that a total of over 40,000 remote sensing data sets can be returned during the entire elliptical orbit phase.

Figure 4.5-9 illustrates the ground tracks provided by the elliptical orbit over the course of a year as well as the locations of the low periapsis tracks, which are centered at mid latitudes.

Throughout the course of the Ganymede orbital phases (including the circular orbit period), extensive remote sensing instrument power cycling will be required. Power limitations with 8 MMRTGs do not permit all the instruments to be operated at 100% duty cycle for extended periods (i.e., longer than ~5 hours). The average power available for remote sensing instruments (including GPR and LA) will be <50% of their normal operating power levels. Instruments will need to have reduced-power modes into which they can be switched thousands of times without incurring damage due to thermal cycling.

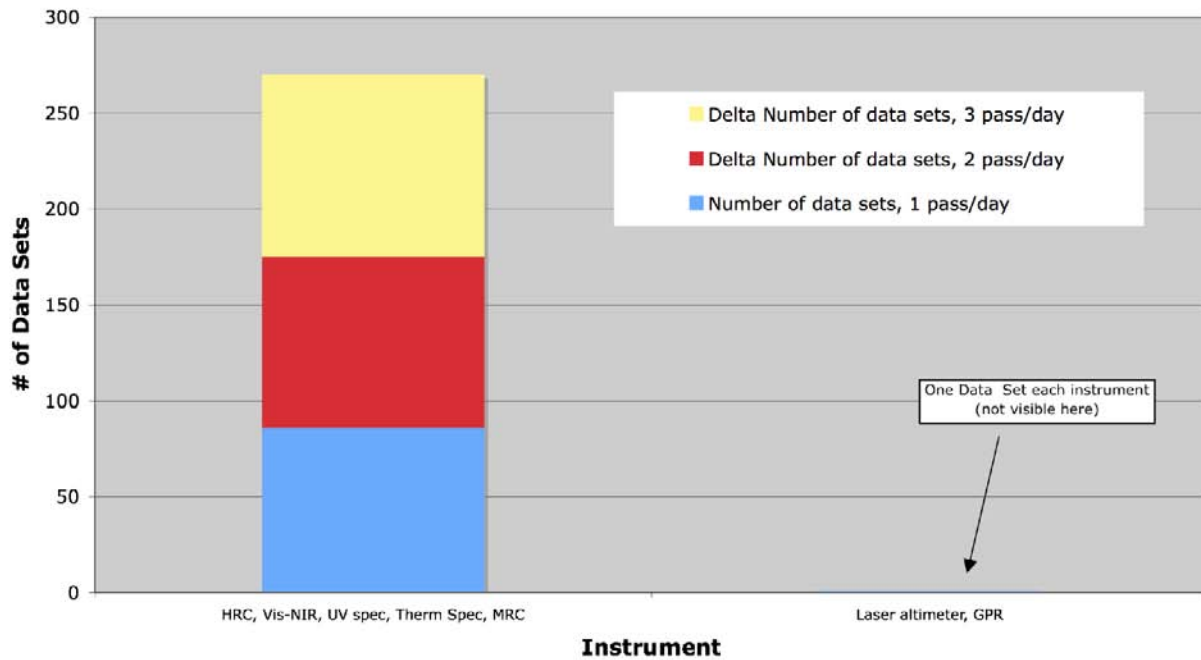
Example: # of Data Sets by Instrument (per elliptical orbit)

Figure 4.5-7. Number of standard remote sensing data sets that can be returned per orbit during the elliptical orbit phase for each level of DSN tracking planned.

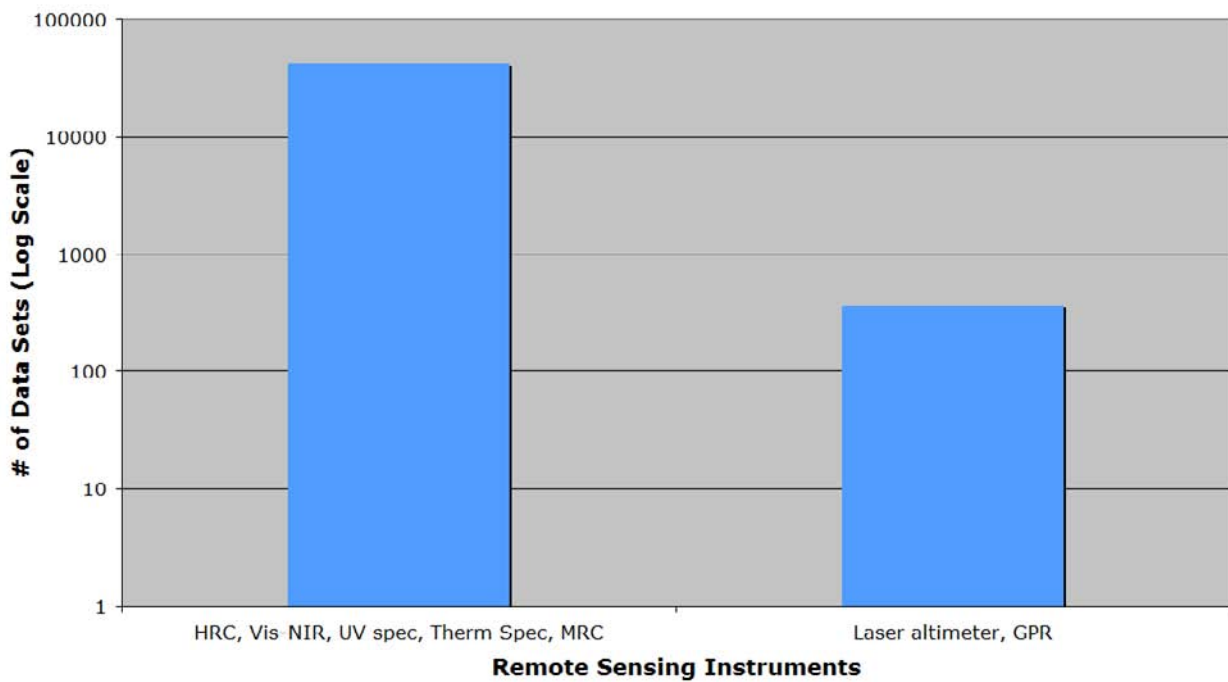
Example: # of Data Sets by Instrument (total elliptical orbit phase)

Figure 4.5-8. Number of standard remote sensing data sets that can be returned during the entire elliptical orbit phase.

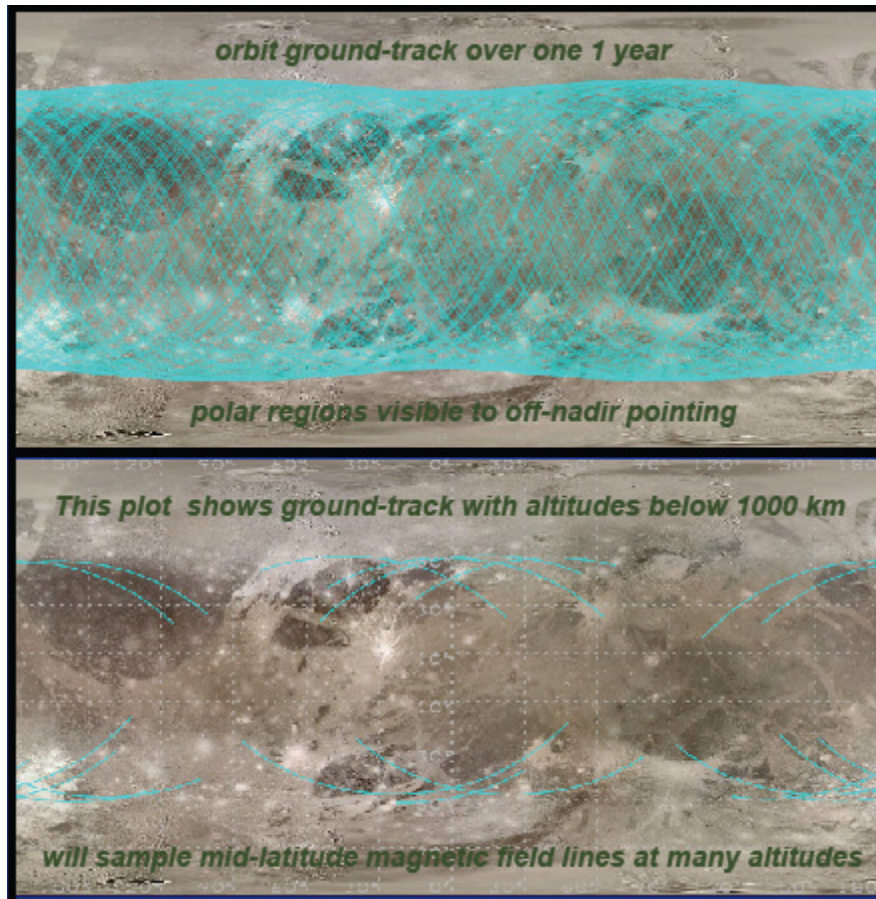


Figure 4.5-9. Elliptical orbit ground tracks provide both global and high-resolution views of Ganymede.

Because of the uncertainties in the gravity field (and therefore uncertain predictions for the spacecraft location one week in the future), the likelihood of significant unexpected science discoveries, and the potential for reactions to radiation induced events and degraded performance, the rapid assessment of science data products and rapid planning and replanning of science data collection will be needed over time spans of about 2 weeks when in orbit about Ganymede. For the most part, response to science discoveries will take the form of re-allocating target data volumes in future days to observe previously unconsidered sites. Recent experience from MRO and MER has shown that rapid data delivery and quick-look processing as well as rapid decision making and activity planning are possible for the planning schedules needed by JSO. MRO has demonstrated the long-term processes for delivering ~100 Gb per day to distributed science centers. Those science centers have shown that they can quickly

produce planning-quality data products in one or a few days. MRO target selection processes take 3 days for nadir-based targets and 1 week for complicated off-nadir coordinated targets. MRO acquires a comparable number of targets per day as JSO is currently considering. MER has shown that one-day turn around of science products to next-day activity plans is possible over mission lifetimes comparable to JSO's.

4.5.3.7 Circular orbit strategy

As for the elliptical orbit phase, the contents of the science observing scenarios during the low circular orbit phase are limited by the downlink data return capability; the SSR can store much more data than can be returned in a day. Downlink outages will occur for up to 40% of each orbit due to occultation of the Earth by Ganymede. During the first month in orbit when 24 hours a day of DSN tracking is planned, improved gravity and magnetic field determinations can be made. Continuous laser altimeter operation is begun

to support global measurements of the shape of Ganymede and how it varies throughout its orbital cycle. Orbit reconstruction accurate to 1 m in the radial direction is required based on Doppler and range data with non-gravitational disturbances due to thruster firings restricted to fewer than one per day for at least the first month. Fields and particles instruments will operate continuously. Data acquisition by the GPR and the other remote sensing instruments will be balanced to use the remaining data volume capacity. Emphasis for these instruments will be on coverage of specific targets of scientific interest selected from previously obtained coverage rather than on global-scale coverage. The number of targets that can be observed will scale with the amount of DSN tracking per day (16 hr/day for months 2 and 3, and 8 hr/day thereafter). The allocations of operating time for the GPR are assumed to be 18% for 24-hr/day DSN coverage, 14% for 16-hr/day coverage, and 7% for 8-hr/day coverage. **Figure 4.5-10** shows the number of remote sensing data sets that can be returned per orbit for each level of DSN tracking and the assumed GPR data

allocations, and **Figure 4.5-11** shows the total number of data sets that can be returned during the 1 year in low circular orbit. An additional nearly 15,000 standard data sets at significantly higher spatial resolution can be returned during this portion of the mission. The remote sensing and GPR instruments will need to be cycled frequently into low-power modes when not taking data to fit within the available power capacity.

FO-2E illustrates the ground tracks provided by the low circular orbit during one ganysol. Over the course of the year in this orbit, the ground tracks will pass nearly directly over any selected target of interest. Ground track coverage can be used as a proxy for the coverage of the profiling instruments (GPR and LA). Frequent, globally distributed ground-track crossover points will provide excellent altimetry results.

Target acquisition will be via on-board, ephemeris driven software. The spacecraft will have a shape model of Ganymede and an orbit ephemeris. Targeting software will calculate the precise time to image a selected site (lat,

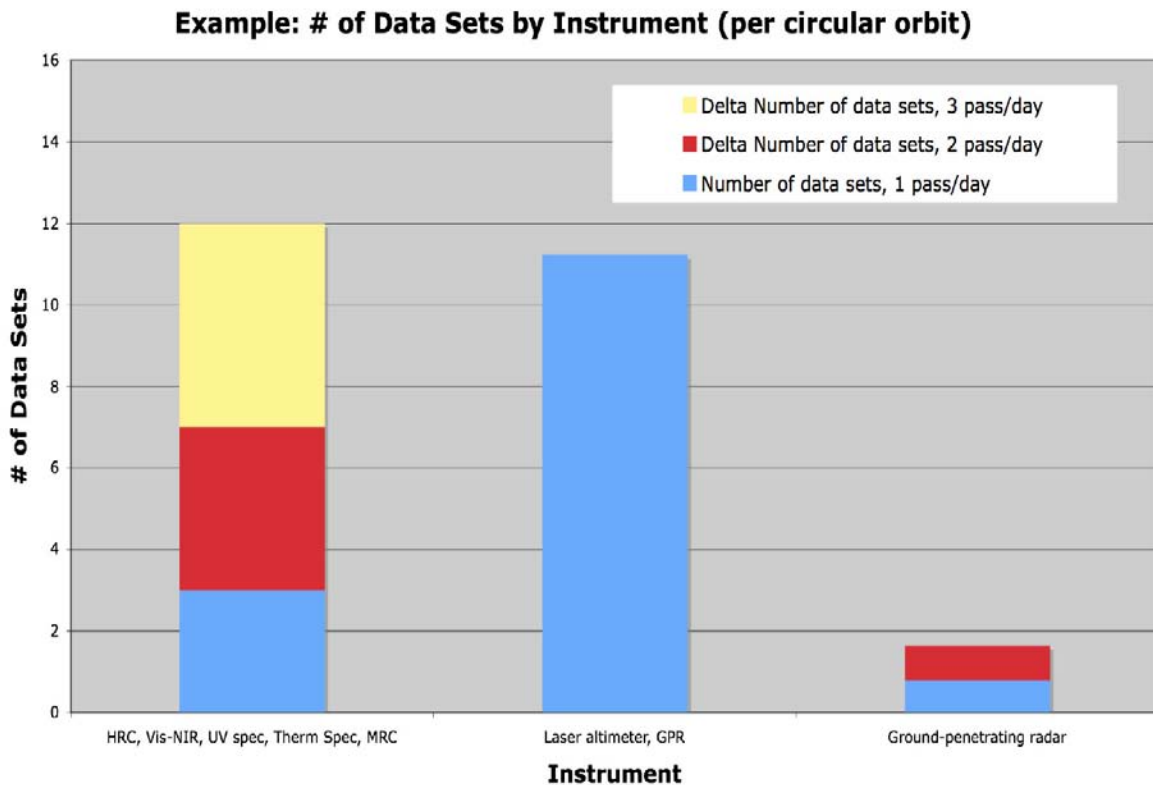


Figure 4.5-10. Number of standard remote sensing data sets that can be returned per orbit during the low circular orbit phase for each level of DSN tracking planned.

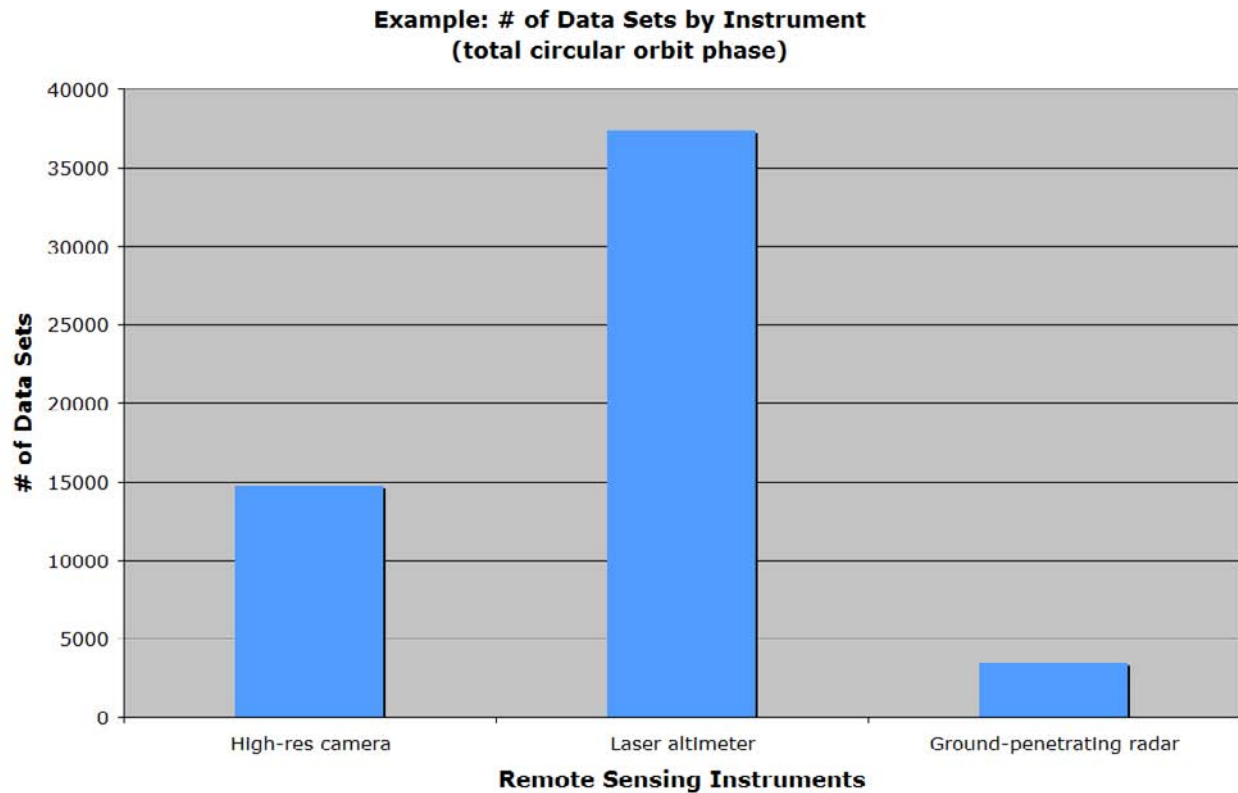


Figure 4.5-11. Number of standard remote sensing data sets that can be returned during the entire low circular orbit phase.

lon, alt) as it passes into the instrument fields of view. Updated ephemeris files will be uplinked to the spacecraft as needed to maintain the desired accuracy. Lists of targets to be acquired and corresponding imaging parameters will be developed and uplinked to the spacecraft every 2 weeks. To speed up the selection and file development process, targets can be selected by ground software using data volume modeling and priority-based selection criteria. Small spacecraft roll maneuvers and/or minor tweaks to the orbital period will be required to ensure that the remote sensing instrument swaths pass over the intended surface targets.

4.6 JSO Planetary Protection

4.6.1 Requirements

As a Jovian System exploration mission, the JSO project must comply with the planetary protection (PP) requirements established by NASA policy NPD 8020.7F and detailed in NPR 8020.12C, “Planetary Protection Provisions for Robotic Extra-terrestrial Missions.”

Given that JSO will be captured into a Ganymede circular orbit and the instability of such an orbit due to Jupiter gravity, the final fate of the spacecraft will be to impact Ganymede. As such, JSO anticipates to be classified as PP mission category IV.

Current PP policy (NPR8020.12C, 2005) specifies requirements for Europa flyby, orbiter, or lander missions as follows:

“Requirements... including microbial reduction, shall be applied in order to reduce the probability of inadvertent contamination of an European ocean to less than 1×10^{-4} per mission. These requirements will be refined in future years, but the calculation of this probability should include a conservative estimate of poorly known parameters and address the following factors, at a minimum:

- Microbial burden at launch.
- Cruise survival for contaminating organisms.
- Organism survival in the radiation environment adjacent to Europa.
- Probability of landing on Europa.

- e. The mechanisms of transport to the European subsurface.
- f. Organism survival and proliferation before, during, and after subsurface transfer.”

The PPO has indicated that the same requirements apply to Ganymede. In addition, there are requirements to avoid harmful contamination of any other of the Jovian satellites.

4.6.2 Implementation

The probability of contamination (P_c) for a Ganymedan mission is dependent on the following terms [Space Studies Board, 2000]:

- Microbial bioburden at launch (N , measurable by classical bioassay)
- Probability of cruise survival (P_{cs} , estimable, but typically a small reduction factor)
- Probability of Jovian tour survival (P_{rad} , estimable based on spacecraft design and radiation dose effects)
- Probability of landing on Ganymede ($P_{lg} = 1$ for JSO)
- Probability of transport to the Ganymedan sub-surface (P_t , estimable, probably small due to the thickness of the Ganymedan ice and the advanced age of the Ganymedan surface)
- Probability of organisms’ survival, dispersion and proliferation (P_g , an item difficult to estimate, but probably small due to the Ganymedan environment, however presence of MMRTGs must be considered)

This will be interpreted for JSO as:

$$P_c = N \times P_{cs} \times P_{rad} \times P_{lg} \times P_t \times P_g \leq 1 \times 10^{-4}$$

Based on guidance from the PPO, the 1×10^{-4} requirement is acceptably met by demonstrating very small values for P_t and P_g and demonstrating an adequate level of hardware cleanliness. JSO will take advantage of the work being done by Juno to estimate P_{cs} and P_{rad} . N at launch will be obtained from direct biological measurement and taking credit where possible of high-temperature processes during manufacture and testing. An estimate of the reduction in N due to exposure to the radiation environment of the Jovian

System will also be used to reduce the N at Ganymede impact.

The requirement to avoid contamination of (impact with) other Jovian satellites will be met through trajectory and reliability analyses. This includes the 10^{-4} requirement to avoid impact with Europa prior to GOI.

JSO will develop estimates of the critical parameters (N , P_t , and P_g for Ganymede; P_t for Europa, Callisto, and Io) early (by early Phase B) in the project schedule. Analyses required to produce these estimates include trajectory, spacecraft reliability, impact and break-up, ice melting, and others as necessary. If any of these parameters is unacceptably high, then the project will develop a new PP approach. Possible alternative approaches include a microbial reduction plan to meet an acceptable bioload, N (may only require dry heat microbial reduction of selected components/subsystems, but it may require system-level sterilization); modifying the mission plan to dispose of the spacecraft into Jupiter; modifying the mission profile to increase the radiation dose to the spacecraft.

4.6.3 Probability of Transport to the Ganymedan Sub-Surface

The Jovian System contains a number of diverse environments, some of which may have the potential for habitability, especially at Europa. This provides a challenge from a planetary protection perspective to formulating a mission to explore this part of the solar system and not risk contamination of these environments. As such, it is necessary to assess the contamination potential for any subsurface ocean.

Oceans and the Icy Satellites

Results from the Galileo Mission suggest that each of the icy satellites likely contain subsurface oceans [Khurana et al., 1998; Neubauer, 1998; Kivelson et al., 1999, 2000, 2002; Zimmer et al., 2000]. The nature and location of the ocean within each satellite is thought to be quite variable and thus, for the purposes of planetary protection, need to be addressed individually. Focus on Europa as a potentially habitable world, with its geologically recent surface and induced magnetic field—attributed to a briny ocean tens of kilometers below the surface [Kivelson et al., 2000]—defines one bound. In comparison, the induced magnetic field at

Callisto suggests that a liquid layer may be present at a depth of ~200 km [Zimmer et al., 2000]. Unlike Europa, where the components of energy, shallow liquid water and an input of carbon material (from meteoric in fall) may make it a likely place where life may have arisen, Callisto lacks a sufficient energy source to mix the key ingredients for habitability. Specifically, the heavily cratered surface—near or at saturation with an age of ~4.0 billion years—suggests that there is no communication between the upper crust and the deep interior. Geologically, Ganymede is a world that falls between that of Europa and Callisto. The surface of Ganymede can be divided into two distinct physiographic provinces, heavily cratered dark terrain and less heavily cratered light/grooved terrain [Smith et al., 1979a, 1979b; Shoemaker et al., 1982]. Based on crater statistics the former of the two terrain types has a surface age of 3.8–4.0 billion years while the latter may be as young as 3.0 billion years [Murchie et al., 1989], suggesting both have not been significantly modified by tectonism or cryovolcanic activity in recent geologic time. A significant discovery of the Galileo mission was the presence of an intrinsic, internally generated magnetic field at Ganymede [Kivelson et al., 2002]. Modeling of the intrinsic and induced components of the magnetic field suggests the presence of an ocean at a depth on the order of 150 km [Kivelson et al., 2002]. Relative to Europa, the liquid layer lies at a level approximately ten times deeper at Ganymede. Based on evidence for an extremely old surface age dating, geologic inactivity, and the significant depth of the Ganymede ocean, it is concluded that there has been little if any direct interaction between the surface and the ocean over recent geologic time.

The final disposition of the JSO spacecraft will most likely be impact onto the surface of Ganymede. From a planetary protection perspective, the concern arises as to the probability of material on the surface having access to a subsurface ocean—a place of biological potential. The evidence from both geologic and geophysical data suggests that an ocean is quite deep and sequestered from surface interaction. Although geologic units span a range of ages, data suggest that the surfaces are billions of years old. As such, the

likelihood of contaminating an ocean is vanishingly small. A more quantitative analysis based on this initial assessment will be conducted during pre-phase A.

4.7 Trades and Open Issues

4.7.1 Descope Options and Floor Mission

The study team considered a single descope mission which uses the Atlas V 551 LV and achieves an elliptical orbit at Ganymede. This option would favor remote sensing of Jupiter's atmosphere and other moons, and fields and particle measurements. A potential descope option could be to reduce the total mass so that an Atlas V 551 would allow capturing into a circular orbit at Ganymede. Areas of descope could be reducing the size of the optical system and reducing or eliminating Io flybys. This becomes a trade between Jupiter system science versus Ganymede interior science.

The study team also did not have time to deliberate on a floor mission. Here, we define a floor mission to be the minimum mission that the science community would deem worth pursuing (the implication being that, if the science capability were reduced further, the appropriate follow-on action would be cancellation). By exploring different mission and architectural level descopes, one may discover different floor missions. That is akin to having different local minima in a valley of potential descopes. Understanding the difference of a particular descope mission to its corresponding floor will help the decision on its selection. This trade was beyond the scope of the current study.

4.7.2 Lagrange Point Dynamics

The current mission concept is to be propulsively captured into Ganymede elliptical orbit. There is potentially some ΔV saving to be captured via the L2 Lagrange Point between Jupiter and Ganymede (L2). L2 is the point about 120,000 km on the far side of Ganymede as viewed from Jupiter where the gravitational attraction of Ganymede on the spacecraft is balanced by its centrifugal force. The region near L2 is inherently unstable, which means a small ΔV in the right direction will send the spacecraft into a capture orbit around Ganymede at very low ΔV cost. This saving in mass with some additional descoped items may enable a Ganymede circular orbit

using an Atlas V 551 LV. This trade was beyond the scope of the current study.

4.7.3 Radiation System Design

The study team recognized that radiation tolerance is a system level trade. It involves availability and selection of parts and materials, which in turn affects system level resources such as mass and power. It also will impact mission design in terms of trading TID with number of flybys at Io and Europa. The current radiation vault and distributed shielding for selected components have not been optimized. It is anticipated that some mass saving can be realized if radiation system design is treated as a global optimization problem. This trade was beyond the scope of the current study.

4.7.4 Radiation Environment Estimation

The JSO team has not modeled the radiation environment while the spacecraft is in orbit at Ganymede. The current assumption is that the radiation environment is equivalent to what would be seen at Ganymede's distance from Jupiter without any potential benefit of shielding from Ganymede. JPL has conducted an assessment of the statistical expected mission lifetime, taking into considerations parts qualification and historical performance and concluded that design margins have been linearly accumulated rather than applied statistically. Therefore, the lifetime prediction of failure due to radiation is too conservative. At the time of this report, JSO has not factored the findings into its design. For instance, the radiation shielding is designed to provide a 5-year mission life using the old conservative approach. Using the statistical approach, one may reduce the shielding or reduce the radiation tolerance of the parts, and still provide a 5-year lifetime. This trade was beyond the scope of the current study.

4.7.5 Ganymede Approach Trajectory

More detailed simulation and analysis is needed to assess the complexity of navigating the spacecraft through successive gravity assists to reduce its orbital energy and match its trajectory parameters prior to Ganymede Orbit Insertion (GOI) to the elliptical orbit parameters. This issue needs to be addressed in the future.

4.7.6 Radio Science Capability

The science requirement states that radio science should provide altitude measurements to an accuracy of 1 meter. The current telecom design includes an Ultra Stable Oscillator (USO) and dual band frequencies to meet this requirement. However, no analysis has been performed to verify that it is achievable. This issue needs to be addressed in the future.

4.7.7 Radiation Monitoring System

JSO has not included in the current design a radiation monitoring system (RMS). An RMS will provide TID information which will provide flexibility in mission and science planning during operations with a small impact on mass and power. The inclusion of an RMS needs to be addressed in the future.

4.7.8 Monopulse Pointing

Trades between attitude control capability and Ka-band pointing requirements will determine whether monopulse will be required.

4.7.9 X-band Downlink

An alternative telecom design to use X-band as the primary communications frequency will be further explored as a back-up to the future Ka-band 70m. A reduction in downlink rate by a factor of 2 will be targeted by increasing the TWTA power and increasing the HGA size. The operational scenarios would be analyzed with this design to assess how well the science objectives would be met, with the expectation that a solution space exists.

4.8 Technology Needs

The study team has generally tried to avoid assuming the use of hardware that would require major technology development for the concept design as that would drive up the risk, and possibly the cost. However, there are several long-lead items that may, upon further investigations, require some technology maturation.

4.8.1 Radiation Tolerant Sensor Design

Currently, JPL has developed a rad-hard APS sun sensor that is at TRL 6. Similarly, Galileo Avionics has developed a rad-hard APS star tracker (described in the Design section above). The ACS design includes spot shielding to be used around the sun sensors and star camera heads to help minimize the

total dose affecting the electronics and detectors.

The Litton Scalable SIRU is advertised as able to survive 100 krad TID. The HRG gyros are robust to radiation as is, but the unit needs rad-hard power supplies and processing electronics. The reaction wheel with Honeywell HR14 heritage requires modifications to the wheel drive electronics and minor modifications to the wheel assembly. The rad-hard gimbal drive electronics used for control of the HGA gimbal mechanism is a new development. All of the modifications and qualification tests of these sensors and electronics are included in the cost basis.

In a high radiation environment, e.g. near Io, there can be relatively numerous false star indications and relatively few persistent true stars in the focal plane. Software must filter out the false stars and identify the true stars. The current estimated maturity for such software is TRL 5. The estimated cost to bring it to TRL 6 is \$3M for development and is included in the cost basis.

Similar rad-hard design and qualification will apply to the instruments. A 25% additional cost has been included in the cost estimate of all the instruments to account for design and qualification for the JSO radiation environment.

4.8.2 Radiation Tolerant Electronic Design

As described in §4.4.3, where possible, MSAP/MSL cards are used and converted to Rad-hard designs. This conversion requires the replacement of the onboard FPGA with Rad-hard ASICs. Though not a tremendous technical hurdle, the conversion is time consuming (18–24 month, first pass) and expensive (\$1M to \$1.5M per variant).

The other board level parts must also be replaced with Rad-hard equivalents. It is not likely that all parts have replacements and the density of components in the I/O (input/output) circuitry may have to be reduced in the final flight configuration, resulting in higher power consumption and greater volumes and associated shielding mass. The rad-hard chalcogenide Solid State Recorder (C-RAM)

based on the BAE 4 Mb chip and its 16 Mb stack configuration is a recent development. The performance and reliability to build to a total 9.6 Gb has not been demonstrated. The development cost includes the non-recurring cost of the design, build, and testing of all of the electronic components upgrades. Early characterization of the electronic design is needed during Phase A to mitigate any unforeseen difficulties.

Similar development effort is needed for instrument electronics. In particular, a 100:1 compression in the hyperspectral imager is executed prior to data transfer to the CDH. The processing power needed to execute such a compression rate in real time could be a technology challenge and its assessment is beyond the scope of this study.

4.8.3 Qualification of Propulsion System

JSO uses the 890 N (200 lbf) Aerojet (Redmond) HiPAT bipropellant engine for primary propulsion. As noted in §4.4.3, the HiPAT engine has not been utilized for deep space missions and has been qualified for less than 30 minutes of continuous operation, but is a well understood technology proposed for Juno and other deep-space missions. Additional qualification is required for JSO applications.

The HiPAT engine uses an iridium-rhenium combustion chamber that has the claimed capability to operate for extended periods with the N_2H_4 /MON-3 propellants. The likelihood of meeting JSO qualification after 2010 is high.

Minimum Impulse Thrusters (MITs) are used for small maneuver and attitude control backup in case of reaction wheel failure. These thrusters have not been flown and full flight qualification is required on the valves that enable the very small impulse bit that will reduce the residual ΔV from an attitude adjustment.

MITs are derived from the Aerojet MR-103 thruster engines with very high heritage and are not considered to be a technology development.

Criteria for Risk Identification and Assessment

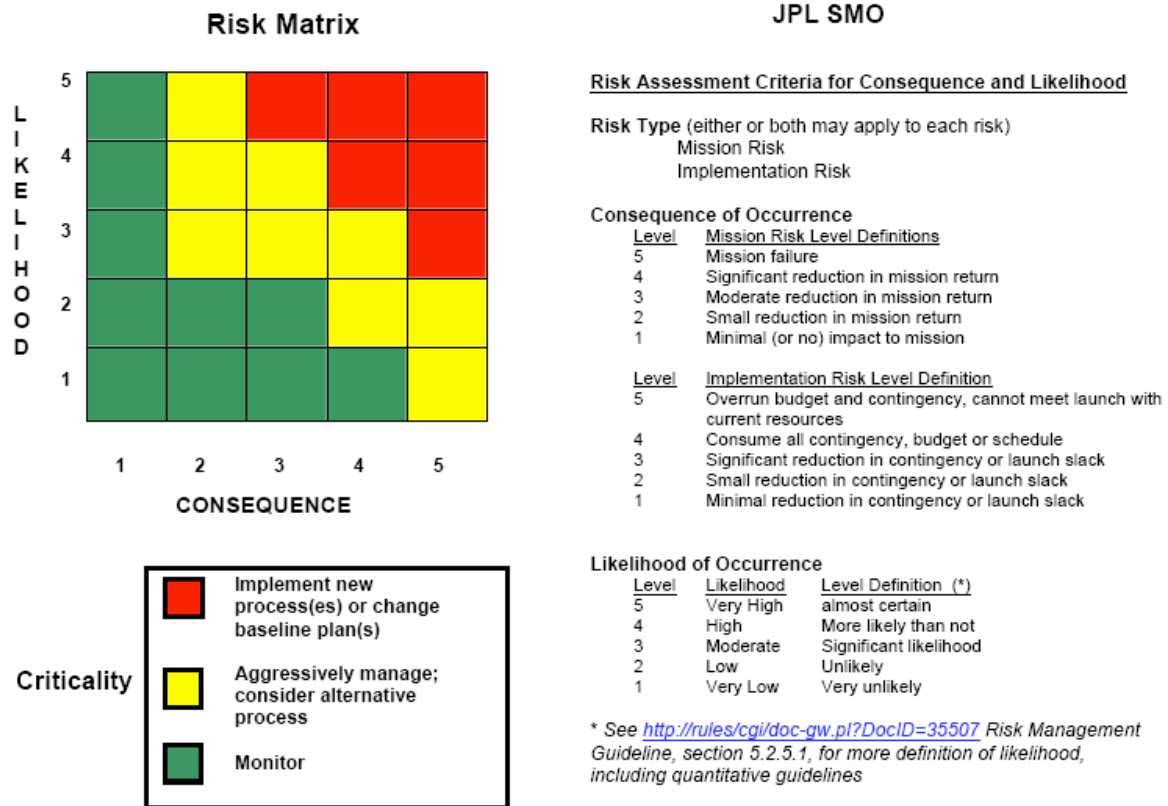


Figure 4.9-1. Criteria for Risk Identification and Assessment.

4.9 Technical Risk Assessment

The JSO team, in coordination with the EE team, has identified a number of risks that could threaten the success of JSO during development (Implementation) or during operations (Mission). The definition of risk is in accordance with JPL Rules DocID 66952, “Criteria for Risk Identification and Assessment” reproduced in Figure 4.9-1.

The identified risk items and their rating are shown in Figure 4.9-2. Table 4.9-1 provides the risk description and the mitigation strategy.

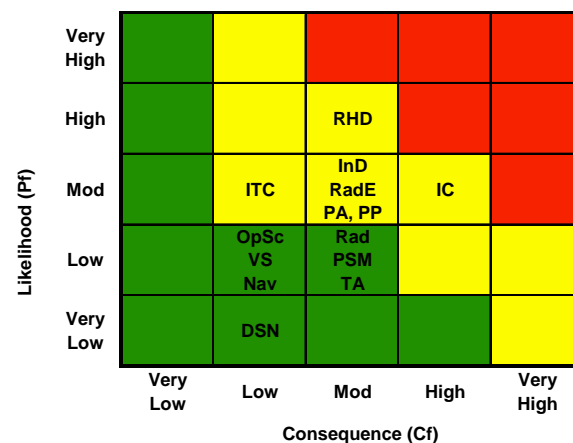


Figure 4.9-2. JSO Project Risk Items.

Table 4.9-1. Risk Description and Mitigation Strategy

	Title	Statement	Cf	Pf	Mitigation Strategy
1	Rad-Hard Design (RHD)	(RHD) A large number of electronics and sensors, including their packaging, have to be re-designed and qualified to accommodate the radiation environment. It is not likely that all parts have replacements and density of components may change resulting in higher mass, power, volume, and shielding, with cost and schedule impact.	3	4	Use the pre-phase A and phase A period to conduct preliminary design of affected systems and assess the availability of parts and materials. Develop rigorous testing program and build in schedule slack for re-design and re-qualification. Include cost in the re-design and build-in cost reserve.
2	Internal charging (IC)	(IC) If high levels of charged particles cause internal charging such that electrostatic discharge occurs and damages materials or electronics.	4	3	Utilize design experience from Galileo and Cassini, provide mission design guidelines early in the design cycle (Phase A), conduct design workshops to train designers. Apply intensive ESD & grounding protection measures in design (i.e. max. ungrounded wire length, bleed path resistors and bleed path analysis, restrictions on use of floating metals, etc.), perform material analysis & test.
3	Instrument Development (InD)	(InD) If instrument development is not managed appropriately, schedule and cost reserves may be needed and/or performance may be inadequate due to planetary protection and radiation requirements.	3	3	Provide resources for dedicated instrument interface and radiation engineers; provide design guidelines and approved parts and materials lists to instrument providers.
4	Radiation Environment and Shielding (RadE)	(RadE) If Radiation environment is greater than predicted could impact spacecraft functions, make shielding inadequate and impact Flight System lifetime.	3	3	Leverage past work, use Galileo data, model environment, apply design margins and design guidelines. Peer review of transport models and simulations, testing to verify models, and use of multi-layer shields to more efficiently absorb secondary particles. Robust cost and schedule reserve allowed for radiation risk mitigation during program.
5	Plutonium Availability (PA)	(PA) If the supply of plutonium remains limited, then the number of MMRTGs available will be reduced.	3	3	Minimize power requirements, prepare power saving descope options for operations and develop plan to demonstrate compatibility with ASRG.
6	Planetary Protection (PP)	(PP) The current PP implementation assumes contamination of Ganymede liquid ocean is vanishingly small with a crashed spacecraft. If this approach is not acceptable, parts of s/c will be required to meet more stringent PP requirements, with significant cost, schedule and design ramifications.	3	3	Schedule PP Implementation Review in Phase B to confirm approach. Define design guidelines and assess parts and materials in time for Instrument AO. Radiation environment will be used for sterilization. Schedule/cost reserve to apply to additional Full System sterilization if needed.
7	Integration & Test Complexity (ITC)	(ITC) The mission uses a large number of instruments, leading to high complexity in integration and test. If not properly managed, schedule and cost reserves may be needed to recover from late problems in I&T.	2	3	Provide cost and schedule reserves for integration and test problems, develop I&T plans early, develop descope plan for instruments.
8	Radiation Parts, Sensors and Materials (RadPSM)	(RadPSM) If radiation effects in parts, sensors and materials are more severe than expected, early failures may occur resulting in loss of science.	3	2	Use experts in radiation effects in devices to define qualification test programs, leverage Galileo/Cassini/JUNO experience, and design techniques that fail gradually with radiation effects. Provide early approved parts and materials lists.
9	Thruster Availability (TA)	(TA) Minimum Impulse Thrusters (MIT) provide backup for reaction wheels for long duration missions, but have not been flight proven. If the development and qualification of the MITs is not completed, the ability to control the spacecraft may be affected	3	2	Increase propulsion system costs for development and qualification, use high heritage thrusters which will provide coarser but acceptable control.
10	Science Operations (OpSc)	(OpSc) If operations and failover options are not coordinated appropriately or if planning tools are not correctly designed and implemented, cost and schedule reserves may be needed.	2	2	Prepare science team plans and tools early, allocate project resource for mission simulations and operation readiness testing and failure scenario operational planning.
11	Vault Size (VS)	(VS) The number of cards to be included in vault is uncertain. If the number grows beyond plans, mass and cost reserves may be needed to accommodate growth.	2	2	Perform more detailed analysis of required vault size in Phase A/B.
12	Navigation (Nav)	(NAV) If the planned multiple, closely spaced flybys are not executed correctly, science may be compromised or lost.	2	2	Program includes early coordinated design of flight and ground software and test sequences to enable quick updates to the spacecraft operations.
13	70-m Equivalent DSN Availability (DSN)	(DSN) If the DSN 70-m antenna equivalent capability or Ka-band downlink is not available then the mission science data could be reduced.	2	1	Define backup operational strategy with arrayed smaller antennas or 34-m antenna availability. Seek alternate antenna assets.

4.10 Programmatic

4.10.1 Schedule

The JSO team selected a development lifecycle duration of 15/15/30/30 months for Phase A/B/C/D respectively. This is within the range of “Rules of Thumb” for flagship missions recommended by the JPL Project Formulation Office with the exception of phase D where the range is between 18 – 24 months. Here, the study team took a more conservative approach of 30 months, particularly in view of potential foreign contribution with the complication of ITAR and Technical Assistant Agreements during test and integration.

Figure 4.10-1 shows the start date of Phase A needed to meet the available launch opportunities. The first available VEEGA opportunity in the 2015 to 2022 time frame is a January 2015 launch. It would require accelerating Phase A with significant investment in 2008 and would incur schedule risk. There is a launch opportunity in July 2015 that was not considered by the JSO team but is currently planned by the Europa Explorer study team. It would require significant investment in 2008 and mass reduction for JSO. There is a launch opportunity in September of 2016 but it arrives at Jupiter later than the January 2017 launch trajectory. With these considerations, the JSO

team selected the January 2017 launch as the baseline.

Figure 4.10-2 shows the key activities and milestones of the major systems that conform to the Principles and Practices recommended by the JPL Project Formulation and Implementation Offices.

The schedule includes a pre-phase A period during 2008 and 2009. This period will be used to reduce risk in several areas and thus reduce cost uncertainty. The current PP implementation assumes the probability of contaminating the Ganymede ocean is vanishingly small and therefore the bus and instrument components do not require sterilization by dry heat. Pre-phase A includes analysis leading to a decision prior to SRR. Pre-phase A also includes the formation of the project science team that will continue to refine the mission architecture, help establish level 1 requirements, identify descope options and define the science floor. The engineering teams will conduct trades and generate scenarios that will lead to definition of the instrument performances and interfaces (mass, power, volume, data, electrical, mechanical, thermal, radiation tolerance, reliability, pointing, alignment, shared optics, operations, data products, and team responsibilities) in support of the instrument Announcement of Opportunity.

Project Start					Launch
Jul 2007	Accelerate Φ A, significant investment 2008 with schedule risk				Jan2015
	Φ A 15 mo	Φ B 15 mo	Φ C 30 mo	Φ D 30 mo	
Jan 2008	Significant investment 2008, need mass reduction				July2015
	Φ A 15 mo	Φ B 15 mo	Φ C 30 mo	Φ D 30 mo	
Mar 2009	Has later arrival date than Jan 2017 launch				Sep2016
	Φ A 15 mo	Φ B 15 mo	Φ C 30 mo	Φ D 30 mo	
July 2009	Pre-A in 2008, refine architecture, science definition, & payload req				Jan2017
	Φ A 15 mo	Φ B 15 mo	Φ C 30 mo	Φ D 30 mo	

Figure 4.10-1. 2017 launch date provides good lead time for start of Phase A.

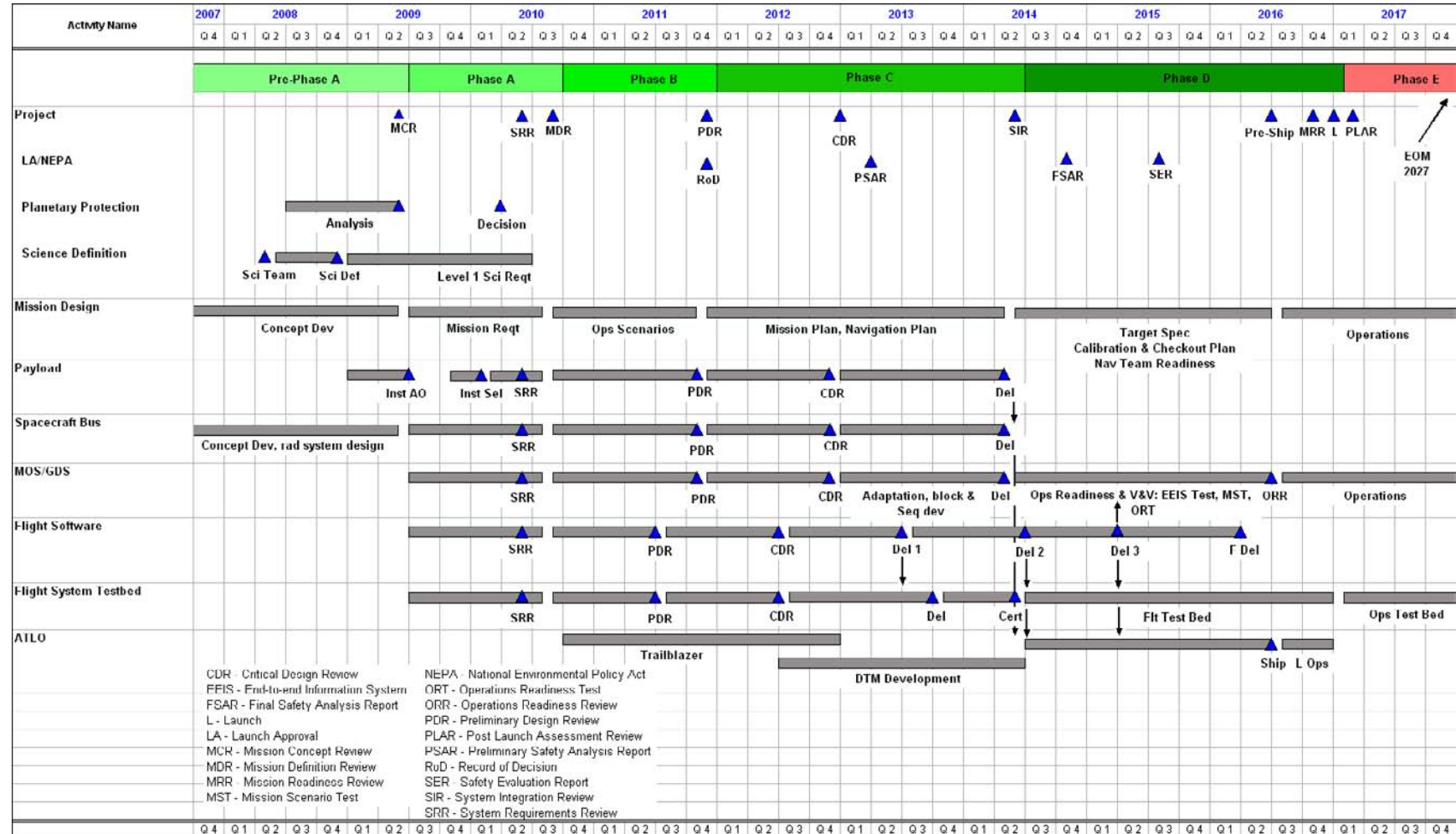


Fig. 4.10-2. JSO Project Schedule.

4.10.2 Cost

The total estimated life cycle cost (phase A/B/C/D/E) including the launch vehicle and Radioisotope Power System is \$3.1B (2007 fixed year \$) for the baseline mission. The estimate includes 35% reserve¹ for phase B/C/D based on evaluation of cost/risk sub-factors. The Basis Of Estimate (BOE) is based on a combination of semi-grass roots and parametric relationship developed by the JPL Technical Sections and incorporated into the Team X concurrent engineering methodology.

The JSO project cycle phase durations are assumed to be 15 months for Phase A, 15 months for Phase B, 60 months for Phase C/D, and 12 years for Phase E. So the total cost covers launching on any VEEGA trajectory that lasts as long as 7 years, plus the 5 years at Jupiter.

Table 4.10-1 provides a project summary of the cost based on the JPL standard WBS.

The uncertainty of the cost estimates based on the study maturity would be large. In the past, similar studies would include -10% to +20% uncertainty in the estimate. So the baseline mission would have a range of \$2.8B to \$3.7B.

4.10.3 NEPA Compliance and Launch Approval

Environmental review requirements will be satisfied by the completion of a mission-specific Environmental Impact Statement (EIS) for the JSO mission. In accordance with the requirements described by NPR 7120.5D, the Record of Decision (ROD) for this EIS would be finalized prior to or concurrent with Project PDR.

The JSO launch approval engineering (LAE) Plan will be completed no later than the MDR. This plan will describe the approach for satisfying NASA's NEPA requirements for the JSO mission, and the approach for complying with the nuclear safety launch approval process described by Presidential Directive/National Security Council Memorandum #25 (PD/NSC-25) and satisfying the nuclear safety requirements of NPR 8715.3. The LAE Plan will provide a description of responsibilities, data sources, schedule, and an overall summary plan for preparing:

Table 4.10-1. JSO Baseline Cost by Level 2 WBS

Team X In-house Build	
Project Cost	FY 2007 M\$
Minimum (-10%)	2,805.0
Expected	3,116.6
Maximum (+20%)	3,739.9
WBS Elements	Baseline FY 2007 M\$ Team X In-house Build
Jupiter System Observer Baseline	3,116.6
Phase A Total	45.0
Phase B Total	135.1
Phase C/D Total	1,730.9
Development Total	1,911.0
1.0 Project Management	102.0
2.0 Project System Engineering	41.3
3.0 Mission Assurance	102.4
4.0 Science	48.0
5.0 Payload System	398.6
6.0 S/C Bus	664.4
7.0 Mission Operations System	45.8
9.0 Ground Data System	39.7
10.0 ATLO	30.5
11.0 Education & Public Outreach	6.0
12 Mission Design	22.1
Reserves (ABCD)	410.2
Phase E Total	719.6
1.0 Project Management	26.9
2.0 Project System Engineering	0.2
3.0 Mission Assurance	20.2
4.0 Science	175.6
7.0 Mission Operations	249.3
9.0 Ground Data System	143.5
11.0 Education & Public Outreach	10.1
Reserves (E)	93.9
8.0 Launch Vehicle	486.0

- a mission-specific environmental review document and supporting nuclear safety risk assessment efforts;
- launch vehicle and spacecraft/mission design data requirements to support nuclear risk assessment and safety analyses in compliance with the requirements of NPR 8715.3 and the PD/NSC-25 nuclear safety launch approval process;
- support of launch site radiological contingency planning efforts; and
- risk communication activities and products pertaining to the NEPA process, nuclear safety and planetary protection aspects of the project.

NASA HQ will initiate the JSO environmental review document development as soon as a clear definition of the baseline plan and option space has been formulated. DOE will provide a nuclear risk assessment to

¹ Applies to total mission cost minus the LV and RPS.

support the environmental review document, based upon a representative set of environments and accident scenarios compiled by the KSC/Launch Services Program working with JPL. This deliverable may be modeled after the approach used on the Mars Science Laboratory (MSL) EIS.

DOE will provide a nuclear safety analysis report (SAR) based upon NASA-provided mission-specific launch system and spacecraft data to support the PD/NSC-25 compliance effort. The SAR will be delivered to an ad hoc interagency nuclear safety review panel (INSRP) organized for the JSO mission. This INSRP will review the SAR's methodology and conclusions and prepare a Safety Evaluation Report (SER). Both the SER and the SAR will then be provided by NASA to EPA, DoD, and DOE for agency review. Following agency review of the documents and resolution of any outstanding issues, NASA, as the sponsoring agency, will submit a request for launch approval to the Director of the Office of Science and Technology Policy (OSTP). The Director of the OSTP will review the request for nuclear safety launch approval and either approve the launch or defer the decision to the President. Key dates and deliverables for the NEPA and nuclear safety launch approval processes are shown in [Figure 4.10-2](#).

As part of broader nuclear safety considerations, JSO will adopt ATLO, spacecraft, trajectory, and operations requirements, which satisfy the nuclear safety requirements described by NPR 8715.3.

Development of coordinated launch site radiological contingency response plans for NASA launches is the responsibility of the launch site radiation safety organization. Comprehensive radiological contingency response plans, compliant with the National Response Plan and appropriate annexes, would be developed and put in place prior to launch as required by NPR 8715.2 and NPR 8715.3. The JSO project will support the development of plans for on-orbit contingency actions to complement these ground-based response plans.

A project-specific Risk Communication Plan will be completed no later than the MDR. The Risk Communication Plan will detail the rationale, proactive strategy, process and

products of communicating risk aspects of the Project, including nuclear safety and planetary protection. The communication strategy and process will comply with the approach and requirements outlined in the NASA Office of Space Science Risk Communication Plan for Deep Space Missions (1999) JPL D-16993 and the JPL Risk Communication Plan, 2002, JPL D-24012

5.0 DESCOPED MISSION IMPLEMENTATION

5.1 Mission Architecture Overview

The descope mission very strongly resembles the baseline mission, with the following key differences between the two architectures:

- Launch vehicle (Atlas V 551 vs. Delta IV-H). The Atlas V 551, which has a 5-meter fairing, 5 strap-on solid boosters, and a single Centaur engine for the second stage. Atlas V 551 LV uses SLC 36, located at CCAFS.
- Payload (reduced capability in Med-res and PS/EPD instruments)
- Descoped mission performs two year elliptical orbit vs. one year elliptical and one year circular
- One fewer MMRTG

5.2 Science Investigation

5.2.1 Planning Payload

The difference in the payload complement between the baseline and descope missions is in two instruments, the MRC and the PS/EPD. The planning payload is largely intact because the major descope is the loss of propellant to achieve a close circular orbit at Ganymede. The SDT concluded that the need to achieve a circular orbit for gravity and magnetic observations would result in significant science advancement and so it was determined

that potential payload mass should be used for propellant to achieve a circular orbit.

5.2.2 Payload Accommodation

Same as the baseline. Refer to §4.2.2.

5.2.3 Instrument Description

Medium-Res Camera

For the descope mission, only a single camera will be included pointed directly at nadir. See [Table 5.2-1](#).

Plasma Spectrometer/Energetic Particle Detector

For the descope mission, the PS/EPD is simplified by removing the ion composition measurement capability provided by the TOF spectrometer. See [Table 5.2-1](#).

The other payload instruments are the same as for the baseline. Refer to §4.2.3.

5.3 Mission Design

Same as the baseline, except that the spacecraft stays in the elliptical orbit for a second year. Refer to §4.3.

5.4 Spacecraft Design and Development

5.4.1 Spacecraft Overview

The spacecraft for the descope architecture is essentially the same. The main source for differences is that it is launched by the Atlas V 551 launch vehicle limiting the launch capability to 5300 kg. The ΔV was reduced to 2045 m/s, thereby reducing the propulsion

Table 5.2-1. JSO Planning Payload Resource Requirements for the Descoped Mission

Mission Option 1: Example Main S/C Payload, Atlas V 551, Ganymede Orbit						
Instrument	CBE Mass (kg)	CBE Power (W)	Native Rate (Mbps)	Data Reduction Factor (at Instrument)	Rate to C&DH (Mbps)	Notes
High-res Camera	70	95	126	3	40	Same as for baseline
VIS-NIR Hyperspectral Imager System			3500	89	40	Same as for baseline
Medium-res Context Camera (per camera)	15	15	25	3	8	Monochrome, IFOV = 20 μ rad, 6-cm aperture, f/6, nadir viewing
UV Spectrometer	15	10	12	100	0.12	Same as for baseline
Thermal Spectrometer	43	26	32	3	11	Same as for baseline
Ground-Penetrating Radar	36	45	30	100	0.30	Same as for baseline
Laser Altimeter	15	21	0.012	1	0.012	Same as for baseline
Magnetometer	4	2	0.004	1	0.004	Same as for baseline
Plasma Spectrometer/Energetic Particle Detector	10	10	0.002	1	0.002	Plasma moments and differential directional fluxes for energetic charged particles (protons, electrons, ions) at eV to MeV energies, 1 - 30-s time resolution, elemental mass, energy, and angle distributions
Radio Science – Gravity Investigation	-	-	-	-	-	Same as for baseline
Radio Science – Atmospheres	-	-	-	-	-	Same as for baseline
Total	208	224	-	-	-	

system tank capacity and mass. The power modes were reduced to be able to remove one MMRTG for a total of 7. A very modest reduction in instrument payload (see §5.2.3) by 10 kg was also settled on. Other mass deltas came from sizing the spacecraft for these changes: less structure, smaller thermal radiator size, less cabling, radiation shielding mass, etc.

Configuration

The only differences between the baseline and descope architectures for the configuration are the number and mass of instruments carried on the instrument platform, the size of the propellant and oxidizer tanks and a difference of 1 in the quantity of MMRTGs carried. A separate configuration drawing was not developed.

5.4.2 System Design Approach

The system design approach for the Descope Architecture is identical to the baseline except for those noted in the section below.

5.4.2.1 Radiation

The radiation environment was assumed the same for both concepts, and the same design

approach for shielding was used. The only difference was the total number of electronic boards to be shielded. The number of instrument electronics cards is 17 6U. This results in 1 instrument chassis (vs. 2 for the baseline architecture). **Table 5.4-1** details the radiation vault components breakdown.

The total radiation vault mass for the descope mission is 152 kg.

5.4.2.2 Fault Protection

For this concept study, the fault protection strategy is essentially the same. There likely will be fewer fault modes without the low circular orbit phase, but this level of detail was not studied in this concept study. Further details would be studied in future efforts.

5.4.2.3 Resource Margin Summary

Mass

The descope spacecraft mass totals and margin are shown in **Table 5.4-2**. Current JSO design shows contingencies averaging about 27% of the total CBE. With the launch vehicle capability (M_{launch}) of 5300 kg, the $M_{\text{propellant}}$ is 2627 kg and the $M_{\text{s/c}}$ allocation is 2648 kg providing a system margin of $M_{\text{s/c}}$ allocation - MEV = 663 kg, or 33% of the MEV. Together,

Table 5.4-1. Radiation Vault Component Breakdown for the Descope Mission

Descope Architecture										
Subsystem	Component	krad (RDF 1)	# of Units	L (cm)	W (cm)	H (cm)	Volume	Type of Shielding Techniques/Comments	Shielding Material	mass (kg)
Telecom	SDST X-up/X&Ka down	300	2	42.2	46.0	20.2	39234.2	Enclosed shielding, added 5 cm to height for cable connections. All MGA and HGA hardware are on the back of the HGA. LGA hardware is on spacecraft	75%W-25%Cu	68.56
	USO, 1E-12		2	15.2	15.2	20.2	4700.9			38.09
	Ka-band TWTA, RF-50W		2	20.3	15.2	15.2	4694.7			8.49
	X-Band sspa, RF-5W		2	17.78	12.7	15.16	3423.2			8.59
	Waveguide Transfer Switch (WGTS)		5	5.1	5.1	15.2	391.2			6.94
	Hybrid Coupler		2	2.5	2.5	6.0	38.8			4.53
	Coax Transfer switch		2	5.1	5.1	7.5	193.5			0.39
	x4 Multiplier		2	2.5	2.5	7.5	48.6			1.05
ACS									0.47	13.26
	Sun Sensors	600	4	7.6	4.5	6.1	208.6	Enclosed shielding, added 5 cm to height for cable connection	75%W-25%Cu	1.07
	Star Camera Head		4	11.5	11.5	15	1983.8			4.64
	IMUs	1000	2	26.7	17.3	16.4	7575.3	1.95		
	Reaction Wheel		4	31.6	15.9	20.9	10501.0	4.91		
	Rad Hard Reaction Wheel Electronics		2					0.23		
	Rad Hard Gimbal Drive Electronics (HGA and Main Engine)		4					0.46		
CDS										38.49
	MSAP Chassis 203x27x204	300	2	25.2	22.9	27.9	16089.1	Holds 9 cards	75%W-25%Cu	11.22
	RADHard RAD750 (6U 200MHz) w/256MB SRAM [NR]		2				6U chassis vault. 6 U Card that takes up two card slots	0.95		
	RADHard 6U C-RAM card for JSO mission (NR)		2					0.95		
	RADHard MTIF Card (6U) for JSO mission (NR)		2					0.95		
	RADHard SIA Card (6U) for JSO mission (NR)		4				6U chassis vault. 6 U Card	1.89		
	RADHard MAGIC Card (6U) for JSO mission (NR)		2					0.95		
	Data Compressor co-processor card (NR)		2					0.95		
	RADHARD PCC DC-DC Converter: 5 V, 3.3V and +/-12V. (NR)		2					0.95		
	MREU Chassis		1	25.2	24.8	27.9	17461.4	Holds 10 cards (will hold the 6 ACS cards)		5.76
	RADHard Analog/Discrete MREU (NR)		4					1.89		
	CDS Backplane: MSAP Backplane		2				6U chassis vault. 6 U Card	0.95		
	RADHard 9.6 Gbit SSR for JSO Mission (NR)		1	25.2	26.9	27.9	18940.0	Holds 11 cards		5.92
	Memory Card		8					3.78		
	Controller		2					0.95		
	Power Supply		1					0.47		
	Instruments									
	Chassis	300	2	25.2	22.9	27.9	16089.1	Holds 9 cards	75%W-25%Cu	11.22
	High-res monochrome camera		3					1.4175		
	VIS-NIR hyperspectral imager		3					1.4175		
	UV imaging spectrometer		2					0.945		
	Thermal spectrometer		3					1.4175		
	Laser altimeter		3					1.4175		
	Magnetometer		1					0.4725		
	Plasma spectrometer/ energetic particle detector		2					0.945		
Propulsion										13.53
	Pressure Transducer	100	12	13.3	3	3	119.7		75%W-25%Cu	13.53
Power										
	Chassis	2000	1	25.2	57.4	27.9	40414.7	Holds 26 cards	Aluminum	No additional shielding needed
	Load Switching*		10							
	Thruster Drivers		4							
	Pyro Switching		2							
	Converters*		2							
	Shunt Regulators		4							
	Battery Control*		2							
	RTG Interface Card		2							
Total Mass										153.09

the contingency and system margin provide 1079 kg over the CBE. This margin and contingency exceed JPL's design principles for a >30% margin over the $M_{s/c}$ allocation.

Power

The main difference for the descope architecture is that the number of MMRTGs is 7 (vs 8 in the baseline design) reducing the EOL power output to 681 W. Power output after 7 years is 738 W and after 10 years is 703 W. This reduces the net power margin in the key driving modes, as shown in [Table 5.4-3](#) and requires more supplemental energy from the rechargeable batteries in certain modes. Note that the energy used on batteries shows a depth of discharge on two batteries for this design. The most power demanding mode, encounter mode, also further increases the amount of duty cycling that will be needed during those flybys. As in the baseline, the number of these events will be under 100, and so JSO's estimate of 42% DoD is well below the DoD of 70% per JPL's design principles.

5.4.3 Subsystem Descriptions

Structures and Mechanisms

The structural design approach for the

Table 5.4-2. Descoped Architecture Mass Summary

Jupiter System Observer 2007-07-10 Systems Comparison	Descoped Architecture (kg)		
	CBE (kg)	Cont. (%)	CBE+ Cont. (kg)
Payload			
Instruments	208	37%	284
Bus			
Attitude Control	51	31%	67
Command & Data	49	37%	67
Power (non-MMRTG)	54	26%	68
MMRTGs	329	5%	345
Propulsion	204	24%	254
Structures & Mechanisms	315	30%	410
Cabling	99	30%	129
Telecom	58	20%	69
Thermal	48	28%	61
Bus Total	1207	22%	1470
Radiation Vault	153	50%	230
Spacecraft			
Spacecraft Dry Mass	1568	27%	1984
Propellant & Pressurant			2627
Wet Mass			4612
Mass (kg)			
System Margin *		33%	663
Spacecraft Dry Mass Allocation			2648
Launch Vehicle Adapter (LV side)			25
Launch Vehicle Capability	Atlas V 551		5300

* Margin = Remaining LV Mass/Spacecraft Dry Mass (CBE+Cont)

descope design is the same. The mechanisms are the same. The only differences between the baseline design and the descope design is the number and mass of instruments carried on the instrument platform, the size of the propellant and oxidizer tanks and a difference of 1 in the quantity of MMRTGs carried. The mass estimates of the structure, ballast, and cabling are based on parametric models that scaled with the spacecraft system.

Telecommunications

The telecom system design is the same as for the baseline. Refer to §4.4.3.

Command and Data Handling

The command and data handling system design is the same as for the baseline. Refer to §4.4.3.

Flight Software

For this concept study, the software is essentially the same. The number of instruments is the same. Further details would be studied in future efforts.

Attitude Control

The attitude control system design is the same as for the baseline. Refer to §4.4.3.

Propulsion

The propulsion system design is the same except for the size of the propellant tanks, given the smaller propellant load. The duty cycle on the HiPAT engine decreases to 110 minutes for four events (from 200 minutes in five events in the baseline design).

Power

The descope spacecraft carries only 7 MMRTGs vs. (8 in the baseline design). With lower power loads, the power dissipation is lower and accounted for in the power modes analysis, as reflected in [Table 5.4-3](#).

Thermal

The thermal design of the descope spacecraft is almost identical to that of the baseline. The difference is the change in the mechanical design to support a slightly smaller instrument complement and the change in the orbit during the Ganymede science orbits, which requires a smaller propulsion system and therefore a corresponding smaller Thermal subsystem.

One of the more significant assemblies difference is the thermal radiator for the

Table 5.4-3. Descope Architecture Power Modes

Descope Architecture	Power	Power	Power	Power	Power	Power	Power	Power	Power
Subsystem	(W)	(W)	(W)	(W)	(W)	(W)	(W)	(W)	(W)
	Launch	Cruise	Critical Mnvr	Jupiter System Tour	Encounter Mode	Ganymede Elliptical (Sci/RS/Tel.)	Ganymede Elliptical (Science)	Fault Recovery	Safe Mode
Power Mode Duration (hours)	8	24	1.5	24	6	1	8	1	Indefinite
Payload	0	59	59	85	145	77	77	49	49
C&DH	89	89	140	103	121	113	113	68	68
ACS	31	87	97	87	87	94	87	87	87
Telecom	107	112	112	112	112	154	112	112	112
Propulsion	58	58	217	10	58	10	10	90	52
Thermal	13	11	11	11	11	11	11	43	43
Power	38	51	75	52	64	57	53	52	49
Bus	336	409	652	376	453	440	386	453	412
TOTAL (W)	336	468	711	461	599	517	463	502	461
Total with Contingency (30%) *	437	608	924	599	778	672	602	652	599
Available Power, (W)**	826	738	738	703	703	681	681	681	681
Net Power Margin (W)	389	130	-186	104	-75	9	79	29	82
Battery Energy Used (W-Hr)			279			451			
DoD (%), one battery			25%			41%			

* Blanket 30% contingency is applied conservatively; many assembly uncertainties understood better than 30%.

** Power computed for end of BOM (mode 1), 7 years (modes 2, 3), 10 years (modes 3, 4), and 12 years (modes 6-9).

descope design: it is 2 m² (vs. 2.5 m² for the baseline design).

5.4.4 Verification and Validation

Same as the baseline. Refer to §4.4.4.

5.5 Operational Scenarios

Same as the elliptical mission subphase of the baseline. Refer to §4.5.

5.6 JSO Planetary Protection

Same as the baseline. Refer to §4.6 in its entirety.

5.7 Trades and Open Issues

Same as the baseline. Refer to §4.7 in its entirety.

5.8 Technology Needs

Same as the baseline. Refer to §4.8 in its entirety.

5.9 Technical Risk Assessment

Same as baseline. Refer to §4.9 in its entirety.

5.10 Programmatics

5.10.1 Schedule

Same as the baseline. Refer to §4.10 in its entirety.

5.10.2 Cost

The total estimated life cycle cost (phase A/B/C/D/E) including the launch vehicle and Radioisotope Power System is \$2.7B (2007 fixed year \$) for the descope mission.

Table 5.10-1 provides a project summary of the cost. A -10% to +20% uncertainty in the estimate would have a range of \$2.4B to \$3.2B.

The major cost reduction is in the launch vehicle, slight reduction in the payload, reduction of one MMRTG in the spacecraft bus.

5.10.3 NEPA Compliance & Launch Approval

Same as the baseline. Refer to §4.12.

*Table 5.10-1. JSO Descoped Cost by Level
2 WBS*

WBS Elements	Team X In-house Build	
	Project Cost	FY 2007 M\$
	Minimum (-10%)	2,429.0
	Expected	2,698.9
	Maximum (+20%)	3,238.7
	FY 2007 M\$ Team X In-house Build	
Jupiter System Observer Descoped	2,698.9	
Phase A Total	43.2	
Phase B Total	129.5	
Phase C/D Total	1,667.4	
Development Total	1,840.1	
1.0 Project Management	105.0	
2.0 Project System Engineering	41.3	
3.0 Mission Assurance	98.2	
4.0 Science	46.6	
5.0 Payload System	381.6	
6.0 S/C Bus	622.4	
7.0 Mission Operations Systems	45.7	
9.0 Ground Data System	39.7	
10.0 ATLO	30.7	
11.0 Education & Public Outreach	5.9	
12.0 Mission & Navigation Design	21.8	
Reserves (ABCD)	401.3	
Phase E Total	667.9	
1.0 Project Management	26.9	
2.0 Project System Engineering	0.2	
3.0 Mission Assurance	18.7	
4.0 Science	169.6	
7.0 Mission Operations	247.4	
9.0 Ground Data System	125.9	
11.0 Education & Public Outreach	9.9	
Reserves (E)	69.4	
8.0 Launch Vehicle	191.0	

This page is intentionally left blank.

6.0 BACK-UP LAUNCH OPPORTUNITIES

Table 6.0-1 shows two backup launch opportunities to the 2017 baseline launch. The 2017 baseline mission is shown for comparison.

It is interesting to note that the 2020 VEEGA launches a year and a half later than the 2018 VEEGA, but arrives only four months later. After accounting for the lower

ΔV for the backup missions, the delivered mass into Ganymede orbit is comparable for the three missions. The only potential spacecraft discriminator between the missions would be the significantly lower perihelion of the 2018 VEEGA, which could affect the thermal design for the sunshade.

Table 6.0-1. Back-Up VEEGAs Provide Comparable Performance to the Baseline

	Baseline	2018 Backup	2020 Backup
Trajectory Type	VEEGA	VEEGA	VEEGA
Launch Period (days)	21	21	21
Launch date	Jan 2017	Sept 2018	Mar 2020
C_3 (km ² /s ²)	10	13.4	9.8
Minimum Heliocentric Range (AU)	0.72	0.62	0.70
Flight Time to Jupiter (years)	5.7	7.0	5.9
Deep Space ΔV (m/s)	265	0	30
Jupiter Arrival	Sep 2022	Oct 2025	Feb 2026
Jupiter Arrival V_∞ (km/s)	6.1	6.2	5.6
Total ΔV	2705	2440	2470
Atlas V 551 Launch Mass (kg)	5300	4985	5315
Delta IV-H Launch Mass (kg)	7810	7325	7840

7.0 SUMMARY

The overview of the report is provided in the Executive Summary (§1). Both the baseline and descoped missions have been designed to mitigate the radiation risks associated with operating in the Jovian environment. These risks are well understood from past experiences of Cassini and Galileo and are addressed in details in §4.9. The estimated cost of both missions are comparable to the Cassini experience, and sufficient reserves are included to guard against unforeseen problems as the mission develops. The cost and reserve approach are discussed in detailed in §10.2. The following section specifically addresses the science evaluation of the two mission concepts against the science measurements that resulted in applying the operations concept described in §4.5.

7.1 Science Value

To achieve the best Jupiter system science, the SDT derived a set of goals, objectives, investigations, and measurements that are far-reaching and comprehensive. The corresponding “ideal” instruments to make these measurements are equally comprehensive. As the trade space is narrowed to formulate the Baseline and Descoped architecture, it is necessary to evaluate the ability of each mission concept to accomplish the desired measurements. This provides an overall assessment as to the science value of a given mission strategy. To begin, the SDT did not attempt to generate an overall “super” priority list of the more than 300 measurements defined in Appendix C. Instead, each science theme group ranked its Objectives and Investigations in priority order. For the Satellites group, each target (Io, Europa, Ganymede, Callisto and Rings/Small Satellites) was prioritized separately. Secondly, it must be stated that overall science value is inherently subjective and thus it is not possible to establish an accurate quantitative assessment. However, the SDT has provided a qualitative rating as to the ability of each measurement to be accomplished for both the baseline and descoped missions ([Figures 7.1-1 and 7.1-2](#)). By their nature, the ability to

achieve geophysical magnetosphere and gravity measurements is dependent on the type of orbit that can be achieved. Because of this, a finer level of evaluation was performed, that for measurements in orbit at Ganymede and that for fly-bys of other targets.

The criteria used to rate science value are:

- 0 (red) – Not Applicable—Does not address the science investigation
- 1 (deep orange) – Poor—Touches on the science investigation
- 2 (orange) – Fair—May address partially the science investigation
- 3 (yellow) – Good—Definitely addresses partially the science investigation
- 4 (light green) – Very Good—May address fully the science investigation
- 5 (dark green) – Excellent—Definitely addresses fully the science investigation

For both the baseline and descoped missions, there is very little variation between the ratings for Satellites and Jupiter Atmospheres. This is not surprising as there are only small differences between the instrument payloads for the two missions. For the descoped mission, the stereo capability of the medium resolution camera is eliminated. Operationally, this will require repeat coverage of targets to achieve stereo objectives. In addition, some of the ability of the plasma spectrometer to provide compositional information is removed in the descoped concept. The greatest variation in science value is expressed in the Magnetosphere and Interiors groups. The inability to achieve a close circular orbit around Ganymede for the descoped mission has a significant impact on the science that can be done. In both cases, the number of measurements that rate “Excellent” decreases by ~50%.

The results of this evaluation show that significant and revolutionary new science can be achieved by both mission concepts. The fact that very few measurements fall into the category of “Not Applicable” demonstrates the robustness of the investigation strategy and implementation.

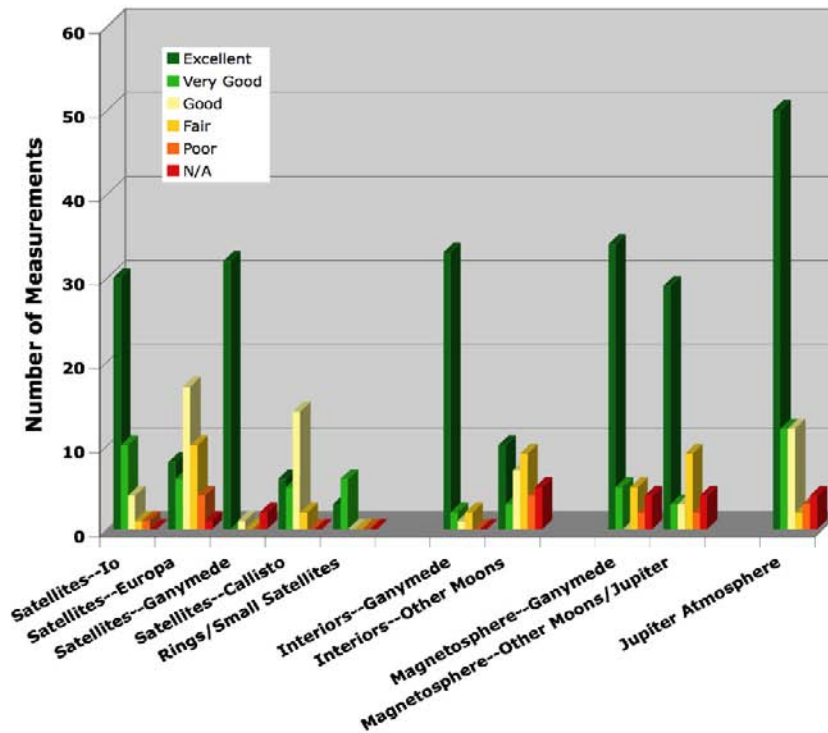


Figure 7.1-1. Graph showing the SDT ranking, by each theme group, of the ability of the baseline mission to achieve the required measurements. Over 80% were rated as good to excellent showing that outstanding science will be returned by this mission.

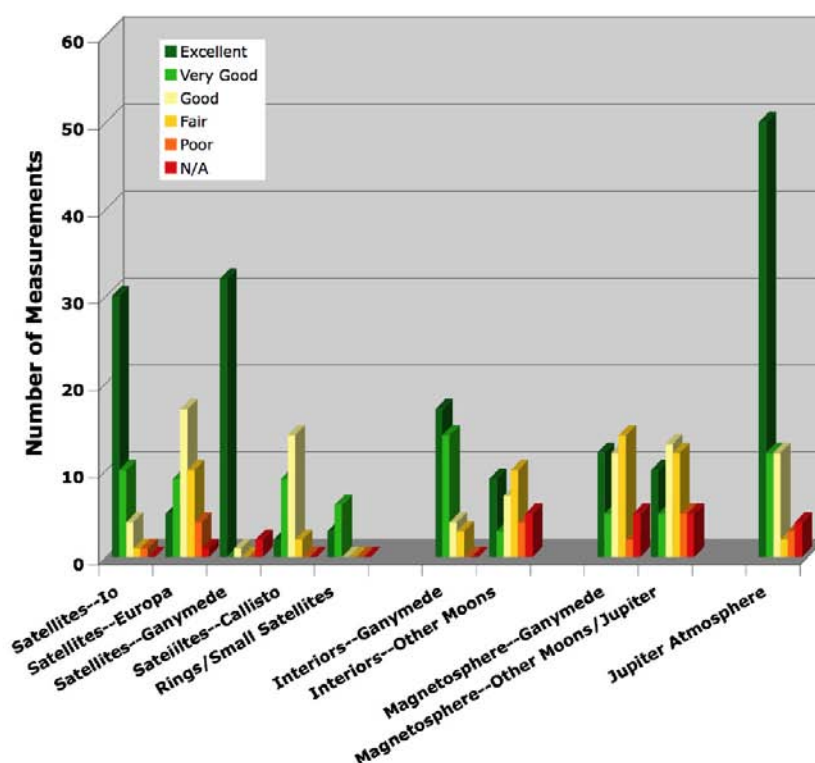


Figure 7.1-2. Graph showing the SDT ranking, by theme group, of the descoped mission to achieve the required science measurements. The greatest loss of science occurs for the Interiors and Magnetospheres groups where there is the strongest dependence on orbit type—showing the importance of the circular orbit at Ganymede. For these two groups, the excellent scores are reduced by ~50% relative to the baseline. Overall, 75% of the measurements rated good to excellent, showing that even for the descoped mission, a significant scientific return can be accomplished.

8.0 TEAM MEMBERS AND ROLES

8.1 Team Overview

The study was conducted by two closely interacting teams. The NASA-chartered Science Definition Team ([Figure 8.1-1](#)) focused on the science aspects of the mission concept while the JPL Engineering Team focused on the technical and programmatic aspects of the mission concept. There was extensive interaction between the two teams throughout the study ensuring that the science goals and objectives were feasible given the technical and programmatic constraints and approaches. A listing of the science team members, their affiliations and their areas of expertise are given in [Table 8.1-1](#).

The SDT held five face-to-face meetings along with weekly telecons. When areas were identified for which additional science expertise was required, the team invited specific individuals to present at the SDT meetings to ensure a broad input on the science and potential investigational methods. Specific presentations were provided by: Mark Showalter (SETI Institute—Jovian Rings); John Spencer (SWRI—Distant observations of the Jovian System from New Horizons); Nick Schneider (University of Colorado—Io torus); Brian Drouin (JPL—Radar Spectrometer); Soren Madsen (JPL—InSAR Topomapper); Robert Green (JPL—Imaging Spectrometer); Sami Asmar (JPL—Radio and Gravity Science).

The SDT was divided into four subgroups that focused on identifying goals, objectives, investigations and measurements for broad science themes—Satellite Science, Interiors, Magnetospheres and Jovian Atmosphere.

Additionally, the JSO SDT worked closely with the Europa Explorer SDT to understand and evaluate the ability of each mission concept to achieve the science objectives of the alternate concept. A joint White Paper is being prepared to document this evaluation and is expected to be completed later this year.

8.2 APL-JPL Outer Planets Steering Group

The Study Team interacted with and was advised by a steering group consisting of the following people:

Walt Faulconer—APL: Civilian Space Business Area Executive

Rob Strain—APL: Space Department Head



Figure 8.1-1. The Jupiter System Observer Science Definition Team. Back row (from left to right): Adam Showman, Dave Williams, John Cooper, Dave Senske; Middle row: Geoff Collins, Jerry Schubert, Elizabeth Turtle, Louise Prockter; Front row: Glenn Orton, Margy Kivelson, Amanda Hendrix, Karl Hibbitts.

Rob Gold—APL: Space Department Chief Technologist

Chris Jones—JPL: Director for Solar System Exploration

Doug Stetson—JPL: Manager of the Solar System Mission Formulation Office

Jim Cutts—JPL: Chief Technologist for Solar System Exploration and Manager of the Strategic Mission and Advanced Concepts Office

8.3 Study Results Review

Different parts of this concept study report have been reviewed by independent sets of discipline specialists and by APL/JPL management as follows:

1. A JPL standing review board provided oversight for the NASA interim reviews.
2. The implementation has been reviewed by a technical, management, and cost review board internal to JPL.
3. Finally, the overall concept study report was reviewed by both JPL and APL management prior to submission.

Table 8.1-1. Science Definition Team

Member	Affiliation	Expertise
Louise Prockter—Co-Chair	APL	Icy Satellite Geology
Dave Senske—Co-Chair	JPL	Icy Satellite Geology
Elizabeth Turtle	APL	Satellite Geology/Geophysics
Karl Hibbitts	APL	Satellite Remote Sensing
Amanda Hendrix	JPL	Satellite/Atmospheres Remote Sensing
Dave Williams	ASU	Satellite Geology--Io
Geoff Collins	Wheaton College	Satellite Geology--Ganymede
Adam Showman	University of Arizona	Geophysics/Jupiter Atmosphere
Jerry Schubert	UCLA	Geophysics/Jupiter Atmosphere
Glenn Orton	JPL	Jupiter Atmosphere
John Cooper	GSFC	Magnetospheres
Margy Kivelson	UCLA	Magnetospheres

A. ACRONYMS AND ABBREVIATIONS

Δ V-EGA	Delta Velocity – Earth Gravity Assist
Δ DOR	Delta Differential One-way Ranging
μ C	Microcontroller
A/D	Analog-to-Digital
AACS	Attitude and Articulation Control Subsystem
AA-STR	APS Autonomous
ACS	Attitude Control (Sub)system
ADC	Analog-to-Digital Converter
AHSE	Assembly Handling Support Equipment
AO	Announcement of Opportunity
APD	Avalanche Photodiode
APL	Applied Physics Laboratory
APS	Active Pixel Sensor
ARR	ATLO Readiness Review
ARTG	Advanced Radioisotope Thermoelectric Generator
ASIC	Application-Specific Integrated Circuit
ASRG	Advanced Sterling Radioisotope Generator
ASU	Arizona State University
ATLO	Assembly, Test, and Launch Operations
AU	Astronomical Unit
B	Magnetic field
BCE	Basis for Cost Estimate
BCE	Backup Control Electronics
BER	Bit Error Rate
BOL	Beginning Of Life
BOM	Beginning Of Mission
C&DH	Command and Data Handling (subsystem)
CAPS	Cassini Plasma Spectrometer
CBE	Current Best Estimate
CCAFS/KSC	Cape Canaveral Air Force Station/Kennedy Space Center
CCD	Charge Coupled Device
CCSDS	Consultative Committee for Space Data Systems
CDH	Command & Data Handling
CDR	Critical Design Review
CDS	Command & Data Subsystem
cg	Center of Gravity
CIRS	Composite Infrared Spectrometer
CM	Center of Mass (star trackers)
CMMI	Capability Maturity Model Integration
CMOS	Complementary Metal Oxide Semiconductor
COMPLEX	Committee on Planetary and Lunar Exploration
COPV	Composite Overwrapped Pressure Vessels
COTS	Commercial Off-The-Shelf
CPU	Central Processing Unit

CRAM	Chalcogenide Memory
DC	Direct Current
DI	Deep Impact
DOD	Depth-of-Discharge
DP	Design Principles
DPMR	Deputy Project Manager for Radiation Development
DPSR	Deputy Project System Engineer of Radiation
DSCC	Deep Space Communications Complex
DSM	Deep Space Maneuver
DSN	Deep Space Network
DSOC	Deep Space Operation Center
DTM	Developmental Test Model
E/PO	Education and Public Outreach
EDAC	Error Detection and Correction
EDL	Entry, Descent and Landing
EE	Europa Explorer
EGC	Europa, Ganymede, Callisto
EGE	Europa Geophysical Explorer
EM	Engineering Model
EMC	Electromagnetic Compatibility
EMI	Electromagnetic Interference
EO	Europa Orbiter
EOI	Europa Orbit Insertion
EOL	End of Life
EOM	End of Mission
EPD	Energetic Particle Detector
EPF	Europa Pathfinder
ER	Eastern Range
ESA	European Space Agency
ESD	Electrostatic Discharge
ESG	Europa Sub-group
ESSP	Europa Surface Science Package
EUV	Extreme Ultraviolet
EUVE	Extreme Ultraviolet Explorer
EUV-FUV	Extreme Ultraviolet-Far Ultraviolet
F&P	Fields & Particles
FER	Frame Error Rate
FOC	Flight Operations Center
FODA	Fiber Optic Delay Assembly
FOV	Field of View
FPGA	Field-Programmable Gate Array
FPP	Flight Project Practices
FTE	Flux Transfer Event
FTE	Full-Time Equivalent
FTS	Fourier Transform Spectrometer
FUV	Far Ultraviolet

G&C	Guidance and Control
GDS	Ground Data System
G-G	Gravity Gradient
GIRE	Galileo Interim Radiation Electron
GLL	Galileo
GOI	Ganymede Orbit Insertion
GPHS	General Purpose Heat Source
GPR	Ground-Penetrating Radar
GRACE	Gravity Recovery And Climate Experiment
GRC	Galactic Cosmic Rays
GSE	Ground Support Equipment
H/W	Hardware
HGA	High Gain Antenna
HiPat	High Performance Apogee Thruster
HiRes	High Resolution
HiRISE	High Resolution Imaging Science Experiment
HRC	High-Resolution Camera
HRGs	Hemispherical Resonating Gyros
HRI	High Resolution Imager
HRI	High Resolution Instrument
HRSC	High Resolution Stereo Camera
HST	Hubble Space Telescope
I&T	Integration and Test
IC	Internal Charging
IC&DH	Instrument Command & Data Handling
IESD	Internal Electrostatic Discharge
IFOV	Instantaneous Field of View
InD	Instrument Development
IR	Infrared
IRS	Infrared Spectrometer
IRU	Inertial Reference Unit
ITC	Integration and Test Complexity
JIMO	Jupiter Icy Moons Orbiter
JMI	Jovian Moon Impactor
JOI	Jupiter Orbit Insertion
JPL	Jet Propulsion Laboratory
JSO	Jupiter System Observer
KLOC	Thousands of Lines of Code (for space data systems)
LA	Laser Altimeter
LGA	Low Gain Antenna
LOLA	Lunar Orbiter Laser Altimeter
LORRI	Long Range Reconnaissance Imager
LOS	Line of Sight
LRO	Lunar Reconnaissance Orbiter
LST	Local Solar Time
LV	Launch Vehicle

LVA	Launch Vehicle Adapter
LVDS	Low-Voltage Differential Signaling
LVPS	Low-Voltage Power Supply
M	Mass
MAG	Magnetometer
MAGIC	Motor Actuation GN&C Interface Cards
MAM	Mission Assurance Manager
MARSIS	Mars Advanced Radar for Subsurface and Ionospheric Sounding
MCP	Microchannel Plate (detectors)
MER	Mars Exploration Rovers
MEV	Maximum Expected Value
MGA	Medium Gain Antenna
MGs	Mars Global Surveyor
MIT	Minimum Impulse Thruster
MLI	Multilayer Insulation
MMRTG	Multi-Mission Radioisotope Thermoelectric Generator
MOLA	Mars Orbiter Laser Altimeter
MOS	Mission Operation System
MRC	Medium-Resolution Camera
MREU	MSAP Remote Engineering Unit
MRO	Mars Reconnaissance Orbiter
MSA	Mission Support Area
MSAP	Multi-Mission Spacecraft Architectural Platform
MSIA	MSAP System Interface Assembly
MSL	Mars Science Laboratory
MST	Mission System Testbed
MTIF	MSAP Telecommunications Interface
MVPS	Medium-Voltage Power Supply
NAC	Narrow-Angle Camera
NASA	National Aeronautics Space Agency
Nav	Navigation
NAVCAM	Navigation Camera
NEAR	Near-Earth Asteroid Rendezvous
NICM	NASA Instrument Cost Model
NIR	Near Infrared
NLR	Near-Earth Asteroid Rendezvous Laser Rangefinder
NPD	NASA Policy Document
NPR	NASA Procedural Requirements
NRC	National Research Council
NUV	Near Ultraviolet
NVM	Non-Volatile Memory
OPAG	Outer Planets Assessment Group
OpSc	Science Operations
ORT	Operational Readiness Test
PA	Plutonium Availability
PAF	Payload Attach Fitting

PCC	Power Converter Card
PCI	Peripheral Controller Interface
PDR	Preliminary Design Review
PJR	Perijove Raise
PM	Project Manager
PMCM	Planet Mission Cost Model
PMD	Propellant Management Device
POP	Program Operating Plan
PP	Planetary Protection
PPO	Planetary Protection Office
PROM	Programmable Read Only Memory
PS	Project Scientist
PS/EPD	Plasma Spectrometer/Energetic Particle Detector
PSE	Project System Engineer
PWB	Printed Wiring Board
QQO	Quasi-Quadrennial Oscillation
R	Radius
RadE	Radiation Environment and Shielding
RadPSM	Radiation Parts, Sensors, and Materials
RAM	Random Access Memory
RCS	Reaction Control System
RDF	required design factor
RDF	Radiation Design Factor
REU	Remote Engineering Unit
RHU	Radioisotope Heater Unit
RMS	Radiation Monitoring System
RPS	Radioisotope Power Source
RT	Remote Terminal
RTG	Radioisotope Thermoelectric Generator
RWA	Reaction Wheel Assembly
S/C	Spacecraft
SDST	Small Deep Space Transponder
SDT	Science Definition Team
SEP	Solar Electric Propulsion
SEU	Single Event Upset
SFC	Spacecraft Flight Computer
SHARAD	Shallow Radar
SIA	System Interface Assembly
SLC	Space Launch Complex
SNR	Signal-to-Noise Ratio
SOC	Science Operations Center
SRAM	Static Random Access Memory
SSE	Solar System Exploration
SSES	Solar System Exploration Subcommittee?
SSIRU	Scalable Space Inertial Reference Unit
SSPA	Solid State Power Amplifier

SSR	Solid-State Recorder
ST5	Space Technology 5
TA	Thruster Availability
TBD	To Be Determined
TCM	Trajectory Correction Maneuver
TI	Thermal Instrument
TID	Total Ionizing Dose
TLM	Telemetry Data
TOF	Time-of-Flight
TRL	Technology Readiness Level
TS	Thermal Spectrometer
TVC	Thrust Vector Control
TWTA	Traveling Wave Tube Amplifier
U of A	University of Arizona
U of Col	University of Colorado
U of H	University of Houston
UCLA	University of California Los Angeles
USO	Ultra Stable Oscillators
UTJ	Ultra Triple Junction
UV	Ultraviolet
UV-IR	Ultraviolet-Infrared
UVIS	Ultraviolet Imaging Spectrometer
UVS	Ultraviolet Spectrometer
V&V	Verification and Validation
VEEGA	Venus-Earth-Earth Gravity Assist
VHS	VIS-NIR Hyperspectral Imager System
VIS-IR	Visible-Infrared
VIS-NIR	Visible-Near Infrared
VkEmMnGA	multiple Venus, Earth, Mars Gravity Assists
VNIR	Visible-Near Infrared
VPS	Voyager Plasma Science
VRHU	Variable Radioisotope Heater Unit
VS	Vault Size
WAC	Wide-Angle Camera
WBS	Work Breakdown Structure
W-Cu	tungsten-copper
WGS	Wave Guide Switch

B REFERENCES

- Ajello, J. M., et al. (2005), The Cassini Campaign observations of the Jupiter aurora by the Ultraviolet Imaging Spectrograph and the Space Telescope Imaging Spectrograph, *Icarus*, 178, 327–345.
- Anderson, J. D., E. L. Lau, W. L. Sjogren, G. Schubert, and W. B. Moore (1996), Gravitational constraints on the internal structure of Ganymede, *Nature*, 384, 541–543.
- Anderson, J. D., G. Schubert, R. A. Jacobson, E. L. Lau, W. B. Moore, and W. L. Sjogren (1998), Distribution of rock, metals, and ices on Callisto, *Science*, 280, 1573–1576.
- Anderson, J. D., R. A., Jacobson, E. L., Lau, W. B., Moore, and G. Schubert (2001), Io's gravity field and interior structure, *J. Geophys. Res.*, 106, E12, 32963–32970.
- Anderson, J. D., G. Schubert, R. A. Jacobson, E. L. Lau, W. B. Moore, and J. L. Palguta (2004), Discovery of Mass Anomalies on Ganymede, *Science*, 305, 989–991.
- Anderson, J. D., T. V. Johnson, G. Schubert, S. Asmar, R. A. Jacobson, D. Johnston, E. L. Lau, G. Lewis, W. B. Moore, A. Taylor, P. C. Thomas, and G. Weinwurm (2005), Amalthea's density is less than that of water, *Science* 27, Vol. 308. no. 5726, pp. 1291–1293, DOI: 10.1126/science.1110422
- Bagenal, F., W. B. McKinnon, and T. E. Dowling (Eds.) (2004), *Jupiter - The Planet, Satellites and Magnetosphere*, Cambridge Univ. Press, pp. 748.
- Bhattacharya, B., R. M. Thorne, D. J. Williams, K. K. Khurana, and D. A. Gurnett (2005), Diffuse auroral precipitation in the jovian upper atmosphere and magnetospheric electron flux variability, *Icarus*, 178, 406–416.
- Bills, B. G. (2005), Free and forced obliquities of the Galilean satellites of Jupiter, *Icarus*, 175, 233–247.
- Borucki, W. J. and M. A. Williams (1986), Lightning in the jovian water cloud, *J. Geophys. Res.*, 91, 9893–9903.
- Burns, J. A. (2004), Planetary Rings: Structure, Evolution and Origin (abs), *Bull. American Astron. Soc.*, 36, pp. 1404.
- Canup, R. M. and W. R. Ward (2002), Formation of the Galilean Satellites: Conditions of Accretion, *The Astronomical Journal*, 124, 3404–3423.
- Carr, M. H., A. S. McEwen, K. A. Howard, F. C. Chuang, P. Thomas, P. Schuster, J. Oberst, G. Neukum, and G. Schubert (1998), Mountains and Calderas on Io: Possible Implications for Lithosphere Structure and Magma Generation, *Icarus*, 135, Issue, 146–165.
- Clarke, J. T., D. Grodent, S. W. H. Cowley, E. J. Bunce, P. Zarka, J. E. P. Connerney, and T. Satoh (2004), Jupiter's aurora, in *Jupiter - The Planet, Satellites and Magnetosphere*, F. Bagenal, W. B. McKinnon, and T. E. Dowling (Eds.), pp. 639–670, Cambridge Univ. Press.
- Carlson, R. W. (1999), A tenuous carbon dioxide atmosphere on Jupiter's moon Callisto, *Science*, 283, 820–821.
- Cole, T. D. (1998), NEAR Laser Rangefinder: A Tool for the Mapping and Topologic Study of Asteroid 433 Eros, *Johns Hopkins APL Technical Digest*, Vol. 19, No 2.
- Cooper, J. F., R. E. Johnson, B. H. Mauk, H. B. Garrett, and N. Gehrels (2001), Energetic ion and electron irradiation of the icy Galilean satellites, *Icarus*, 149, 133–159.
- Cooper, J. F. and K. K. Khurana (Eds.) (2005), Jovian System Magnetospheric Science (special collection), *Icarus*, 178.
- Del Genio, A. D., J. M. Barbara, J. Ferrier, A. P. Ingersoll, R. A. West, A. R. Vasavada, J. Spitale, and C. C. Porco (2007), Saturn eddy momentum fluxes and convection: First estimates from Cassini images, *Icarus*, In press.
- Elsner, R. F., et al. (2005a), Simultaneous Chandra X-ray, Hubble Space Telescope ultraviolet, and Ulysses radio observations of Jupiter's aurora, *J. Geophys. Res.*, 110, A01207, doi:10.1029/2004JA010717.
- Elsner, R. F., B. D. Ramsey, J. H. Waite, P. Rehak, R. E. Johnson, J. F. Cooper, and D. A. Swartz (2005b), X-ray probes of magnetospheric interactions with Jupiter's auroral zones, the Galilean satellites, and the Io plasma torus, *Icarus*, 178, 417–428.

- Geissler, P. E. (2003), Volcanic Activity on Io During the Galileo Era, *Annual Review Earth Planetary Science*, 31, 175–211.
- Gierasch, P. J., B. J. Conrath, and P. L. Read (2004), Nonconservation of potential vorticity in hydrogen atmospheres, *J. Atmos. Sci.*, 61, 1953–1965.
- Greeley, R., J. Klemaszewski, R. Wagner, and the Galileo Imaging Team (2000a), Galileo views of the geology of Callisto, *Planet. & Space Sci.*, 48, 829–853.
- Greeley, R., et al. (2004a), *Report of the NASA Science Definition Team for the Jupiter Icy Moons Orbiter (JIMO)*, NASA.
- Greeley, R., C. F. Chyba, J. W. Head III, T. B. McCord, W. B. McKinnon, R. T. Pappalardo, and P. H. Figueredo (2004b), in *Jupiter - The Planet, Satellites and Magnetosphere*, F. Bagenal, W. B. McKinnon, and T. E. Dowling (Eds.), pp. 329–362, Cambridge Univ. Press.
- Hand, K. P., C. F. Chyba, R. W. Carlson, and J. F. Cooper (2006), Clathrate hydrates of oxidants in the ice shell of Europa, *Astrobiology*, 6(3), 463–482.
- Hansen, G. B. and T. B. McCord (2004), Amorphous and crystalline ice on the Galilean satellites: a balance between thermal and radiolytic processes, *J. Geophys. Res.*, 109, doi: 10.1029/2003JE002149.
- Harrington, J., I. De Pater, S. J. Brecht, D. Deming, V. Meadows, K. Zahnle, P. D. Nicholson (2004), Lessons from Shoemaker-Levy 9 about Jupiter and planetary impacts, in *Jupiter: The Planet, Satellites and Magnetosphere*, (Bagenal, Dowling and McKinnon, Eds.) Cambridge Univ. Press. Cambridge, UK, pp. 159–184.
- Hibbitts, C. A., J. E. Klemaszewski, T. B. McCord, G. B. Hansen, R. Greeley (2002), CO₂-rich impact craters on Callisto, *J. Geophys. Res.*, 107, E10, 5084.
- Ingersoll, A. P., T. E. Dowling, P. J. Gierasch, G. S. Orton, P. L. Read, A. Sánchez-Lavega, A. P. Showman, A. A. Simon-Miller, A. R. Vasavada (2004), Dynamics of Jupiter's atmosphere, in *Jupiter: The Planet, Satellites and Magnetosphere*, (Bagenal, Dowling and McKinnon, Eds.) Cambridge Univ. Press. Cambridge, UK, pp. 105–128.
- Jaeger, W. L., E. P. Turtle, L. P. Keszthelyi, J. Radebaugh, A. S. McEwen, and R. T. Pappalardo (2003), Orogenic tectonism on Io, *J. Geophys. Res.*, 108, E8, 12-1, DOI 10.1029/2002JE001946.
- Jewitt, D. C., S. Sheppard, and C. Porco (2004), Jupiter's outer satellites and Trojans, in *Jupiter - The Planet, Satellites and Magnetosphere*, F. Bagenal, W. B. McKinnon, and T. E. Dowling (Eds.), pp. 263–280, Cambridge Univ. Press.
- Johnson, R. E., R. W. Carlson, J. F. Cooper, C. Paranicas, M. H. Moore, and M. Wong, Radiation Effects on the Surfaces of the Galilean Satellites (2004), in *Jupiter - The Planet, Satellites and Magnetosphere*, F. Bagenal, W. B. McKinnon, and T. E. Dowling (Eds.), pp. 485–512, Cambridge Univ. Press.
- Jun, I., H. B. Garrett, R. Swimm, R. W. Evans, and G. Clough (2005), Statistics of the variations of the high-energy electron population between 7 and 28 jovian radii as measured by the Galileo spacecraft, *Icarus*, 178, 386–394.
- Khurana, K. K., M. G. Kivelson, D. J. Stevenson, G. Schubert, C. T. Russell, R. J. Walker, and C. Polanskey (1998), Induced magnetic fields as evidence for subsurface oceans in Europa and Callisto, *Nature*, 395 (6704), 777–780.
- Khurana, K. K., M. G. Kivelson, V. M. Vasyliunas, N. Krupp, J. Woch, A. Lagg, B. H. Mauk, and W. S. Kurth (2004), The configuration of Jupiter's magnetosphere, in *Jupiter - The Planet, Satellites and Magnetosphere*, F. Bagenal, W. B. McKinnon, and T. E. Dowling (Eds.), pp. 593–616, Cambridge Univ. Press.
- Khurana, K., R. T. Pappalardo, N. Murphy, and T. Denk (2007), The origin of Ganymede's polar caps, *Icarus*, in press.
- Kivelson, M. G., K. K. Khurana, C. T. Russell, R. J. Walker, J. Warnecke, F. V. Coroniti, C. Polanskey, D. J. Southwood, and G. Schubert (1996), Discovery of Ganymede's magnetic field by the Galileo spacecraft, *Nature*, 384, 537–541.

- Kivelson, M. G., K. K. Khurana, D. J. Stevenson, L. Bennett, S. Joy, C. T. Russell, R. J. Walker, and C. Polanskey (1999), Europa and Callisto: induced or intrinsic fields in a periodically varying plasma environment, *J. Geophys. Res.*, 104, 4609–4625.
- Kivelson, M. G., K. K. Khurana, C. T. Russell, M. Volwerk, R. J. Walker, and C. Zimmer (2000), Galileo magnetometer measurements: a stronger case for a subsurface ocean at Europa, *Science*, 289, 1340–1343.
- Kivelson, M. G., K. K. Khurana, and M. Volwerk (2002), The Permanent and Inductive Magnetic Moments of Ganymede, *Icarus*, 157, 507–522.
- Kivelson, M. G., F. Bagenal, W. S. Kurth, F. M. Neubauer, C. Paranicas, and J. Saur (2004), Magnetospheric interactions with satellites, in *Jupiter - The Planet, Satellites and Magnetosphere*, F. Bagenal, W. B. McKinnon, and T. E. Dowling (Eds.), pp. 513–536, Cambridge Univ. Press.
- Kliore, A. J., A. Anabtawi, R. G. Herrera, S. W. Asmar, A. F. Nagy, D. P. Hinson, and F. M. Flasar (2002), ionosphere of Callisto from Galileo radio occultation observations, *J. Geophys. Res. (Space Physics)*, 107, A11, pp. SIA 19-1, DOI 10.1029/2002JA009365.
- Krupp, N., et al. (2004), Dynamics of the Jovian magnetosphere, in *Jupiter - The Planet, Satellites and Magnetosphere*, F. Bagenal, W. B. McKinnon, and T. E. Dowling (Eds.), pp. 617–638, Cambridge Univ. Press.
- Leblanc, F., A. E. Potter, R. M. Killen, and R. E. Johnson (2005), Origins of Europa Na cloud and torus, *Icarus*, 178, 367–385.
- Leovy, C. B., A. J. Friedson, and G. S. Orton (1991), The quasiquadrennial oscillation of Jupiter's equatorial stratosphere, *Nature*, 354, 380–382.
- Little, B., C. D. Anger, A. P. Ingersoll, A. R. Vasavada, D. A. Senske, H. H. Breneman, and W. J. Borucki, The Galileo SSI Team (1999), Galileo Images of Lightning on Jupiter, *Icarus*, 142, 306–323.
- Lopes, R. M. C. and D. A. Williams (2005), Io after Galileo, *Reports on Progress in Physics*, 68, 303–340.
- Lopes, R. M. and J. R. Spencer (2007), *Io After Galileo: A New View of Jupiter's Volcanic Moon*, Cambridge Planetary Science Series, Cambridge University Press, Cambridge, UK, 342 pp.
- Malin, M. C. and D. C. Pieri (1986), Europa, in *Satellites*, Tucson, AZ, University of Arizona Press, 1986, p. 689–717.
- McCord, T. B., et al. (1998), Non-water-ice constituents in the surface material of the icy Galilean satellites from the Galileo Near Infrared Mapping Spectrometer investigation, *J. Geophys. Res.*, 103, 8603–8626.
- McCord, T. B., G. B. Hansen, D. L. Matson, T. V. Johnson, J. K. Crowley, F. P. Fanale, R. W. Carlson, W. D. Smythe, D. William, P. D. Martin, C. A. Hibbitts, J. C. Granahan, and A. Ocampo (1999), Hydrated salt minerals on Europa's surface from the Galileo near-infrared mapping spectrometer (NIMS) investigation, *J. Geophys. Res.*, 104, E5, 11827–11852.
- McEwen, A. S., L. P. Keszthelyi, R. Lopes, P. M. Schenk, and J. R. Spencer (2004), The lithosphere and Surface of Io, in *Jupiter: The Planet, Satellites and Magnetosphere*, F. Bagenal, T. Dowling, and W. McKinnon, eds., Cambridge Planetary Science Series, Cambridge University Press, Cambridge, UK, pp. 307–328.
- McGrath, M. A., E. Lellouch, D. F. Strobel, P. D. Feldman, and R. E. Johnson (2004), Satellite atmospheres, in *Jupiter - The Planet, Satellites and Magnetosphere*, F. Bagenal, W. B. McKinnon, and T. E. Dowling (Eds.), pp. 457–483, Cambridge Univ. Press.
- McKinnon, W. B. and E. M. Parmentier (1986), Ganymede and Callisto, in *Satellites*, Tucson, AZ, University of Arizona Press, 1986, p. 718–763.
- Moore, W. B. (2001), The Thermal State of Io, *Icarus*, 154, 2, 548–550.
- Moore, W. B., G. Schubert, J. D. Anderson and J. R. Spencer (2007), The Interior of Io, in *Io After Galileo* (Eds. R. M. C. Lopes and J. R. Spencer), pp. 89–105, Springer-Praxis.
- Moore, J. M., et al. (1999), Mass movement and landform degradation on the icy

- Galilean satellites: Results of the Galileo nominal mission, *Icarus*, 140, 294–312.
- Moore, J. M., E. Asphaug, M. J. S. Belton, B. Bierhaus, H. H. Breneman, S. M. Brooks, C. R. Chapman, F. C. Chuang, G. C. Collins, B. Giese, R. Greeley, J. W. Head, S. Kadel, K. P. Klaasen, J. E. Klemaszewski, K. P. Magee, J. Moreau, D. Morrison, G. Neukum, R. T. Pappalardo, C. B. Phillips, P. M. Schenk, D. A. Senske, R. J. Sullivan, E. P. Turtle, and K. Williams (2001), Impact Features on Europa: Results of the Galileo Europa Mission (GEM), *Icarus*, 151, 93–111.
- Moore, J. M., et al. (2004), Callisto, in *Jupiter - The Planet, Satellites and Magnetosphere*, F. Bagenal, W. B. McKinnon, and T. E. Dowling (Eds.), pp. 397–426, Cambridge Univ. Press.
- Moses, J. I., T. Fouchet, B. Bézard, G. R. Gladstone, E. Lellouch, and H. Feuchtgruber (2005), Photochemistry and diffusion in Jupiter's stratosphere: Constraints from ISO observations and comparisons with other giant planets, *J. Geophys. Res.*, 110, E8, 10.1029/2005JE002411.
- Moses, J. I., T. Fouchet, R. V. Yelle, A. J. Friedson, S. G. Orton, B. Beard, P. Drossart, G. R. Gladstone, T. Kostiuik, and T. A. Livengood (2004), The stratosphere of Jupiter, in *Jupiter: The Planet, Satellites and Magnetosphere*, (Bagenal, Dowling and McKinnon, Eds.) Cambridge Univ. Press. Cambridge, UK, pp. 129–158.
- Mosqueira, I. and P. R. Estrada (2003), Formation of the regular satellites of giant planets in an extended gaseous nebula I: subnebula model and accretion of satellites, *Icarus*, 163, 198–231.
- Murchie, S. L., J. W. Head, and J. B. Plescia (1989), Crater densities and crater ages of different terrain types on Ganymede, *Icarus*, 81, 271–297.
- Nash, D. B., C. F. Yoder, M. H. Carr, J. Gradie, D. M. Hunten (1986), Io, in *Satellites*, Tucson, AZ, University of Arizona Press, 629–688.
- Neubauer, F. (1998), Planetary science—oceans inside Jupiter's moons, *Nature*, 395, 749.
- O'Reilly, T. C. and G. F. Davies (1981), Magma transport of heat on Io - A mechanism allowing a thick lithosphere, *Geophys. Res. Lett.*, 8, 313–316.
- Orton, G. S. and 15 co-authors (1998), Characteristics of the Galileo Probe entry site from earth-based remote sensing observations, *J. Geophys. Res.*, 103, 22791–22814.
- Ostro, S. J. et al. (1992), Europa, Ganymede, and Callisto: New radar results from Arecibo and Goldstone, *J. Geophys. Res.*, 97, 18227.
- Ott, M.N. (1998), Fiber optic cable assemblies for space flight: II. Thermal and radiation effects, *Proceedings of the SPIE*, v. 3440, pp. 37–46.
- Palguta, J., J. D. Anderson, G. Schubert, and W. B. Moore (2006), Mass Anomalies on Ganymede, *Icarus*, 180, 428–441.
- Pappalardo, R. T., J. W. Head, R. Greeley, R. J. Sullivan, C. Pilcher, G. Schubert, W. B. Moore, M. H. Carr, J. M. Moore, M. J. S. Belton, and D. L. Goldsby (1998a), Geological evidence for solid-state convection in Europa's ice shell, *Nature*, 391, 365.
- Pappalardo, R. T., J. W. Head, G. C. Collins, R. L. Kirk, G. Neukum, J. Oberst, B. Giese, R. Greeley, C. R. Chapman, P. Helfenstein, J. M. Moore, A. McEwen, B. R. Tufts, D. A. Senske, H. H. Breneman, and K. K. Klaasen (1998b), Grooved Terrain on Ganymede: First Results from Galileo High-Resolution Imaging, *Icarus*, 135, 276–302.
- Pappalardo, R. T., M. J. S., Belton, H. H. Breneman, M. H. Carr, C. R. Chapman, G. C. Collins, T. Denk, S. Fagents, P. E. Geissler, B. Giese, R. Greeley, R. Greenberg, J. W. Head, P. Helfenstein, G. Hoppa, S. Kadel, K. P. Klaasen, J. E. Klemaszewski, K. Magee, A. S. McEwen, J. M. Moore, W. B. Moore, G. Neukum, C. B. Phillips, L. M. Prockter, G. Schubert, D. A. Senske, R. J. Sullivan, B. R. Tufts, E. P. Turtle, R. Wagner, and K. K. Williams (1999), Does Europa have a subsurface ocean? Evaluation of the geological evidence, *J. Geophys. Res.*, 104, E10, 24015–24056.

- Pappalardo, R. T., et al. (2004), Geology of Ganymede, in *Jupiter - The Planet, Satellites and Magnetosphere*, F. Bagenal, W. B. McKinnon, and T. E. Dowling (Eds.), pp. 363–396, Cambridge Univ. Press.
- Parmentier, E. M., S. W. Squyres, J. W. Head, and M. L. Allison (1982), The tectonics of Ganymede, *Nature*, 295, 290–293.
- Porco, C. and 23 co-authors (2003), Cassini imaging of Jupiter's atmosphere, satellites and rings, *Science*, 299, 1541–1547.
- Prockter, L. M., J. W. Head, R. T. Pappalardo, D. A. Senske, G. Neukum, R. Wagner, U. Wolf, J. Oberst, B. Giese, J. M. Moore, C. R. Chapman, P. Helfenstein, R. Greeley, H. H. Breneman, and M. J. S. Belton (1998), Dark Terrain on Ganymede: Geological Mapping and Interpretation of Galileo Regio at High Resolution, *Icarus*, 135, 317–344.
- Pryor, W. R., et al. (2005), Cassini UVIS observations of Jupiter's auroral variability, *Icarus*, 178, 312–326.
- Salyk, C., A. P. Ingersoll, J. Lorre, A. Vasavada, and A. D. Del Genio (2006), Interaction between eddies and mean flow in Jupiter's atmosphere: Analysis of Cassini imaging data, *Icarus*, 185, 430–442.
- Saur, J., F. M. Neubauer, J. E. P. Connerney, P. Zarka, and M. G. Kivelson (2004) Plasma interaction of Io with its plasma torus, in *Jupiter - The Planet, Satellites and Magnetosphere*, F. Bagenal, W. B. McKinnon, and T. E. Dowling (Eds.), pp. 537–560, Cambridge Univ. Press.
- Schenk, P. M. and M. H. Bulmer (1998), Origin of Mountains on Io by Thrust Faulting and Large-Scale Mass Movements, *Science*, 279, 1514.
- Schenk, P. M., C. R. Chapman, K. Zahnle, and J. M. Moore (2004), Ages and interiors: the cratering record of the Galilean satellites, in *Jupiter - The Planet, Satellites and Magnetosphere*, F. Bagenal, W. B. McKinnon, and T. E. Dowling (Eds.), pp. 427–456, Cambridge Univ. Press.
- Schubert, G., T. Spohn, and R. T. Reynolds, (1986), Thermal histories, compositions and internal structures of the moons of the solar system, in *Satellites*, Tucson, AZ, University of Arizona Press, 224–292.
- Schubert, G., K. Zhang, M. G. Kivelson, and J. D. Anderson (1996), The magnetic field and internal structure of Ganymede, *Nature*, 384, 544–545.
- Schubert, G., J. D. Anderson, T. Spohn, and W. B. McKinnon (2004), Interior composition, structure, and dynamics of the Galilean satellites, in *Jupiter: The Planet, Satellites and Magnetosphere*, F. Bagenal, T. Dowling, and W. McKinnon (Eds.), Cambridge Planetary Science Series, Cambridge University Press, Cambridge, UK, pp. 281–306 pp.
- Shoemaker, E. M., B. K. Lucchitta, J. B. Plescia, S. W. Squyres, and D. E. Wilhelms (1982), The geology of Ganymede, in *Satellites of Jupiter* (D. Morrison, Ed.), pp. 435–520, Univ. of Arizona Press, Tucson.
- Showman, A. P. and R. Malhotra (1997), Tidal Evolution into the Laplace Resonance and the Resurfacing of Ganymede, *Icarus*, 127, 93–111.
- Showman, A. P., I. Mosqueira, and J. W. Head (2004), On the resurfacing of Ganymede by liquid-water volcanism, *Icarus*, 172, 625–640.
- Showman, A. P., P. J. Gierasch, and Y. Lian (2006), Deep zonal winds can result from shallow driving in a giant-planet atmosphere, *Icarus*, 182, 513–526.
- Simon-Miller, A. A., N. L. Chanover, G. S. Orton, M. Sussman, and E. Karkoschka (2006), Jupiter's white oval turns red, *Icarus*, 185, 558–562.
- Smith, B. A., and the Voyager Imaging Team (1979a), The Jupiter system through the eyes of Voyager 1, *Science*, 204, 951–972.
- Smith, B. A., and the Voyager Imaging Team (1979b), The Galilean Satellites and Jupiter: Voyager 2 imaging science results, *Science*, 206, 927–950.
- Space Studies Board, (2000) *Preventing the Forward Contamination of Europa*, National Academy Press, Washington, DC.
- Spencer, J. R. (1987), Thermal segregation of water ice on the Galilean satellites, *Icarus*, 69, 297–313.
- SSES, Solar System Exploration Survey (2003), Space Studies Board, National

- Research Council, (2003) *New Frontiers in the Solar System: An Integrated Exploration Strategy*, National Academy Press, Washington, DC.
- Strobel, D. F., J. Saur, P. D. Feldman, and M. A. McGrath (2002), Hubble Space Telescope Space Telescope Imaging Spectrograph Search for an Atmosphere on Callisto: A Jovian Unipolar Inductor, *The Astrophysical Journal*, 581, L51–L54.
- Takahashi, S., H. Misawa, H. Nozawa, A. Morioka, S. Okano, and R. Sood (2005), Dynamic features of Io's extended sodium distributions, *Icarus*, 178, 346–359.
- Taylor, F. W., S. K. Atreya, T. Encrenaz, D. M. Hunten, P. J. G. Irwin, T. C. Owen (2004), The composition of the atmosphere of Jupiter, in *Jupiter: The Planet, Satellites and Magnetosphere*, (Bagenal, Dowling and McKinnon, Eds.) Cambridge, Univ. Press. Cambridge, UK, pp. 59–78.
- Thomas, N., F. Bagenal, T. W. Hill, and J. K. Wilson (2004), The Io neutral clouds and plasma torus, in *Jupiter - The Planet, Satellites and Magnetosphere*, F. Bagenal, W. B. McKinnon, and T. E. Dowling (Eds.), pp. 561–591, Cambridge Univ. Press.
- Turtle, E. P., W. L. Jaeger, L. P. Keszthelyi, A. S. McEwen, M. Milazzo, J. Moore, C. B. Phillips, J. Radebaugh, D. Simonelli, F. Chuang, P. Schuster, and Galileo SSI Team (2001), Mountains on Io: High-resolution Galileo observations, initial interpretations, and formation models, *J. Geophys. Res.*, 106, E12, 33175–33200.
- Veeder, G. J., D. L. Matson, T. V. Johnson, A. G. Davies, and D. L. Blaney (2004), The polar contribution to the heat flow of Io, *Icarus*, Volume 169, 264–270.
- Vincent, M. and 18 co-authors (2000), Jupiter's polar regions in the ultraviolet as imaged by HST/WFPC2: Auroral-aligned features and zonal motions, *Icarus*, 143, 205–222.
- West, R. A., K. H. Baines, A. J. Friedson, D. Banfield, B. Ragent, and R. W. Taylor (2004), Jovian clouds and haze, in *Jupiter: The Planet, Satellites and Magnetosphere*, (Bagenal, Dowling and McKinnon, Eds.) Cambridge Univ. Press. Cambridge, UK, pp. 79–104.
- Wienbruch, U. and T. Spohn (1995), A self sustained magnetic field on Io?, *Planetary and Space Science*, 43, 1045–1057,
- Yelle, R. V., L. A. Young, R. J. Vervack, R. Young, L. Pfister, and B. R. Sandel (1996), Structure of Jupiter's upper atmosphere: Predictions for Galileo, *J. Geophys. Res.*, 101, 2149–2162.
- Yelle, R. V. and S. Miller (2004), Jupiter's thermosphere and ionosphere, in *Jupiter: The Planet, Satellites and Magnetosphere*, (Bagenal, Dowling and McKinnon, Eds.) Cambridge Univ. Press. Cambridge, UK, pp. 185–218.
- Yoder, C. F. and S. J. Peale (1981), The tides of Io, *Icarus*, 47, 1–35
- Young, R.E. (2003), The Galileo probe: how it has changed our understanding of Jupiter, *New Astronomy Reviews*, 47,1, 1–51.
- Vasavada, A. R. and A. Showman (2005), Jovian atmospheric dynamics: an update after Galileo and Cassini, *Reports on Progress in Physics*, 68, 8, 1935–1996.
- Zahnle, K., P. Schenk, H. Levison, and L. Dones (2003), Cratering rates in the outer Solar System, *Icarus*, 163, 263–289.
- Zimmer, C., K. K. Khurana, and M. G. Kivelson (2000), Subsurface oceans on Europa and Callisto: constraints from Galileo magnetometer observations, *Icarus*, 147, 329–347.

C. SCIENCE VALUE SUPPORTING DETAIL

This Appendix establishes the detailed measurements for each of the JSO Investigations identified in **FO-1** of §2.2. Within each theme group (Jupiter Atmosphere, Magnetosphere, Satellites and Interiors), the objectives and investigations are in priority order. For the Satellites group, the objectives and investigations for each target are prioritized separately. Based on the requirements for specific measurements, notional instrument types are identified that would achieve each measurement. The planning payloads for the baseline and descoped mission concepts will be seen to have varying ability to achieve each indicated measurement.

The SDT evaluated the potential science value of the baseline and the descoped payloads based on their ability to achieve each measurement. A scale from 0-Not Applicable to 5-Excellent was used to make this evaluation.

Contents

Foldout C1. Jupiter Atmosphere	C-2
Foldout C2. Magnetosphere	C-7
Foldout C3a. Satellites—Io	C-11
Foldout C3b. Satellites—Europa	C-14
Foldout C3c. Satellites—Ganymede	C-17
Foldout C3d. Satellites—Callisto	C-19
Foldout C3e. Satellites—Rings and Small Satellites	C-21
Foldout C4. Interiors	C-22

Foldout C1. Jupiter Atmosphere

GOAL	OBJECTIVE	INVESTIGATION	MEASUREMENT	Instrument Type	Baseline Pavload Science Value	Descoped Payload Science Value
		Understand the processes that maintain the composition, structure and dynamics of the Jovian atmosphere as a Type Example of a Gas Giant Planet				
		Study the composition, structure, chemistry, and dynamics of Jupiter's atmosphere				
		Study atmospheric dynamics at scales ranging from less than one scale height to the planetary scale				
			Image the atmosphere at high spatial resolution (10 km/pixel) and frequent temporal (20 min-1day) sampling to characterize the winds/cloud patterns of zonal jets, vortices, eddies, and their interactions. [This will provide an unprecedented climate database that will help determine whether eddies pump momentum upgradient into the jets, and it will provide constraints on the structure below the clouds, etc.]	Hi-res (<10 mrad/pixel) camera	5	5
			Measure the dynamics of individual thunderstorms and cloud features over their life cycles at a resolution of 10 km/ pixel with a sampling rate of 1000 sec. Requires near-uv, visible and near-IR imaging in at least two broad bands which sense the atmosphere at different levels, e.g. 255 nm, 893 nm or 2.3 microns to sense at high altitude, and wavelengths inbetween methane bands to sense the continuum.	Hi-res (<10 mrad/pixel) color camera	5	5
			Measure the water variability at and above the clouds with global coverage and 100 km spatial resolution. Use 5-micron imaging spectroscopy with spectral resolution R > 3000	Hyperspectral imager	5	5
			Measure the 3-D gaseous ammonia distribution with 5000 km horizontal spatial resolution at 1-5 bars and 200 km resolution at .01-.5 bars. Use 5-micron imaging spectroscopy with spectral resolution R>3000, mid-IR (10 microns) imaging spectroscopy for the .1 to .5 bar region, R > 1000.	Hyperspectral imager Thermal imaging spectrometer	4	4
			Use submillimeter sounding in the 0.5-2 mm range to sense the .5 to 2-bar region.	Submm sounder	4	4
			Passive microwave radiometry at 1-5 cm wavelength, possibly using the telecom antenna as a receiver for 1- 5-bar region	Mircowave radiometer	0	0
			Measure the poleward eddy heat flux from simultaneous maps of wind and temperature at horizontal scales of 100 km or better. At 7-8 microns, R > 1000. At 14-40 microns, R > 50	Moderate-res (<0.1 mrad/pixel) thermal imaging spectrometer	5	5
			Obtain global temperature maps for vertical temperature structure and horizontal gradients (for deriving thermal wind shears). Pressure range 1-10,100–500 mbar. with global coverage and horizontal scale of 20-40 km at the limb, 100 km global	Moderate-res (<0.1 mrad/pixel) thermal imaging spectrometer	5	5
			Obtain global temperature maps for vertical temperature structure and waves. Mid-IR (10 microns) imaging spectroscopy , R > 1000. Limb sensing with full latitudinal coverage and horizontal scale of 20-40 km at the limb. Pressure range 10-100 mbar.	Hi-res (<40 mrad/pixel) thermal imager	2	2
		Study the temperature and energy balance of the planet to improve our understanding of the relative roles of radiative solar radiative heating, winds and eddies in driving atmospheric circulation and convection				
			Measure repeated radio occultations to obtain vertical temperature profiles closely spaced in space and time (e.g. at the same latitude +/-10 degrees, once every 2 weeks) to investigate wave propagation in the stratosphere and upper troposphere	Dual-frequency radio transmitter with USO	5	5
			Radio occultations over a wide range of latitudes to obtain high vertical resolution temperature structure in the upper troposphere and lower to middle stratosphere, filling in vertical structure information for remote sensing of various latitudes and longitudes.	Dual-frequency radio transmitter with USO	5	5
			Stellar and solar occultations over a wide range of latitudes to obtain high vertical resolution temperature structure and composition in the upper stratosphere (1-km at 20 K per measurement).	UV spectrometer	5	5
		Study Jupiter's clouds and hazes.				
			Retrieve global and regional cloud vertical structure from 0.1 to 5 bars. Requires simultaneous visible and near IR spectral imaging with comparable spatial resolutions, to best identify the locations and composition of the clouds. Resolution sufficient to resolve molecular absorption bands (R > 300). Middle IR spectral imaging (~8 micron) with R > 1000. Far IR spectral imaging with R > 500.	Multispectral camera Hyperspectral imager Thermal imaging spectrometer	5	5
			Measure spatial distribution of lightning at spatial resolution of 10 km, from visible or near-IR imaging	Hi-res (<10 mrad/pixel) camera	5	5
			Characterize the photochemical hazes from ultraviolet imaging, visible wavelength polarization and infrared mapping (0.3 – 5 microns) at multiple incidence angles. R ~50-500, spatial resolution of 100 km	UV camera VIS polarimeter Hyperspectral imager	4	4
			Search for direct detection of NH3, NH4SH and H2O ice signatures with spatial resolution of 10 km. Requires near through far-IR mapping, R ~20-500	Hi-res hyperspectral imager Hi-res (<10 mrad/pixel) thermal imager	3	3
		Study the composition and chemistry of Jupiter's atmosphere to understand sources and sinks, and dynamics from disequilibrium species				
			Measure the 3-D distribution of disequilibrium species: PH3, CO, AsH3, GeH4 at 5 microns at 100-km resolution and R>3000. PH3, CO using mid and far-IR wavelengths at 100 km resolution. R > 2000-5000	Thermal imaging spectrometer	4	4
			Measure the para H2 fraction above the visible clouds. Requires 17 - 35 micron mapping with 100 km spatial resolution and R > 100	Thermal imager	3	3
			Measure the 3-D distribution of hydrocarbon and other molecules in the stratosphere, particularly water, at 100 km spatial resolution with global coverage and spectral resolution R > 10000 in the mid-IR (8-16 microns). Limb spectroscopy with 20-40 km vertical spatial resolution for vertical distribution	Hi-res (<20 mrad/pixel) thermal hyperspectral imager	2	2
		Study the auroral emissions and dynamic effects of the magnetosphere on the upper atmosphere				
			Floor field and plasma measurements	Magnetometer, plasma spectrometer	5	5
			Measure Jovian aurora at IR, UV wavelengths continuously while making direct measurements of the magnetosphere	X-ray imager	4	4

GOAL	OBJECTIVE	INVESTIGATION	MEASUREMENT	Instrument Type	Baseline Pavload Science Value	Descoped Payload Science Value
				UV imager IR imager Radio receiver		
	<i>Study the structure and dynamics of the Jovian magnetosphere, including processes that generate Jupiter's aurora</i>					
		Determine the coupling of magnetosphere/ionosphere/atmosphere				
			Measure Jovian aurora at IR, UV,wavelengths continuously while making direct measurements of the magnetosphere	X-ray imager UV imager IR imager Radio receiver	3	3
	<i>Characterize the spatial distribution and temporal variability of minor atmospheric species to understand Jupiter's origin and present state</i>					
		Determine the bulk abundance of water in the deep atmosphere				
			Measure the water below the clouds with global coverage and 100 km spatial resolution. Use 5-micron imaging spectroscopy with spectral resolution R > 3000	Hyperspectral imager	5	5
		Determine the 3-D concentrations of the condensable gases water and ammonia and disequilibrium species				
			Measure the water variability below the clouds with global coverage and 100 km spatial resolution. Use 5-micron imaging spectroscopy with spectral resolution R > 3000	Hyperspectral imager	5	5
			Measure the 3-D gaseous ammonia distribution with 5000 km horizontal spatial resolution at 1-5 bars and 200 km resolution at 0.01-0.5 bars. Use 5-micron imaging spectroscopy with spectral resolution R>3000, mid-IR (10 microns) imaging spectroscopy for the 0.1 to 0.5 bar region, R > 1000.	Hyperspectral imager Thermal imaging spectrometer	5	5
			Use submillimeter sounding in the 0.5-2 mm range to sense the 0.5 to 2-bar region.	Submm sounder	4	4
			Passive microwave radiometry at 1-5 cm wavelength, possibly using the telecom antenna as a receiver for 1- 5-bar region	Mircowave radiometer	0	0
			Measure the 3-D distribution of disequilibrium species: PH ₃ , CO, AsH ₃ , GeH ₄ at 100-km resolution. Measure PH ₃ , CO, AsH ₃ , GeH ₄ at 5 microns with R>3000. PH ₃ , CO using mid and far-IR wavelengths with R > 2000-5000	Hyperspectral imager in 4.8-5.3 micron region	4	4
			Measure the para H ₂ fraction above the visible clouds. Requires 17 - 35 micron mapping with 100 km spatial resolution and R > 100	Mid-IR spectrometer	4	4
			Measure the 3-D distribution of hydrocarbons and other molecules in the stratosphere, particularly water, at 100 km spatial resolution with global coverage. Spectral resolution R > 1000 in the mid-IR (8-16 microns).	Med-res (<100 mrad/pixel) thermal hyperspectral imager	3	3
			Measure the 3-D distribution of hydrocarbons and other molecules in the stratosphere, particularly water, with full latitudinal coverage. Spectral resolution R > 1000 in the mid-IR (8-16 microns). Limb spectroscopy with 20-40 km vertical spatial resolution for vertical distribution	Hi-res (<20 mrad/pixel) thermal hyperspectral imager	3	3
			Stellar and solar occultations over a wide range of latitudes to obtain high vertical resolution temperature structure and composition in the upper stratosphere (1-km at 20 K per measurement).	UV spectrometer	5	5
	<i>Characterize Jupiter's clouds and hazes and the processes that maintain them</i>					
		Determine the height, composition, optical thickness, and particle size distribution of clouds and hazes				
			Image the atmosphere at high spatial resolution (10 km/pixel) and frequent temporal (20 min-1day) sampling and multiple wavelengths to sound many pressure levels	Hi-res (<10 mrad/pixel) color camera	5	5
			Radio occultations over a wide range of latitudes to obtain high vertical resolution temperature structure in the upper troposphere and lower to middle stratosphere, filling in vertical structure information for remote sensing of various latitudes and longitudes.	Dual-frequency radio transmitter with USO	5	5
			Stellar and solar occultations over a wide range of latitudes to obtain high vertical resolution temperature structure and composition in the upper stratosphere (1-km at 20 K per measurement).	UV spectrometer	5	5
		Determine the concentrations of condensable atmospheric gases				
			Measure the 3-D gaseous ammonia distribution with 5000 km horizontal spatial resolution at 1-5 bars and 200 km resolution at 0.01-0.5 bars. Use 5-micron imaging spectroscopy with spectral resolution R>3000, mid-IR (10 microns) imaging spectroscopy for the 0.1 to 0.5 bar region, R > 1000.	Hyperspectral imager Thermal imaging spectrometer	4	4
			Use submillimeter sounding in the 0.5-2 mm range to sense the 0.5 to 2-bar region.	Submm sounder	4	4
			Passive microwave radiometry at 1-5 cm wavelength, possibly using the telecom antenna as a receiver for 1- 5-bar region	Mircowave radiometer	0	0
			Measure the water variability below the clouds with global coverage and 100 km spatial resolution. Use 5-micron imaging spectroscopy with spectral resolution R > 3000	Hyperspectral imager	5	5
	<i>Understand the processes that maintain the hot thermosphere</i>					
		Characterize the vertical structure of the thermosphere and its spatial and temporal variability				
			Obtain global temperature maps for vertical temperature structure and horizontal gradients (for deriving thermal wind shears). Pressure range 1-10,100–500 mbar. Same spectral requirements as Meas. 10 with global coverage and horizontal scale of 20-40 km at the limb, 100 km global	Moderate-res (<0.1 mrad/pixel) thermal imaging spectrometer	5	5
			Obtain global temperature maps for vertical temperature structure and waves. Mid-IR (10 microns) imaging spectroscopy , R > 1000. Limb sensing with full latitudinal coverage and horizontal scale of 20-40 km at the limb. Pressure range 10-100 mbar.	Hi-res (<40 mrad/pixel) thermal imager	3	3

GOAL	OBJECTIVE	INVESTIGATION	MEASUREMENT	Instrument Type	Baseline Pavload Science Value	Descoped Payload Science Value
			Stellar and solar occultations over a wide range of latitudes to obtain high vertical resolution temperature structure and composition in the upper stratosphere (1-km at 20 K per measurement).	UV spectrometer	5	5
		Determine the properties and fluxes of vertically propagating waves				
			Repeated radio occultations to obtain vertical temperature profiles closely spaced in space and time (e.g. at the same latitude +/-10 degrees, once every 2 weeks) to investigate wave propagation in the stratosphere and upper troposphere	Dual-frequency radio transmitter with USO	5	5
			Stellar and solar occultations over a wide range of latitudes to obtain high vertical resolution temperature structure and composition in the upper stratosphere (1-km at 20 K per measurement).	UV spectrometer	5	5
			Image the atmosphere at high spatial resolution (10 km/pixel) and frequent temporal (20 min-1day) sampling and multiple wavelengths to sound many pressure levels	Hi-res (<10 mrad/pixel) color camera	5	5
		Characterize the atmosphere-magnetosphere interaction, including the contribution of aurorae to the thermal structure of the upper atmosphere.				
			Measure Jovian aurora at IR, UV wavelengths continuously while making direct measurements of the magnetosphere	X-ray imager UV imager IR imager Radio receiver	3	3
		Determine the latitudinal variation of solar-energy absorption and thermal radiation				
			Image the atmosphere at moderate spatial resolution (100 km/pixel), sampling to characterize the zonal mean cloud properties of clouds and their reflectivity over wavelength, emission angle and phase angle.	Hi-res (<10 mrad/pixel) color camera	5	5
			Obtain global temperature, ammonia and trace constituent maps for 100 km/pixel to model accurately the zonal mean of total thermal emission.	Moderate-res (<0.1 mrad/pixel) thermal imaging spectrometer	3	3
	Study the temperature and energy balance of the planet to improve our understanding of the relative roles of internal and solar heating in controlling the structure and dynamics of the atmosphere					
		Determine the global, 3-D temperature structure from the thermosphere to the upper troposphere				
			Obtain global temperature maps for vertical temperature structure and horizontal gradients (for deriving thermal wind shears). Pressure range 1-10,100–500 mbar. Same spectral requirements as Meas. 2 with global coverage and horizontal scale of 20-40 km at the limb, 100 km global	Moderate-res (<0.1 mrad/pixel) thermal imaging spectrometer	3	3
			Obtain global temperature maps for vertical temperature structure and waves. Mid-IR (10 microns) imaging spectroscopy , R > 1000. Limb sensing with full latitudinal coverage and horizontal scale of 20-40 km at the limb. Pressure range 10-100 mbar.	Hi-res (<40 mrad/pixel) thermal imager	1	1
			Measure repeated radio occultations to obtain vertical temperature profiles closely spaced in space and time (e.g. at the same latitude +/-10 degrees, once every 2 weeks) to investigate wave propagation in the stratosphere and upper troposphere	Dual-frequency radio transmitter with USO	5	5
			Measure stellar and solar occultations over a wide range of latitudes to obtain high vertical resolution temperature structure and composition in the upper stratosphere (1-km at 20 K per measurement).	UV spectrometer	5	5
		Determine the dynamical contributions to the latitudinal energy transport				
			Image the atmosphere at high spatial resolution (10 km/pixel) and frequent temporal (20 min-1day) sampling and multiple wavelengths to sound many pressure levels	Hi-res (<10 mrad/pixel) color camera	5	5
			Measure the poleward eddy heat flux from simultaneous maps of wind and temperature at horizontal scales of 100 km or better. At 7-8 microns, R > 1000. At 14-40 microns, R > 50	Moderate-res (<0.1 mrad/pixel) thermal imaging spectrometer	3	3
			Measure radio occultations over a wide range of latitudes to obtain high vertical resolution temperature structure in the upper troposphere and lower to middle stratosphere, filling in vertical structure information for remote sensing of various latitudes and longitudes.	Dual-frequency radio transmitter with USO	5	5
			Measure stellar and solar occultations over a wide range of latitudes to obtain high vertical resolution temperature structure and composition in the upper stratosphere (1-km at 20 K per measurement).	UV spectrometer	5	5
	Determine the processes that maintain the jet streams, polar vortex circulations, large vortices, quasi-quadrennial oscillation, and planetary-scale waves such as the hot spots, equatorial plumes, and slowly moving thermal features					
		Determine the wind speeds, temperatures, and variability of atmospheric features				
			Image the atmosphere at high spatial resolution (10 km/pixel) and frequent temporal (20 min-1day) sampling and multiple wavelengths to sound many pressure levels	Hi-res (<10 mrad/pixel) color camera	5	5
			Obtain global temperature maps for vertical temperature structure and horizontal gradients (for deriving thermal wind shears). Pressure range 1-10,100–500 mbar. Same spectral requirements as Meas. 10 with global coverage and horizontal scale of 20-40 km at the limb, 100 km global	Moderate-res (<0.1 mrad/pixel) thermal imaging spectrometer	5	5
			Obtain global temperature maps for vertical temperature structure and waves. Mid-IR (10 microns) imaging spectroscopy , R > 1000. Limb sensing with full latitudinal coverage and horizontal scale of 20-40 km at the limb. Pressure range 10-100 mbar.	Hi-res (<40 mrad/pixel) thermal imager	1	1
			Stellar and solar occultations over a wide range of latitudes to obtain high vertical resolution temperature structure and composition in the upper stratosphere (1-km at 20 K per measurement).	UV spectrometer	5	5
		Determine the latitudinal momentum and heat fluxes of waves and eddies				

GOAL	OBJECTIVE	INVESTIGATION	MEASUREMENT	Instrument Type	Baseline Pavload Science Value	Descoped Payload Science Value
			Image the atmosphere at high spatial resolution (10 km/pixel) and frequent temporal (20 min-1day) sampling and multiple wavelengths to sound many pressure levels	Hi-res (<10 mrad/pixel) color camera	5	5
			Measure the poleward eddy heat flux from simultaneous maps of wind and temperature at horizontal scales of 100 km or better. At 7-8 microns, R > 1000. At 14-40 microns, R > 50	Moderate-res (<0.1 mrad/pixel) thermal imaging spectrometer	3	3
			Radio occultations over a wide range of latitudes to obtain high vertical resolution temperature structure in the upper troposphere and lower to middle stratosphere, filling in vertical structure information for remote sensing of various latitudes and longitudes.	Dual-frequency radio transmitter with USO	5	5
			Stellar and solar occultations over a wide range of latitudes to obtain high vertical resolution temperature structure and composition in the upper stratosphere (1-km at 20 K per measurement).	UV spectrometer	5	5
		Characterize the existence, horizontal wavelengths, and speeds of small-scale atmospheric waves to constrain the vertical stability structure (Brunt-Vaisala frequency) of the upper troposphere				
			Repeated radio occultations to obtain vertical temperature profiles closely spaced in space and time (e.g. at the same latitude +-10 degrees, once every 2 weeks) to investigate wave propagation in the stratosphere and upper troposphere	Dual-frequency radio transmitter with USO	5	5
			Image the atmosphere at high spatial resolution (10 km/pixel) and frequent temporal (20 min-1day) sampling and multiple wavelengths to sound many pressure levels	Hi-res (<10 mrad/pixel) color camera	5	5
			Radio occultations over a wide range of latitudes to obtain high vertical resolution temperature structure in the upper troposphere and lower to middle stratosphere, filling in vertical structure information for remote sensing of various latitudes and longitudes.	Dual-frequency radio transmitter with USO	5	5
			Stellar and solar occultations over a wide range of latitudes to obtain high vertical resolution temperature structure and composition in the upper stratosphere (1-km at 20 K per measurement).	UV spectrometer	5	5
		Determine the concentrations of condensable atmospheric gases				
			Measure the 3-D gaseous ammonia distribution with 5000 km horizontal spatial resolution at 1-5 bars and 200 km resolution at 0.01-0.5 bars. Use 5-micron imaging spectroscopy with spectral resolution R>3000, mid-IR (10 microns) imaging spectroscopy for the 0.1 to 0.5 bar region, R > 1000.	Hyperspectral imager Thermal imaging spectrometer	4	4
			Use submillimeter sounding in the 0.5-2 mm range to sense the 0.5 to 2-bar region.	Submm sounder	4	4
			Passive microwave radiometry at 1-5 cm wavelength, possibly using the telecom antenna as a receiver for 1- 5-bar region	Mircowave radiometer	0	0
			Measure the water variability below the clouds with global coverage and 100 km spatial resolution. Use 5-micron imaging spectroscopy with spectral resolution R > 3000	Hyperspectral imager	5	5
		Characterize the morphology, spatial distribution, and role of thunderstorms and small-scale waves and eddies in driving the large-scale circulation				
			Determine the occurrence frequency, locations, pressures, and temporal evolution of thunderstorms			
			Near-UV, visible and near-IR imaging in at least two broad bands which sense the atmosphere at different levels, e.g. 255 nm, 893 nm or 2.3 microns to sense at high altitude, and wavelengths in between methane bands to sense the continuum. Measurements must achieve 10 km/pixel and sample individual storms at 20-min intervals over storm life cycles	Hi-res (<10 mrad/pixel) UV camera Hi-res (<10 mrad/pixel) VIS camera Hi-res (<10 mrad/pixel) IR camera	5	5
			Measure the water variability below the clouds with global coverage and 100 km spatial resolution. Use 5-micron imaging spectroscopy with spectral resolution R > 3000	Hyperspectral imager	5	5
		Determine the occurrence frequency, locations, amplitude, spectrum, and depth of lightning				
			Image the atmosphere at high spatial resolution (10 km/pixel) and frequent temporal (20 min-1day) sampling and multiple wavelengths spanning H-alpha, H-beta, etc.	Hi-res (<10 mrad/pixel) color camera	5	5
		Determine the latitudinal momentum and heat fluxes of waves and eddies				
			Image the atmosphere at high spatial resolution (10 km/pixel) and frequent temporal (20 min-1day) sampling and multiple wavelengths to sound many pressure levels	Hi-res (<10 mrad/pixel) color camera	5	5
			Measure the poleward eddy heat flux from simultaneous maps of wind and temperature at horizontal scales of 100 km or better. At 7-8 microns, R > 1000. At 14-40 microns, R > 50	Moderate-res (<0.1 mrad/pixel) thermal imaging spectrometer	3	3
			Radio occultations over a wide range of latitudes to obtain high vertical resolution temperature structure in the upper troposphere and lower to middle stratosphere, filling in vertical structure information for remote sensing of various latitudes and longitudes.	Dual-frequency radio transmitter with USO	5	5
			Stellar and solar occultations over a wide range of latitudes to obtain high vertical resolution temperature structure and composition in the upper stratosphere (1-km at 20 K per measurement).	UV spectrometer	5	5
		Understand the structure and circulation of the middle and upper atmosphere				
			Determine the global, 3-D temperature structure, radiative heating rates, and wind speeds from the thermosphere to the upper troposphere			
			Repeated radio occultations to obtain vertical temperature profiles closely spaced in space and time (e.g. at the same latitude +-10 degrees, once every 2 weeks) to investigate wave propagation in the stratosphere and upper troposphere	Dual-frequency radio transmitter with USO	5	5
			Obtain global temperature maps for vertical temperature structure and horizontal gradients (for deriving thermal wind shears). Pressure range 1-10,100–500 mbar. Same spectral requirements as Meas. 10 with global coverage and horizontal scale of 20-40 km at the limb, 100 km global	Moderate-res (<0.1 mrad/pixel) thermal imaging spectrometer	5	5

GOAL	OBJECTIVE	INVESTIGATION	MEASUREMENT	Instrument Type	Baseline Payload Science Value	Descoped Payload Science Value
			Obtain global temperature maps for vertical temperature structure and waves. Mid-IR (10 microns) imaging spectroscopy , R > 1000. Limb sensing with full latitudinal coverage and horizontal scale of 20-40 km at the limb. Pressure range 10-100 mbar.	Hi-res (<40 mrad/pixel) thermal imager	1	1
			Stellar and solar occultations over a wide range of latitudes to obtain high vertical resolution temperature structure and composition in the upper stratosphere (1-km at 20 K per measurement).	UV spectrometer	5	5



Foldout C2. Magnetosphere

GOAL	OBJECTIVE	INVESTIGATION	MEASUREMENT	Instrument Type	Baseline Payload Science Value		Descoped Payload Science Value		
Understand the magnetospheric environments of Jupiter, its moons and their interactions					Ganymede	Other	Ganymede	Other	
	A. Moon Interior Structure. Establish internal structure of icy moons including presence and properties of putative conducting layers, measurement of higher harmonics and secular variations of Ganymede's magnetic field and set limits on intrinsic magnetic fields for Europa and Callisto								
		A1. Magnetic Field of Ganymede. Investigate and confirm presence of a conducting layer at Ganymede and deeper conducting layers by monitoring steady and time-varying magnetic configurations.							
			In-situ measurement of intrinsic and/or induced components of moon vector magnetic field at 0.05-sec time resolution in low altitude high-inclination orbit over at least 10 orbital periods of the moon	Magnetometer	5	5	3	3	
		A2. Plasma and Energetic Particle Environment of Ganymede. Investigate response of local magnetospheric plasma, energetic particle, and ionospheric environment at Ganymede to changing total and induced magnetic fields							
			In-situ measurement at 10-sec time resolution of plasma moments and directional fluxes for energetic charged particles at keV to MeV energies	Plasma Energetic Particle Detector	5	5	3	3	
		A3. Magnetic Fields of Europa and Callisto. Investigate and confirm presence of a conducting layer at Europa and Callisto and deeper conducting layers by monitoring steady and time-varying magnetic configurations.							
			In situ measurement on flyby trajectory of intrinsic and/or induced components of moon vector magnetic field.	Magnetometer	4	4	4	4	
		A4. Plasma and Energetic Particle Environment of Europa and Callisto. Investigate response of local magnetospheric plasma, energetic particle and ionospheric environment at Europa and Callisto to changing magnetic fields.							
			In-situ measurement at 10-sec time resolution of plasma moments and directional fluxes for energetic charged particles at keV to MeV energies	Plasma Energetic Particle Detector	4	4	2	2	
	B. Ganymede's Intrinsic Magnetosphere. Investigate the magnetic field, particle populations, and dynamics of Ganymede's magnetosphere.								
		B1. Magnetic Reconnection. Investigate the magnetopause to establish spatial distribution of reconnecting field lines and to characterize the spatial distribution and temporal distribution of reconnection, including possible intermittency of reconnection.							
			Measure magnetic field vectors with 0.05 s time resolution.		Magnetometer	5	5	4	4
			Measure differential directional fluxes of energetic ions and electrons		Plasma Energetic Particle Detector	5	5	3	3
			Measure the velocity space distribution of thermal plasma		Plasma Energetic Particle Detector	5	5	4	4
			Measurement of the intensity of remote radio and local plasma waves vs. frequency		Plasma Wave spectrometer	0	0	0	0
		B2. Magnetospheric structure. Investigate Ganymede's magnetospheric structure, in particular the spatial structure and energy distributions of particle populations, including time variability in response to external Jovian magnetospheric perturbations.							
			In-situ measurement of differential directional fluxes at 1-sec to 60-sec time resolution for the suprathermal and energetic particle fluxes for protons, major and minor ions, and electrons.		Plasma Energetic Particle Detector	5	5	4	4
			Measure magnetic field vectors with 0.05 s time resolution.		Magnetometer	5	5	5	5
		B3. Investigate the generation of Ganymede's aurora							
			UV imaging (0.1-0.35 microns) of Ganymede (at 0.3 nm spectral resolution) at 1 km spatial resolution and at cadences of a minute or longer.		UV Imaging Spectrometer	5	5	5	5
		B4. Surface Interaction. Investigate the modification of surface composition and structure on open vs. closed field line regions.							
			Imaging of Ganymede at FUV-NIR wavelengths (0.1-3 microns) at 1 km spatial resolution.		FUV imaging spectrometer, UV imaging spectrometer, Hyperspectral imager	5	5	5	5
		C. Moon-Magnetosphere Interactions. Determine the effect of the Jovian magnetosphere on the icy moons. Understand effects of the moons on the magnetosphere and Jupiter's auroral ionosphere.							
		C1. Magnetospheric Environment. Investigate the magnetic field, plasma, energetic particle, electromagnetic, and dust distribution in the Jovian magnetosphere, at the jovicentric orbits of the moons, including spatial and temporal variations.							
			In-situ measurement at 1-minute time resolution of the magnetospheric vector magnetic field, and the plasma ion and	Magnetometer; Plasma Energetic	5	5	4	4	

GOAL	OBJECTIVE	INVESTIGATION	MEASUREMENT	Instrument Type	Baseline Pavload Science Value		Descoped Payload Science Value	
			electron velocity space distribution.	Particle Detector				
			In-situ measurement at 1-minute time resolution of energetic (10 keV to 10 MeV) charged particle fluxes with elemental mass, energy, and angle distributions for protons, major and minor heavy ions, and electrons.	Plasma Energetic Particle Detector	5	5	3	3
			In-situ measurement at 15-minute time resolution of the isotopic mass abundances of plasma and energetic ions.	Plasma Energetic Particle Detector	4	4	2	2
			In-situ measurement of high energy (> 10 MeV) protons, electrons and heavy ions	Plasma Energetic Particle Detector	5	5	2	2
		C2. Moon Environment. Investigate the changes of magnetospheric properties (the magnetic field, plasma, energetic particle, electromagnetic, and dust environments) in the near vicinity of the moons in order to establish effects of the magnetosphere on the moons and to characterize the moons as sources of gas and dust tori..						
			In-situ measurement at 1-sec to 30-sec time resolution for the major energy and compositional environment parameters including the total vector magnetic field 0.05-second time resolution), bulk plasma ion and electron moments, and energetic particle fluxes with elemental mass, energy, and angle for protons, major heavy ions including charge states, and electrons.	Magnetometer; Plasma Energetic Particle Detector	5	5	3	3
		C3. Moon Surface & Atmospheric Interaction Effects. Investigate effects of direct magnetospheric plasma, energetic particle, solar UV, and interplanetary dust interactions with the moon surfaces & atmospheres, and associated temporal variations						
			Global UV-NIR measurements (0.1-3 microns) of hemispherical distributions of radiation products (sulfates, H2O2, O2, CO2) at 10 km resolution, and via repeated observations (timescale of months)	Hyperspectral imager; UV Spectrometer	5-Ganymede	3	5-Ganymede	3
			Ultraviolet (0.1-0.35 microns) airglow measurements at 10-km resolution.	Hyperspectral imager; UV Spectrometer	5-Ganymede	3	5 -Ganymede	3
			In-situ correlation of low-energy plasma ion composition with elemental and isotopic mass resolution at 10-sec low-altitude time resolution along local magnetic lines connected to sources of sputtering in geological distinct regions of the surface at 10-km resolution.	Plasma Energetic Particle Detector; Magnetormeter; Visible imager	5-Ganymede	2	2-Ganymede	1
			Remote spot compositional imaging of selected surface features at 100-meter visible (400-meter infrared) maximum resolution with different local topographic exposures to magnetospheric irradiation to assess future landing sites and determine correlation of local composition to measured or expected total ionization dosage rate.	Hi-Res Hyperspectral Imager	4-Ganymede	2	2-Ganymede	1
			Remote spot compositional imaging of selected surface features at 100-meter visible (400-meter infrared) maximum resolution with minimum exposure to radiation for determination of measurement limits on endogenic chemical sources and signs of life.	Hi-Res Hyperspectral Imager	4-Ganymede	2	2-Ganymede	1
			In-situ measurement at 10-sec to 1-min time resolution for the magnetospheric vector magnetic field, bulk plasma ion and electron moments, and energetic particle fluxes with elemental mass, energy, angle, and charge state distributions for protons, major heavy ions, and electrons in moon wake region of downstream corotating plasma flow.	Magnetometer; Plasma Energetic Particle Detector	5-Ganymede	2	3 -Ganymede	2
			In-situ measurement at 1-min time resolution for density and composition of plasma ions associated with moon torus cloud in jovicentric coordinates and with longitudinal distance from the moon.	Plasma Energetic Particle Detector	5	5	3	3
			In-situ measurement at 1-min time resolution of ion cyclotron waves in near-moon and wake region for constraints on pickup ion composition.	Plasma Wave Detector	5	5	5	5
			In-situ measurement of anisotropic high energy >10 MeV heavy ion interactions with moon surface & atmosphere for surface irradiation and magnetic field modeling	Plasma Energetic Particle Detector	5-Ganymede	3	2	2
			In-situ correlation of low-energy neutral atom composition at 30-sec low-altitude time resolution to sputtering sources in geologically distinct regions of the underlying surface at 100-km resolution.	Plasma Energetic Particle Detector, Visible Imager	2	2	0	0
		C4. Moon Auroral Interaction. Investigate the coupling of the moons with the low altitude magnetosphere and the Jovian atmosphere, including formation processes of the satellite footprint and wake aurora in the Jovian polar atmosphere to understand the electrodynamic circuit connecting them						
			In-situ measurement of vector magnetic field for Alfvénic divergence and fluctuations of the local magnetospheric magnetic field lines connecting the moon to the Jovian atmosphere.	Magnetometer	5	5	2	2
			In-situ measurement at 30-sec time resolution of plasma and energetic particle pitch angle distributions, including loss cone fluxes, for protons, major ions, and electrons with respect to the local magnetospheric magnetic field lines connecting	Magnetometer, Plasma Enegetic Particle Detector	5	5	2	2

GOAL	OBJECTIVE	INVESTIGATION	MEASUREMENT	Instrument Type	Baseline Payload Science Value		Descoped Payload Science Value	
			the moon to the Jovian atmosphere.					
			In-situ measurement at 30-sec time resolution of electromagnetic plasma wave intensity and angular distributions as functions of wave frequency with respect to the local magnetospheric magnetic field lines connecting the moon to the Jovian atmosphere.	Plasma wave detector	0	0	0	0
			UV (0.1-0.2 microns) measurements at 1-min resolution of emission from moon magnetic footpoints in the Jovian auroral region.	UV Spectrometer	1	1	1	1
			Measure electric and magnetic fluctuations from 10s of Hz to MHz.	Magnetometer	0	0	0	0
	D. Io torus. Understand the contributions of Io to the composition, and to the transient and periodic dynamics, of the Jovian magnetosphere							
		D1. Io Activity. Investigate the relationship between temporal variations of volcanic activity on Io, the Io torus and the magnetosphere.						
			UV-VIS (0.05-0.7 microns) imaging of the torus and Io with wide and narrow angle cameras over a range of temporal scales (e.g. hourly, daily weekly, monthly.)	UV Spectrometer, Visible Imager	5	5	5	5
			UV Imaging of Jovian auroral emissions from Io footprint	Visible Imager	1	1	1	1
			In-situ plasma and energetic ion measurements with compositional resolution for transport of iogenic ions from the Io torus region throughout the Jovian magnetosphere	Plasma Energetic Particle Detector	5	5	3	3
		D2. Composition. Determine the composition of the plasma torus and iogenic neutrals.						
			UV-Vis measurements (0.05-0.7 microns) of the Io plasma torus.	UV Spectrometer, Visible Imager	5	5	5	5
	E. Jupiter Magnetosphere. Study the global dynamics of the Jovian magnetosphere including processes that generate the planetary aurora. Identify internal particle sources, acceleration processes, transport and loss processes that shape and drive the Jovian magnetosphere. Understand injection events in the inner magnetosphere.							
		E1. Magnetospheric Ion Sources. Identify locations and activity levels for sources of major and minor plasma ions						
			In-situ measurement of plasma and energetic major and minor ion composition, including elemental mass and ionic charge, especially those ions that differ for sources in the Jovian ionosphere, the moons, and the solar wind.	Plasma Energetic Particle Detector	5	5	3	3
			UV-Vis (100-700 nm) measurements of emissions from the Io plasma torus and other moon tori for ion composition at ~1 nm spectral resolution.	UV Spectrometer, VIS Spectrometer	5	5	5	5
		E2. Magnetospheric Transport Processes. Investigate internal transport acceleration and loss processes that shape and drive the Jovian magnetosphere and produce observed local time asymmetries.						
			Measure differential directional fluxes of protons, major ions, and electrons from eV to MeV energies at 1 minute or better time resolution over a broad range of positions within the jovian magnetosphere	Plasma Energetic Particle Detector	5	5	3	3
			Measure time varying magnetic field at time resolutions up to 20 samples/sec.	Magnetometer	5	5	5	5
			Measure high frequency fluctuations of electric and magnetic fields from a few 10 Hz to MHz.	Magnetometer	0	0	0	0
			In-situ measurement MHD turbulence and flux tube interchange through correlated measurements of fluctuations in vector magnetic field and plasma moments over time scales from seconds to hours.	Magnetometer, Plasma Energetic Particle Detector	5	5	5	5
			UV imaging (0.05-0.35 microns) at 0.3 nm spectral resolution of Io torus emissions at time scales of hours and at spatial resolution of 0.1 RJ	UV Imaging Spectrometer	5	5	5	5
		E3. Injection Events. Investigate the phenomenon of energetic particle injection in the inner magnetosphere.						
			Measure differential directional fluxes of protons, major ions, and electrons from eV to MeV energies at 1 minute or better time resolution in the inner jovian magnetosphere	Plasma Energetic Particle Detector	5	5	3	3
		E4. Auroral Energy Sources. Investigate magnetospheric and solar wind energy sources and dynamics for the Jupiter planetary aurora						
			UV-VIS (0.1-0.7 microns) imaging of auroral emissions at 100-km spatial resolution at cadences of up to 1 minute.	UV Spectrometer, Visible Imaging	2	2	2	2
		E5. Boundary Layers. Investigate the important boundary layers of the magnetosphere (Bow shock, magnetopause, plasma sheet boundary layer, high energy particle radiation belt boundaries, equatorial plasma disk)						
			In-situ measurement at 1-min resolution of magnetic field vectors, plasma moments, and energetic particles at equatorial plasma disk crossings.	Magnetometer, Plasma Energetic Particle Detector	5	5	3	3

GOAL	OBJECTIVE	INVESTIGATION	MEASUREMENT	Instrument Type	Baseline Payload Science Value		Descoped Payload Science Value	
			In-situ measurement at 1-min resolution of high energy protons and ions near boundaries of radiation belt trapping	Plasma Energetic Particle Detector	5	5	2	2
			In-situ measurement of upstream energetic particle events in the solar wind from sources at or within the outer magnetospheric boundaries	Plasma Energetic Particle Detector	2	2	2	2
			In-situ measurements of magnetic field, plasma, and energetic particles to identify and study outer boundary crossings	Magnetometer, Plasma, Energetic Particle Detector	2	2	2	2
			Remote measurement of auroral and internal magnetospheric activity correlated to movement of outer magnetospheric boundaries	UV spectrometer, VIS spectrometer, Magnetometer, Plasma, Energetic Particle detector	2	2	2	2



Foldout C3a. Satellites—Io

GOAL	OBJECTIVE	INVESTIGATION	MEASUREMENT	Instrument Type	Baseline Payload Science Value	Descoped Payload Science Value
	Target Body -- Io					
Understand the mechanisms responsible for formation of surface features and implications for geological history, evolution, and levels of current activity						
	Understand heat balance, tidal dissipation, relationship to volcanism, and the coupling of its thermal/orbital evolution to that of the icy satellites					
		Determine regional and global heat flow				
			IR imaging of thermal emission at < 100-km/pixel spatial scale, absolute accuracy 2K, from ~80K to silicate melt temperatures, over a range of temporal scales (e.g. hourly, daily, weekly, monthly). Desire < 20-km/pixel spatial resolution	IR imaging spectrometer (<90 mrad/pixel)	3	3
		Determine regional and global time-varying topography/shape				
			Measure absolute topography at 1 m vertical scale repeated at several orbital positions	Super-hi-res (0.25 mrad/pixel) imager	1	1
	Monitor Io's active volcanism for insight into its geological history and evolution, and the mechanisms of surface changes					
		Perform long-term and high-temporal-resolution monitoring of volcanic activity				
			Repeated (daily to monthly) monochromatic imaging of selected active volcanic features at ~1 km/pixel spatial resolution	Hi-Res Imager	5	5
			IR imaging of volcanic thermal emission at < 100-km/pixel spatial scale, absolute accuracy 2K, at silicate melt temperatures, over a range of temporal scales (e.g. hourly, daily, weekly, monthly). Desire < 20-km/pixel spatial resolution	Vis-NIR hyperspectral imager	4	4
			Frequent multispectral global mapping (minimum 3 colors) at better than or equal to 10-km/pixel. Violet, green, NIR over a range of temporal scales (e.g. hourly, daily, weekly, monthly)	Hi-res imager	5	5
			High-resolution visible imaging (<100-m spatial resolution) of selected volcanic features for change detection (e.g. with Galileo and Voyager data)	Hi-res imager	3	3
		Determine global distribution of volcanic activity and styles				
			Global (>80%) monochromatic imaging at ~1 km/pixel spatial resolution at available opportunities	Hi-res imager	5	5
			IR imaging of volcanic thermal emission at < 100-km/pixel spatial scale, absolute accuracy 2K, at silicate melt temperatures, over a range of temporal scales (e.g. hourly, daily, weekly, monthly). Desire < 20-km/pixel spatial resolution	Vis-NIR hyperspectral imager	4	4
			Frequent multispectral global mapping (minimum 3 colors) at better than or equal to 10-km/pixel. Violet, green, NIR over a range of temporal scales (e.g. hourly, daily, weekly, monthly)	Hi-res imager	5	5
			UV - VIS plume imaging: high phase angle plume monitoring (for dust and gas emissions) and low phase angle observations (for gas absorptions) over a range of temporal scales. Spatial resolution <20 km/pixel vis, <50 km/pixel UV	Hi-res imager & UV	3	3
		Characterize crustal recycling of volatiles				
			Frequent multispectral global mapping (minimum 3 colors) at better than or equal to 10-km/pixel. Violet, green, IR over a range of temporal scales (e.g. hourly, daily, weekly, monthly)	Hi-res imager	4	4
		Determine eruption temperatures (implications for superheating)				
			Measure silicate melt temperatures of selected volcanic features at <1-km/pixel resolution	Vis-NIR hyperspectral imager	4	4
		Determine local, regional, and global topography				
			Global (>80%) monochromatic imaging at ~1 km/pixel spatial resolution at available opportunities	Hi-res imager	5	5
			Topographic mapping of representative features at better than 100-m/pixel and better than or equal to 10-m vertical accuracy.	LIDAR. Stereo Camera, LASER altimeter	3	3
			Topographic mapping as widely distributed as possible at the global scale at better than 1 km/pixel and better than or equal to 100-m vertical accuracy.	Altimeter, Stereo Camera	2	2
			Obtain high-resolution (< 100 m/pixel) monochromatic images of representative features at low sun angle	Stereo Camera & Hi-res imager	4	4
		Understand Io's surface geology, including the relationships between volcanism and tectonism, erosion and deposition processes				
		Determine distribution of geologic structures				
			Global (>80%) monochromatic imaging at ~1 km/pixel spatial resolution at available opportunities	Hi-res imager	5	5
			Multispectral vis-NIR global mapping (minimum 3 colors) at better than or equal to 10-km/pixel	Hi-res (<10 mrad/pixel) color imager	5	5
			Obtain high-resolution (< 100 m/pixel) monochromatic images of representative features at low sun angle	Super-hi-res (0.25 mrad/pixel) imager	4	4
		Characterize distribution and transport of volatiles				
			Frequent multispectral global mapping (minimum 3 colors) at better than or equal to 10-km/pixel. Violet, green, IR over a range of temporal scales (e.g. hourly, daily, weekly, monthly)	Hi-res (<10 mrad/pixel) color imager	5	5
Global mapping of surface at UV-NIR wavelengths (eg for SO2 frost variations) at ~10 (NIR)-500 km/pix (UV) on a range of temporal scales (~days) Range 1 - 5 microns at 20 nm spectral resolution in IR and 2 nm for UV/VNIR			IR imaging spectrometer (<90 mrad/pixel) VNIR imaging spectrometer (<90 mrad/pixel) UV imaging spectrometer (<90 mrad/pixel)	5	5	

GOAL	OBJECTIVE	INVESTIGATION	MEASUREMENT	Instrument Type	Baseline Payload Science Value	Descoped Payload Science Value	
		Determine regional and global topography					
			Global (>80%) monochromatic imaging at ~1 km/pixel spatial resolution at available opportunities	Super-hi-res (0.25 mrad/pixel) imager	5	5	
			Topographic mapping of representative features at spatial and vertical scales of ~100 m or better (relative topography)		Stereo Camera	5	5
			Obtain high-resolution visible images (<100-m spatial resolution) of selected features at low sun angle		Super-hi-res (0.25 mrad/pixel) imager	4	4
		Characterize morphology and structure of geologic features					
			Global (>80%) monochromatic imaging at ~1 km/pixel spatial resolution at available opportunities	Super-hi-res (0.25 mrad/pixel) imager	5	5	
			Topographic mapping of representative features at spatial and vertical scales of ~100 m or better (relative topography)		Super-hi-res (0.25 mrad/pixel) imager	5	5
			Multispectral vis-NIR global mapping (minimum 3 colors) at better than or equal to 10-km/pixel		Hi-res (<10 mrad/pixel) color imager	5	5
			Obtain high-resolution visible images (<100-m spatial resolution) of selected features at low sun angle during flybys		Super-hi-res (0.25 mrad/pixel) imager	4	4
		Perform surface monitoring for change detection					
			Repeated (daily to monthly) monochromatic imaging of selected active volcanic features at <1 km/pixel spatial resolution	Hi-Res Imager	4	4	
			IR imaging of thermal emission at < 100-km/pixel spatial scale, absolute accuracy 2K, from ~80K to silicate melt temperatures, over a range of temporal scales (e.g. hourly, daily, weekly, monthly). Desire < 20-km/pixel spatial resolution		IR imaging spectrometer (<90 mrad/pixel)	4	4
			Frequent multispectral global mapping (minimum 3 colors) at better than or equal to 10-km/pixel. Violet, green, IR over a range of temporal scales (e.g. hourly, daily, weekly, monthly)		Hi-res (<10 mrad/pixel) color imager	5	5
			Obtain high-resolution observations (<100-m spatial resolution) of selected volcanic features in visible and infrared wavelengths		Super-hi-res (0.25 mrad/pixel) imager	5	5
Determine the surface compositions and implications for the origin, evolution and transport of surface materials							
	Understand the volatile component of Io's crust and its behavior						
		Characterize volatile cycle: document composition, physical state, distribution, and transport of surface volatiles					
			Global mapping of surface at UV-NIR wavelengths (eg for SO2 frost variations) at ~10-500 km/pix on a range of temporal scales (~days) Range 1 - 5 microns at 20 nm spectral resolution in IR and 2 nm for UV/VNIR		IR imaging spectrometer (<90 mrad/pixel) VNIR imaging spectrometer (<90 mrad/pixel) UV imaging spectrometer (<90 mrad/pixel)	5	5
			Dayside, nightside and eclipse coverage at UV wavelengths, 0.1-0.35 microns (for SO2 and other gas density) at 0.3 nm spectral res, <500 km/pix spatial resolution		IR imaging spectrometer (<90 mrad/pixel) UV imaging spectrometer (<90 mrad/pixel)	5	5
			Determine roles and rates of sublimation, sputtering, and radiation darkening				
			Global mapping of surface at UV-IR wavelengths at ~10-500 km/pix at <10 nm spectral resolution from 1-5 microns, ~2 nm for UV/Vis) over a wide range of longitudes (i.e. to facilitate comparisons between leading and trailing hemispheres, especially in non-plume regions)		IR imaging spectrometer (<90 mrad/pixel) VNIR imaging spectrometer (<90 mrad/pixel) UV imaging spectrometer (<90 mrad/pixel)	5	5
	Understand the silicate component of Io's crust						
		Identify compositions (including the source(s) of the 1.0- and 3.915-µm bands) and physical characteristics (e.g., particle size, porosity) of silicates					
		Hyperspectral Vis-IR (0.4-5 microns) observations of representative features at ≤ 1 km/pixel and < 10 nm spectral resolution		Hi-res (<1 mrad/pixel) hyperspectral imager	5	5	
		Determine distribution of silicates					
		Multispectral Vis-NIR global mapping (minimum 3 colors) at better than or equal to 10-km/pixel		Hi-res (<10 mrad/pixel) color imager	5	5	
		Search for compositional variability among silicates					
	Hyperspectral Vis-IR (0.4-5 microns) observations of representative features at ≤ 1 km/pixel and < 10 nm spectral resolution		Hyperspectral imager	5	5		
	Determine the compositions, origins, and evolution of the atmosphere, including transport of material throughout the Jovian system						
	Understand the sources (volcanism, sublimation, surface sputtering) and sinks (freezing out, plasma pickup/sputtering, thermal escape) of atmospheric components						
		Determine column densities of atmospheric/plume species across the globe and document correlations with plumes, geologic features and local albedo variations					
			Global EUV - VNIR (0.06-1 micron) surface and limb spectroscopy at <50 km resolution (VNIR). UV spectral resolution of 0.3 nm. UV spatial resolution of <500 km/pix	UV hyperspectral imager (<10 mrad/pixel) VNIR hyperspectral imager (<10 mrad/pixel)	5	5	
			UV stellar occultations (FUV-NUV) over a range of latitude/longitude space and a range of temporal scales/periodically throughout the mission. UV spectral resolution of 0.3 nm, 0.1-0.35 microns	UV hyperspectral imager (<10 mrad/pixel) VNIR hyperspectral imager (<10 mrad/pixel)	5	5	
	Perform long-term and high-temporal-resolution monitoring of atmosphere, plumes, limb-glow, and equatorial spots						
		Obtain EUV - VNIR (0.06-1 micron) hyperspectral imaging limb observations of plumes, atmosphere, neutral clouds at ≤10km/px over a range of temporal scales (e.g. hourly, daily, weekly, monthly). UV spectral resolution of 0.3 nm, spatial res of <500 km/pix	UV hyperspectral imager (<10 mrad/pixel) VNIR hyperspectral imager (<10 mrad/pixel)	5	5		
	Monitor Io torus						
		Obtain EUV through VNIR (0.06-1 micron) hyperspectral imaging observations of torus at 0.1 RJ/px and <1 nm spectral resolution over a range of temporal scales (e.g. hourly, daily, weekly, monthly). UV spectral resolution of 0.3 nm	UV hyperspectral imager (<10 mrad/pixel) VNIR hyperspectral imager (<10 mrad/pixel)	5	5		

GOAL	OBJECTIVE	INVESTIGATION	MEASUREMENT	Instrument Type	Baseline Payload Science Value	Descoped Payload Science Value
		Determine the composition, distribution and physical characteristics (grain-size, crystallinity) of volatile materials on the surface, including SO2 frost				
			Obtain vis-IR (0.4-5 micron) hyperspectral imaging on a global scale (<10 km/px for yellow and white-gray units), and at higher resolution for green and red units (~1 km/px).	IR hyperspectral imager (<10 mrad/pixel) VNIR hyperspectral imager (<10 mrad/pixel)	5	5
	<i>Understand the temporal, spatial, and compositional variability of the atmosphere</i>					
		Perform long-term and high-temporal-resolution monitoring				
			Obtain EUV through VNIR (0.06-1 micron) hyperspectral imaging limb observations of plumes, atmosphere, neutral clouds at ≤10km/px over a range of temporal scales (e.g. hourly, daily, weekly, monthly). UV spectral resolution of 0.3 nm, spatial res of <500 km/pix	UV hyperspectral imager (<10 mrad/pixel) VNIR hyperspectral imager (<10 mrad/pixel)	5	5
		Determine column densities and compositions of atmospheric/plume species across the globe				
			Obtain EUV through VNIR (0.06-1 micron) hyperspectral imaging limb observations of plumes, atmosphere, neutral clouds at ≤10km/px and <1 nm spectral resolution over a range of temporal scales (e.g. hourly, daily, weekly, monthly). UV spectral resolution of 0.3 nm, spatial res of <500 km/pix	UV hyperspectral imager (<10 mrad/pixel) VNIR hyperspectral imager (<10 mrad/pixel)	5	5
		Determine temperatures of gas in plumes and atmosphere				
			UV/NIR and thermal IR imaging of thermal emission from plumes and atmosphere at < 100-km/pixel spatial scale. Desire < 20-km/pixel spatial resolution. UV spectral resolution of 0.3 nm	IR imaging spectrometer (<90 mrad/pixel) VNIR imaging spectrometer (<90 mrad/pixel)	5	5



Foldout C3b. Satellites—Europa

GOAL	OBJECTIVE	INVESTIGATION	MEASUREMENT	Instrument Type	Baseline Pavload Science Value	Descoped Pavload Science Value
	Target Body -- Europa					
			Understand the mechanisms responsible for formation of surface features and implications for geological history, evolution, and levels of current activity			
			Understand geologic history, potential for current activity, and the implications for Jupiter's satellite system			
		Determine distribution of geologic structures				
			Global monochromatic imaging at <0.5 km/pixel, widely distributed regional imaging at <100 m/pixel	Super hi-res (<0.1 mrad/pixel) imager	3	3
		Determine differences in crater morphology and cratering rates over time and between satellites				
			Global monochromatic imaging at <0.5 km/pixel, widely distributed regional imaging at <100 m/pixel	Super hi-res (<0.1 mrad/pixel) imager	3	3
		Constrain past non-synchronous rotation				
			Repeat selected near-terminator Voyager and Galileo observations	Super hi-res (<0.1 mrad/pixel) imager	3	3
		Search for evidence of current activity through surface monitoring for change detection, thermal anomalies, plumes				
			UV stellar occultations (0.06-0.35 microns at 0.3 nm resolution) over a range of latitude/longitude space, periodically throughout the mission	UV spectrometer	5	5
			High-phase (>140 deg), full-disk visible limb imaging at a variety of longitudes, repeated weekly to monthly	Hi-res (<1 mrad/pixel) imager	5	5
			Thermal imaging, 2K absolute accuracy, from ~80K to >160K, spatial resolution <10 km/pixel, prefer <500-m/pixel, within 30 degrees of the noon meridian and at night	Far-IR imaging radiometer (<10 mrad/pixel)	3	3
			Understand heat balance and tidal dissipation			
		Determine regional and global heat flow				
			Thermal imaging, 2K absolute accuracy, from ~80K to >160K, spatial resolution <10 km/pixel, prefer <500-m/pixel, within 30 degrees of the noon meridian and at night	Far-IR imaging radiometer (<10 mrad/pixel)	3	3
		Determine regional and global time-varying topography/shape				
			Measure absolute topography of tidal bulge at 1 m vertical scale repeated at several orbital positions		1	1
			Understand the processes responsible for the observed geologic features and as analogs for surface geology of other icy satellites			
		Characterize morphology and structure of geologic features				
			Topographic mapping of representative features at spatial and vertical scales of ~100 m or better (relative topography)	Hi-res (<10 mrad/pixel) stereo imager from a distance or SAR for close flybys	5	4
			Subsurface profiling of thermal, compositional, and structural horizons, including the distribution of brines, beneath representative features, and at depths of 100 m to 2 km (or as far as possible) at ~10-m vertical resolution and ~100-m horizontal resolution.	Ice penetrating radar	2	2
			Global monochromatic imaging at <0.5 km/pixel, widely distributed regional imaging at <100 m/pixel	Super hi-res (<0.1 mrad/pixel) imager	3	3
		Understand compositional variations and role in formation mechanisms				
			Coregistered visible imaging of representative features with IR hyperspectral imaging: 1 to 5 micron with IR spectral resolution better than 10nm and IR spatial resolution <1km/pixel	Hi-res (<1 mrad/pixel) IR imaging spectrometer	5	5
			Shallow subsurface profiling of representative features to depths of 10s of m (or as far as possible) at ~1-m vertical resolution and ~100-m horizontal resolution.	Ice penetrating radar	2	2
		Determine regional and global topography and relationship to surface features				
			Topographic mapping of representative features at spatial and vertical scales of ~100 m or better (relative topography)	Hi-res (<10 mrad/pixel) stereo imager from a distance or SAR for close flybys	5	4
			Globally distributed measurements of topography (e.g. limb profiles, altimetric profiles, stereo imaging) to vertical scales of ≤50 m absolute topography and horizontal scales of 2 km.	Hi-res (<10 mrad/pixel) stereo imager	3	3
		Determine the role of regolith formation and mass wasting in the modification of surface features				
			Topographic mapping of representative features at spatial and vertical scales of ~100 m or better (relative topography)	Hi-res (<10 mrad/pixel) VIS imager	5	4
			Super-high resolution monochrome images of selected target areas (with intermediate context imaging) down to 1 m/pixel scale	Super hi-res (<0.1 mrad/pixel) imager Hi-res (<1 mrad/pixel) imager	2 2	2 2
			Shallow subsurface profiling widely distributed across the globe to depths of 10s of m (or as far as possible) at ~1-m vertical resolution and ~100-m horizontal resolution.	Ice penetrating radar	2	2
			Search for evidence of recent activity (e.g., thermal anomalies; the presence of short-lived species; the absence of radiolytic products such as H2O2; chemical disequilibrium).			

GOAL	OBJECTIVE	INVESTIGATION	MEASUREMENT	Instrument Type	Baseline Pavload Science Value	Descoped Pavload Science Value			
		Search for changes in surface heat flowby mapping regolith thermal and thermophysical properties, and performing long-term monitoring of changes							
			Repeated thermal imaging, 2K absolute accuracy, from ~80K to >160K, spatial resolution <10 km/pixel, prefer <500-m/pixel, within 30 degrees of the noon meridian and at night	Far-IR imaging radiometer (<10 mrad/pixel)	3	3			
		Identify and map accumulation of radiation products and compounds which are unstable to radiation; Monitor long-term changes in abundances of these materials							
			UV imaging spectroscopy with wavelength range of 0.2 to 0.4 micron with spectral resolution of <2 nm. Globally distributed observations with spatial resolution <1km/pixel, with representative areas at 100m/pixel; repeated coverage to look for changes.	Hi-res (<1 mrad/pixel) UV imaging spectrometer Hi-res (<1 mrad/pixel) VNIR imaging spectrometer	2	2			
			Visible hyperspectral imaging: 0.55 to 0.75 microns, spectral resolution of <2 nm. Globally distributed observations with spatial resolution <1km/pixel, with representative areas at 100m/pixel; repeated coverage to look for changes.	Super hi-res (<0.1 mrad/pixel) imager Hi-res (<1 mrad/pixel) imager	2	2			
			IR hyperspectral imaging: 1 to 2.5 microns with spectral resolution <2 nm, 2.5 to 5 micron with <10 nm spectral resolution. Globally distributed observations with spatial resolution <1km/pixel, with representative areas at 100m/pixel; repeated coverage to look for changes.	Hyperspectral imager	2	2			
	Characterize suitability of surface for future lander missions								
	Evaluate surface structure, characteristics and properties at local scales (spatial scales of centimeters)								
		Super-high resolution monochrome images of selected target areas (with intermediate context imaging) at 1-m/pixel at incidence angles ~60° -70°.	Super hi-res (<0.1 mrad/pixel) imager Hi-res (<1 mrad/pixel) imager	0	0				
Determine the surface compositions and implications for the origin, evolution and transport of surface materials									
Understand composition, physical characteristics, distribution, and evolution of surface materials									
	Identify bulk material compositions, grain size, porosity, crystallinity, and physical state								
		Globally distributed IR hyperspectral imaging (0.8-2.5 microns). Spectral resolution: 4 nm IFOV<50m	Hi-res (<1 mrad/pixel) imager Hi-res (<1 mrad/pixel) VNIR imaging spectrometer Thermal IR imaging spectrometer				3	3	
		Globally distributed thermal imaging, 2K absolute accuracy, from ~80K to >160K, spatial resolution <10 km/pixel	Thermal Imager				4	4	
		Globally distributed UV hyperspectral imaging (0.1 to 0.4 microns) with spectral resolution of 2 nm and spatial resolution <1km/pixel.	UV hyperspectral imager (<10 mrad/pixel)				3	3	
	Map distributions of different materials, including radiolytic materials (e.g. SOx, O3, H2O2, OH, O2), and document variability over a range of timescales.								
		Global IR hyperspectral imaging (0.8-5 microns). Spectral resolution: <10nm (1-2.5 micron: 4 nm). IFOV<1km.	Hi-res (<1 mrad/pixel) imager VNIR imaging spectrometer (<2.5 mrad/pixel) UV imaging spectrometer (<2.5 mrad/pixel)				2	2	
		Global UV hyperspectral imaging (0.1 to 0.4 microns) with spectral resolution of 2 nm and spatial resolution <1km/pixel.	UV hyperspectral imager (<10 mrad/pixel)				1	1	
	Determine origin and evolution of non-ice materials, including the role of geologic processes								
		IR hyperspectral imaging of representative features (0.8-5 microns). Spectral resolution: <10nm. IFOV<1km. Co-registered with higher-resolution panchromatic imaging.	Hi-res (<1 mrad/pixel) imager VNIR imaging spectrometer (<2.5 mrad/pixel)				4	4	
	Characterize volatile cycle: document composition, physical state, distribution, and transport of surface volatiles, e.g. sublimation								
		UV wavelength range of 0.2 to 0.4 micron with spectral resolution of 2 nm and spatial resolution <1km/pixel. Spatial coverage of 50% to search for short – lived or mobile species and repeated coverage to look for changes.	VNIR imaging spectrometer (<2.5 mrad/pixel) UV imaging spectrometer (<2.5 mrad/pixel)				1	1	
		VNIR hyperspectral imaging: 0.55 to 0.75 microns, spectral resolution of 1 nm. 50% global coverage with spatial resolution <1km/pixel; repeated coverage to look for changes.	Hyperspectral imager				2	2	
		Hyperspectral IR imaging (0.8-5 microns). Spectral resolution: <10nm. 50% global coverage with spatial resolution <1km/pixel; repeated coverage to look for changes.	Hyperspectral imager				1	1	
Determine if and how material is interchanged between surface and ocean									
	Profiling of thermal, compositional, and structural horizons								
		Subsurface profiling of thermal, compositional, and structural horizons, including the distribution of brines, beneath representative features, and at depths of 100 m to 2 km (or as far as possible) at ~10-m vertical resolution and ~100-m horizontal resolution.	Ice penetrating radar				2	2	
	Perform coordinated overlapping topographic, compositional, and thermal measurements to assess diagnostic geologic and compositional interrelationships								
		Hyperspectral NUV imaging (0.2-0.35 microns) (2 nm spectr res) (1km spat res), coverage of representative features.	Super hi-res (<0.1 mrad/pixel) imager Hi-res (<2.5 mrad/pixel) imager UV imaging spectrometer (<2.5 mrad/pixel) VNIR imaging spectrometer (<2.5 mrad/pixel) Thermal IR imaging spectrometer (<2.5 mrad/pixel) Thermal imager (<25 mrad/pixel)				3	3	

GOAL	OBJECTIVE	INVESTIGATION	MEASUREMENT	Instrument Type	Baseline Payload Science Value	Descoped Payload Science Value	
			Hyperspectral IR imaging of representative features (0.8-5 microns). Spectral resolution: <10nm IFOV<1km	Hyperspectral imager	4	4	
			Hyperspectral TIR imaging of representative features. 8-15microns. Spectral resolution: 4cm-1 or 25nm. IFOV<1km	Hyperspectral imager	4	4	
			3-color (visible to near-IR) imaging of representative features at 100 m/pix, co-registered with multi-spectral data	Hi-res (<1 mrad/pixel) imager Hi-res (<1 mrad/pixel) VNIR imaging spectrometer Thermal IR imaging spectrometer	5	5	
			Topography at 100-m horizontal and 10-m vertical resolution, coverage of representative features.	Super-hi-res (0.25 mrad/pixel) imager	4	4	
			Thermal imaging of representative features, 2K absolute accuracy, from ~80K to >160K, spatial resolution <10 km/pixel, prefer <500-m/pixel, within 30 degrees of the noon meridian and at night	Thermal Imager	3	3	
			<i>Determine the compositions, origins, and evolution of the atmosphere, including transport of material throughout the Jovian system</i>				
	<i>Understand the sources (sublimation, surface sputtering) and sinks (freezing out, plasma pickup/sputtering, thermal escape) of atmospheric components</i>						
		Determine column densities of atmospheric species across the globe					
			Global EUV - VNIR (0.06-1 micron) surface and limb spectroscopy at <50 km resolution. UV spectral resolution of 0.3 nm		UV imaging spectrometer (<50 mrad/pixel) VNIR imaging spectrometer (<50 mrad/pixel)	3	3
			UV stellar occultations (0.06-0.35 microns) over a range of latitude/longitude space periodically throughout the mission. UV spectral resolution of 0.3 nm		UV spectrometer	5	5
		Perform long-term and high-temporal-resolution monitoring of atmosphere in context of plasma bombardment and potential endogenic variations					
			EUV - VNIR (0.06-1 micron) surface and limb spectroscopy at <50 km spatial resolution at temporal resolution on the scale of days. UV spectral resolution of 0.3 nm.		UV imaging spectrometer (<50 mrad/pixel) VNIR imaging spectrometer (<50 mrad/pixel)	3	3
			Perform UV (0.06-0.35 microns) stellar occultations frequently (~daily) and at high time resolution. UV spectral resolution of 0.3 nm		UV spectrometer	4	4
		Determine the composition, distribution and physical characteristics (grain-size, crystallinity, physical state) of volatile materials on the surface					
			Global FUV - IR (0.1-5 micron) spectroscopy at <50 km spatial resolution, <10nm spectral resolution		FUV imaging spectrometer (<50 mrad/pixel) VNIR imaging spectrometer (<50 mrad/pixel)	3	3
			Investigate sputtering processes at high latitudes as compared with lower latitudes				
				Global FUV - IR (0.1-5 micron) spectroscopy at <50 km spatial resolution. UV spectral resolution of 1 nm; IR spectral resolution <10 nm		FUV imaging spectrometer (<50 mrad/pixel) VNIR imaging spectrometer (<50 mrad/pixel)	3
	<i>Understand the temporal, spatial, and compositional variability of the atmosphere</i>						
			Determine column densities, compositions and temperatures of atmospheric species across the globe				
			Global EUV - VNIR (0.06-1 micron) surface and limb spectroscopy at <50 km spatial resolution; spectral resolution of 0.3 nm		FUV imaging spectrometer (<50 mrad/pixel) VNIR imaging spectrometer (<50 mrad/pixel)	3	3



Foldout C3c. Satellites—Ganymede

GOAL	OBJECTIVE	INVESTIGATION	MEASUREMENT	Instrument Type	Baseline Payload Science Value	Descoped Payload Science Value
	Target Body -- Ganymede					
	Understand the mechanisms responsible for formation of surface features and implications for geological history, evolution, and levels of current activity					
	Understand geologic history, potential for current activity, and the implications for Jupiter's satellite system					
		Determine distribution of geologic structures	Global monochromatic imaging at <50 m/pixel	Hi-res (<10 mrad/pixel) VIS imager	5	5
		Determine differences in crater morphology and cratering rates over time and between satellites				
			Global monochromatic imaging at <50 m/pixel	Hi-res (<10 mrad/pixel) VIS imager	5	5
			Topographic mapping of representative features at spatial and vertical scales of ~100 m or better (relative topography)	Medium-res camera (<25 mrad/pixel)	5	5
			Super-high resolution monochrome images of selected target areas (with intermediate context imaging) down to 25-cm/pixel scale.	Super hi-res (<0.1 mrad/pixel) imager	0	0
			Subsurface profiling of thermal, compositional, and structural horizons, widely distributed across the globe, and at depths of 100 m to 2 km (or as far as possible) at ~10-m vertical resolution and ~100-m horizontal resolution.	Ice penetrating radar	5	5
		Constrain whether non-synchronous rotation has occurred in the past				
			Map distribution of catenae through global monochromatic imaging at <500 m/pixel	Medium-res camera (<25 mrad/pixel)	5	5
		Search for evidence of current activity through surface monitoring for change detection, thermal anomalies, plumes				
			UV stellar occultations (0.06-0.35 microns; 0.3 nm spectr res) over a range of latitude/longitude space periodically throughout the mission	UV spectrometer	5	5
			High-phase (>140 deg), full-disk visible limb imaging over a range of longitudes over the duration of the mission	Hi-res (<2.5 mrad/pixel) imager UV imaging spectrometer (<2.5 mrad/pixel)	5	5
			Thermal imaging, 2K absolute accuracy, from ~80K to >160K, spatial resolution <10 km/pixel, prefer <500-m/pixel, within 30 degrees of the noon meridian and at night	Far-IR imaging radiometer (<100 mrad/pixel)	5	5
			Global monochrome imaging at a spatial resolution of 500m-1km, for comparison to previous datasets, with repeated imaging as possible.	Medium-res camera (<25 mrad/pixel)	5	5
		Understand the processes responsible for the observed geologic features				
		Characterize morphology and structure of geologic features				
			Topographic mapping of representative features at spatial and vertical scales of ~100 m or better (relative topography)	Hi-res (<10 mrad/pixel) stereo imager from a distance or SAR for close flybys	5	5
			Subsurface profiling of thermal, compositional, and structural horizons, beneath representative features, and at depths of 100 m to 2 km (or as far as possible) at ~10-m vertical resolution and ~100-m horizontal resolution.	Ice penetrating radar	5	5
			Global monochromatic imaging at <50 m/pixel	Hi-res (<10 mrad/pixel) VIS imager	5	5
		Determine regional and global topography and relationship to surface features				
			Global measurement of absolute topography to vertical scales of ≤50 m and horizontal scales of ~2 km.	Medium-res camera (<25 mrad/pixel)	5	5
		Understand compositional variations and role in formation mechanisms				
			Coregistered visible imaging of representative features at spatial scales of 100 m with spectral imaging at 1-5 microns at 20nm spectral resolution at 0.5 km/px.	Hi-res (<10 mrad/pixel) VIS imager IR imaging spectrometer (<50 mrad/pixel)	5	5
		Determine the role of regolith formation and mass wasting in the modification of surface features				
			Topographic mapping of representative features at spatial and vertical scales of ~100 m or better (relative topography)	Hi-res (<10 mrad/pixel) stereo imager from a distance or SAR for close flybys	5	5
			Super-high resolution monochrome images of selected target areas (with intermediate context imaging) down to 25-cm/pixel scale.	Hi-res (<1 mrad/pixel) imager	0	0
			Shallow subsurface profiling widely distributed across the globe to depths of 10s of m (or as far as possible) at ~1-m vertical resolution and ~100-m horizontal resolution.	Ice penetrating radar	5	5
		Understand heat balance and tidal dissipation				
		Determine regional and global time-varying topography/shape				
			Measure absolute topography of tidal bulge at 1 m vertical scale repeated at several orbital positions	Hi-res (<1 mrad/pixel) imager	5	5
		Determine regional and global heat flow				
			Thermal imaging, 2K absolute accuracy, from ~80K to >160K, spatial resolution <10 km/pixel, prefer <500-m/pixel, within 30 degrees of the noon meridian and	Hi-res (<1 mrad/pixel) imager	5	5

GOAL	OBJECTIVE	INVESTIGATION	MEASUREMENT	Instrument Type	Baseline Payload Science Value	Descoped Payload Science Value	
			at night				
Determine the surface compositions and implications for the origin, evolution and transport of surface materials							
	Understand composition, physical characteristics, distribution, and evolution of surface materials						
		Identify bulk material compositions, grain size, porosity, crystallinity, and physical state					
			Globally-distributed hyperspectral IR imaging (0.8-2.5 microns). Spectral resolution: 4 nm IFOV<100m.		Hyperspectral imager	5	5
			Globally-distributed thermal imaging, 2K absolute accuracy, from ~80K to >160K, spatial resolution <10 km/pixel		Thermal Imager	5	5
		Map distributions of different materials, including radiolytic materials (e.g. SOx, O3, H2O2, OH, O2), and document variability over a range of timescales.					
			Global hyperspectral IR imaging (0.8-5 microns). Spectral resolution: <10nm (1-2.5 micron: 4 nm). IFOV<1km.		Hyperspectral imager	5	5
			UV imaging (0.1 to 0.4 microns) with spectral resolution of <2 nm and spatial resolution <1km/pixel.		UV imager	5	5
		Determine origin and evolution of non-ice materials, including the role of geologic processes					
			Hyperspectral IR imaging of representative features (0.8-5 microns). Spectral resolution: <10nm. IFOV<1km. Co-registered with higher-resolution panchromatic images.		Hyperspectral imager	5	5
		Characterize volatile cycle: document composition, physical state, distribution, and transport of surface volatiles, e.g. sublimation					
			UV wavelength range of 0.2 to 0.4 micron with spectral resolution of 2 nm and spatial resolution <1km/pixel. Spatial coverage of 50% to search for short – lived or mobile species and repeated coverage to look for changes.		UV imaging spectrometer (<90 mrad/pixel)	5	5
			Visible hyperspectral imaging: 0.55 to 0.75 microns, spectral resolution of 1 nm. 50% global coverage with spatial resolution <1km/pixel; repeated coverage to look for changes.		VNIR imaging spectrometer (<25 mrad/pixel)	3	3
IR imaging spectrometer (0.8-5 microns). Spectral resolution: <10nm. FWHM<10nm. IFOV<1km. 50% global coverage with spatial resolution <1km/pixel; repeated coverage to look for changes.			VNIR imaging spectrometer (<25 mrad/pixel)	5	5		
Determine the compositions, origins, and evolution of the atmosphere, including transport of material throughout the Jovian system							
	Understand the sources (sublimation, surface sputtering) and sinks (freezing out, plasma pickup/sputtering, thermal escape) of atmospheric components						
		Determine column densities of atmospheric species across the globe					
			Global EUV - VNIR (0.06-1 micron) surface and limb spectroscopy at <50 km resolution. UV spectral resolution of 0.3 nm		UV imaging spectrometer VNIR imaging spectrometer	5	5
			UV stellar occultations (0.06-0.35 microns) over a range of latitude/longitude space periodically throughout the mission. UV spectral resolution of 0.3 nm		UV spectrometer	5	5
		Perform long-term and high-temporal-resolution monitoring of atmosphere in context of magnetospheric variations					
			EUV - VNIR (0.06-1 micron) surface and limb spectroscopy at <50 km spatial resolution at temporal resolution on the scale of days. UV spectral resolution of 0.3 nm		UV imaging spectrometer VNIR imaging spectrometer	5	5
			Perform UV stellar occultations frequently (~daily) and at high time resolution. UV spectral resolution of 0.3 nm, range of 0.06-0.35 microns.		UV spectrometer	5	5
		Determine the composition, distribution and physical characteristics (grain-size, crystallinity, physical state) of volatile materials on the surface					
			Global FUV - IR (0.1-5 micron) spectroscopy at <50 km spatial resolution;IR spectral resolution <10 nm		UV imaging spectrometer VNIR imaging spectrometer	5	5
		Investigate sputtering processes at high latitudes as compared with lower latitudes					
			FUV - IR (0.1-5 micron) spectroscopy at <50 km spatial resolution. UV spectral resolution of <1 nm; IR spectral resolution <10 nm		UV imaging spectrometer VNIR imaging spectrometer	5	5
	Understand the temporal, spatial, and compositional variability of the atmosphere						
		Determine column densities, compositions and temperatures of atmospheric species across the globe					
		EUV - VNIR (0.06-1 micron) surface and limb spectroscopy at <50 km spatial resolution; spectral resolution of 0.3 nm		UV imaging spectrometer VNIR imaging spectrometer	5	5	



Foldout C3d. Satellites—Callisto

GOAL	OBJECTIVE	INVESTIGATION	MEASUREMENT	Instrument Type	Baseline Pavload Science Value	Descoped Pavload Science Value
	Target Body -- Callisto					
	Understand the mechanisms responsible for formation of surface features and implications for geological history, evolution, and levels of current activity					
	Understand geologic history and implications for Jupiter's satellite system					
		Determine differences in crater morphology and cratering rates over time and between satellites				
			Global monochromatic imaging at <200 m/pixel	Hi-res (<1 mrad/pixel) imager	3	3
			Topographic mapping of representative features at spatial and vertical scales of ~100 m or better (relative topography)	Hi-res (<10 mrad/pixel) VIS imager	5	4
			Super-high resolution monochrome images of selected target areas (with intermediate context imaging) down to 1 m/pixel scale	Super hi-res (<0.1 mrad/pixel) imager Hi-res (<1 mrad/pixel) imager	2	2
			Subsurface profiling of thermal, compositional, and structural horizons, widely distributed across the globe, and at depths of 100 m to 2 km (or as far as possible) at ~10-m vertical resolution and ~100-m horizontal resolution.	Ice penetrating radar	3	3
		Identify and map distribution of other geologic structures				
			Global monochromatic imaging at <200-m/pixel	Hi-res (<1 mrad/pixel) imager	3	3
	Understand the processes responsible for the observed geologic features					
		Characterize morphology and structure of geologic features				
			Topographic mapping of representative features at spatial and vertical scales of ~100 m or better (relative topography)	Hi-res (<10 mrad/pixel) VIS imager	5	4
			Subsurface profiling of thermal, compositional, and structural horizons, beneath representative features, and at depths of 100 m to 2 km (or as far as possible) at ~10-m vertical resolution and ~100-m horizontal resolution.	Ice penetrating radar	3	3
			Global monochromatic imaging at <200 m/pixel	Super hi-res (<0.1 mrad/pixel) imager	3	3
		Determine the role of regolith formation and mass wasting in the modification of surface features				
			Topographic mapping of representative features at spatial and vertical scales of ~100 m or better (relative topography)	Hi-res (<10 mrad/pixel) VIS imager	5	4
			Super-high resolution monochrome images of selected target areas (with intermediate context imaging) down to 1 m/pixel scale	Super hi-res (<0.1 mrad/pixel) imager Hi-res (<1 mrad/pixel) imager	2	2
			Shallow subsurface profiling widely distributed across the globe to depths of 10s of m (or as far as possible) at ~1-m vertical resolution and ~100-m horizontal resolution.	Ice penetrating radar	3	3
		Determine regional and global topography and relationship to surface features				
			Measurement of the topography of globally significant geologic features (e.g. impact basins) to vertical scales of ~100 m and horizontal scales of 10 km.	Medium-res camera (<25 mrad/pixel)	5	4
		Understand compositional variations and role in formation mechanisms				
			Coregistered visible imaging of representative features at spatial scales of 100 m with IR hyperspectral imaging at 1-5 microns at 20nm spectral resolution at 0.5 km/px.	Hi-res (<10 mrad/pixel) VIS imager IR imaging spectrometer (<50 mrad/pixel)	5	5
	Determine the surface compositions and implications for the origin, evolution and transport of surface materials					
	Understand composition, physical characteristics, distribution, and evolution of surface materials					
		Identify bulk material compositions, grain size, porosity, crystallinity, and physical state				
			Globally distributed hyperspectral IR imaging (0.8-2.5 microns). Spectral resolution: 4 nm IFOV<100m.	Hi-res (<1 mrad/pixel) VNIR imaging spectrometer	4	4
			Globally distributed thermal imaging, 2K absolute accuracy, from ~80K to >160K, spatial resolution <10 km/pixel	Thermal IR imaging spectrometer	4	4
		Map distributions of different materials, including radiolytic materials (e.g. SOx, O3, H2O2, OH, O2), and document variability over a range of timescales.				
			Global hyperspectral IR imaging (0.8-5 microns). Spectral resolution: <10nm (1-2.5 micron: 4 nm). IFOV<1km.	Hi-res (<1 mrad/pixel) VNIR imaging spectrometer	3	3
			Global UV imaging spectroscopy (0.1 to 0.4 microns) with spectral resolution of <2 nm and spatial resolution <100 km/px resolution, <1 km desired.	UV Spectrometer	3	3
		Determine origin and evolution of non-ice materials, including the role of geologic processes				
			Globally distributed hyperspectral IR imaging of representative features (0.8-5 microns). Spectral resolution: <10nm. IFOV<1km. Co-registered with higher-resolution panchromatic imaging.	Hi-res (<1 mrad/pixel) VNIR imaging spectrometer	4	4
		Characterize volatile cycle: document composition, physical state, distribution, and transport of surface volatiles, e.g. sublimation				
			UV imaging spectroscopy with wavelength range of 0.1 to 0.4 micron with spectral resolution of 2 nm and spatial resolution <100 km/pixel (<1km/pixel desired). Spatial coverage of 50% to search for short – lived or mobile species and repeated coverage to look for changes.	UV Spectrometer	4	4

GOAL	OBJECTIVE	INVESTIGATION	MEASUREMENT	Instrument Type	Baseline Payload Science Value	Descoped Payload Science Value	
			VNIR hyperspectral imaging: 0.55 to 0.75 microns, spectral resolution of 1 nm. 50% global coverage with spatial resolution <1km/pixel; repeated coverage to look for changes.	Hi-res (<1 mrad/pixel) VNIR imaging spectrometer	3	3	
			Hyperspectral IR imaging (0.8-5 microns). Spectral resolution: <10nm, 50% global coverage with spatial resolution <1km/pixel; repeated coverage to look for changes.	Hi-res (<1 mrad/pixel) VNIR imaging spectrometer	4	4	
Determine the compositions, origins, and evolution of the atmosphere, including transport of material throughout the Jovian system							
	Understand the sources (sublimation, surface sputtering) and sinks (freezing out, plasma pickup/sputtering, thermal escape) of atmospheric components						
		Determine column densities of atmospheric species across the globe					
			Global EUV - VNIR (0.06-1 micron) surface and limb spectroscopy at <50 km resolution. UV spectral resolution of 0.3 nm		UV imaging spectrometer (<90 mrad/pixel) VNIR imaging spectrometer (<90 mrad/pixel)	3	3
			UV stellar occultations (0.06-0.35 microns) over a range of latitude/longitude space periodically throughout the mission. UV spectral resolution of 0.3 nm		UV spectrometer	5	5
		Perform long-term and high-temporal-resolution monitoring of atmosphere in context of plasma bombardment variations					
			Global EUV - VNIR (0.06-1 micron) surface and limb spectroscopy at <50 km spatial resolution. UV spectral resolution of 0.3 nm		UV imaging spectrometer (<90 mrad/pixel) VNIR imaging spectrometer (<90 mrad/pixel)	3	3
			Determine the composition, distribution and physical characteristics (grain-size, crystallinity, physical state) of volatile materials on the surface				
			Global FUV - IR (0.1-5 micron) spectroscopy at <50 km spatial resolution; UV spectral resolution of 1 nm;IR spectral resolution <10 nm		UV imaging spectrometer (<90 mrad/pixel) VNIR imaging spectrometer (<90 mrad/pixel)	3	3
			Investigate sputtering processes at high latitudes as compared with lower latitudes				
			Global FUV - IR (0.1-5 micron) spectroscopy at <50 km spatial resolution. UV spectral resolution of 1 nm;IR spectral resolution <10 nm		UV imaging spectrometer (<90 mrad/pixel) VNIR imaging spectrometer (<90 mrad/pixel)	3	3
	Understand the temporal, spatial, and compositional variability of the atmosphere						
		Determine column densities, compositions and temperatures of atmospheric species across the globe					
			Global EUV - VNIR (0.06-1 micron) surface and limb spectroscopy at <50 km spatial resolution; spectral resolution of 0.3 nm		UV imaging spectrometer (<90 mrad/pixel) VNIR imaging spectrometer (<90 mrad/pixel)	3	3



Foldout C3e. Satellites—Rings and Small Satellites

GOAL	OBJECTIVE	INVESTIGATION	MEASUREMENT	Instrument Type	Baseline Payload Science Value	Descoped Payload Science Value	
	Target Body -- Rings & Small Satellites						
Determine how the components of the Jovian system operate and interact							
	Determine the structure and particle properties of the Jovian ring system						
		Determine the size distribution in each ring component					
			Broad-band imaging of each ring component at visual to near IR (0.4 to 2 micron) wavelengths and multiple phase angles. Include phase angles > 178 degrees and < 5 degrees. Phase angle sampling < 10 degrees. Signal-to-noise > 100. Spatial resolution < 10 km. Field of view > 10,000 km.		Hi-Res Imaging; VNIR Spectrometer	5	5
			Visual to IR (0.5 to 5 micron) spectral image cubes of each ring component. Signal-to-noise > 100. Spectral resolution < 0.02 microns. Spatial resolution < 50 km. Field of view > 15,000 km. At least 5 phase angles including < 10 degrees and > 175 degrees		Hi-Res Imaging; VNIR Spectrometer	5	5
			Far IR emission spectra of the main ring. Signal-to-noise > 100. Wavelength range 5 to 300 microns		Thermal Imaging Spectrometer	4	4
		Determine the 3-D structure Jovian ring system					
			Edge-on imaging of the entire ring system < 10 km resolution. Multiple (> 5) phase angles including < 10 degrees and > 170 degrees. Several visual and near-IR wavelengths. Multiple longitudes relative to the nodes of Amalthea's and Thebe's orbits to look for orbital concentrations.		Hi-Res Imaging	4	4
			Broad-band imaging of the halo crossing into the Jovian shadow, as viewed from within the shadow. Multiple broadband filters in the visual and near-IR. Resolution < 10 km. Field of view > 10,000 km.		Hi-Res Imaging	4	4
			Fine resolution (< 1 km resolution) imaging of the main ring. Multiple (> 5) phase angles including < 10 degrees and > 175 degrees. Several visual and near-IR wavelengths		Hi-Res Imaging	5	5
		Determine the composition of the rings and embedded moons					
			Visual to IR (0.5 to 5 micron) spectral image cubes of Adrastea, Metis, Amalthea and Thebe. Spectral resolution < 0.02 microns. Phase angle < 20 degrees. Multiple rotational phases.		Hi-Res Imaging; VNIR Spectrometer	4	4
			Visual to IR (0.5 to 5 micron) spectral image cubes of each ring component. Signal-to-noise > 100. Spectral resolution < 0.02 microns. Phase angle < 20 degrees. Spatial resolution < 10 km. Field of view > 15,000 km.		Hi-Res Imaging; VNIR Spectrometer	4	4
		Complete a comprehensive search for small inner moons of Jupiter, down to a size of 100 m					
				Broad-band visual imaging at low phase angles, using long exposures to achieve needed sensitivities. Repeated observations over >1 year to obtain well-defined orbits.		Hi-Res Imaging	4



Foldout C4. Interiors

GOAL	OBJECTIVE	INVESTIGATION	MEASUREMENT	Instrument Type	Baseline Payload Science Value		Descoped Payload Science Value	
	Determine the interior structures and processes operating in the Galilean Satellites in relation to the formation and history of the Jupiter system and potential habitability of the moons.					Ganymede	Other	GanymedeOther
	Characterize the formation & chemical evolution of the Jupiter system							
		Place bounds on the orbital evolution of the satellites						
			Secular acceleration of all the moons to 5m/yr ² (corresponds to ~ a few meters in orbit location). Particularly important for Europa, although the signal is likely largest at Io.	Doppler radio tracking Hi-res imager	2-Ganymede;	1	2-Ganymede;	1
			Io heat flow constraints. Thermal: wavelength range of 8 to 100mm with a spectral resolution of 2 and spatial resolution ≤30-km/pixel; Observation collected several times of day and at night.	Thermal imager	3	3	3	3
			Thermal IR (10-30 micron) monitoring of Jupiter's stratosphere to search for waves associated with tides raised on Jupiter by the moons (especially Io). If detected, the amplitudes of such waves could help constrain the tidal Q of Jupiter. Sounding needs to occur globally and repeatedly (binning the data at the known wave periods will be needed to extract the weak signal from unrelated stratospheric activity).	Thermal imager	2	2	2	2
		Determine the sizes and states of the cores of the moons.						
			Global steady magnetic fields. Global field; Desired accuracy of 0.1nT	Magnetometer	5-Ganymede;	0	3-Ganymede;	0
	Determine the presence and location of water within these moons.							
		Determine the extent of differentiation of the three icy satellites						
			Low order gravity (static & dynamic) J ₂ and C ₂₂ ; constraints on nonhydrostatic components from higher harmonics and test of hydrostaticity. At 10 ⁻⁷ accuracy for the non-dimensional gravitational harmonics of all three moons.	Doppler radio tracking Laser altimeter	5	5	5	5
			Determination of degree 2 static topography to at least ten-meter accuracy	Doppler radio tracking Laser altimeter	5-Ganymede	2-Caillisto, 1-Others	4-Ganymede;	2-Callisto; 1- Others
			Globally characterize the intrinsic magnetic fields, if any. Global magnetic field. Desired accuracy of 0.1nT	Magnetometer	5-Ganymede;	1	4-Ganymede;	1
			Measure the pole position to 10-m accuracy to determine the obliquity of the spin axis. If the shell is decoupled this would provide a constraint on the shell thickness through the Cassini relation	Hi-res imager	5-Ganymede;	2	5-Ganymede;	2
		Establish the presence of oceans						
			Time-dependent altimetry and gravity to determine Love numbers h ₂ and k ₂ for the time-variable tide. Requires determination of the surface motion that correlates with the eccentricity tidal potential to 1-meter accuracy (if performed from orbit requires equivalent radial orbit determination accuracy), and a determination of the time dependent degree-2 gravitational acceleration to 0.1 mgal at Ganymede and Callisto, and 1 mgal at Europa.	Doppler radio tracking Laser altimeter	5-Ganymede;	4-Callisto, 2-Others	4-Ganymede;	4-Callisto; 2- Others
			Induced magnetic field. Global determination of induction response at orbital (as well as Jupiter rotation) time scales for all the satellites to an accuracy of 0.1 nT.	Magnetometer	5-Ganymede;	3	4-Ganymede;	3
			Libration amplitude. Determination of the libration amplitude to 10-m accuracy for Europa, Ganymede, and Callisto	Hi-res imager	5-Ganymede;	2	5-Ganymede;	2
		Characterize the extent and location of water (including brines) in 3D within Europa, Ganymede and Callisto						
			Global profiling of thermal, compositional and structural horizons for Europa, Ganymede, and Callisto's icy shells, at 5 degree equatorial separations, at depths from 2 up to 30 km at 100 m vertical resolution, and at depths from 100m – 2 km at 10 m vertical resolution	Ice-penetrating radar	5-Ganymede;	2	3-Ganymede;	2
			Magnetic field. Global magnetic field. Desired accuracy of 0.1nT	Magnetometer	4-Ganymede;	3	4-Ganymede;	3
			Heat flow by thermal IR. Global coverage at 5-30 micron wavelength, spectral resolution >10, and spatial resolution of 100 km/pixel. Coverage should be repeated at many geometries relative to the Sun to distinguish heat flow from albedo/thermal inertia effects.	Thermal imager	5	5	5	5
		Determine the thickness of the ice layer for all Icy Satellites						
			Altimetry (in combination with gravity) for the eccentricity tide. Determination of eccentricity tidal response to meter accuracy. (This includes but is not restricted to degree 2 response). This includes determining k ₂ and h ₂ to accuracy of 0.005 at all the satellites. In terms of percentage uncertainty in the result, this is a higher measurement requirement at Europa than at the other icy moons.	Doppler radio tracking Laser altimeter	5-Ganymede;	3	4-Ganymede;	3

GOAL	OBJECTIVE	INVESTIGATION	MEASUREMENT	Instrument Type	Baseline Payload Science Value		Descoped Payload Science Value	
			Induced magnetic field at periods from Jupiter's rotation to several weeks. Determination of induction response at orbital (as well as Jupiter rotation) time scales for all the satellites to an accuracy of 0.1 nT	Magnetometer	5-Ganymede;	0	5-Ganymede;	0
			Subsurface sounding. Profiling of thermal, compositional and structural horizons for Europa, Ganymede, and Callisto's icy shells, at ~ 5 deg. equatorial separations, at depths from 2 up to 30 km at 100 m vertical resolution, and at depths from 100m – 2 km at 10 m vertical resolution. Global coverage not required; even a small number of close flybys could sound bottom of a thin ice shell and hence determine ice shell thickness. But global coverage strongly desired because (i) it would help remove ambiguities between bottom of ice shell and other internal horizons (compositional boundaries or faults), and (ii) it would provide constraints on spatial variations in the thickness of the ice shell.	Ice-penetrating radar	5	5	5	5
			Heat flow by thermal IR. Thermal: wavelength range of 8 to 100mm with a spectral resolution of 2 and spatial resolution ≤30-km/pixel; Observation collected several times of day and at night.	Thermal imager	5	5	5	5
	Characterize the operation of magnetic dynamo processes in the Jovian system and their interaction with the surrounding magnetic field							
		Globally characterize Ganymede's intrinsic magnetic field and search for temporal variability in the field						
			Perform near-surface (100-200 km altitude) global magnetic sounding at spatial resolutions of ~300 km. Repeat global coverage every <3 months to characterize temporal variability in the intrinsic field and separate it from spatial variability in the intrinsic field. Coverage at a given Ganymede latitude/longitude should be repeated at multiple Jupiter System III longitudes to separate the induced field from the intrinsic field. Desired spacecraft inclination > 60 degrees.	Magnetometer	5	5	2	2
		Characterize the interaction of Ganymede's magnetosphere with Jupiter's magnetosphere						
			Perform global magnetic, electric, and charged-particle sounding at (i) a range of distances from near-Ganymede-surface to several Ganymede radii, (ii) a range of longitudes/latitudes to cover trailing hemisphere, leading hemisphere, equator, and poles, and (iii) a range of temporal scales ranging from weeks to years.	Magnetometer Plasma spectrometer Plasma wave spectrometer Energetic particle detector Heavy ion counter	5	5	5	5
		Monitoring of Jupiter's magnetic-field environment, with the goal of searching for changes in the intrinsic Jovian field and characterizing plasma processes in the Jovian magnetosphere						
		Perform magnetic, electric, and charged-particle measurements at a range of distances from Jupiter over a period of years, with spatial coverage including equatorial, polar, sub-solar, and anti-solar locations	Magnetometer Plasma spectrometer Plasma wave spectrometer Energetic particle detector Heavy ion counter	5	5	5	5	
	Identify the dynamical processes that cause internal evolution and near-surface tectonics of all four moons							
		Determine the extent of differentiation of all four satellites						
			Low order gravity (static & dynamic) J ₂ and C ₂₂ ; constraints on nonhydrostatic components from higher harmonics and test of hydrostaticity. At 10 ⁻⁷ accuracy for the non-dimensional gravitational harmonics of all three moons.	Doppler radio tracking Laser altimeter	5-Ganymede;	4	4	4
			Determination of degree 2 static topography to at least ten-meter accuracy	Doppler radio tracking Laser altimeter	5-Ganymede;	2-Callisto; 1-Others	4-Ganymede;	2-Callisto; 1- Others
			Globally characterize the intrinsic magnetic field, if any. Desired accuracy of 0.1nT	Magnetometer	5-Ganymede;	1	4-Ganymede;	1
			Measure the pole position to 10-m accuracy to determine the obliquity of the spin axis. If the shell is decoupled this would provide a constraint on the shell thickness through the Cassini relation	Hi-res imager	5-Ganymede;	2	5-Ganymede;	2
			Time dependent altimetry and gravity to determine tidal k ₂ and h ₂ of the time-variable tide Requires determination of the surface motion that correlates with the eccentricity tidal potential to 1-meter accuracy (if performed from orbit requires equivalent radial orbit determination accuracy), and a determination of the time dependent degree-2 gravitational acceleration to 0.1mgal at Ganymede and Callisto, and 1mgal at Europa. Alternatively, the eccentricity tidal k ₂ and h ₂ at accuracy 0.01. For Io, this will determine whether low-rigidity regions exist (asthenosphere and/or liquid-iron core); for the icy moons, it will determine whether oceans exist.	Doppler radio tracking Laser altimeter	5-Ganymede;	4-Callisto; 2-Others	4-Ganymede;	4-Callisto; 2- Others
		Characterize the near-surface tectonic and volcanic processes and their relation to interior processes						
			Globally distributed altimetry to 1-m vertical resolution and better than 1-km horizontal resolution (100-m horizontal resolution preferable, at least along specific spacecraft tracks if not globally)	Doppler radio tracking Laser altimeter	5-Ganymede;	3-Io, Europa; 4- Callisto	5-Ganymede;	3-Io, Europa' 4- Callisto
		Global high-order gravity sounding to ~300 km horizontal resolution from an altitude of < 100-200 km	Doppler radio tracking Laser altimeter	5-Ganymede;	0	3-Ganymede;	0	

GOAL	OBJECTIVE	INVESTIGATION	MEASUREMENT	Instrument Type	Baseline Payload Science Value		Descoped Payload Science Value	
			Global (>80% coverage) visible imaging at 100-m/pixel spatial resolution. Additionally, desire ~10-20% coverage at 10-m/pixel.	Moderate-res imager Hi-res imager		4-Io		4-Io
			Thermal and compositional horizons. Global profiling of thermal, compositional and structural horizons for Europa, Ganymede, and Callisto's icy shells, at £ 5 deg. equatorial separations, at depths from 2 up to 30 km at 100 m vertical resolution, and at depths from 100m – 2 km at 10 m vertical resolution	Ice-penetrating radar	5-Ganymede	2	4-Ganymede	2
			Measurement of, or upper limit on, heat flow (thermal IR). Thermal: wavelength range of 8 to 100mm with a spectral resolution of 2 and spatial resolution ≤30-km/pixel; Observation collected several times of day and at night. Additionally, for Io, global coverage at 1-5 micron wavelength and spatial resolution of 100 km/pixel to search for localized hot spots. Desire < 20-km/pixel spatial resolution.	Thermal imager Hi-res thermal imager	5	5	5	5
			Topographic change arising from internal processes. Requirement is the ability to detect vertical or horizontal displacement of 10-m. Baseline requirement is 1 m. Require double coverage of candidate features (e.g., once near beginning of mission and once near end to maximize temporal baseline). For especially promising or active features, prefer coverage multiple times throughout the mission.	Topographic mapping via stereo imaging or SAR mapping Laser altimeter	5-Ganymede	1	4-Ganymede;	1
			Subsurface change. Global profiling of thermal, compositional and structural horizons for Europa, Ganymede, and Callisto's icy shells, at £ 5 deg. equatorial separations, at depths from 2 up to 30 km at 100 m vertical resolution, and at depths from 100m – 2 km at 10 m vertical resolution	Ice-penetrating radar	5-Ganymede	2	4-Ganymede	2
			Search for changes in pole position (obliquity) over periods of years. This should include both changes in the rotation-axis orientation in inertial space and movements of the rotation poles relative to the satellite figure (polar wander). Predictions (Bills 2005) are that Io, Europa, Ganymede, and Calliso undergo obliquity oscillations with amplitudes of ~0.005, 0.1, 0.1, and 1 degree over periods of ~10, ~40, 40, and 500 years. This implies total surface movements of pole position of ~160 m, 3 km, 5 km, and 40 km, respectively, over the respective periods. Over a 5-year interval, the predicted movement in pole position would be ~160 m, 300 m, 600 m, and 400 m for Io, Europa, Ganymede, and Callisto. Requirement is therefore to image selected portions of the surface at 10 m/pixel and to determine the absolute latitude/longitude location of the imaged terrain to 10 m/pixel. This must be done multiple times during the mission, with a total temporal baseline >1 year (and >3 years strongly desired).	Hi-res stereo imaging or SAR mapping				
					4-Ganymede	0	4-Ganymede	0
			Magnetic field. Determination of induction response at orbital (as well as Jupiter rotation) time scales for all the satellites to an accuracy of 0.1 nT but with the emphasis on looking for secular variation of the “steady” field or variation in the induction signal since Galileo	Magnetometer	5-Ganymede	4	5-Ganymede	4
			Magnetotelluric effects from ocean currents. Sensitivity to 0.1 nT.	Magnetometer	5-Ganymede	0	5-Ganymede	0
			Heat flow by thermal IR. Thermal: wavelength range of 8 to 100mm with a spectral resolution of 2 and spatial resolution ≤30-km/pixel; Observation collected several times of day and at night.	Thermal imager	5	5	5	5
			Io monitoring. Requirement is long-distance visible and thermal characterization (e.g., from Ganymede or Jupiter orbit) over a period of years. Desire close flybys of Io to characterize terrains/active features/change at high resolution	Hi-res imager Hi-res thermal imager	5	5	5	5



D. TELECOMMUNICATIONS LINK ANALYSIS

D1. Introduction

This appendix contains the performance estimates for the Jupiter System Observer (JSO) telecommunication links. The telecommunications subsystem is described in §4.4. The following paragraphs detail the assumptions within the link analysis, as well as present the results of the analysis with charts and link design control tables where appropriate.

D2. Requirements

The link shall provide for command, telemetry, and radiometric navigation:

Radiometric Navigation Performance

1. Doppler: < 0.1 mm/sec in 60 sec
2. Ranging: 4 m in 10 min
3. DDOR (VLBI): 0.12 ns

Command Performance at BER < 1E-5

4. Minimum rate: 7.8125 bps
5. Maximum rate: 2000 bps

Engineering Telemetry Performance FER < 1E-4

6. Minimum rate: 10 bps
7. Maximum rate: ~1600 kbps at 3.95 AU

Key functions:

8. Initial acquisition
9. Safe mode telecom & command
10. Critical event data & monitoring
11. Single fault immunity

D3. Telecommunications Subsystem Overview

The maximum range is 6.5 AU for the JSO science phase. In order to minimize transmit circuit losses, the telecom hardware is mounted on the back of the HGA which reduces the loss between the output of the high-power amplifiers and the 2.75 m, X/Ka-band HGA.

Flight system communication is primarily via X-band for the uplink and Ka-band for the downlink, with additional use of X-band downlink and Ka-band uplink for dual-band gravity science. Dual string, cross-strapped SDSTs and 50-W Ka-Band TWTAs provide X up/Ka down command and telemetry capability. In addition, there are two 5 W X-Band SSPAs for the X-Band downlink carrier-only reference signal for gravity and radio science

experiments. The Ka band downlink can be operated with the HGA, MGA or one of 2 LGAs. The X-band downlink can be operated with the HGA, or one of the LGAs.

The high rate links are designed to communicate to DSN 70-m equivalent antennas at Ka-Band. Link performance for cruise and Jupiter system tour does not constrain the design. The MGA link example is for safe modes during the Jupiter science phase to a 70-m equivalent antenna.

D4. Assumptions

Assumptions made for the link analysis include:

- 90% Cumulative Weather Distribution
- 20 deg station elevation
- 89K receiver noise temperature
- No Jupiter Hot body noise in the antenna field of view (Jupiter will only occupy the beam rarely and for a brief period)
- BPSK suppressed carrier modulation
- Turbo 1/6 encoding
- 8920 bit frame length
- Ranging is OFF for high rate science TLM

D5. Link Design Control Tables

The link Design Control Tables (DCT) shown in [Tables D5-1](#) through [D5-3](#) were constructed for the baseline telecom concept and design assumptions. Because the detailed design has not yet been determined, some parameters, such as circuit losses, were assumed based on actual designs from previous projects.

Table D5-1. 50-W Ka-Band TWTA, 2.75-m HGA, 70m DSN, Turbo 1/6, 1.2-mradian Pointing

50W TWTA										9.724E+08 6.5000 0.000		Range, km RF band AU CW L1, NS	
Ka-Band HGA, 2.75 m antenna diameter, 0.07° off-point DSN 34 m station Configuration: X/Ka RCP Camera Az deg, elevation 90% L/W camera (year average) Hot body noise = 0 K 1 way										0.00		SEP, deg	
Carrier Loop Bandwidth = 100 Hz Symbol Rate to the SLS T = 360000 sps Data Bit Rate Before All Encoding = 600000 bps										20		Elev. Angle, deg	
Tim channel (Turbo 1/6, 8920 bit/frame) FER=10^-4										Ka 32050		RF band Freq, MHz	
Link Parameter Unit										50.0		Xmit Pwr, W (BOL)	
TRANSMITTER PARAMETERS										0.24		3 dB Beamwidth	
1 SC RF Power Output dBm 46.99 0.30 -0.30 46.99 0.0150 T										HGA		SC Antenna	
2 Total Circuit Loss dB -2.00 0.20 -0.20 -2.00 0.0134 U													
3 Antenna Gain (on boresight) dBi 57.44 0.00 0.00 57.44 0.0000 T													
4 Ant Pointing Loss dB -1.04 0.99 -0.99 -1.04 0.3275 U													
5 EIRP (1+2+3+4) dBm 101.39 0.3559													
PATH PARAMETERS													
6 Space Loss dB -302.32 0.00 0.00 -302.32 0.0000 D										90		Weather%	
7 Atmospheric Attn dB -1.18 0.00 0.00 -1.18 0.0000 D										Year Average		Distribution Type 7	
RECEIVER PARAMETERS										Carberra: 34m BWG, DSS34			
8 DSN Antenna Gain dBi 84.80 0.30 -0.30 84.80 0.0150 T										n/a		LNA Selection	
9 Ant Pointing Loss dB -0.20 0.00 0.00 -0.20 0.0000 U										X/Ka RCP		DSS Config	
10 Polarization Loss dB -0.04 0.00 0.00 -0.04 0.0000 U													
TOTAL POWER SUMMARY										70m Ka-Band equivalent			
11 Total Rxd Pwr (Pt) dBm 117.56 0.3709 G													
12 Noise Spec Dens dBm/Hz -179.11 -0.05 0.10 -179.09 0.0006 G													
System Noise Temp K 88.88 -1.00 2.00													
Vacuum, zenith K 21.33 -1.00 2.00										1		WAY	
Elevation K 1.47 0.00 0.00													
Atmosphere K 66.08 0.00 0.00													
Hot Body Noise K 0.00 0.00 0.00													
13 Received P/N0 dBHz 61.53 0.3715 G													
13a Received P/N0 - 2 sigma dBHz 60.31													
CARRIER PERFORMANCE (at threshold)										TRUE		TLM ON?	
14 Tim Carrier Supp dB -15.21 5.01 -13.94 -18.18 16.0797 T										0 deg		RNG MI?	
15 Rng Carrier Supp dB 0.00 0.00 0.00 0.00 0.0000 T										FALSE		DOR ON?	
16 DOR Carrier Supp dB 0.00 0.00 0.00 0.00 0.0000 T													
17 Received P/N0 (39+14+15+16) dBHz 39.99 16.4512 T										10.0		Carrier Bl, Hz	
18a Carrier Loop Bandwidth, Bl dBHz 10.00 0.00 0.00 10.00 0.0000 T										-30		Carrier Phase Noise	
Phase Noise Variance rad^2 0.00										Type 2: SuperOptically Damped			
Thermal Noise Contribution rad^2 0.0010													
Transmitter Noise Contribution rad^2 0.0002													
Solar Noise Contribution rad^2 0.0000													
19 Loop SNR dB 29.37 16.4512 U													
20 Required Carrier Loop SNR dB 10.00 0.0000 D													
21 Carrier Loop SNR Margin dB 19.37 16.4512 U													
SUBCARRIER PERFORMANCE at Req. P/N0										500		Sub Carr Bl, mHz	
22 Sub Carr. L. SNR dB 51.20										1		Sub Carr window f.	
23 Required Loop SNR dB 20.00													
24 Sub Carrier Loop SNR Margin dB 31.20													
SYMBOL LOOP PERFORMANCE at Req. P/N0										50		Sym Bl, mHz	
25 Sym. Loop SNR dB 49.44										1		Sym window f.	
26 Required Loop SNR dB 15.00													
27 Sub Carrier Loop SNR Margin dB 34.44													
TELEMETRY PERFORMANCE at Required P/N0										80.0		tim MI, deg	
28 Tim Data Supp dB -0.13 0.13 -0.30 -0.19 0.0082 T										0.00		peaking MI, deg	
29 Rng Data Supp dB 0.00 0.00 0.00 0.00 0.0000 T													
30 DOR Data Supp dB 0.00 0.00 0.00 0.00 0.0000 T													
30a Pd/N0 (39 +28 +29 +30) dBHz 57.98										600,000.0		data bit rate, bps	
31 Data Rate dB 57.78 0.00 0.00 57.78 0.0000 D										3,600,000		ch symbol rate, bps	
32 Radio Loss dB -0.10 -0.10													
33 Sub Carrier Demod. Loss dB -0.01 -0.01													
34 Symbol Sync Loss dB -0.01 -0.01													
35 Waveform Distortion Loss dB -0.15 -0.15													
36 Decoder Loss dB 0.00													
37 Baseline Eb/N0 dB -0.10										D Turbo 1/6, 8920 bit/frame		Coding	
38 Output Eb/N0 (required to close all loops) dB 0.20										FER=10^-4		BER at BVR output	
38a Eb/N0 margin dB 0.30													
39 Required P/N0 dBHz 58.17 0.3107 U													
Performance Margin (39-13) dB 3.36													
40 Sigma dB 0.83													
42 Margin -2 sigma dB 1.71													
Wind Loading Loss dB 0.00 0.00 0.00 0.00 0.0000 U										0		wind speed, mph	
Pointing Loss due to Wind (BWG) dB 0.00 0.00 0.00 0.00 0.0000 U										99		wind CD %	
Adjusted Performance Margin dB 3.36													

Table D5-2. 50-W Ka-Band TWTA, MGA, 70m DSN, Safe Mode Downlink

500W TWTA										9.724E+08 6.5000 0.50		Range, km Range, AU UV L1, hrs
Ka-Band MGA, 5.0° offpoint DSN 34 m station Configuration: X/Ka RCP Carrier BW (deg): 0.000000000 0.0 W carrier (1 deg average) Hot body noise = 0 K 1 way										0.00		SEP, deg
Tim channel/ (Turbo 1/2, 1/84 bit frame) FER=10^-4										20		Elev. Angle, deg
Camera Loop Bandwidth = 30 Hz Symbol Rate to the SLS 1 = 20 sps Data Bit Rate Before All Encoding= 10 tps												
	Link Parameter	Unit	Design Value	Fav Tol	Adv Tol	Mean Value	Var	S	Ka 32050	RF band Freq, MHz		
TRANSMITTER PARAMETERS												
1	SCRF Power Output	dBm	46.99	0.30	-0.30	46.99	0.0150	T	50.0	Xmtr Pwr, W (BOL)		
2	Total Circuit Loss	dB	-2.00	0.30	-0.30	-2.00	0.0301	U				
3	Antenna Gain (on boresight)	dBi	19.24	0.00	0.00	19.24	0.0000	T	5.00	Boresight Angle, deg		
4	Ant Pointing Loss	dB	-0.87	-1.38	1.38	-0.87	0.6400	U	MGA	S/C Antenna		
5	EIRP (1+2+3+4)	dBm				63.36	0.6851					
PATH PARAMETERS												
6	Space Loss	dB	-302.32	0.00	0.00	-302.32	0.0000	D	90	Weather%		
7	Atmospheric Attn	dB	-1.18	0.00	0.00	-1.18	0.0000	D	Year Average	▼ Distribution Type		
RECEIVER PARAMETERS												
8	DSN Antenna Gain	dBi	84.80	0.30	-0.30	84.80	0.0150	T	Canberra: 34m BWG, DSS34	▼		
9	Ant Pointing Loss	dB	-0.10	0.00	0.00	-0.10	0.0000	U	n/a	▼ LNA Selection		
10	Polarization Loss	dB	-0.03	0.00	0.00	-0.03	0.0000	U	X/Ka RCP	▼ DSS Config		
TOTAL POWER SUMMARY										70m Ka-Band equivalent		
11	Total Rad Pwr (Pt) (5+6+7+8+9+10)	dBm				-155.48	0.7001	G				
12	Noise Spec Dens	dBm/Hz	-179.11	-0.05	0.10	-179.09	0.0006	G				
	System Noise Temp	K	88.88	-1.00	2.00			G				
	Vacuum, zenith	K	21.33	-1.00	2.00			T	1	WAY		
	Elevation	K	1.47	0.00	0.00			G				
	Atmosphere	K	66.08	0.00	0.00			G				
	Hot Body Noise	K	0.00	0.00	0.00			G				
13	Received PtNo	dBHz				23.61	0.7007	G				
13a	Received PtNo - 2sigma	dBHz				21.94						
CARRIER PERFORMANCE (at threshold)												
14	Tim Carrier Supp	dB	-5.23	1.19	-1.47	-5.33	0.2966	T	TRUE	TLM ON?		
15	Rng Carrier Supp	dB	0.00	0.00	0.00	0.00	0.0000	T	0 deg	▼ RNG MI?		
16	DOR Carrier Supp	dB	0.00	0.00	0.00	0.00	0.0000	T	FALSE	DOR ON?		
17	Received PoNo (39+14+15+16)	dBHz				14.74	0.9972	T				
18	Carrier Loop Bandwidth, BI	dBHz	4.77	0.00	0.00	4.77	0.0000	T	3.0	Carrier BI, Hz		
18a	Phase Noise Variance	rad^2				0.10			-30	Carrier Phase Noise		
	Thermal Noise Contribution	rad^2				0.1007			Type 2: SuperCritically Damped			
	Transmitter Noise Contribution	rad^2				0.0017						
	Solar Noise Contribution	rad^2				0.0000						
19	Loop SNR	dB				9.90	0.9972	U				
20	Required Carrier Loop SNR	dB				10.00	0.0000	D				
21	Carrier Loop SNR Margin	dB				-0.10	0.9972	U				
SUBCARRIER PERFORMANCE at Req. PtNo												
22	SubCar L. SNR	dB				20.00						
23	Required Loop SNR	dB				20.00			500	SubCar BI, mHz		
24	SubCarrier Loop SNR Margin	dB				0.00			0.5	SubCar window.f.		
SYMBOL LOOP PERFORMANCE at Req. PtNo												
25	Sym. Loop SNR	dB				21.42			50	Sym BI, mHz		
26	Required Loop SNR	dB				15.00			0.5	Sym window.f.		
27	SubCarrier Loop SNR Margin	dB				6.42						
TELEMETRY PERFORMANCE at Required PtNo												
28	Tim Data Supp	dB	-1.55	0.50	-0.63	-1.59	0.0537	T	56.8	tIm MI, deg		
29	Rng Data Supp	dB	0.00	0.00	0.00	0.00	0.0000	T	0.00	peakng MI, deg		
30	DOR Data Supp	dB	0.00	0.00	0.00	0.00	0.0000	T				
30a	PdNo (39+28+29+30)	dBHz				18.48						
31	Data Rate	dB	10.00	0.00	0.00	10.00	0.0000	D	10.0	data bit rate, bps		
32	Radio Loss	dB	-0.47			-0.47		T	20	ch symbol rate, bps		
33	SubCarrier Demod. Loss	dB	-0.46			-0.46		T				
34	Symbol Sync. Loss	dB	-0.19			-0.19		T				
35	Waveform Distortion Loss	dB	-0.15			-0.15		T				
36	Decoder Loss	dB				0.00						
37	Baseline Eb/No	dB				1.50		D	Turbo 1/2, 1/84 bit frame	▼ Coding		
	Output Eb/No (required to close all loops)	dB				8.48			FER=10^-4 BER at BVR output			
38a	Eb/No margin	dB				6.98						
39	Required PtNo	dBHz				20.07	0.3562	U				
40	Performance Margin (39-13)	dB				3.54						
41	Sigma	dB				1.03						
42	Margin -2 sigma	dB				1.49						
	Wind Loading Loss	dB	0.00	0.00	0.00	0.00	0.0000	U	0	▼ wind speed, mph		
	Pointing Loss due to Wind (BWG)	dB	0.00	0.00	0.00	0.00	0.0000	U	99	wind CD%		
	Adjusted Performance Margin	dB				3.54						

Table D5-3. 5-W X-Band SSPA, HGA, 34m DSN, Carrier Only

5.0 W SSPA									
X-Band HGA, 3 m antenna diameter, 0.10° off-point								9.724E+08 Range, km	
DSN 34 m station /Configuration: X/Ka duplexed RCP								6.5000 Range, AU	
Canberra/15 deg. elevation/90% CD Weather (Year Average)								0.90 OWLT, hrs	
Hot body noise = 0 K									
1 way								0.00 SEP, deg	
Block V receiver/residual carrier mode/TLM-21 Models									
11m channel/ (1 turbo 1/6, 8920 bit frame) F/R=10^4								15 Elev. Angle, deg	
	Link Parameter	Unit	Design Value	Fav Tol	Adv Tol	Mean Value	Var	S	X RF band
TRANSMITTER PARAMETERS									8439.44 Freq, MHz
1	S/C RF Power Output	dBm	36.99	0.30	-0.30	36.99	0.0150	T	5.0 Xmrtr Pwr, W (BOL)
2	Total Circult Loss	dB	-2.00	0.20	-0.20	-2.00	0.0134	U	
3	Antenna Gain (on boresight)	dB	46.60	0.00	0.00	46.60	0.0000	T	0.83 3 dB Beamwidth
4	Ant Pointing Loss	dB	-0.17	2.32	-2.32	-0.17	1.8007	U	HGA S/C Antenna
5	EIRP (1+2+3+4)	dBm				81.42	1.8291		
PATH PARAMETERS									
6	Space Loss	dB	-290.73	0.00	0.00	-290.73	0.0000	D	
7	Atmospheric Attn	dB	-0.22	0.00	0.00	-0.22	0.0000	D	90 Weather %
RECEIVER PARAMETERS									Year Average Distribution Type
8	DSN Antenna Gain	dB	68.26	0.10	-0.20	68.23	0.0039	T	Canberra: 34mBWG, DSS34
9	Ant Pointing Loss	dB	-0.10	0.00	0.00	-0.10	0.0000	U	n/a LNA Selection
10	Polarization Loss	dB	-0.03	0.00	0.00	-0.03	0.0000	U	X/Ka duplexed RCP DSS Config
TOTAL POWER SUMMARY									
11	Total Rcvd Pwr (Pt)	dBm				-141.43	1.8330	G	
			(5+6+7+8+9+10)						
12	Noise Spec Dens	dBm/Hz	-183.39	-0.13	0.25	-183.33	0.0039	G	
	System Noise Temp	K	33.16	-1.00	2.00			G	
	Vacuum, zenith	K	18.97	-1.00	2.00			T	1 WAY
	Elevation	K	0.70	0.00	0.00			G	
	Atmosphere	K	13.49	0.00	0.00			G	
	Hot Body Noise	K	0.00	0.00	0.00			G	
13	Received P/No	dB-Hz				41.90	1.8369	G	
13a	Received P/No - 2sigma	dB-Hz				39.19			

E MEL AND PEL

Details not available for public release.